NASA Contractor Report 189235

Analysis of Large Quasistatic Deformations of Inelastic Solids by a New Stress Based Finite Element Method

Kenneth W. Reed
Georgia Institute of Technology
Atlanta, Georgia

September 1992

Prepared for
Lewis Research Center
Under Grant NAG3–38

National Aeronautics and Space Administration

ACKNOWLEDGMENTS

The author is deeply indebted to Professor S. N. Atluri, teacher and counselor, whose support, encouragement, and guidance made this work possible. The author is grateful for the suggestions of Professors Fitzgerald and Will, members of the reading committee, and for the recommendations of Professors Stallybrass and Lai, members of the guidance committee.

The author expresses his sincere appreciation to Dr. S. L. Passman for his interest in the author's progress, and to those at Sandia National Laboratories who made the author's stay there rewarding.

The author gratefully acknowledges the many valuable discussions he had with Dr. H. Murakawa during the early stages of this work. His influence was certainly felt throughout.

The author acknowledges the financial support provided by NASA-Lewis Research Center through a grant, NAG 3-38, to Georgia Tech with S. N. Atluri as principal investigator.

The author thanks his family for their unwavering support and encouragement during this work. Finally, to his wife, Carol, this work is dedicated.

TABLE OF CONTENTS

LIST OF TABLES

LIST OF ILLUSTRATIONS

Figure Page

CHAPTER I

INTRODUCTION

In his *Treatise on the Mathematical Theory of Elasticity*, Love* observed that "When the general equations had been obtained, all questions of the small strain of elastic bodies were reduced to a matter of mathematical calculation." To this day, that 'matter of mathematical calculation' figures prominently in applied mechanics.

The early mecanicians realized that the general equations of elasticity were too difficult to solve except in a few special cases, so a large part of their effort was focused on methods for finding approximate solutions to problems of technological interest. Some of the techniques they used in deriving approximate theories for rods, plates, and shells are, in fundamental ways, very similar to the finite element technique.

Today it is well understood that the classical theories of rods, plates, and shells may all be systematically derived from elasticity theory by introduction of approximations for the displacement to the principle of virtual work. Kirchhoff is the first person mentioned by Love [1] as having used this methodology,** and in using it Kirchhoff managed to give a clear interpretation of the boundary

---

*Love [1], p. 2.

**to derive a theory of elastic rods; later, elastic plates.

conditions in the plate theory with which his name is now associated. In two respects Kirchhoff's methodology is the same as the finite element methodology. First of all, he made kinematic approximations, and secondly, he used an energy principle to maintain consistency between his generalized stresses and strains, and to arrive at the correct boundary conditions. The principal difference between Kirchhoff's methodology and the finite element methodology lies in the degree to which the kinematic field is approximated. Because of the similarities in the construction of the classical rod, plate, and shell theories to the construction of finite element equations, the successes and failures of the classical structural theories reflect, at least qualitatively, upon the performance of the finite element method.

No special theory in the realm of solid mechanics has enjoyed greater success than that of elastic beams, for there the general equations of elasticity are effectively replaced by a single ordinary differential equation. The theory is not only reasonably accurate, but extremely easy to understand because of its displacement based derivation. The classical plate and shell theories provide equations less easy to understand and less easy to solve than the beam equations, but still regarded as simpler than the general equations of elasticity.

A major failing of the classical theories of beams, plates, and shells is their inability to account for the effects of 'transverse shear stress'; that is, the shear stress acting on plane sections through the thickness of the structure. As a direct consequence, those theories always give a higher estimate of the stiffness

of a structure than does the general theory. Secondly, the twisting moment and shear force are coupled on the edge of such a plate or shell. In spite of these shortcomings, it was not until after Reissner's [2] investigation into the effect of shear stress on the bending of plates that satisfactory alternatives to the classical theories became available. But Reissner's methodology has had a greater impact on the methods used in applied mechanics than did his plate theory of itself. In its derivation his theory is distinguished from the classical theories by the fact that both assumed stresses and displacements are used. Since that time the use of assumed stresses in the derivation of plate and shell theories has become common.

It is not surprising that the finite element method has evolved along similar lines. The motive--finding approximate solutions for problems of technological interest--was the same for the early finite element researchers as it had been for the early plate and shell theorists. The finite element method in which one introduces kinematic approximations to the virtual work principle is the direct counterpart of Kirchhoff's rod and plate theories. The same types of advantages and defects are inherent.

The principal advantage of the displacement based finite element methods is their conceptual simplicity. For application to beams, the simplicity rivals the simplicity of the beam theory itself. In the cases of plates and shells though, it proves difficult to construct 'compatible' shape functions for the displacement. Finite elements for thin plates based on kinematic approximations sometimes overestimate the stiffness of the plate so badly that they are

described as 'locking.' As a means of avoiding locking, and just for simpler construction of shape functions, some researchers have presented 'incompatible' plate bending elements, elements which do not satisfy slope continuity at element interfaces. A second problem with displacement based finite element methods (in general) is their ability only to satisfy traction boundary conditions in an average sense. One of the principal advantages of the finite element method over the method of finite differences is its ability to satisfy higher order boundary conditions accurately; but this potential is not fully realized in a purely kinematic formulation.

It was Pian's [3] investigation into the derivation of element stiffness matrices that brought widespread attention to the potential advantages of introducing the stress as an independent variable. By his formulation, which was based on the complementary energy principle of linear elasticity, an energy-consistent alternative to incompatible elements was made available. Also, as was the case in Reissner's plate theory, the stress formulation made possible considerably more accurate satisfaction of traction type boundary conditions. Finally, Pian observed a marked acceleration in the convergence of the components of the stiffness matrix when the stress method was used. Since that time, the study of finite element methods related to Pian's (which have come to be known as 'hybrid stress methods') has produced a number of special methods which may be applied where conventional displacement based finite elements fail.

The failure of the conventional finite element method seems always to be attributable to the presence of kinematic constraints

which cannot be satisfied by approximated displacement fields. In the case of plates and shells, that constraint is interelement slope continuity. When the algorithm is based on an energy principle, it is always possible to 'relax' the constraint by the introduction of a Lagrange multiplier. That multiplier always will be a generalized stress, the 'energy-conjugate' of the kinematic constraint.

One particular class of problems in which the conventional displacement-based finite element method fails is composed of problems involving incompressible or nearly incompressible bodies. The constitutive equation for such bodies is nearly or precisely singular for the mode of dilitation. The shape functions for the displacement used in the conventional finite element method are incapable of producing any motion other than pure shearing which does not contain (loosely speaking) 'excessive' dilitation. As a consequence, the conventional finite element method drastically overestimates the resistance to deformation of nearly and precisely incompressible bodies. In a key paper by Herrmann [4], it was shown that the difficulty could be avoided if only the mean stress were introduced as an independent variable. In this case the kinematic constraint was incompressibility and the energy-conjugate stress was the pressure. His assumed pressure formulation of finite elements for such bodies is now a standard practice.

Problems involving finite deformations of strain-softening bodies resemble problems involving nearly incompressible bodies in the sense that the body's shear compliance is much greater than its bulk compliance. For the most part, finite element analyses of such

deformations have been accomplished only at considerable expense, even when the pressure is introduced as an independent variable. No finite deformation counterpart to the complementary energy principle of linear elasticity was known, so no pure stress or hybrid stress finite element algorithm was found.

The door to stress based finite element analysis of finite deformation problems was opened in 1972 by Fraeijs de Veubeke [5] with his presentation of a complementary energy principle for finite deformation elasticity.* The stationary conditions of this principle are both the equations of compatibility and angular momentum balance. To date, variants of the principle have been used by de Veubeke and Millard [6], Sander and Carnoy [7], Koiter [8], Wunderlich and Obrecht [9], Murakawa [10], Murakawa and Atluri [11], [12], Murakawa et al. [13], and Atluri and Murakawa [14], in problems ranging from elastic membrane theory to beam, plate, and shell theories.

A considerable generalization of de Veubeke's principle was given by Atluri [15]. His formulation of the complementary principle for stress rates and spin opened the way for the current work, that of developing a stress-rate based finite element algorithm for analysis of large deformations of inelastic bodies. It appears that the sole other analysis of large deformations of inelastic bodies by any similar algorithm is that presented by Atluri and Murakawa [14], in

*an invalid principle was presented by Levinson [16], and again by Zubov [17]. The failure of that principle is discussed by Dill [18].

which necking of an elastic-plastic bar and postbifurcation analysis of a thin elastic-plastic plate was performed. The finite element algorithm used by those researchers was based on stress increments, rather than stress rates, and the motion of the elastic-plastic body was found by summation of increments. It was assumed that the accumulated error in this procedure could be kept small by minimizing 'residual loads,' as may be done in elasticity. This procedure has a firm foundation for problems involving elastic bodies (whose deformations were the subject of Murakawa's earlier research), but is of questionable validity when the body is not elastic. In their assessment of incremental solution methods for inelastic rate problems, Argyris et al. [19] conclude that

> Inelastic rate processes are in general path-dependent; therefore, the drift (i.e. the accumulation of numerical integration errors) cannot be eliminated by residual load iteration, e.g. at the end of each time step.

Moreover, when the body exhibits relaxation effects, this solution technique's numerical stability becomes extremely sensitive to the time step size. Hughes and Taylor [20] observe that the time steps required for stability in the explicit time stepping technique are much smaller than required for accuracy when only quasistatic deformations are to be analyzed.

A final objection to 'incremental' finite element formulations may be raised on the grounds that there always results an artificial coupling between the boundary value problem and the initial value problem. When dealing with 'flow law' type solids it is possible to treat the boundary value problem (for the rates) and the initial value

problem (for the total stress and deformation) separately. Typically the boundary value problem for the rates is either precisely linear, or equivalent to a linear problem (without approximation). All of the nonlinearity falls into the initial value problem. Nonlinear initial value problems are perhaps the single type of nonlinear problem which we are best equipped to deal with numerically. In any case, we are better equipped to handle them than we are nonlinear boundary value problems. The incremental approach has the effect of actually transferring that nonlinearity to the boundary value problem, where it is dealt with by residual load iterations.

The objective of the present work is to develop a stress (-rate) based finite element algorithm for analysis of large quasistatic deformations of inelastic bodies. In doing so, we discard the notion of 'increments' entirely. As a direct result, the boundary value problem and the initial value problem may be dealt with separately. The algorithm which results is applied to analyze large deformations of hypoelastic, hypoelastic/plastic, and hypoelastic/viscoplastic bodies.

As is true in large deformation problems in general, the formulation of the boundary value problem and initial value problem is more complicated than in an infinitesimal deformation problem. The first part of this work is devoted to presenting, with reasonable completeness, the development of the problem. The finite element algorithm is not presented until Chapter VII. The initial value problem is presented in Chapter VIII. Example problems are presented in Chapter IX. We note from the outset that the finite element

algorithm is considerably more complicated, and involves more computation, than velocity based algorithms. However from the results it is clear that the improvement in accuracy over velocity based methods is substantial; so much so, that in view of the difficulties encountered in the application of velocity based methods to finite deformation problems, the present stress based approach appears to be the more efficient of the two.

CHAPTER II

KINEMATICS

Kinematics is the study of deformations of bodies in space, without regard for the forces which cause them. Mathematically we represent natural space as a three dimensional Euclidean space E. Consider the motion of a body through space. The image of the body in E at the time t is the *configuration* C(t). As time passes, the configuration changes, and we say that the body *deforms*. In order to study aspects of deformations, we must be equipped to compare configurations assumed by the body at different times. We set out to equip ourselves thus. Let $\underline{X}$ be the position in E that was occupied by the material point X at the time τ, and let $\underline{x}$ be the position of that same material point at the present time t. To indicate the dependence of $\underline{x}$ upon $\underline{X}$, τ, and t, we write

$$\underline{x} = \underline{\chi}_\tau(\underline{X},t) \ . \tag{2.1}$$

The function $\underline{\chi}_\tau$ describes the deformation of the body relative to the configuration $C(\tau)$ by 'tracking' each material point from its position in $C(\tau)$. It is easily seen that at the time $t = \tau$

$$\underline{\chi}_\tau(\underline{X},t)\Big|_{t=\tau} = \underline{X} \ . \tag{2.2}$$

The gradient of $\underline{\chi}_\tau$ with respect to $\underline{X}$

$$\underset{\sim}{F}_\tau(\underline{X},t) = [\nabla_{\underline{X}}\underline{\chi}_\tau(\underline{X},t)]^T \qquad (2.3)^*$$

is called the deformation gradient, and J_τ is written for the determinant of $\underset{\sim}{F}_\tau$:

$$J_\tau(\underline{X},t) = \det \underset{\sim}{F}_\tau(\underline{X},t) \ . \qquad (2.4)$$

In view of (2.2), it is clear that

$$\underset{\sim}{F}_\tau(\underline{X},t)\Big|_{t=\tau} = \underset{\sim}{1} \qquad (2.5)$$

and

$$J_\tau(\underline{X},t)\Big|_{t=\tau} = +1 \ . \qquad (2.6)$$

The time derivative of $\underline{\chi}_\tau$ is the velocity function $\underline{v}_\tau$:

$$\underline{v}_\tau(\underline{X},t) = \frac{d}{dt}\,\underline{\chi}_\tau(\underline{X},t) \ . \qquad (2.7)$$

The spatial velocity distribution is obtained by putting $\underline{\chi}_\tau^{-1}(\underline{x},t)$ for $\underline{X}$ in (2.7):

---

*For an explanation of the special notations used in this work, see Appendix A.

$$\underset{\sim}{v}(\underset{\sim}{x},t) = \underset{\sim}{v}_\tau(\underset{\sim}{\chi}_\tau^{-1}(\underset{\sim}{x},t),t) \ . \tag{2.8}$$

It is clear that at the time $t = \tau$

$$\underset{\sim}{v}_\tau(\underset{\sim}{X},t)\Big|_{t=\tau} = \underset{\sim}{v}(\underset{\sim}{x},\tau) \ .$$

We caution the reader by pointing out that $\underset{\sim}{v}(\underset{\sim}{x},t)$ and $\underset{\sim}{v}_\tau(\underset{\sim}{X},t)$ are entirely different functions.

The velocity gradient $\underset{\sim}{L}$ is defined by

$$\underset{\sim}{L}(\underset{\sim}{x},t) = [\nabla \underset{\sim}{v}(\underset{\sim}{x},t)]^T \ , \tag{2.9}$$

and it is clear that when $t = \tau$,

$$\dot{\underset{\sim}{F}}_\tau(\underset{\sim}{X},t)\Big|_{t=\tau} = \underset{\sim}{L}(\underset{\sim}{x},\tau) \ .$$

The symmetric and skew-symmetric parts of $\underset{\sim}{L}$

$$\underset{\sim}{\varepsilon} = \tfrac{1}{2}(\underset{\sim}{L} + \underset{\sim}{L}^T) \tag{2.10}$$

and

$$\underset{\sim}{\omega} = \tfrac{1}{2}(\underset{\sim}{L} - \underset{\sim}{L}^T) \tag{2.11}$$

have the physical significance of *stretching* and *spin*, and are thus

named. The trace of $\underset{\sim}{L}$ has the physical significance of *dilitation*

$$\text{tr } \underset{\sim}{L} = \nabla \cdot \underline{v} \ . \tag{2.12}$$

The equation

$$\dot{J}_\tau = J_\tau (\nabla \cdot \underline{v}) \tag{2.13}$$

is called Euler's expansion formula* in fluid mechanics. In view of (2.6), when $t = \tau$,

$$\dot{J}_\tau (\underline{X}, t)\Big|_{t=\tau} = \nabla \cdot \underline{v}(\underline{x}, \tau) \ .$$

We shall frequently write $\dot{J}$ for $(\nabla \cdot \underline{v})$.

Of course not any tensor field $\underset{\sim}{L}$ is the gradient of a velocity field. The integrability condition (henceforth called *compatibility equation*) is

$$\nabla \times (\underset{\sim}{L}^T) = \underset{\sim}{0} \ . \tag{2.14}$$

The general solution of the partial differential equation (2.14) is

$$\underset{\sim}{L}^T = \nabla \underline{v}(\underline{x}, t) \ . \tag{2.15}$$

---

*Marris, lectures on fluid mechanics, Georgia Institute of Technology, Fall 1978.

Likewise, if $\underset{\sim}{\varepsilon}$ is a symmetric tensor field and $\underset{\sim}{\omega}$ is a skew-symmetric tensor field, and $(\underset{\sim}{\varepsilon} - \underset{\sim}{\omega})$ satisfies the compatibility equation

$$\nabla \times (\underset{\sim}{\varepsilon} - \underset{\sim}{\omega}) = \underset{\sim}{0} , \tag{2.16}$$

then there is a twice differentiable vector field $\underline{v}$ for which

$$\underset{\sim}{\varepsilon} = \tfrac{1}{2}(\nabla \underline{v}^{T} + \nabla \underline{v}) \tag{2.17}$$

and

$$\underset{\sim}{\omega} = \tfrac{1}{2}(\nabla \underline{v}^{T} - \nabla \underline{v}) . \tag{2.18}$$

CHAPTER III

DYNAMICS

Dynamics is "that branch of . . . mechanics which deals . . . with the action of forces on bodies in motion or at rest."* The fundamental laws of dynamics are called *balance of linear momentum* and *balance of angular momentum.* They are expressed by the equations

$$\frac{d}{dt}\underline{H} - \underline{F} = \underline{0} \tag{3.1}$$

and

$$\frac{d}{dt}\underline{L} - \underline{M} = \underline{0} \tag{3.2}$$

where $\underline{H}$ is the linear momentum of the body, $\underline{L}$ is the angular momentum, $\underline{F}$ is the aggregate force, and $\underline{M}$ is the aggregate moment. If no concentrated or distributed couples are present, and if the reference frame is inertial, then $\underline{H}$, $\underline{L}$, $\underline{F}$, and $\underline{M}$ are given in their classical forms by

$$\underline{H} = \int_V \underline{v}(\underline{x},t)\rho(\underline{x},t)\,dV \tag{3.3}$$**

American College Dictionary, Random House, 1970.

**V is the region in E occupied by the body at the present time.

$$\underline{L} = \int_V \underline{x} \times \underline{v}(\underline{x},t)\rho(\underline{x},t)dV \tag{3.4}$$

$$\underline{F} = \int_V \underline{b}(\underline{x},t)\rho(\underline{x},t)dV + \int_S \underline{T}\,dS \tag{3.5}*$$

$$\underline{M} = \int_V \underline{x} \times \underline{b}(\underline{x},t)\rho(\underline{x},t)dV + \int_S \underline{x} \times \underline{T}\,dS \tag{3.6}$$

where ρ is the spatial mass density, $\underline{b}$ is the spatial body force intensity, and $\underline{T}$ is the true traction acting on the surface of the body. We now introduce $\underline{X}_\tau(\underline{X},t)$ for $\underline{x}$ in (3.3) through (3.6), thus obtaining

$$\underline{H} = \int_{V_\tau} \underline{v}_\tau(\underline{X},t)\rho_\tau(\underline{X})dV \tag{3.7}**$$

$$\underline{L} = \int_{V_\tau} \underline{X}_\tau(\underline{X},t) \times \underline{v}_\tau(\underline{X},t)\rho_\tau(\underline{X})dV \tag{3.8}$$

$$\underline{F} = \int_{V_\tau} \underline{b}_\tau(\underline{X},t)\rho_\tau(\underline{X})dV + \int_{S_\tau} \underline{T}_\tau dS \tag{3.9}***$$

$$\underline{M} = \int_{V_\tau} \underline{X}_\tau(\underline{X},t) \times \underline{b}_\tau(\underline{X},t)\rho_\tau(\underline{X})dV + \int_{S_\tau} \underline{X}_\tau(\underline{X},t) \times \underline{T}_\tau dS. \tag{3.10}$$

---

*S is the surface of V.

**V_τ is the region in E occupied by the body at time τ.

***S_τ is the surface of V_τ.

The terms $\rho_\tau(\underline{X})$, $\underline{b}_\tau(\underline{X},t)$, and $\underline{T}_\tau$ are defined by

$$\rho_\tau(\underline{X}) = \rho(\underline{X},\tau)$$

$$\underline{b}_\tau(\underline{X},t) = \underline{b}(\underline{\chi}_\tau(\underline{X},t),t)$$

and

$$\underline{T}_\tau = \underline{T}(dS_t/dS_\tau) \ .$$

We shall consistently refer to $\underline{b}_\tau$ as the nominal body force and to $\underline{T}_\tau$ as the nominal traction. Inserting (3.7) through (3.10) into the dynamical equations (3.1) and (3.2), one may deduce by the usual arguments that

$$\underline{T}_\tau^+ + \underline{T}_\tau^- = \underline{0} \qquad (3.11)^*$$

$$\underline{T}_\tau = \underline{n}_\tau \cdot \underset{\sim}{t}_\tau \qquad (3.12)^{**}$$

$$\nabla_X \cdot \underset{\sim}{t}_\tau + \rho_\tau \underline{b}_\tau = \rho_\tau \dot{\underline{v}}_\tau \qquad (3.13)$$

$$\underset{\sim}{F}_\tau \cdot \underset{\sim}{t}_\tau - (\underset{\sim}{F}_\tau \cdot \underset{\sim}{t}_\tau)^T = \underset{\sim}{0} \qquad (3.14)$$

---

*the + and - indicates that the two tractions act on opposing sides of a surface with a well defined normal.

**$\underline{n}_\tau(\underline{X}) = \underline{n}(\underline{\chi},\tau)$

called traction reciprocity, the stress principle, and the local forms of linear momentum balance and angular momentum balance, respectively. The stress $\underset{\sim}{t}_\tau$ is called the nominal stress.* If the reference configuration and present configurations coincide ($t = \tau$), then it is easily seen that

$$\underset{\sim}{T}_\tau(\underset{\sim}{X},t)\Big|_{t=\tau} = \underset{\sim}{T}(\underset{\sim}{X},\tau)$$

and

$$\underset{\sim}{t}_\tau(\underset{\sim}{X},t)\Big|_{t=\tau} = \underset{\sim}{\tau}(\underset{\sim}{X},\tau) \ .$$

The familiar dynamic equations are thus recovered:

$$\underset{\sim}{T}^+ + \underset{\sim}{T}^- = \underset{\sim}{0} \tag{3.15}$$

$$\underset{\sim}{T} = \underset{\sim}{n} \cdot \underset{\sim}{\tau} \tag{3.16}$$

$$\nabla \cdot \underset{\sim}{\tau} + \rho \underset{\sim}{b} = \rho \dot{\underset{\sim}{v}} \tag{3.17}$$

$$\underset{\sim}{\tau} - \underset{\sim}{\tau}^T = \underset{\sim}{0} \tag{3.18}$$

---

*called the Lagrange stress by Prager [21], the First Piola-Kirchhoff stress by Truesdell and Noll [22]; other definitions result if $\underset{\sim}{T}_\tau = \underset{\sim}{t}_\tau \cdot \underset{\sim}{n}_\tau$ instead of (3.12).

where $\underset{\sim}{\tau}$ is the true stress.*

According to their definitions, the nominal tractions $\underset{\sim}{T}_\tau$ and $\underset{\sim}{T}_\zeta$ obey

$$\underset{\sim}{T}_\tau dS_\tau = \underset{\sim}{T}_\zeta dS_\zeta \ . \tag{3.19}$$

Using the stress principle (3.12) and the kinematical relation

$$\underset{\sim}{n}_\zeta dS_\zeta = J_\tau(\zeta)\underset{\sim}{n}_\tau \cdot \underset{\sim}{F}_\tau^{-1}(\zeta) dS_\tau \tag{3.20}$$

we obtain from (3.19) the relation between the nominal stresses $\underset{\sim}{t}_\tau$ and $\underset{\sim}{t}_\zeta$:

$$\underset{\sim}{t}_\tau(t) = J_\tau(\zeta)\underset{\sim}{F}_\tau^{-1}(\zeta) \cdot \underset{\sim}{t}_\zeta(t) \ . \tag{3.21}$$

When one of the configurations $C(\tau)$ or $C(\zeta)$ coincides with the present configuration, say $\zeta \to t$, then we obtain

$$\underset{\sim}{t}_\tau(t) = J_\tau(t)\underset{\sim}{F}_\tau^{-1}(t) \cdot \underset{\sim}{\tau}(t) \ , \tag{3.22}$$

relating the true stress $\underset{\sim}{\tau}$ to the nominal stress $\underset{\sim}{t}_\tau$. Of course, equations (3.19) through (3.22) are for application at a material point (as opposed to a spatial point).

---

*also called the Cauchy stress.

We now set (3.11) through (3.14) for traction rates and stress rates.* By stress rate we mean the actual time derivative of stress. This distinction is necessary because in some instances (not in this work) the word 'rate' is used interchangeably with the word 'increment.' In this work a superposed dot indicates a material derivative; that is, the time rate at a material point (as opposed to a spatial point).

The rate forms of (3.11) through (3.14) are found by ordinary differentiation. We thus obtain

$$\dot{\underline{T}}^{+}_{\tau} + \dot{\underline{T}}^{-}_{\tau} = \underline{0} \tag{3.23}$$

$$\dot{\underline{T}}_{\tau} = \underline{n}_{\tau} \cdot \dot{\underline{t}}_{\tau} \tag{3.24}$$

$$\nabla_{\chi} \cdot \dot{\underline{t}}_{\tau} + \rho_{\tau} \dot{\underline{b}}_{\tau} = \rho_{\tau} \ddot{\underline{v}}_{\tau} \tag{3.25}$$

$$(\dot{\underline{F}}_{\tau} \cdot \underline{t}_{\tau} + \underline{F}_{\tau} \cdot \dot{\underline{t}}_{\tau}) - (\dot{\underline{F}}_{\tau} \cdot \underline{t}_{\tau} + \underline{F}_{\tau} \cdot \dot{\underline{t}}_{\tau})^{T} = \underline{0} \ . \tag{3.26}$$

From equations (3.21) and (3.22) we obtain

$$\dot{\underline{t}}_{\tau} = J_{\tau} \underline{F}^{-1}_{\tau} \cdot \dot{\underline{t}} \tag{3.27}$$

---

*this discussion is unrelated to the controversy surrounding the definition of an 'appropriate stress rate' for constitutive theory.

and

$$\dot{\underset{\sim}{t}} = -(\underset{\sim}{\varepsilon} + \underset{\sim}{\omega}) \cdot \underset{\sim}{\tau} + \dot{J}\underset{\sim}{\tau} + \dot{\underset{\sim}{\tau}} \ . \tag{3.28}$$

For the stress rate $\dot{\underset{\sim}{t}}$, equations (3.23) through (3.26) become

$$\dot{\underline{T}}_t^+ + \dot{\underline{T}}_t^- = \underline{0} \tag{3.29}$$

$$\dot{\underline{T}}_t = \underline{n} \cdot \dot{\underset{\sim}{t}} \tag{3.30}$$

$$\nabla \cdot \dot{\underset{\sim}{t}} + \rho \dot{\underline{b}} = \rho \ddot{\underline{v}} \tag{3.31}$$

$$(\underset{\sim}{\varepsilon} + \underset{\sim}{\omega}) \cdot \underset{\sim}{\tau} + \dot{\underset{\sim}{t}} - \dot{\underset{\sim}{t}}^T - \underset{\sim}{\tau} \cdot (\underset{\sim}{\varepsilon} - \underset{\sim}{\omega}) = \underset{\sim}{0} \ . \tag{3.32}$$

Equation (3.27) will prove essential in the eventual integration of the stress rate. Equation (3.28) is important in the reformulation of the constitutive equations. It is clear that at the time $t = \tau$

$$\dot{\underset{\sim}{t}}_\tau(\underline{X},t)\Big|_{t=\tau} = \dot{\underset{\sim}{t}}(\underline{X},\tau) \ .$$

We now discuss the difference between the nominal traction rate $\dot{\underline{T}}_t$ and the true traction rate $\dot{\underline{T}}$. Differentiation of (3.16) yields

$$\dot{\underline{T}} = \dot{\underline{n}} \cdot \underset{\sim}{\tau} + \underline{n} \cdot \dot{\underset{\sim}{\tau}} \ . \tag{3.33}$$

The rate of change of the normal vector $\underline{n}$ is

$$\dot{\underline{n}} = \underline{n} \cdot [-(\underset{\sim}{\varepsilon} + \underset{\sim}{\omega}) + (\underline{n} \cdot \underset{\sim}{\varepsilon} \cdot \underline{n})\underset{\sim}{I}] \ . \tag{3.34}$$

Elimination of $\dot{\underline{n}}$ from (3.33) yields

$$\dot{\underline{T}} = \underline{n} \cdot [-(\underset{\sim}{\varepsilon} + \underset{\sim}{\omega}) \cdot \underset{\sim}{\tau} + (\underline{n} \cdot \underset{\sim}{\varepsilon} \cdot \underline{n})\underset{\sim}{\tau} + \dot{\underset{\sim}{\tau}}] \ . \tag{3.35}$$

From (3.28) $[-(\underset{\sim}{\varepsilon} + \underset{\sim}{\omega}) \cdot \underset{\sim}{\tau} + \dot{\underset{\sim}{\tau}}] = [\dot{\underset{\sim}{t}} - \dot{J}\underset{\sim}{\tau}]$, and since $\underline{n} \cdot \dot{\underset{\sim}{t}} = \dot{\underline{T}}_t$, and $\underline{n} \cdot \underset{\sim}{\tau} = \underline{T}$, we finally arrive at

$$\dot{\underline{T}} = \dot{\underline{T}}_t - (\dot{J} - \underline{n} \cdot \underset{\sim}{\varepsilon} \cdot \underline{n})\underline{T} \ , \tag{3.36}$$

Though (3.36) was arrived at by manipulation, its physical significance is easily found out. Consider a force $\underline{P}$ acting uniformly over a flat surface S of area A. Then the nominal traction rate $\dot{\underline{T}}_t$ is given by

$$\dot{\underline{T}}_t = (\dot{\underline{P}}/A) \ ,$$

and the true traction rate $\dot{\underline{T}}$ by

$$\dot{\underline{T}} = (\dot{\underline{P}}/A) - (\dot{A}/A)(\underline{P}/A) \ .$$

However, since $(\dot{\underline{P}}/A) = \dot{\underline{T}}_t$ and $(\underline{P}/A) = \underline{T}$, this last equation may be written as

$$\dot{\underline{T}} = \dot{\underline{T}}_t - (\dot{A}/A)\underline{T} \ .$$

Glancing back at (3.36), it is now clear that the difference between the true traction rate and the nominal traction rate is due to straining of the surface. In applications a hydrostatic pressure may be prescribed on a straining surface. In such a case the formula (3.36) must be used to relate the nominal traction rate to the true traction rate.

Some other practical information can be drawn from equation (3.36). Suppose part of the surface of a body is to be traction-free during a deformation; that is, $\underline{T}(t) = \underline{0}$. Then $\dot{\underline{T}}_t = \underline{0}$ is the appropriate boundary condition for the nominal traction rate. The boundary condition $\dot{\underline{T}}_t = \underline{0}$ and equation (3.36) yield

$$\dot{\underline{T}} + (\dot{J} - \underline{n} \cdot \underset{\sim}{\varepsilon} \cdot \underline{n})\underline{T} = \underline{0} \; ; \qquad \underline{T}(0) = \underline{0} \; . \tag{3.37}$$

This is an initial value problem for $\underline{T}(t)$. The solution is $\underline{T}(t) = \underline{0}$. However, in a numerical integration of the boundary value problem we should expect errors in $\underline{T}$ to be amplified or attenuated as the surface contracts or expands* (that is, as the coefficient of $\underline{T}$ above is negative or positive). This example is simple, yet suggestive of the types of problems associated with traction boundary conditions on surfaces which experience large strains.

For notational convenience we define the Kirchhoff stress $\underset{\sim}{\sigma}_\tau$ as

---

*the stability of solutions of the traction reciprocity equation (3.29) depends on the surface stretching in the same manner.

$$\underset{\sim}{\sigma}_{\tau} = J_{\tau}\underset{\sim}{\tau} \ . \tag{3.38}$$

It is clear that at the time $t = \tau$

$$\underset{\sim}{\sigma}_{\tau}(\underline{X},t)\Big|_{t=\tau} = \underset{\sim}{\tau}(\underline{X},\tau) \ . \tag{3.39}$$

The rate of the Kirchhoff stress is related to the rate of the true stress by

$$\dot{\underset{\sim}{\sigma}}_{\tau} = \dot{J}_{\tau}\underset{\sim}{\tau} + J_{\tau}\dot{\underset{\sim}{\tau}} \ , \tag{3.40}$$

and it is clear that when the reference configuration and present configuration coincide

$$\dot{\underset{\sim}{\sigma}} = \dot{J}\underset{\sim}{\tau} + \dot{\underset{\sim}{\tau}} \ . \tag{3.41}$$

From the last two equations and Euler's expansion formula we find the relation between $\dot{\underset{\sim}{\sigma}}_{\tau}$ and $\dot{\underset{\sim}{\sigma}}$ to be

$$\dot{\underset{\sim}{\sigma}}_{\tau} = J_{\tau}\dot{\underset{\sim}{\sigma}} \ , \tag{3.42}$$

and it is clear that when $t = \tau$

$$\dot{\underset{\sim}{\sigma}}_{\tau}(t)\Big|_{t=\tau} = \dot{\underset{\sim}{\sigma}}(\tau) \ . \tag{3.43}$$

The relationship between the Kirchhoff stress rate and the nominal stress rate may be drawn from (3.28) and (3.41) as

$$\dot{\underset{\sim}{t}} = -(\underset{\sim}{\varepsilon} + \underset{\sim}{\omega}) \cdot \underset{\sim}{\tau} + \dot{\underset{\sim}{\sigma}} \ . \tag{3.44}$$

This equation shall be used in the reformulation of the constitutive equations.

The final topic in this chapter is construction of the general solution of the linear momentum balance (3.25). That equation is of the form

$$D_1 f_1 + D_2 f_2 = 0 \tag{3.45}$$

where $D_1 = \nabla_{\chi^*}$, $D_2 = \frac{d}{dt}$, $f_1 = \dot{\underset{\sim}{t}}_\tau$, and $f_2 = \rho_\tau(\underset{\sim}{b}_\tau - \dot{\underset{\sim}{v}}_\tau)$. Just as for differentials in the plane, the general solution of (3.45) is (formally)

$$f_1 = D_2\phi + k_1 \ ; \qquad f_2 = -D_1\phi + k_2 \ ; \tag{3.46}$$

where ϕ is arbitrary and k_i is any function which satisfies

$$D_i k_i = 0 \qquad \text{(no sum)} \ .$$

It follows immediately that the general solution of the rate form of the linear momentum balance is

$$\dot{\underset{\sim}{t}}_\tau(\underline{X},t) = \frac{d}{dt}\,\underset{\sim}{\phi}_\tau(\underline{X},t) + \nabla_X \times \underset{\sim}{\Phi}_\tau(\underline{X},t) \tag{3.47}$$

$$\rho_\tau(\underline{X})(\underline{b}_\tau(\underline{X},t) - \dot{\underline{v}}_\tau(\underline{X},t)) = -\nabla_X \cdot \underset{\sim}{\phi}_\tau(\underline{X},t) + \underline{\gamma}_\tau(\underline{X}) \tag{3.48}$$

where $\underset{\sim}{\phi}_\tau$, $\underset{\sim}{\Phi}_\tau$, and $\underline{\gamma}_\tau$ are arbitrary functions of the indicated arguments.

From our experience with natural bodies, we often expect a gradually applied statically balanced load to produce a 'gradual' deformation of a solid body. The obvious counterexamples are snap-through phenomena, but it is the very failure of the gradually applied load to produce a gradual deformation which leads us to call such behavior 'unstable.' The general mathematical model for the motion and deformation of bodies is not so well understood that one can ascertain the stability of the motion of a body (subjected to gradually applied loads) without actually determining that motion and 'inspecting' it. Of course this is not practical, so it has become common to anticipate stability (for gradually applied loads).

If we assume that, for sufficiently gradual application of loads, the ensuing motion of a body is stable, then it is reasonable to ignore the inertial terms $\dot{\underline{H}}$ and $\dot{\underline{L}}$ in the dynamical principles (3.1) and (3.2). This is known as the quasistatic assumption (or less accurately, the quasistatic approximation). In such a case the general solution of the linear momentum balance may be simplified.* We write $\dot{\underset{\sim}{t}}$ as the sum of a homogeneous and a particular solution

*only the quasistatic solution of (3.31) is recorded here.

$$\dot{\underset{\sim}{t}} = \dot{\underset{\sim}{t}}^{o} + \dot{\underset{\sim}{t}}^{b} \tag{3.49}$$

where $\dot{\underset{\sim}{t}}^{o}$ is the solution of the homogeneous equation $\nabla \cdot \underset{\sim}{t} = \underline{0}$,

$$\dot{\underset{\sim}{t}}^{o}(\underline{x},t) = \nabla \times \underset{\sim}{\Phi}(\underline{x},t) \tag{3.50}$$

and $\dot{\underset{\sim}{t}}^{b}$ is any particular solution of

$$\nabla \cdot \underset{\sim}{t}^{b}(\underline{x},t) = -\rho(\underline{x},t)\left[\frac{\partial}{\partial t}\underline{b}(\underline{x},t) + \underline{v}(\underline{x},t) \cdot \nabla \underline{b}(\underline{x},t)\right] . \tag{3.51}$$

A particular solution $\dot{\underset{\sim}{t}}^{b}$ may be constructed in cartesian coordinates using indefinite integrals

$$t^{b}_{ij} = -\delta_{ij} \int \left\{ \rho \left[\frac{\partial}{\partial t} b_i + \underline{v} \cdot \nabla b_i \right] \right\} dx_i \quad \text{(no sum)} . \tag{3.52}$$

Notice that $\dot{\underset{\sim}{t}}^{b}$ will depend upon $\underline{v}$ unless $\underline{v} \cdot \nabla \underline{b} = \underline{0}$. If the only body force is due to gravity then one sets $\nabla \underline{b} = \underline{0}$. However, if D'Alembert's principle is used, then $\dot{\underset{\sim}{t}}^{b}$ will depend upon $\underline{v} \cdot \nabla \dot{\underline{v}}$.*

The angular momentum balance for $\dot{\underset{\sim}{t}}$ (3.32) involves the stretching and spin, as well as $\dot{\underset{\sim}{t}}$. For this reason we cannot form the general solution of that equation by judicious choice of stress functions, as may be done in the case of the true stress. The function $\underset{\sim}{\Phi}$ is therefore called a first order stress function.

---

*In a steadily spinning disk $\underline{v} \cdot \nabla \dot{\underline{v}} = \underline{0}$, since the radial velocity vanishes and the acceleration is entirely radial.

CHAPTER IV

CONSTITUTIVE EQUATIONS

Introduction

A material is characterized by its response to loads and deformations. The mathematical model for the load-response behavior of a material is called its constitutive equation. A constitutive equation of the form

$$\underset{\sim}{L} = \underset{\sim}{B}(\overset{\bullet}{\underset{\sim}{t}}, \underset{\sim}{\tau}) \tag{4.1}$$

would enable us to set a boundary value problem involving the stress rate $\overset{\bullet}{\underset{\sim}{t}}$ alone.* The possibility of finding such a constitutive equation is now discussed. Consider a deformation for which $\underset{\sim}{L}$, $\overset{\bullet}{\underset{\sim}{t}}$, and $\underset{\sim}{\tau}$ are the observed velocity gradient, nominal stress rate, and true stress. If a rigid motion

$$\underset{\sim}{x}' = \underset{\sim}{Q}(t) \cdot (\underset{\sim}{x} - \underset{\sim}{x}_o) + \underset{\sim}{x}_1(t) \tag{4.2}$$

is superposed upon this deformation, then the apparent velocity gradient, nominal stress rate, and true stress are $\underset{\sim}{L}'$, $\overset{\bullet}{\underset{\sim}{t}}'$, and $\underset{\sim}{\tau}'$

*this form has appeared in the literature; see Hill [23].

(distinguished by a prime). The tensors $\underset{\sim}{L}'$, $\dot{\underset{\sim}{t}}'$, and $\underset{\sim}{\tau}'$ are related to the tensors $\underset{\sim}{L}$, $\dot{\underset{\sim}{t}}$, and $\underset{\sim}{\tau}$ by the formulas

$$\underset{\sim}{L}' = \underset{\sim}{Q} \cdot \underset{\sim}{L} \cdot \underset{\sim}{Q}^T + \dot{\underset{\sim}{Q}} \cdot \underset{\sim}{Q}^T \tag{4.3}$$

$$\dot{\underset{\sim}{t}}' = \underset{\sim}{Q} \cdot \dot{\underset{\sim}{t}} \cdot \underset{\sim}{Q}^T + \underset{\sim}{Q} \cdot \underset{\sim}{\tau} \cdot \dot{\underset{\sim}{Q}}^T \tag{4.4}$$

$$\underset{\sim}{\tau}' = \underset{\sim}{Q} \cdot \underset{\sim}{\tau} \cdot \underset{\sim}{Q}^T \, . \tag{4.5}$$

The principle of material frame indifference states that the mechanical behavior of the material is indifferent to rigid motions such as (4.2). Therefore, the constitutive function $\underset{\sim}{B}$ must satisfy

$$\underset{\sim}{L}' = \underset{\sim}{B}(\dot{\underset{\sim}{t}}', \underset{\sim}{\tau}') \tag{4.6}$$

for the same function $\underset{\sim}{B}$. To establish whether or not $\underset{\sim}{B}$ satisfies frame indifference, we use (4.3) through (4.5) to eliminate the primed quantities from (4.6), thus obtaining

$$\underset{\sim}{Q} \cdot \underset{\sim}{B}(\dot{\underset{\sim}{t}}, \underset{\sim}{\tau}) \cdot \underset{\sim}{Q}^T + \dot{\underset{\sim}{Q}} \cdot \underset{\sim}{Q}^T = \underset{\sim}{B}(\underset{\sim}{Q} \cdot \dot{\underset{\sim}{t}} \cdot \underset{\sim}{Q}^T + \underset{\sim}{Q} \cdot \underset{\sim}{\tau} \cdot \dot{\underset{\sim}{Q}}^T, \underset{\sim}{Q} \cdot \underset{\sim}{\tau} \cdot \underset{\sim}{Q}^T), \tag{4.7}$$

which must be satisfied by all orthogonal $\underset{\sim}{Q}$ and all skew symmetric $\dot{\underset{\sim}{Q}} \cdot \underset{\sim}{Q}^T$ at every moment of time. In particular, it must be satisfied when

$$\underset{\sim}{Q} = \underset{\sim}{1} \; ; \qquad \dot{\underset{\sim}{Q}} = -\dot{\underset{\sim}{Q}}^{T} . \tag{4.8}$$

Then (4.7) serves to restrict the form of $\underset{\sim}{B}$:

$$\underset{\sim}{B}(\dot{\underset{\sim}{t}},\underset{\sim}{\tau}) = \underset{\sim}{B}(\dot{\underset{\sim}{t}} + \underset{\sim}{\tau} \cdot \dot{\underset{\sim}{Q}}^{T},\underset{\sim}{\tau}) - \dot{\underset{\sim}{Q}} \tag{4.9}$$

for arbitrary skew symmetric $\dot{\underset{\sim}{Q}}$. The right hand side of (4.9) depends upon $\dot{\underset{\sim}{Q}}$ but the left does not. Thus (4.9) can be satisfied (for arbitrary $\dot{\underset{\sim}{Q}}$) only if $\dot{\underset{\sim}{Q}}$ cancels out on the right hand side of (4.9). This is not possible in general; that is, no functional form for $\underset{\sim}{B}$ assures that $\dot{\underset{\sim}{Q}}$ cancels.*

This difficulty may be overcome by postulating a new constitutive function $\underset{\sim}{B}$ which depends not only upon $\dot{\underset{\sim}{t}}$ and $\underset{\sim}{\tau}$, but also upon $\underset{\sim}{\omega}$.** Then we easily replace (4.9) by

$$\underset{\sim}{B}(\dot{\underset{\sim}{t}},\underset{\sim}{\tau},\underset{\sim}{\omega}) = \underset{\sim}{B}(\dot{\underset{\sim}{t}} + \underset{\sim}{\tau} \cdot \dot{\underset{\sim}{Q}}^{T},\underset{\sim}{\tau},\underset{\sim}{\omega} + \dot{\underset{\sim}{Q}}) - \dot{\underset{\sim}{Q}} \; , \tag{4.10}$$

to be satisfied for arbitrary skew symmetric $\dot{\underset{\sim}{Q}}$. Again, this is only possible if $\dot{\underset{\sim}{Q}}$ cancels out on the right hand side. Therefore $\underset{\sim}{B}$ must be of the form

$$\underset{\sim}{B}(\underset{\sim}{a},\underset{\sim}{b},\underset{\sim}{c}) = \underset{\sim}{F}(\underset{\sim}{a} + \underset{\sim}{b} \cdot \underset{\sim}{c},\underset{\sim}{b}) + \underset{\sim}{c} \; ; \tag{4.11}$$

---

*further light is shed on this problem by Ogden [24].

**or for that matter, any tensor $\underset{\sim}{T}$ which transforms by the rule $\underset{\sim}{T}' = \underset{\sim}{Q} \cdot \underset{\sim}{T} \cdot \underset{\sim}{Q}^{T} + \dot{\underset{\sim}{Q}} \cdot \underset{\sim}{Q}^{T}$.

in other words,

$$\underset{\sim}{L} = \underset{\sim}{\mathcal{F}}(\dot{\underset{\sim}{t}} + \underset{\sim}{\tau} \cdot \underset{\sim}{\omega}, \underset{\sim}{\tau}) + \underset{\sim}{\omega} \ . \tag{4.12}$$

Defining a stress rate $\dot{\underset{\sim}{p}}$ as

$$\dot{\underset{\sim}{p}} = \dot{\underset{\sim}{t}} + \underset{\sim}{\tau} \cdot \underset{\sim}{\omega} \tag{4.13}$$

and recalling that $\underset{\sim}{L} - \underset{\sim}{\omega} = \underset{\sim}{\varepsilon}$, we replace (4.12) by

$$\underset{\sim}{\varepsilon} = \underset{\sim}{\mathcal{F}}(\dot{\underset{\sim}{p}}, \underset{\sim}{\tau}) \ . \tag{4.14}$$

The stress rate $\dot{\underset{\sim}{p}}$ is called the Luré stress rate in this work * Frame indifference requires that $\underset{\sim}{\mathcal{F}}$ satisfy, for all orthogonal $\underset{\sim}{Q}$,

$$\underset{\sim}{Q} \cdot \underset{\sim}{\mathcal{F}}(\dot{\underset{\sim}{p}}, \underset{\sim}{\tau}) \cdot \underset{\sim}{Q}^T = \underset{\sim}{\mathcal{F}}(\underset{\sim}{Q} \cdot \dot{\underset{\sim}{p}} \cdot \underset{\sim}{Q}^T, \underset{\sim}{Q} \cdot \underset{\sim}{\tau} \cdot \underset{\sim}{Q}^T) \ . \tag{4.15}$$

A tensor function possessing this property is called isotropic. From the theory of matrix polynomials [25], we know that if $\underset{\sim}{\mathcal{F}}$ is a symmetric isotropic function, at most affine** with respect to $\dot{\underset{\sim}{p}}$, then $\underset{\sim}{\mathcal{F}}$

---

*$\dot{p}$ has the physical significance of a 'corotational nominal stress; $\tilde{T}$t has been used by Wunderlich and Obrecht [9] for beams.

**an affine function is composed of linear and inhomogeneous parts; for example, if $f(x) = ax + b$, then f is affine w.r.t. x so long as a and b are independent of x.

may be represented as a linear combination of the six tensors

$$\underset{\sim}{I} \qquad \underset{\sim}{\tau}' \qquad \underset{\sim}{s}$$

$$\dot{\underset{\sim}{r}} \qquad \tfrac{1}{2}(\dot{\underset{\sim}{r}} \cdot \underset{\sim}{\tau}' + \underset{\sim}{\tau}' \cdot \dot{\underset{\sim}{r}}) \qquad \tfrac{1}{2}(\dot{\underset{\sim}{r}} \cdot \underset{\sim}{s} + \underset{\sim}{s} \cdot \dot{\underset{\sim}{r}}) \ ,$$

where $\dot{\underset{\sim}{r}} = \frac{1}{2}(\dot{\underset{\sim}{p}} + \dot{\underset{\sim}{p}}^{T})$ and $\underset{\sim}{s} = \underset{\sim}{\tau}' \cdot \underset{\sim}{\tau}'$. However a more useful representation of $\underset{\sim}{F}$ can be found which depends upon the traditional form of the constitutive equation. Thus, we defer further discussion of $\underset{\sim}{F}$ until after the traditional form has been presented.

Traditionally one assumes a constitutive equation of the form

$$\dot{\underset{\sim}{\sigma}} = \underset{\sim}{E}(\underset{\sim}{\varepsilon}, \underset{\sim}{\omega}, \underset{\sim}{\tau}) \ . \tag{4.16}$$

It is a simple application of the frame indifference principle to show that $\underset{\sim}{E}$ must be of the form

$$\underset{\sim}{E}(\underset{\sim}{a}, \underset{\sim}{b}, \underset{\sim}{c}) = \underset{\sim}{\mathcal{L}}(\underset{\sim}{a}, \underset{\sim}{c}) + \underset{\sim}{b} \cdot \underset{\sim}{c} - \underset{\sim}{c} \cdot \underset{\sim}{b} \tag{4.17}$$

so we replace (4.16) by

$$\dot{\underset{\sim}{\sigma}} - \underset{\sim}{\omega} \cdot \underset{\sim}{\tau} + \underset{\sim}{\tau} \cdot \underset{\sim}{\omega} = \underset{\sim}{\mathcal{L}}(\underset{\sim}{\varepsilon}, \underset{\sim}{\tau}) \ , \tag{4.18}$$

where $\underset{\sim}{\mathcal{L}}$ is a symmetric isotropic function. For convenience we define

the *corotational stress rate* $\overset{\nabla}{\underset{\sim}{\sigma}}{}^{*}$ by

$$\overset{\nabla}{\underset{\sim}{\sigma}}{}^{*} = \dot{\underset{\sim}{\sigma}} - \underset{\sim}{\omega}\cdot\underset{\sim}{\tau} + \underset{\sim}{\tau}\cdot\underset{\sim}{\omega} \,. \qquad (4.19)^{*}$$

If $\underset{\sim}{\mathcal{L}}$ is at most affine with respect to $\underset{\sim}{\varepsilon}$, then the general form for (4.18) is

$$\overset{\nabla}{\underset{\sim}{\sigma}}{}^{*} = \underset{\sim}{\underset{\sim}{V}} : \underset{\sim}{\varepsilon} + \underset{\sim}{\Sigma} \qquad (4.20)$$

where the fourth order tensor $\underset{\sim}{\underset{\sim}{V}}$ and the second order symmetric tensor $\underset{\sim}{\Sigma}$ depend upon the stress. The components of $\underset{\sim}{\underset{\sim}{V}}$ and $\underset{\sim}{\Sigma}$, in cartesian coordinates may be set in the forms

$$\begin{aligned} V_{ijkl} = {} & \lambda^{11}(\delta_{ij}\delta_{kl}) + \lambda^{12}(\delta_{ij}\tau'_{kl}) + \lambda^{13}(\delta_{ij}s_{kl}) \\ & + \lambda^{21}(\tau'_{ij}\delta_{kl}) + \lambda^{22}(\tau'_{ij}\tau'_{kl}) + \lambda^{23}(\tau'_{ij}s_{kl}) \\ & + \lambda^{31}(s_{ij}\delta_{kl}) + \lambda^{32}(s_{ij}\tau'_{kl}) + \lambda^{33}(s_{ij}s_{kl}) \\ & + 2\mu^{1}(\delta_{ik}\delta_{jl}) + \mu^{2}(\delta_{ik}\tau'_{lj} + \tau'_{ik}\delta_{lj}) + \mu^{3}(\delta_{ik}s_{lj} + s_{ik}\delta_{lj}) \end{aligned} \qquad (4.21)$$

---

*the essential property of this stress rate, or any other stress rate described as 'corotational' in this work, is that it is absolutely insensitive to rigid spin of the body. In frames in which the spin vanishes, such stress rates always reduce to ordinary time derivatives of stress.

and

$$\Sigma_{ij} = \eta^1 \delta_{ij} + \eta^2 \tau'_{ij} + \eta^3 s_{ij} \ . \tag{4.22}$$

In (4.21) and (4.22) τ'_{ij} is the stress deviator, $s_{ij} = \tau'_{ik}\tau'_{kj}$, and λ^{ij}, μ^i, and η^i are functions of the invariants of $\underset{\sim}{\tau}$. If $\lambda^{ij} = \lambda^{ji}$ then $V_{ijkl} = V_{klij}$, and we describe $\underset{\approx}{V}$ as symmetric. Equations (4.20) through (4.22) include, as special cases, the theories of hypoelastic and hypoelastic/viscoplastic bodies, and with slight modification, plastic bodies. These shall be discussed individually at the end of this chapter.

We now construct from (4.20) a representation for $\underset{\sim}{\mathcal{F}}$ (4.14). Recalling from (3.44) that the nominal stress rate and the Kirchhoff stress rate are related as

$$\dot{\underset{\sim}{t}} = [\dot{\underset{\sim}{\sigma}} - (\underset{\sim}{\varepsilon} + \underset{\sim}{\omega}) \cdot \underset{\sim}{\tau}] \ ,$$

it is easily seen that the relationship between the Luré stress rate and the Kirchhoff stress rate is

$$\dot{\underset{\sim}{p}} = \dot{\underset{\sim}{t}} + \underset{\sim}{\tau} \cdot \underset{\sim}{\omega} = [\dot{\underset{\sim}{\sigma}} - (\underset{\sim}{\varepsilon} + \underset{\sim}{\omega}) \cdot \underset{\sim}{\tau}] + \underset{\sim}{\tau} \cdot \underset{\sim}{\omega} \ .$$

This yields, using the definition of the corotational stress rate,

$$\dot{\underset{\sim}{p}} = \dot{\underset{\sim}{\sigma}}^* - \underset{\sim}{\varepsilon} \cdot \underset{\sim}{\tau} \ . \tag{4.23}$$

The symmetric and skew symmetric parts of $\dot{\underset{\sim}{p}}$ are given by

$$\tfrac{1}{2}(\dot{\underset{\sim}{p}} + \dot{\underset{\sim}{p}}^T) = \dot{\underset{\sim}{\sigma}}^* - \tfrac{1}{2}(\underset{\sim}{\varepsilon} \cdot \underset{\sim}{\tau} + \underset{\sim}{\tau} \cdot \underset{\sim}{\varepsilon}) \tag{4.24}$$

and

$$\tfrac{1}{2}(\dot{\underset{\sim}{p}} - \dot{\underset{\sim}{p}}^T) = -\tfrac{1}{2}(\underset{\sim}{\varepsilon} \cdot \underset{\sim}{\tau} - \underset{\sim}{\tau} \cdot \underset{\sim}{\varepsilon}) \ . \tag{4.25}$$

According to angular momentum balance, the latter of these (4.25) must be an identity. Using (4.20) to eliminate $\dot{\underset{\sim}{\sigma}}^*$ from (4.24) yields

$$\dot{\underset{\sim}{r}} = \underset{\approx}{W} : \underset{\sim}{\varepsilon} + \underset{\sim}{\Sigma} \ , \tag{4.26}$$

where $\underset{\approx}{W}$ is defined by

$$W_{ijkl} = V_{ijkl} - \tfrac{1}{2}(\delta_{ik}\tau'_{lj} + \tau'_{ik}\delta_{lj}) - \frac{1}{3}\tau_{mm}(\delta_{ik}\delta_{lj}) \ . \tag{4.27}$$

Note that if $\underset{\approx}{V}$ is symmetric then $\underset{\approx}{W}$ is symmetric also.

The stress rate $\dot{\underset{\sim}{r}}$

$$\dot{\underset{\sim}{r}} = \tfrac{1}{2}(\dot{\underset{\sim}{p}} + \dot{\underset{\sim}{p}}^T) = \tfrac{1}{2}(\dot{\underset{\sim}{t}} + \underset{\sim}{\tau} \cdot \underset{\sim}{\omega} - \underset{\sim}{\omega} \cdot \underset{\sim}{\tau} + \dot{\underset{\sim}{t}}^T) \tag{4.28}$$

is called the symmetrized Luré stress rate in this work. It is the time rate of a symmetric nominal stress used recently by de Veubeke [26], and called by him the Jaumann stress. Since the corotational stress rate ($\dot{\underset{\sim}{\tau}}^*$) is often called the Zaremba-Jaumann rigid-body stress

rate, different from the rate of the stress used by de Veubeke ($\overset{\circ}{\underset{\sim}{\tau}}$), it would be likely to cause confusion if the name Jaumann were assigned to any stress rate in this work.*

If $\underset{\approx}{W}$ is invertible, then the constitutive equation (4.26) may be written

$$\underset{\sim}{\varepsilon} = \underset{\approx}{W}^{-1} : (\overset{\circ}{\underset{\sim}{\tau}} - \underset{\sim}{\Sigma}) \tag{4.29}$$

and we see that the function $\underset{\sim}{F}$ (4.14) corresponding to (4.20) is represented by

$$\underset{\sim}{F}(\overset{\circ}{\underset{\sim}{p}}, \underset{\sim}{\tau}) = \underset{\approx}{W}^{-1} : [\tfrac{1}{2}(\overset{\circ}{\underset{\sim}{p}} + \overset{\circ}{\underset{\sim}{p}}^{T}) - \underset{\sim}{\Sigma}], \tag{4.30}$$

where $\underset{\approx}{W}$ is defined by (4.27).

In applications one is usually given the constitutive equation in the traditional form (4.20), (4.21), and (4.22). To obtain the form (4.30), one must construct $\underset{\sim}{W}$ according to (4.27) and then invert $\underset{\approx}{W}$, if possible. This is a major undertaking from a computational point of view, for $\underset{\approx}{W}$ will generally be different at each point of a stressed body, even when $\underset{\approx}{V}$ is constant. Therefore special attention is given to practical methods for construction of $\underset{\approx}{W}^{-1}$. For plane problems $\underset{\approx}{W}^{-1}$ can be found in closed form. For general problems in which $\underset{\approx}{V}^{-1}$ is known a truncated power series for $\underset{\approx}{W}^{-1}$ is often of acceptable accuracy. The details of these two special cases are discussed in Appendix B.

*see Atluri [15].

Hypoelastic Bodies

If $\underset{\sim}{\Sigma} = \underset{\sim}{0}$ in equation (4.20), and the coefficients λ^{ij} and μ^{i} are analytic functions of the stress invariants, at least in some open region of stress space (containing the origin), then the body is said to behave hypoelastically in that region [26]. No relaxation phenomena will be exhibited by the body so long as $\underset{\sim}{\Sigma} = \underset{\sim}{0}$. The state of stress at a material point will depend upon the deformation history, but not upon the speed of the deformation. This makes it possible for us to use any monotonically increasing parameter, such as a characteristic displacement, in place of natural time when studying the deformations of hypoelastic bodies.

The first approximation to the behavior of any hypoelastic body for small deformations from the stress-free state is obtained by setting $\underset{\sim}{\tau} = \underset{\sim}{0}$ in (4.21). Then $\underset{\approx}{V}$ may be written as

$$V_{ijkl} = \lambda(\delta_{ij}\delta_{kl}) + 2\mu(\delta_{ik}\delta_{lj}) \ , \tag{4.31}$$

where λ (Lame's constant) and μ (the shear modulus) are defined

$$\lambda = \lambda^{11}\Big|_{\underset{\sim}{\tau}=\underset{\sim}{0}} \qquad \mu = \mu^{1}\Big|_{\underset{\sim}{\tau}=\underset{\sim}{0}} \ .$$

Referring to (4.27), we construct $\underset{\approx}{W}$ as

$$W_{ijkl} = \lambda(\delta_{ij}\delta_{kl}) + (2\mu - \tfrac{1}{3}\tau_{mm})(\delta_{ik}\delta_{lj}) \tag{4.32}$$

$$- \tfrac{1}{2}(\delta_{ik}\tau'_{lj} + \tau'_{ik}\delta_{lj}) \ .$$

The constitutive equation given by (4.31) must be regarded as the simplest possible model of solid behavior. It is doubtful that any real material behaves as predicted by (4.31) when deformations are finite. Its popularity stems not only from its simplicity, but from the success it has enjoyed in infinitesimal strain theories, and the lack of physical data needed to use more sophisticated models. Nevertheless, there is a point beyond which any semblance of real material behavior vanishes from (4.31). Consider rectilinear shearing from a stress-free state:

$$v^1 = kx^2 \; ; \qquad v^2 = v^3 = 0 \; ; \qquad \underset{\sim}{\tau}\Big|_{t=0} = \underset{\sim}{0} \; .$$

The constitutive equation (4.31) predicts the following stresses [27]:

$$\tau_{12} = \mu \sin(kt) \; ; \qquad \tau_{11} = -\tau_{22} = \mu(1 - \cos(kt)) \; .$$

Until the time that $kt = \frac{1}{2}\pi$, the shear stress τ_{12} increases. After that time τ_{12} decreases, even though the shear strain continues to increase. In this particular problem we may take (kt) to be a measure of the strain; beyond the strain $kt = \frac{1}{2}\pi$, (4.31) fails to provide an acceptable model of any material's behavior.

The rectilinear shearing example above is such a simple deformation that we were able to rely on intuition alone in deciding the limit of applicability of the equation (4.31). For more complicated deformations (and/or more complicated materials) our intuition

is not so strong. The notion of 'realistic material behavior' needs to be set down in a form which (minimally) allows us to distinguish between 'realistic' and 'unrealistic' deformation processes. This is the role played by thermodynamics in modern continuum mechanics [28].

Yield Surfaces

It is well known that metals exhibit behavior which is more or less elastic so long as strains are small. In other words, when moderate loads are imposed, then removed, the elastic body returns to its original shape. If more severe loads are applied to the body, then removed, some permanent distortion of the material may occur. The mechanisms of inelastic behavior may become active very suddenly, as in mild steel, or only gradually, as for lead or copper [29]. In any case, one way of idealizing the transition is to introduce a *yield surface* to stress space, inside of which the mechanism of inelasticity is dormant, on or outside of which the mechanism is active. The yield surface may change during the deformation as dictated by the change in the yield behavior of the real material being modeled. After the initial yield of the material, the surface is usually called the loading surface.

The von Mises' yield criterion is the most common of those found in the engineering literature. The equation of von Mises' surface is expressed by either of

$$\left.\begin{aligned} &J_o\sqrt{\tfrac{3}{2}\, I'} - \sigma_e^{11}(k) = 0; \\ &J_o\sqrt{\tfrac{1}{2}\, I'} - \sigma_e^{12}(k) = 0\ ; \\ &(I' = \underset{\sim}{\tau}' : \underset{\sim}{\tau}') \end{aligned}\right\} \qquad (4.33)$$

where σ_e^{11} and σ_e^{12} are material functions called the effective uniaxial stress and effective shear stress, respectively. The parameter k is a monotonically increasing invariant of the local plastic deformation history. The function $\sigma_e^{11}(k)$ must be determined from uniaxial test data, and the function $\sigma_e^{12}(k)$ must be determined from plane stress or strain rectilinear shearing test data. The scalar J_o is the volumetric strain relative to the stress-free state. It must be included in the first of (4.33) because in uniaxial tests, the total load P and length l are measurable. The initial dimensions of the specimen are known, so the measurable stress is σ_o^{11}:

$$\sigma_o^{11} = J_o\tau^{11} = (Al/A_o l_o)(P/A) = P(l/A_o l_o)\ . \qquad (4.34)$$

Similar arguments may be given for inclusion of J_o in the second of (4.33). The usual Mises' criterion is recovered by dividing (4.33) through by J_o. In practice J_o would usually be expressed as a function of the mean stress:

$$J_o = (3\lambda + 2\mu)/(3\lambda + 2\mu - \underset{\sim}{\tau} : \underset{\sim}{1})\ . \qquad (4.35)$$

Of course σ_e^{11} and σ_e^{12} cannot be independent; in view of (4.33) they must be related as

$$\sigma_e^{11}(k) = \sqrt{3}\, \sigma_e^{12}(k) \ . \tag{4.36}$$

If physical data cannot be reconciled to this condition, then the body in question does not admit von Mises' representation of the loading surface.

One might suspect that von Mises' criterion is no more than an extreme idealization. However, according to Hill:*

> experimental data for mild steel . . . suggests that the yield locus changes over from a hexagon to a circle with progressive cold work. However, for other steels, and for copper and aluminum, von Mises' criterion appears to fit the data equally well no matter what degree of prestrain.

So, while it is indeed an idealization, its agreement with physical data for some metals is quite good. Nevertheless, the small differences may be important. According to Christoffersen and Hutchinson [31], who have proposed a class of 'corner theories' of plasticity,

> it is generally agreed that the simplest flow theory built upon the assumption of isotropic hardening using the Mises yield surface underestimates certain crucial plastic strain components in a non-proportional stress history such as encountered in buckling or necking.
>
> In contrast to a smooth yield surface characterization, a corner theory will most likely overestimate certain components of the plastic strain increments in the vicinity of an abrupt change from proportional loading.

*Hill [30], p. 24.

As a consequence, "calculations based on a flow theory with a smooth yield surface give necking-type bifurcations at strain levels which far exceed realistic values" [31], while calculations based on corner theory can be expected to provide conservative estimates of the bifurcation strain. Finally, according to Tvergaard et al. [32], who have presented a numerical study of flow localization in the plane tensile test,

> Analyses carried out within a theoretical framework . . . reveal that the classical elastic-plastic solid with a smooth yield surface is quite resistant to the localization of deformation into a shear band.

The resistance of the classical elastic-plastic body to intense local deformation may even be sensitive to the yield criterion's independence from the mean stress (such as that induced by a distribution of voids). Thus, the circumstances under which von Mises' criterion can be expected to provide reasonable results have not been resolved.

We observe that, as a rule, smooth deformations are found when a smooth yield criterion is used. This may be an over-simplification, but it is borne out by the weight of solved problems in the literature. Regarding finite elements, and the goals of the present work, this is important because we may be reasonably confident that intense local deformations, which would require a much finer finite element mesh than has been used, do not occur. In view of the discussions of Tvergaard et al. [32], it would seem less safe to make such an assumption if the most common alternative to von Mises' criterion, the Tresca 'maximum shear stress criterion,' were used, since that surface has vertices. In this work, von Mises' criterion is used exclusively.

The parameter k is usually chosen as either the 'plastic work' W^P or some variant of Odquist's 'plastic strain' q, defined by Kachanov [29] as

$$W^P = \int_0^t \underset{\sim}{\tau} : \underset{\sim}{\varepsilon}^P \, dt \; ; \qquad q_a = \int_0^t \sqrt{a\underset{\sim}{\varepsilon}^P : \underset{\sim}{\varepsilon}^P} \; dt \; . \tag{4.37}$$

Notice that both of these increase monotonically during plastic deformation. In uniaxial extension

$$\dot{W}^P = \tau^{11}\varepsilon^P_{11} \; ; \qquad \dot{q}_{\frac{2}{3}} = \sqrt{\tfrac{2}{3}\,\underset{\sim}{\varepsilon}^P : \underset{\sim}{\varepsilon}^P} = \varepsilon^P_{11} \; ;$$

or in rectilinear shear (plane strain)

$$\dot{W}^P = 2\tau^{12}\varepsilon^P_{12} \; ; \qquad \dot{q}_2 = \sqrt{2\underset{\sim}{\varepsilon}^P : \underset{\sim}{\varepsilon}^P} = 2\varepsilon^P_{12} \; .$$

In any case we can find a functional dependence between W^P and q_a since

$$dW^P/dq_a = (\underset{\sim}{\tau} : \underset{\sim}{\varepsilon}^P)/(a\underset{\sim}{\varepsilon}^P : \underset{\sim}{\varepsilon}^P)^{\frac{1}{2}} > 0 \; ,$$

so the choice of parameter is largely a matter of convenience.

Hypoelastic/Plastic Bodies

We give a brief sketch of the theory of hypoelastic/plastic bodies. The reader is referred to Hill [30], Prager [33], and Kachanov [29] for extended treatments of the theory.

As was discussed in the main text of this chapter, the mechanical behavior of an isotropic body is completely known once material functions λ^{ij}, μ^i, and η^i are known (see equations 4.20 through 4.22). However, no series of physical tests can be devised that would determine these material functions completely. In the face of such indeterminancy, it is customary to choose λ^{ij}, μ^i, and η^i which produce the simplest constitutive equation capable of explaining the behavior which has been observed.* The classical theory of plasticity for polycrystalline metals is just such a theory.

Suppose the plastic stretching $\underset{\sim}{\varepsilon}^P$ depends upon the stress and stress rate as

$$\underset{\sim}{\varepsilon}^P = \underset{\approx}{V}' : \overset{\circ}{\underset{\sim}{\sigma}}^* + \underset{\sim}{\Sigma}'$$

where $\underset{\approx}{V}'$ and $\underset{\sim}{\Sigma}'$ are of the *forms* (4.21) and (4.22). Then from the apparent absence of relaxation phenomena, at least for quasistatic cold-working of the material, one concludes that $\underset{\sim}{\Sigma}'$ must vanish. The physically observed incompressibility of plastic deformation places the following restriction on $\underset{\approx}{V}'$:

$$\underset{\sim}{I} : \underset{\approx}{V}' = \underset{\sim}{0} \ . \qquad (4.38)$$

*It is entirely possible that (4.20)-(4.22) and the physical data cannot be reconciled; in such a case one must discard (4.20)-(4.22).

From a series of uniaxial tests in which the Kirchhoff stress σ_o^{11} is found as a function of the logarithmic strain

$$\int_0^t \varepsilon_{11} dt = \ln(l/l_o)$$

we establish the following relation between $\dot{\sigma}_o^{11}$ and ε_{11}:

$$\left.\begin{aligned} \dot{\sigma}_o^{11}/\varepsilon_{11} &= \{J_o E_t(k)\} \quad \text{when} \quad \sigma_o^{11} = \sigma_e^{11}(k) \\ &\qquad\qquad \text{and} \quad \sigma_o^{11}\varepsilon_{11} > 0 \\ \dot{\sigma}_o^{11}/\varepsilon_{11} &= \{J_o E(k)\} \quad \text{otherwise} \end{aligned}\right\} \tag{4.39}$$

which is used to further restrict $\underset{\approx}{V}'$. The material functions in the general representation for $\underset{\approx}{V}'$ cannot be determined uniquely from the restrictions (4.38) and (4.39). However, a very simple solution may be found as follows: we assume that

$$\underset{\sim}{V}' = \Lambda^{22}\underset{\sim}{\tau}'\underset{\sim}{\tau}' \ . \tag{4.40}$$

This form satisfies (4.38). Now we define Λ^{22} so that (4.39) is satisfied. The plastic stretching is given by

$$\Lambda^{22}\underset{\sim}{\tau}'(\underset{\sim}{\tau}' : \overset{\circ}{\underset{\sim}{\sigma}}{}^{*}) = \underset{\sim}{\varepsilon}^{P} \ . \tag{4.41}$$

The scalar product $\underset{\sim}{\tau}' : \underset{\sim}{\varepsilon}^{P}$ is therefore

$$\Lambda^{22}(\underset{\sim}{\tau}' : \underset{\sim}{\tau}')(\underset{\sim}{\tau}' : \dot{\underset{\sim}{\sigma}}^*) = \underset{\sim}{\tau}' : \underset{\sim}{\varepsilon}^P \ .$$

Putting $I' = (\underset{\sim}{\tau}' : \underset{\sim}{\tau}')$, $I'_\tau = J_\tau^2 I'$, and $W^P = \underset{\sim}{\tau} : \underset{\sim}{\varepsilon}^P$, from this last equation we find that

$$\Lambda^{22} = (2/I')(dW^P/dI'_t) \ . \tag{4.42}$$

The function (dW^P/dI'_t) may be determined from the uniaxial test data (4.39) as follows:

$$dW^P = \tau^{11}\varepsilon^P_{11}dt \ ; \qquad dI'_t = \frac{4}{3}\tau^{11}\dot{\sigma}^{11}dt \ ;$$

so

$$(dW^P/dI'_t) = \frac{3}{4}(\varepsilon^P_{11}/\dot{\sigma}^{11}) \ . \tag{4.43}$$

Recalling that $\dot{\underset{\sim}{\sigma}}_o = J_o\dot{\underset{\sim}{\sigma}}$, we get from the test data

$$(\varepsilon^P_{11}/\dot{\sigma}^{11}) = J_o[(\dot{\varepsilon} - \dot{\varepsilon}^e)/\dot{\sigma}^{11}_o] = [\{E_t(k)\}^{-1} - \{E(k)\}^{-1}]$$

$$\equiv (1/h) \ . \tag{4.44}$$

On replacing σ^{11}_o by $J_o\sqrt{\frac{3}{2}I'}$, and recalling (4.42) and (4.43), we finally obtain Λ^{22} as

$$\Lambda^{22} = \left(\frac{3}{2}\, \underset{\sim}{\tau}' : \underset{\sim}{\tau}'\right)^{-1} \left(\frac{9}{4}\right)\left[\{E_t(k)\}^{-1} - \{E(k)\}^{-1}\right] \quad \text{for loading}$$

$$\left(\text{if } J_o\sqrt{\frac{3}{2}\, \underset{\sim}{\tau}' : \underset{\sim}{\tau}'} = \sigma_e^{11}(k) \text{ and } \underset{\sim}{\tau} : \underset{\sim}{\varepsilon} \geq 0\right)$$

$$= 0 \qquad \text{otherwise} \tag{4.45}$$

or, in terms of the function h, defined in (4.44) above,

$$\Lambda^{22} = \left(\frac{3}{2}\, \underset{\sim}{\tau}' : \underset{\sim}{\tau}' h\right)^{-1} \left(\frac{9}{4}\right) \qquad \text{for loading} \tag{4.46}$$

$$= 0 \qquad \text{otherwise.}$$

Values of the function $E_t(\cdot)$ are called the tangent modulus. Values of $E(\cdot)$ are the instantaneous Young's modulus. The function Λ^{22} is multivalued on the loading surface; this is the sole source of nonlinearity in plasticity theory. If the dependence of Λ^{22} upon $\dot{k}$ were removed then Λ^{22} would be single valued on the yield surface. The resulting hypothetical material is encountered in the context of uniqueness theory, and is called the 'linear comparison solid' there.

The complete constitutive equation is obtained when we consider the total stretching* to be the sum of elastic and plastic parts:

$$\underset{\sim}{\varepsilon} = \underset{\sim}{\varepsilon}^e + \underset{\sim}{\varepsilon}^p = \underset{\approx}{V}^{-1} : \overset{\circ}{\underset{\sim}{\sigma}}^* \tag{4.47}$$

$$V^{-1}_{ijkl} = \left(\frac{1+\nu}{E}\right)(\delta_{ik}\delta_{lj}) - \frac{\nu}{E}(\delta_{ij}\delta_{kl}) + \Lambda^{22}\tau'_{ij}\tau'_{kl} \ .$$

*i.e., the symmetric part of the velocity gradient.

Notice that $\underset{\approx}{V}^{-1}$ thus defined is symmetric; that is

$$V^{-1}_{ijkl} = V^{-1}_{klij} .$$

Since Λ^{22} is multivalued on the yield surface (4.47) is not linear. We note the agreement between the present equations and those of McMeeking and Rice [34].

Hypoelastic/Viscoplastic Bodies

The theory of viscoplasticity is similar to classical plasticity theory in the sense that it provides the simplest constitutive equation capable of explaining the uniaxial test data of certain materials. The difference is that the materials being modeled exhibit creep and relaxation. The viscoplastic model common in the literature is compatible with

isotropic yield behavior

plastic incompressibility

uniaxial creep and relaxation tests.

The representation of the viscoplastic stretching $\underset{\sim}{\varepsilon}^{vp}$ found in the monograph of Perzyna [35] is of the form

$$\underset{\sim}{\varepsilon}^{vp} = \gamma \underset{\sim}{\tau}' \tag{4.48}$$

where γ is a function of the stress invariants and perhaps the deformation history. It may be determined from uniaxial test data in basically the same manner as Λ^{22} was determined for a plastic body.

Suppose that from uniaxial tests we establish

$$\left.\begin{aligned} \varepsilon_{11}^{vp} &= \phi(\sigma_o^{11},k) \qquad \text{when} \quad \sigma_o^{11} \geq \sigma_e^{11}(k) \\ &= 0 \qquad\qquad\quad \text{otherwise.} \end{aligned}\right\} \tag{4.49}$$

For uniaxial tests, the general equation (4.48) reduces to

$$\varepsilon_{11}^{vp} = \frac{2}{3}\gamma\sigma_o^{11}/J_o \qquad \text{when} \quad \sigma_o^{11} \geq \sigma_e^{11}(k) \ . \tag{4.50}$$

Using the result of the uniaxial tests, we find γ as

$$\left.\begin{aligned} \gamma &= \frac{3}{2} J_o \frac{\varepsilon_{11}^{vp}}{\sigma_o^{11}} = \frac{3}{2} J_o \phi(\sigma^{11}{}_o,k)/\sigma_o^{11} \quad \text{when } \sigma_o^{11} \geq \sigma_e^{11}(k) \\ &= 0 \qquad \text{otherwise .} \end{aligned}\right\} \tag{4.51}$$

The complete constitutive equation is obtained when we consider the total stretching to be the sum of elastic and viscoplastic parts:

$$\underset{\sim}{\varepsilon} = \underset{\sim}{\varepsilon}^{e} + \underset{\sim}{\varepsilon}^{vp} = \underset{\approx}{V}^{-1} : \overset{\cdot}{\underset{\sim}{\sigma}}{}^{*} + \gamma\underset{\sim}{\tau}' \tag{4.52}$$

where

$$V_{ijkl}^{-1} = \left(\frac{1+\nu}{E}\right)(\delta_{ik}\delta_{lj}) - \frac{\nu}{E}(\delta_{ij}\delta_{kl}) \tag{4.53}$$

and γ is defined in (4.51). Notice that $\underset{\sim}{V}^{-1}$ is symmetric. Only this simple model of viscoplasticity is used in the examples accompanying this work.

CHAPTER V

BOUNDARY VALUE PROBLEMS

In the preceding sections we have treated kinematics, dynamics, and material behavior as distinct subjects. We obtained equations of compatibility (2.16), linear momentum balance (3.31), angular momentum balance (3.32), and the constitutive equations (4.20) and (4.26). Presently we regard these equations as a system of coupled partial differential equations. It is worthy of special note that all of these equations are linear, with the exception of the constitutive equation in the case of a plastic body. For ease of reference we collect these equations below:

$$\nabla \times (\underset{\sim}{\varepsilon} - \underset{\sim}{\omega}) = \underline{0} \quad \text{in} \quad V ; \qquad \underline{s} \cdot (-\underset{\sim}{\varepsilon} + \underset{\sim}{\omega} + \nabla \underline{v}) = \underline{0} \ \text{on} \ S ; \tag{5.1}$$

$$\nabla \cdot \dot{\underset{\sim}{t}} + \rho \dot{\underline{b}} = \underline{0} \quad \text{in} \quad V ; \qquad \underline{n} \cdot \dot{\underset{\sim}{t}} = \dot{\underline{T}}_t \quad \text{on} \quad S ; \tag{5.2}$$

$$\tfrac{1}{2}[(\underset{\sim}{\varepsilon} + \underset{\sim}{\omega}) \cdot \underset{\sim}{\tau} + \dot{\underset{\sim}{t}} - \dot{\underset{\sim}{t}}^T - \underset{\sim}{\tau} \cdot (\underset{\sim}{\varepsilon} - \underset{\sim}{\omega})] = \underline{0} \quad \text{in} \quad V ; \tag{5.3}$$

$$\dot{\underset{\sim}{t}} = \underset{\approx}{V} : \underset{\sim}{\varepsilon} - \underset{\sim}{\varepsilon} \cdot \underset{\sim}{\tau} - \underset{\sim}{\tau} \cdot \underset{\sim}{\omega} + \underset{\sim}{\Sigma} ; \tag{5.4}$$

$$\dot{\underset{\sim}{\varepsilon}} = \underset{\approx}{W}^{-1} : [\tfrac{1}{2}(\dot{\underset{\sim}{t}} + \underset{\sim}{\tau} \cdot \underset{\sim}{\omega} - \underset{\sim}{\omega} \cdot \underset{\sim}{\tau} + \dot{\underset{\sim}{t}}^T) - \underset{\sim}{\Sigma}] ; \tag{5.5}$$

$$\underline{v} = \bar{\underline{v}} \quad \text{on} \quad S_v ; \tag{5.6}$$

$$\dot{\underline{T}}_t = \dot{\overline{\underline{T}}}_t \quad \text{on} \quad S_\sigma \, . \tag{5.7}$$

These equations have been discussed individually in the preceding chapters, with the exception of the second of (5.1), and (5.4). The constitutive equation (5.4) follows directly from (4.20) and

$$\dot{\underline{t}} = \dot{\underline{\sigma}}^* - \underline{\varepsilon} \cdot \underline{\tau} - \underline{\tau} \cdot \underline{\omega} \, .$$

In the second of (5.1) $\underline{s}$ is an arbitrary surface tangent; the equation is essentially a counterpart to the stress principle, as it relates the (two-dimensional) surface-velocity gradient to the (three-dimensional) velocity gradient. We shall imply only symmetric tensors by writing

$$\underline{\varepsilon}: \quad \underline{\varepsilon} - \underline{\varepsilon}^T = \underline{0} \tag{5.8}$$

and only skew symmetric tensors by writing

$$\underline{\omega}: \quad \underline{\omega} + \underline{\omega}^T = \underline{0} \, . \tag{5.9}$$

This is rather trivial, but nonetheless necessary to complete the system of equations (5.1) through (5.7). For the sake of clarity we shall often refer to (5.1) as 'compatibility,' (5.2) and 'LMB' (linear momentum balance), (5.3) as 'AMB' (angular momentum balance), (5.6) as 'VBC' (velocity boundary condition), and (5.7) as 'TBC' (traction boundary condition). We call the system of equations (5.1) through

(5.9) 'the general boundary value problem.'

As discussed, the general solutions of compatibility (5.1) and LMB (5.2) are given by

$$\left.\begin{aligned} \underset{\sim}{\varepsilon} &= \tfrac{1}{2}(\nabla \underset{\sim}{v}^{T} + \nabla \underset{\sim}{v}) \\ \underset{\sim}{\omega} &= \tfrac{1}{2}(\nabla \underset{\sim}{v}^{T} - \nabla \underset{\sim}{v}) \end{aligned}\right\} \tag{5.10}$$

and

$$\left.\begin{aligned} \dot{\underset{\sim}{t}} &= \dot{\underset{\sim}{t}}^{o} + \dot{\underset{\sim}{t}}^{b} \\ \dot{\underset{\sim}{t}} &= \nabla \times \underset{\sim}{\Phi} \; ; \qquad \nabla \cdot \dot{\underset{\sim}{t}}^{b} = - \rho \dot{\underset{\sim}{b}} \end{aligned}\right\} \tag{5.11}$$

respectively. The remaining equations of the general boundary value problem (5.3) through (5.9) are algebraic in character. Derived boundary value problems are those obtained from the general boundary value problem through use of (5.10) or (5.11). Usually one uses (5.10) to eliminate $\underset{\sim}{\varepsilon}$ and $\underset{\sim}{\omega}$ as variables from the constitutive equation (5.4), so that $\underset{\sim}{\varepsilon}$, $\underset{\sim}{\omega}$, and $\dot{\underset{\sim}{t}}$ are all determined by $\underset{\sim}{v}$. Owing to the special structure of the constitutive equation (5.4), AMB is satisfied implicitly for all such $\underset{\sim}{\varepsilon}$, $\underset{\sim}{\omega}$, and $\dot{\underset{\sim}{t}}$. Upon elimination of $\dot{\underset{\sim}{t}}$ from LMB, one obtains a single second order partial differential equation in $\underset{\sim}{v}$. We call this the First boundary value problem. Alternatively, one may use (5.11) to eliminate $\dot{\underset{\sim}{t}}$ from the constitutive equation (5.5), so that $\underset{\sim}{\varepsilon}$ is determined by $\underset{\sim}{\Phi}$ and $\underset{\sim}{\omega}$. Subsequent introduction of $\underset{\sim}{\Phi}$ (via $\dot{\underset{\sim}{t}}$ and $\underset{\sim}{\varepsilon}$)

and $\underset{\sim}{\omega}$ to compatibility (5.1) and AMB (5.3) yields a first order and a second order partial differential equation for $\underset{\sim}{\Phi}$ and $\underset{\sim}{\omega}$. We call this the Second boundary value problem.

The First boundary value problem is appealing to the practitioner because of the clear physical significance of the principal variable, the velocity field, and the simplicity of the boundary conditions. The Second boundary value problem is unattractive because the stress functions lack physical appeal, the boundary conditions are complicated, and because it involves two coupled equations in two unknowns. In either case, construction of closed form solutions is virtually impossible. It is this intractability which leads us to search for and study methods by which the solutions of these two boundary value problems may be approximated.

Two approximation methods for boundary value problems of solid mechanics dominate the current literature, namely, the method of finite differences and the finite element method. The finite difference method is, for the most part, reserved for dynamic (i.e. wave propagation) problems. Only rarely is it used for analysis of quasi-static deformation problems. In using the finite difference method, one attacks the partial differential equations as they stand. However the finite element method requires that one first *generalize* the equations (5.1) through (5.9). In the engineering literature this generalization is accomplished by finding a variational problem which is 'equivalent' to the original problem. Perhaps nowhere can a more lucid exposition of the fundamental variational principles of solid mechanics be found than in the monograph of Washizu [36]. His modus

operandi is adopted here.

The essence of Washizu's method is to use Lagrange multipliers to 'enforce' the equations (5.1) through (5.9) of the general boundary value problem. These multipliers turn out to be the displacement, stress, traction, etc. After discussing two 'virtual work' principles, he supposes the existence of a potential for the stress (the strain energy), and shows that all the variational principles of classical linear elasticity may be systematically derived from the "generalized potential energy principle" now known as the 'Hu-Washizu' principle. The principles discussed in this work are named 'virtual work,' 'potential energy,' 'Hellinger-Reissner,' etc., in analogy to the principles of linear elastostatics.

We begin with the generalization of the linear momentum balance (5.2). Let us momentarily regard $\delta\underset{\sim}{v}$ as a Lagrange multiplier. Then a stress rate $\dot{\underset{\sim}{t}}$ and a traction rate $\dot{\underset{\sim}{T}}_t$ satisfy LMB (5.2) and the stress principle if

$$\int_V [-\nabla \cdot \dot{\underset{\sim}{t}} - \rho\dot{\underset{\sim}{b}}] \cdot \delta\underset{\sim}{v}dV - \int_S (\dot{\underset{\sim}{T}}_t - \underset{\sim}{n} \cdot \dot{\underset{\sim}{t}})\delta\underset{\sim}{v}dS = 0 \qquad (5.13)$$

for arbitrary $\delta\underset{\sim}{v}$. In (5.13), as in (5.2), $\dot{\underset{\sim}{t}}$ apparently must be differentiable, but $\delta\underset{\sim}{v}$ need not even be continuous. Now, by formal integration by parts,* (5.13) may be transformed to

*throughout this chapter, integration by parts is *formal*.

$$\int_V [\dot{\underset{\sim}{t}} : \nabla\delta\underline{v} - \rho\dot{\underline{b}} \cdot \delta\underline{v}]dV - \int_S \dot{\underline{T}}_t \cdot \delta\underline{v}dS = 0 \qquad (5.14)$$

to be satisfied for arbitrary $\delta\underline{v}$. In (5.14) apparently $\dot{\underset{\sim}{t}}$ need not be continuous, but $\delta\underline{v}$ must be once differentiable. Any stress rate $\dot{\underset{\sim}{t}}$ admissible to the classical form of LMB (5.2) is also admitted by (5.14), but the converse is not true.* Therefore we call (5.14) the 'generalized' linear momentum balance, and write LMB (5.14). Any $\dot{\underset{\sim}{t}}$ and $\dot{\underline{T}}_t$ which satisfy the stress principle and LMB (5.2) necessarily satisfy (5.14).

Consider the modified general boundary value problem composed by replacing LMB (5.2) by generalized LMB (5.14) and eliminating compatibility through use of (5.10):

$$\left.\begin{aligned} &\underset{\sim}{\varepsilon} = \tfrac{1}{2}(\nabla\underline{v}^T + \nabla\underline{v}) \ ; \qquad \underset{\sim}{\omega} = \tfrac{1}{2}(\nabla\underline{v}^T - \nabla\underline{v}) \ ; \\ &\int_V [\dot{\underset{\sim}{t}} : \nabla\delta\underline{v} - \rho\dot{\underline{b}} \cdot \delta\underline{v}]dV - \int_S \dot{\underline{T}}_t \cdot \delta\underline{v}dS = 0 \\ &\qquad\qquad \text{for arbitrary } \delta\underline{v} \ ; \\ &\dot{\underset{\sim}{t}} = \underset{\sim}{G}(\underset{\sim}{\varepsilon},\underset{\sim}{\omega},\underset{\sim}{\tau}) \ ; \qquad \dot{\underline{T}}_t = \dot{\overline{\underline{T}}}_t \quad \text{on} \quad S_\sigma \ ; \end{aligned}\right\} \qquad (5.15)$$

$$\underline{v} = \overline{\underline{v}} \quad \text{on} \quad S_v \ . \qquad (5.16)$$

Every solution of the general boundary value problem (5.1) through

*In particular, (5.14) admits piecewise continuous stress rates, whereas (5.2) does not.

(5.9) is a solution of (5.15) and (5.16). If we admit only $\underline{v} = \bar{\underline{v}}$ on S_v, $\delta\underline{v} = \underline{0}$ on S_v, and $\dot{\underline{T}}_t = \dot{\bar{\underline{T}}}_t$ on S_σ, then one easily reduces (5.15) to a functional of the velocity field alone. This comprises the *principle of virtual work*. The virtual work principle is the most common basis for finite element algorithms used in engineering today. Its strong appeal stems from its overall simplicity. In arriving at (5.15) no assumption was made which restricts the from of the constitutive function $\underset{\sim}{G}$, except that all $\dot{\underline{t}} = G(\underset{\sim}{\varepsilon}, \underset{\sim}{\omega}, \underset{\sim}{\tau})$ satisfies AMB (5.3). As an alternative to retaining VBC (5.16) as a subsidiary condition, we may 'enforce' it by introduction of the Lagrange multiplier $\delta\dot{\underline{T}}_t$ on S_v. We replace (5.16) by

$$\int_{S_v} \delta\dot{\underline{T}}_t \cdot (\bar{\underline{v}} - \underline{v}) dS = 0 \quad \text{for arbitrary } \delta\dot{\underline{T}}_t \,. \tag{5.17}$$

If we admit only $\dot{\underline{T}}_t = \dot{\bar{\underline{T}}}_t$ on S_σ, then one easily reduces (5.15) through (5.17) to a functional of only $\underline{v}$ and $\dot{\underline{T}}_t$ (on S_v). We call this the *Second virtual work principle*. It is not used as a basis for finite element algorithms in engineering because the velocity boundary condition is so easily enforced; that is to say, introduction of the extra variable $\dot{\underline{T}}_t$ is a greater effort than a priori satisfaction of VBC and $\delta\underline{v} = \underline{0}$ on S_v.

By a procedure similar to the one above we may obtain the generalization of the compatibility equation. Let us momentarily regard the stress function $\underset{\sim}{\Phi}$ and the surface tangents $\delta\underline{s}^j$ as Lagrange multipliers. We write $(\delta\underline{s}^j \underline{e}_j)$ as $(\underline{n} \times \delta\underset{\sim}{\Phi})$. If $\underset{\sim}{\varepsilon}$ and $\underset{\sim}{\omega}$ (in V),

and $\underset{\sim}{v}$ (on S) satisfy compatibility (5.1), then they necessarily satisfy

$$\int_V [\nabla \times (-\underset{\sim}{\varepsilon} + \underset{\sim}{\omega})] : \delta\underset{\sim}{\Phi} dV + \int_S (\underset{\sim}{n} \times \delta\underset{\sim}{\Phi}) : (-\underset{\sim}{\varepsilon} + \underset{\sim}{\omega} + \nabla \underset{\sim}{v}) dS = 0 \tag{5.18}$$

for arbitrary $\delta\underset{\sim}{\Phi}$. Just as for LMB, we formally integrate by parts in order to relax the smoothness requirement on $\underset{\sim}{\varepsilon}$ and $\underset{\sim}{\omega}$, obtaining

$$\int_V [-\underset{\sim}{\varepsilon} + \underset{\sim}{\omega}] : (\nabla \times \delta\underset{\sim}{\Phi}) dV + \int_S (\underset{\sim}{n} \times \delta\underset{\sim}{\Phi}) : (\nabla \underset{\sim}{v}) dS = 0 \tag{5.19}$$

for arbitrary $\delta\underset{\sim}{\Phi}$. For the same reasons that we called (5.14) a generalization of LMB, we call (5.19) a generalization of compatibility. In this form it is easily seen that only the in-surface components of $(\nabla \underset{\sim}{v})$ influence the value of the functional. If $\underset{\sim}{\varepsilon}$, $\underset{\sim}{\omega}$, and $\underset{\sim}{v}$ are found which satisfy (5.19) identically for all $\delta\underset{\sim}{\Phi}$, it is incorrect to conclude that $(\underset{\sim}{\varepsilon} - \underset{\sim}{\omega}) = \nabla \underset{\sim}{v}$ anywhere in V, or even on S; only the in-surface components of $(\nabla \underset{\sim}{v})$ will agree with $(\underset{\sim}{\varepsilon} - \underset{\sim}{\omega})$ on S. Unfortunately this fact is not brought out in the literature, and is obscured by the conventional form of (5.19), which we now give. Using the formula (integration by parts)

$$\int_S (\underset{\sim}{n} \times \delta\underset{\sim}{\Phi}) : \nabla \underset{\sim}{v} dS = \int_S \underset{\sim}{n} \cdot (\nabla \times \delta\underset{\sim}{\Phi}) \cdot \underset{\sim}{v} dS \tag{5.20}$$

and identifying $(\nabla \times \delta\underset{\sim}{\Phi})$ as $\delta\dot{\underset{\sim}{t}}$ (in agreement with 5.11), equation (5.19) becomes

$$\int_V [-\underset{\sim}{\varepsilon} + \underset{\sim}{\omega}] : \delta\dot{\underset{\sim}{t}} dV + \int_S \underline{n} \cdot \delta\dot{\underset{\sim}{t}} \cdot \underline{v} dS = 0 \ . \tag{5.21}$$

It is clear from the present derivation that $\delta\dot{\underset{\sim}{t}}$ (in 5.21) is subject to no constraint except

$$\delta\dot{\underset{\sim}{t}} = \nabla \times \delta\underset{\sim}{\Phi} \ .$$

Consider the modified general boundary value problem obtained by replacing compatibility (5.1) by generalized compatibility (5.21), and using (5.11) to eliminate LMB:

$$\left.\begin{aligned} &\int_V [-\underset{\sim}{\varepsilon} + \underset{\sim}{\omega}] : \delta\dot{\underset{\sim}{t}} dV + \int_S \underline{n} \cdot \delta\dot{\underset{\sim}{t}} \cdot \underline{v} dS = 0 \\ &\qquad\qquad \text{for all } \delta\dot{\underset{\sim}{t}} = \nabla \times \delta\underset{\sim}{\Phi} \ ; \\ &\dot{\underset{\sim}{t}} = \nabla \times \underset{\sim}{\Phi} + \dot{\underset{\sim}{t}}^b \ ; \quad \underline{n} \cdot \dot{\underset{\sim}{t}} = \dot{\underline{T}}_t ; \quad \underset{\sim}{\omega} + \underset{\sim}{\omega}^T = \underset{\sim}{0} \ ; \\ &(\underset{\sim}{\varepsilon} + \underset{\sim}{\omega}) \cdot \underset{\sim}{\tau} + \dot{\underset{\sim}{t}} - \dot{\underset{\sim}{t}}^T - \underset{\sim}{\tau} \cdot (\underset{\sim}{\varepsilon} - \underset{\sim}{\omega}) = \underset{\sim}{0} \ ; \\ &\underset{\sim}{\varepsilon} = \underset{\sim}{G}'(\dot{\underset{\sim}{r}}, \underset{\sim}{\tau}) ; \quad \dot{\underset{\sim}{r}} = \tfrac{1}{2}(\dot{\underset{\sim}{t}} + \underset{\sim}{\tau} \cdot \underset{\sim}{\omega} - \underset{\sim}{\omega} \cdot \underset{\sim}{\tau} + \dot{\underset{\sim}{t}}^T) \ ; \end{aligned}\right\} \tag{5.22}$$

$$\left.\begin{aligned} &\underline{v} = \overline{\underline{v}} \quad \text{on} \quad S_v \\ &\dot{\underline{T}}_t = \dot{\overline{\underline{T}}}_t \quad \text{on} \quad S_\sigma \ . \end{aligned}\right\} \tag{5.23}$$

Every solution of the general boundary value problem (5.1) through

(5.9) is a solution of (5.22) and (5.23). If we admit to (5.22) only $\underset{\sim}{v} = \bar{\underset{\sim}{v}}$ on S_v, $\underset{\sim}{n} \cdot \dot{\underset{\sim}{t}} = \dot{\bar{\underset{\sim}{T}}}_t$ on S_σ, $\underset{\sim}{n} \cdot \delta\dot{\underset{\sim}{t}} = 0$ on S_σ, and $(\dot{\underset{\sim}{t}}, \underset{\sim}{\omega})$ which satisfy AMB, then we can reduce (5.22) and (5.23) to a single functional. This functional, when we are able to construct such $\dot{\underset{\sim}{t}}$ and $\underset{\sim}{\omega}$, comprises the *principle of complementary virtual work*. Except for pathological cases, construction of those $\dot{\underset{\sim}{t}}$ and $\underset{\sim}{\omega}$ is impracticable. The problems associated with the use of the complementary virtual work principle in its 'pure' form (5.22 and 5.23) may be avoided if AMB (5.3) and TBC (5.7) are incorporated into the principle by introduction of the Lagrange multipliers $\delta\underset{\sim}{\omega}$ and $\delta\underset{\sim}{v}$:

$$\int_V [(\underset{\sim}{\varepsilon} + \underset{\sim}{\omega}) \cdot \underset{\sim}{\tau} + \dot{\underset{\sim}{t}}] : \delta\underset{\sim}{\omega}\, dV = 0 \qquad (5.24)$$

$$\text{for all } \delta\underset{\sim}{\omega}: \ \delta\underset{\sim}{\omega} + \delta\underset{\sim}{\omega}^T = \underset{\sim}{0} \ ;$$

$$\int_{S_\sigma} [\underset{\sim}{n} \cdot \dot{\underset{\sim}{t}} - \dot{\bar{\underset{\sim}{T}}}_t] \cdot \delta\underset{\sim}{v}\, dS = 0 \qquad (5.25)$$

$$\text{for arbitrary } \delta\underset{\sim}{v} \ (\text{on } S_\sigma).$$

We call (5.22) and (5.23) thus modified the *Second complementary virtual work principle.*

For easy reference we collect the equations of the Second complementary virtual work principle below:

$$
\left.
\begin{aligned}
&\int_V [-\underset{\sim}{\varepsilon}+\underset{\sim}{\omega}] : \delta\dot{\underset{\sim}{t}}\,dV + \int_S \underset{\sim}{n}\cdot\delta\dot{\underset{\sim}{t}}\cdot\underset{\sim}{v}\,dS = 0 \\
&\qquad\qquad \text{for all } \delta\dot{\underset{\sim}{t}}\text{: } \delta\dot{\underset{\sim}{t}} = \nabla\times\delta\underset{\sim}{\Phi}\ ; \\
&\dot{\underset{\sim}{t}} = \nabla\times\underset{\sim}{\Phi} + \dot{\underset{\sim}{t}}^{b}; \qquad \underset{\sim}{\omega} + \underset{\sim}{\omega}^{T} = \underset{\sim}{0}\ ; \\
&\int_V [(\underset{\sim}{\varepsilon}+\underset{\sim}{\omega})\cdot\underset{\sim}{\tau} + \dot{\underset{\sim}{t}}] : \delta\underset{\sim}{\omega}\,dV = 0 \\
&\qquad\qquad \text{for all } \delta\underset{\sim}{\omega}\text{: } \delta\underset{\sim}{\omega} + \delta\underset{\sim}{\omega}^{T} = \underset{\sim}{0}\ ; \\
&\underset{\sim}{\varepsilon} = \underset{\sim}{G}'(\dot{\underset{\sim}{r}},\underset{\sim}{\tau})\ ; \qquad \dot{\underset{\sim}{r}} = \tfrac{1}{2}(\dot{\underset{\sim}{t}} + \underset{\sim}{\tau}\cdot\underset{\sim}{\omega} - \underset{\sim}{\omega}\cdot\underset{\sim}{\tau} + \dot{\underset{\sim}{t}}^{T})\ ; \\
&\int_{S_\sigma} (\underset{\sim}{n}\cdot\dot{\underset{\sim}{t}} - \dot{\overline{\underset{\sim}{T}}}_t)\cdot\delta\underset{\sim}{v}\,dS = 0 \\
&\qquad\qquad \text{for all } \delta\underset{\sim}{v} \text{ on } S_\sigma\ ; \\
&\underset{\sim}{v} = \overline{\underset{\sim}{v}} \quad \text{on} \quad S_v\ .
\end{aligned}
\right\} \qquad (5.26)
$$

It is a simple exercise to reduce (5.26) to three functionals involving $\dot{\underset{\sim}{t}}$ and $\underset{\sim}{\omega}$ in V and $\underset{\sim}{v}$ on S_σ. The second complementary virtual work principle used in this manner is the basis for the finite element algorithm presented in this work. In deriving (5.26) no assumption has been made which restricts the form of $\underset{\sim}{G}'$, except that $\underset{\sim}{\varepsilon} = \underset{\sim}{G}'(\dot{\underset{\sim}{r}},\underset{\sim}{\tau})$ must be symmetric.

The most important feature of the virtual work principles is that they admit functions $\underset{\sim}{v}$, $\underset{\sim}{\varepsilon}$, $\underset{\sim}{\omega}$, and $\dot{\underset{\sim}{t}}$ less smooth than did their

partial differential equation counterparts. A second property worthy of special note is that they were derived without restricting the forms of the constitutive functions $\underset{\sim}{G}$ and $\underset{\sim}{G}'$. The various energy principles we are about to derive require such restrictions. Specifically, we require that a stress-rate potential W for $\dot{\underset{\sim}{r}}$ exist such that

$$\dot{\underset{\sim}{r}} = \partial W(\underset{\sim}{\varepsilon},\underset{\sim}{\tau})/\partial \underset{\sim}{\varepsilon} \ . \tag{5.27}$$

Moreover, we consider only cases in which the nominal traction rate $\dot{\underset{\sim}{T}}_t$ is prescribed on S_σ.* For solids of the type (4.20) such a potential exists if and only if $\underset{\approx}{V}$ (and hence $\underset{\approx}{W}$) is symmetric. We remark that the constitutive equations for solids common in the engineering literature all satisfy this symmetry.**

If the conditions above are satisfied, then the first energy principle is found by introduction of the potential (5.27) for the stress rate to the virtual work principle (5.17) and (5.18). But since that principle involves the stress rate $\dot{\underset{\sim}{t}}$, we need a potential U for $\dot{\underset{\sim}{t}}$ such that

$$\dot{\underset{\sim}{t}} = \partial U(\underset{\sim}{L},\underset{\sim}{\tau})/\partial \underset{\sim}{L}^T \ .$$

Recalling the definition of $\dot{\underset{\sim}{t}}$ and $\dot{\underset{\sim}{r}}$, we get

---

*this is actually over-restrictive; see Hill [37], and references to Sewell, therein.

**including all the materials in examples accompanying this work. Some exceptions are noted by McMeeking and Rice [34].

$$\tfrac{1}{2}(\dot{\underset{\sim}{t}} + \dot{\underset{\sim}{t}}^T) = \dot{\underset{\sim}{r}} - \tfrac{1}{2}(\underset{\sim}{\tau}\cdot\underset{\sim}{\omega} - \underset{\sim}{\omega}\cdot\underset{\sim}{\tau}) \tag{5.28}$$

and recalling AMB (5.3) we get

$$\tfrac{1}{2}(\dot{\underset{\sim}{t}} - \dot{\underset{\sim}{t}}^T) = -\tfrac{1}{2}[(\underset{\sim}{\varepsilon} + \underset{\sim}{\omega})\cdot\underset{\sim}{\tau} - \underset{\sim}{\tau}\cdot(\underset{\sim}{\varepsilon} - \underset{\sim}{\omega})] \ . \tag{5.29}$$

Putting $\delta\underset{\sim}{L}^T = \delta\underset{\sim}{\varepsilon} - \delta\underset{\sim}{\omega}$, we get from (5.28) and (5.29)

$$\dot{\underset{\sim}{t}} : \delta\underset{\sim}{L}^T = \dot{\underset{\sim}{r}} : \delta\underset{\sim}{\varepsilon} - (\delta\underset{\sim}{\varepsilon} : \underset{\sim}{\tau}\cdot\underset{\sim}{\omega} + \underset{\sim}{\varepsilon} : \underset{\sim}{\tau}\cdot\delta\underset{\sim}{\omega})$$

$$- \tfrac{1}{2}\underset{\sim}{\tau} : (\underset{\sim}{\omega}\cdot\delta\underset{\sim}{\omega} + \delta\underset{\sim}{\omega}\cdot\underset{\sim}{\omega}) \ . \tag{5.30}$$

It is easily seen by inspection of (5.30) that $\dot{\underset{\sim}{t}} : \delta\underset{\sim}{L}^T$ is a perfect differential if and only if $\dot{\underset{\sim}{r}} : \delta\underset{\sim}{\varepsilon}$ is a perfect differential. When

$$\dot{\underset{\sim}{r}} : \delta\underset{\sim}{\varepsilon} = (\partial W/\partial\underset{\sim}{\varepsilon}) : \delta\underset{\sim}{\varepsilon}$$

then

$$\dot{\underset{\sim}{t}} : \delta\underset{\sim}{L}^T = (\partial U/\partial\underset{\sim}{L}^T) : \delta\underset{\sim}{L}^T \ ,$$

where W is defined by ($\underset{\sim}{\tau}$ is suppressed)

$$W(\underset{\sim}{\varepsilon}) = \tfrac{1}{2}\,\underset{\sim}{\varepsilon} : \underset{\approx}{W} : \underset{\sim}{\varepsilon} + \underset{\sim}{\varepsilon} : \underset{\sim}{\Sigma} \tag{5.31}$$

and U is defined through W as

$$U(\underset{\sim}{\varepsilon},\underset{\sim}{\omega}) = W(\underset{\sim}{\varepsilon}) - \underset{\sim}{\varepsilon} : \underset{\sim}{\tau} \cdot \underset{\sim}{\omega} - \tfrac{1}{2}\underset{\sim}{\tau} : (\underset{\sim}{\omega} \cdot \underset{\sim}{\omega}) \ . \tag{5.32}$$

Now we introduce the potential (5.32) for $\dot{\underset{\sim}{t}}$ to the Second virtual work principle (5.15 - 5.17) to obtain

$$\underset{\sim}{\varepsilon} = \tfrac{1}{2}(\nabla \underset{\sim}{v}^T + \nabla \underset{\sim}{v}) \ ; \qquad \underset{\sim}{\omega} = \tfrac{1}{2}(\nabla \underset{\sim}{v}^T - \nabla \underset{\sim}{v}) \ ; \tag{5.33}$$

$$\delta\pi(\underset{\sim}{v},\underset{\sim}{\varepsilon},\underset{\sim}{\omega},\dot{\underset{\sim}{T}}_t) = 0 \ ; \tag{5.34}$$

$$\pi(\underset{\sim}{v},\underset{\sim}{\varepsilon},\underset{\sim}{\omega},\dot{\underset{\sim}{T}}_t) = \int_V [U(\underset{\sim}{\varepsilon},\underset{\sim}{\omega}) - \rho \dot{\underset{\sim}{b}} \cdot \underset{\sim}{v}]dV - \int_{S_\sigma} \dot{\underset{\sim}{T}}_t \cdot \underset{\sim}{v} dS$$

$$- \int_{S_v} \dot{\underset{\sim}{T}}_t \cdot (\underset{\sim}{v} - \overline{\underset{\sim}{v}}) dS \ .$$

There are two ways to deal with the subsidiary conditions (5.33). It is an easy exercise to reduce (5.33) and (5.34) to a functional of the velocity field and traction rate. Alternatively we may 'enforce' (5.33) by use of Lagrange multipliers.

The first course of action leads us to the *principle of stationary potential energy*

$$\delta\pi_p(\underset{\sim}{v},\dot{\underset{\sim}{T}}_t) = 0 \tag{5.35}$$

$$\pi_p(\underset{\sim}{v},\dot{\underset{\sim}{T}}_t) = \pi(\underset{\sim}{v},\tfrac{1}{2}(\nabla \underset{\sim}{v}^T + \nabla \underset{\sim}{v}),\tfrac{1}{2}(\nabla \underset{\sim}{v}^T - \nabla \underset{\sim}{v}),\dot{\underset{\sim}{T}}_t) \ .$$

Any solution of the general boundary value problem is a solution of

(5.35). In practice one usually satisfies the velocity boundary condition a priori, thereby eliminating $\dot{\underline{T}}_t$ from (5.35).

The alternative course of action leads us to a *Hu-Washizu energy principle*. Let $\dot{\underline{\underline{t}}}$ be regarded momentarily as a Lagrange multiplier. Then (5.33) and (5.44) may be set as

$$\delta\pi_{HW}(\underline{v},\underline{\underline{\varepsilon}},\underline{\underline{\omega}},\dot{\underline{T}}_t,\dot{\underline{\underline{t}}}) = 0 \ ; \tag{5.36}$$

$$\pi_{HW}(\underline{v},\underline{\underline{\varepsilon}},\underline{\underline{\omega}},\dot{\underline{T}}_t,\dot{\underline{\underline{t}}}) = \pi(\underline{v},\underline{\underline{\varepsilon}},\underline{\underline{\omega}},\dot{\underline{T}}_t) + \int_V \dot{\underline{\underline{t}}} : (\nabla\underline{v} - (\underline{\underline{\varepsilon}} - \underline{\underline{\omega}}))dV$$

$$\underline{\underline{\varepsilon}} - \underline{\underline{\varepsilon}}^T = \underline{\underline{0}} \ ; \qquad \underline{\underline{\omega}} + \underline{\underline{\omega}}^T = \underline{\underline{0}} \ .$$

It is possible to enforce both of the conditions (5.33) with the single multiplier so long as only symmetric $\underline{\underline{\varepsilon}}$ and skew symmetric $\underline{\underline{\omega}}$ are admitted to π_{HW}. There are no other subsidiary conditions. Any solution of the general boundary problem (5.1 through 5.9) necessarily satisfies (5.36). We write out the stationary conditions for future references:

$$\delta\pi_{HW}(\underline{v},\underline{\underline{\varepsilon}},\underline{\underline{\omega}},\dot{\underline{T}}_t,\dot{\underline{\underline{t}}}) = 0 :$$

LMB:

$$\int_V [\dot{\underline{\underline{t}}} : \nabla\delta\underline{v} - \rho\dot{\underline{b}} \cdot \delta\underline{v}]dV - \int_{S_\sigma} \dot{\underline{T}}_t \cdot \delta\underline{v}dS - \int_{S_v} \dot{\underline{T}}_t \cdot \delta\underline{v}dS = 0 \tag{5.37}$$

CONSTITUTIVE EQUATION:

$$\int_V [(\partial W/\partial \underset{\sim}{\varepsilon}) - \tfrac{1}{2}(\dot{\underset{\sim}{t}} + \underset{\sim}{\tau}\cdot\underset{\sim}{\omega} - \underset{\sim}{\omega}\cdot\underset{\sim}{\tau} + \dot{\underset{\sim}{t}}^T)] : \delta\underset{\sim}{\varepsilon} dV = 0 \tag{5.38}$$

AMB:

$$\int_V [\tfrac{1}{2}((\underset{\sim}{\varepsilon} + \underset{\sim}{\omega})\cdot\underset{\sim}{\tau} + \dot{\underset{\sim}{t}} - \dot{\underset{\sim}{t}}^T - \underset{\sim}{\tau}\cdot(\underset{\sim}{\varepsilon} - \underset{\sim}{\omega})) : \delta\underset{\sim}{\omega}] dV = 0 \tag{5.39}$$

VBC:

$$\int_{S_v} \delta\dot{\underset{\sim}{T}}_t \cdot (\bar{\underset{\sim}{v}} - \underset{\sim}{v}) dS = 0 \tag{5.40}$$

COMPATIBILITY:

$$\int_V [\nabla\underset{\sim}{v} - (\underset{\sim}{\varepsilon} - \underset{\sim}{\omega})] : \delta\dot{\underset{\sim}{t}} dV = 0 \ . \tag{5.41}$$

Notice that the stationary condition for $\delta\underset{\sim}{v}$ (5.37) is the generalized LMB (5.14).

The main detraction of the Hu-Washizu principle is the large number of unknowns (five). Although a finite element algorithm could be based upon this principle, it is unlikely that it could be made very efficient, and thus would be of diminished practical interest.

We note that solely by rearrangement of terms, (5.26) may be rendered in the form [15]

$$\pi_{HW}(\underset{\sim}{v},\underset{\sim}{\varepsilon},\underset{\sim}{\omega},\dot{\underset{\sim}{T}}_t,\dot{\underset{\sim}{t}}) = \tag{5.42}$$

$$\int_V \left\{[W(\underset{\sim}{\varepsilon}) - \tfrac{1}{2}(\dot{\underset{\sim}{t}} + \underset{\sim}{\tau}\cdot\underset{\sim}{\omega} - \underset{\sim}{\omega}\cdot\underset{\sim}{\tau} + \dot{\underset{\sim}{t}}^T) : \underset{\sim}{\varepsilon}] - \tfrac{1}{2}\underset{\sim}{\tau} : \underset{\sim}{\omega}\cdot\underset{\sim}{\omega} + \dot{\underset{\sim}{t}} : \underset{\sim}{\omega}\right\} dV$$

$$+ \int_V \left\{\dot{\underset{\sim}{t}} : \nabla\underset{\sim}{v} - \rho\dot{\underset{\sim}{b}}\cdot\underset{\sim}{v}\right\} dV - \int_{S_\sigma} \dot{\bar{\underset{\sim}{T}}}_t \cdot \underset{\sim}{v}\, dS - \int_{S_v} \dot{\underset{\sim}{T}}_t \cdot \underset{\sim}{v}\, dS$$

$$+ \int_{S_v} \dot{\underset{\sim}{T}}_t \cdot \bar{\underset{\sim}{v}}\, dS \,.$$

If the constitutive equation (5.5) is used to eliminate $\underset{\sim}{\varepsilon}$ as a variable from (5.42), then, defining

$$-R(\dot{\underset{\sim}{t}},\underset{\sim}{\omega}) = W(\underset{\sim}{\varepsilon}(\dot{\underset{\sim}{t}},\underset{\sim}{\omega})) - \tfrac{1}{2}(\dot{\underset{\sim}{t}} + \underset{\sim}{\tau}\cdot\underset{\sim}{\omega} - \underset{\sim}{\omega}\cdot\underset{\sim}{\tau} + \dot{\underset{\sim}{t}}^T) : \underset{\sim}{\varepsilon}(\dot{\underset{\sim}{t}},\underset{\sim}{\omega}) \,,$$

we obtain a *Hellinger-Reissner variational principle:*

$$\delta\pi_{HR}(\underset{\sim}{v},\underset{\sim}{\omega},\dot{\underset{\sim}{T}}_t,\dot{\underset{\sim}{t}}) = 0 \;; \tag{5.43}$$

$$\pi_{HR}(\underset{\sim}{v},\underset{\sim}{\omega},\dot{\underset{\sim}{T}}_t,\dot{\underset{\sim}{t}}) = \int_V \left\{-R(\dot{\underset{\sim}{t}},\underset{\sim}{\omega}) - \tfrac{1}{2}\underset{\sim}{\tau} : (\underset{\sim}{\omega}\cdot\underset{\sim}{\omega}) + \dot{\underset{\sim}{t}} : \dot{\underset{\sim}{\omega}}\right\} dV$$

$$+ \int_{S_v} \dot{\underset{\sim}{T}}_t \cdot \bar{\underset{\sim}{v}}\, dS$$

$$+ \int_V [\dot{\underset{\sim}{t}} : \nabla\underset{\sim}{v} - \rho\dot{\underset{\sim}{b}}\cdot v]\, dV - \int_{S_\sigma} \dot{\bar{\underset{\sim}{T}}}_t \cdot \underset{\sim}{v}\, dS - \int_{S_v} \dot{\underset{\sim}{T}}_t \cdot \underset{\sim}{v}\, dS \;;$$

$$\underset{\sim}{\omega} + \underset{\sim}{\omega}^T = 0 \,.$$

Any solution of the general boundary value problem is also a solution of (5.43). The stationary conditions are LMB (5.37), AMB (5.39), VBC (5.40), and compatibility (5.41). In the stationary conditions $\underset{\sim}{\varepsilon}$ only appears as a function of $\dot{\underset{\sim}{t}}$ and $\underset{\sim}{\omega}$.

If we admit to π_{HR} (5.43) only stress rates $\dot{\underset{\sim}{t}}$ and traction rates $\dot{\underline{T}}_t$ which satisfy the generalized LMB (5.14) for assigned $\dot{\overline{\underline{T}}}_t$, we obtain the complementary energy principle of Atluri [15]:

$$\delta\pi_c(\underset{\sim}{\omega},\dot{\underset{\sim}{t}}) = 0 \; ; \tag{5.44}$$

$$\pi_c(\underset{\sim}{\omega},\dot{\underset{\sim}{t}}) = \int_V \left\{-R(\dot{\underset{\sim}{t}},\underset{\sim}{\omega}) - \tfrac{1}{2}\underset{\sim}{\tau}:(\underset{\sim}{\omega}\cdot\underset{\sim}{\omega}) + \dot{\underset{\sim}{t}}:\underset{\sim}{\omega}\right\} dV + \int_{S_v} \underline{n}\cdot\dot{\underset{\sim}{t}}\cdot\dot{\overline{\underline{v}}}\, dS$$

$$\dot{\underset{\sim}{t}} = \nabla\times\underset{\sim}{\Phi} + \dot{\underset{\sim}{t}}^b \; ; \qquad \underset{\sim}{\omega} + \underset{\sim}{\omega}^T = \underset{\sim}{0} \; ;$$

$$\underline{n}\cdot\dot{\underset{\sim}{t}} = \dot{\underline{T}}_t \quad \text{on} \quad S_\sigma \; . \tag{5.45}$$

Any solution of the general boundary value problem is a solution of (5.44) and (5.45). The stationary conditions are AMB (5.39), VBC (5.40), and compatibility (5.41). In the stationary conditions $\underset{\sim}{\varepsilon}$ only appears as a function of $\dot{\underset{\sim}{t}}$ and $\underset{\sim}{\omega}$. It is not a simple matter to reduce (5.44) and (5.45) to a single functional of $\dot{\underset{\sim}{t}}$ and $\underset{\sim}{\omega}$ since this would require construction of stress functions satisfying

$$\underline{n}\cdot(\nabla\times\underset{\sim}{\Phi}+\dot{\underset{\sim}{t}}^b) = \dot{\underline{T}}_t \quad \text{on} \quad S_\sigma \; .$$

Therefore (5.44) and (5.45) are not suitable as a basis for a finite element algorithm.

The problems associated with the use of the complementary energy principle in its 'pure' form (above) may be avoided if the traction boundary condition is incorporated into the principle. Let $\underset{\sim}{v}$ be a Lagrange multiplier on S_σ. Then we replace (5.44) and (5.45) by

$$\delta\pi_c^*(\underset{\sim}{v},\underset{\sim}{\omega},\dot{\underset{\sim}{t}}) = 0 \; ; \tag{5.46}$$

$$\pi_c^*(\underset{\sim}{v},\underset{\sim}{\omega},\dot{\underset{\sim}{t}}) = \pi_c(\underset{\sim}{\omega},\dot{\underset{\sim}{t}}) + \int_{S_\sigma} (\underset{\sim}{n}\cdot\dot{\underset{\sim}{t}} - \dot{\bar{\underset{\sim}{T}}}_t)\cdot\underset{\sim}{v}\,dS$$

$$\dot{\underset{\sim}{t}} = \nabla\times\underset{\sim}{\Phi} + \dot{\underset{\sim}{t}}^b \; ; \qquad \underset{\sim}{\omega} + \underset{\sim}{\omega}^T = \underset{\sim}{0} \; .$$

Any solution of the general boundary value problem is a solution of (5.46). The stationary conditions are the same as those of the 'pure' complementary energy principle, except that the traction boundary condition follows from $\delta\pi_c^*/\delta\underset{\sim}{v} = 0$. It is a simple exercise to reduce (5.46) to a single functional of $\underset{\sim}{v}$, $\underset{\sim}{\omega}$, and $\dot{\underset{\sim}{t}}$. The complementary energy principle thus modified serves as the basis for the finite element algorithm presented in this work.

CHAPTER VI

UNIQUENESS OF SOLUTIONS OF BOUNDARY VALUE PROBLEMS

Introduction

Once a solution of a boundary value problem has been found, one may inquire as to the uniqueness of that solution. In the event that multiple solutions exist, a stability criterion is required to distinguish stable solutions from those which are unstable.

Hill [38] has published a number of papers on the subject of uniqueness. For materials of the type (4.20) through (4.22), his criterion is necessary and sufficient for uniqueness. He has also given a practical method for testing the uniqueness of deformations of hypoelastic/plastic bodies (which are nonlinear in a certain way). For extended treatments of the theory, see Hill [38].

In this work we establish (quasistatic) stability of a configuration of a body by inspection of the 'restoring force' that results when the configuration is slightly perturbed. If the forces arising from an admissible* perturbation tend to attenuate the disturbance, then we say the given configuration is stable. The principal shortcoming of this stability criterion is apparent when uniqueness is lost; it provides no means of distinguishing stable solutions from unstable solutions. The

*not violating kinematic constraints.

criterion tests configurations of bodies, not solutions of the boundary value problem. This shortcoming is probably unavoidable when one is using a purely mechanical material model such as (4.20), or the hypoelastic/plastic model.

We construct two uniqueness criteria, one from the virtual work principle, and the other from the Second complementary virtual work principle. These are equivalent to the criteria proposed by Hill [38].

A Uniqueness Criterion Based on the Virtual Work Principle

Let $(\underset{\sim}{v}^1, \underset{\sim}{\varepsilon}^1, \underset{\sim}{\omega}^1, \overset{\cdot}{\underset{\sim}{t}}^1)$ and $(\underset{\sim}{v}^2, \underset{\sim}{\varepsilon}^2, \underset{\sim}{\omega}^2, \overset{\cdot}{\underset{\sim}{t}}^2)$ be two solutions of the general boundary value problem. The same traction boundary condition and velocity boundary condition are satisfied by each of the two solutions above. By the virtual work principle, any solution of the general boundary value problem is also a solution of (5.15) and (5.16), so $(\underset{\sim}{v}^i, \underset{\sim}{\varepsilon}^i, \underset{\sim}{\omega}^i, \overset{\cdot}{\underset{\sim}{t}}^i)$ each satisfy (5.15) and (5.16). Therefore the difference of the two solutions

$$(\Delta\underset{\sim}{v}, \Delta\underset{\sim}{\varepsilon}, \Delta\underset{\sim}{\omega}, \Delta\overset{\cdot}{\underset{\sim}{t}}) = (\underset{\sim}{v}^2 - \underset{\sim}{v}^1, \underset{\sim}{\varepsilon}^2 - \underset{\sim}{\varepsilon}^1, \underset{\sim}{\omega}^2 - \underset{\sim}{\omega}^1, \overset{\cdot}{\underset{\sim}{t}}^2 - \overset{\cdot}{\underset{\sim}{t}}^1) \tag{6.1}$$

necessarily satisfies*

$$\Delta\underset{\sim}{\varepsilon} = \tfrac{1}{2}(\nabla\Delta\underset{\sim}{v}^T + \nabla\Delta\underset{\sim}{v}) \; ; \qquad \Delta\underset{\sim}{\omega} = \tfrac{1}{2}(\nabla\Delta\underset{\sim}{v}^T - \nabla\Delta\underset{\sim}{v}) \; ;$$

*the first of (6.2) applies when nominal tractions are prescribed on S_σ; the second applies when true tractions are prescribed.

$$\text{or} \quad \begin{cases} \int_V [\Delta \dot{\underset{\sim}{t}} : \nabla \delta \underset{\sim}{v} - \rho \Delta \underset{\sim}{v} \cdot \nabla \dot{\underset{\sim}{b}} \cdot \delta \underset{\sim}{v}] dV = 0 \ ; \\ \\ \int_V [\Delta \dot{\underset{\sim}{t}} : \nabla \delta \underset{\sim}{v} - \rho \Delta \underset{\sim}{v} \cdot \nabla \dot{\underset{\sim}{b}} \cdot \delta \underset{\sim}{v}] dV - \int_{S_\sigma} [(\Delta \dot{J} - \underset{\sim}{n} \cdot \Delta \underset{\sim}{\varepsilon} \cdot \underset{\sim}{n}) \underset{\sim}{T} \cdot \delta \underset{\sim}{v}] dS = 0 \ ; \end{cases} \tag{6.2}$$

$$\Delta \dot{\underset{\sim}{t}} = \underset{\sim}{G}(\underset{\sim}{\varepsilon}^2, \underset{\sim}{\omega}^2, \underset{\sim}{\tau}) - \underset{\sim}{G}(\underset{\sim}{\varepsilon}^1, \underset{\sim}{\omega}^1, \underset{\sim}{\tau})$$

$$\underset{\sim}{v} = \underset{\sim}{0} \quad \text{on} \quad S_v \ ; \qquad \delta \underset{\sim}{v} = \underset{\sim}{0} \quad \text{on} \quad S_v \ .$$

A sufficient condition for uniqueness is therefore that (6.2) have no solution among all pairs $\{v^1, v^2\}$ taking the prescribed value $\bar{\underset{\sim}{v}}$ on S_v. Generally we are unable to reduce the expression above to a functional of $\Delta \underset{\sim}{v}$ alone since the constitutive equation involves $\underset{\sim}{\varepsilon}^1$, $\underset{\sim}{\omega}^1$, $\underset{\sim}{\varepsilon}^2$, and $\underset{\sim}{\omega}^2$ distinctly. However, if $\underset{\sim}{G}$ has the distributive property (modulo $\underset{\sim}{G}(\underset{\sim}{0}, \underset{\sim}{0}, \underset{\sim}{\tau})$)

$$\underset{\sim}{G}(\Delta \underset{\sim}{\varepsilon}, \Delta \underset{\sim}{\omega}, \underset{\sim}{\tau}) = \underset{\sim}{G}(\underset{\sim}{\varepsilon}^2, \underset{\sim}{\omega}^2, \underset{\sim}{\tau}) - \underset{\sim}{G}(\underset{\sim}{\varepsilon}^1, \underset{\sim}{\omega}^1, \underset{\sim}{\tau}) + \underset{\sim}{G}(\underset{\sim}{0}, \underset{\sim}{0}, \underset{\sim}{\tau}) \tag{6.3}$$

then it is an easy exercise to reduce (6.2) to a functional of the velocity field alone, and that functional is independent of the particular boundary values $\bar{\underset{\sim}{v}}$. This is important in practice because it means that searching for solutions of (6.2) is precisely equivalent to searching for solutions of virtual work (5.15 and 5.16) with homogeneous boundary conditions and no relaxation.

The condition (6.3) is satisfied by hypoelastic and hypoelastic/viscoplastic materials, but not by hypoelastic/plastic materials.

Hill [38] has shown that if the 'linear comparison solid' associated with a particular plastic body is used in (6.2), then uniqueness of solutions for the linear comparison solid is sufficient for uniqueness of solutions for the plastic body.

A Uniqueness Criterion Based on the Second Complementary Virtual Work Principle

In this section we use the same difference notation as in the previous section. Any two solutions of the general boundary value problem necessarily satisfy the Second complementary virtual work principle. Therefore, their difference satisfies

$$\left.\begin{aligned}
&\int_V [-\Delta\underset{\sim}{\varepsilon} + \Delta\underset{\sim}{\omega}] : \delta\dot{\underset{\sim}{t}}\,dV + \int_{S_\sigma} \underset{\sim}{n} \cdot \delta\dot{\underset{\sim}{t}} \cdot \Delta\underset{\sim}{v}\,dS = 0 \\
&\qquad\qquad \text{for all } \delta\dot{\underset{\sim}{t}} = \nabla \times \delta\underset{\sim}{\Phi} \ ; \\
&\Delta\dot{\underset{\sim}{t}} = \nabla \times \Delta\underset{\sim}{\Phi} \ ;^{*} \qquad \Delta\underset{\sim}{\omega} + \Delta\underset{\sim}{\omega}^{T} = \underset{\sim}{0} \ ; \\
&\int_V [(\Delta\underset{\sim}{\varepsilon} + \Delta\underset{\sim}{\omega}) \cdot \underset{\sim}{\tau} + \dot{\underset{\sim}{t}}] : \delta\underset{\sim}{\omega}\,dV = 0 \\
&\qquad\qquad \text{for all } \delta\underset{\sim}{\omega}: \ \delta\underset{\sim}{\omega} + \delta\underset{\sim}{\omega}^{T} = \underset{\sim}{0} \ ; \\
&\Delta\underset{\sim}{\varepsilon} = \underset{\sim}{G}'(\dot{\underset{\sim}{r}}^{2}, \underset{\sim}{\tau}) - \underset{\sim}{G}'(\dot{\underset{\sim}{r}}^{1}, \underset{\sim}{\tau}) \ ; \\
&\dot{\underset{\sim}{r}} = \tfrac{1}{2}(\dot{\underset{\sim}{t}} + \underset{\sim}{\tau} \cdot \underset{\sim}{\omega} - \underset{\sim}{\omega} \cdot \underset{\sim}{\tau} + \dot{\underset{\sim}{t}}^{T}) \ ;
\end{aligned}\right\} \qquad (6.4)$$

*for convenience, we have assumed that $\Delta\underset{\sim}{v} \cdot \nabla\dot{\underset{\sim}{b}} = \underset{\sim}{0}$.

or

$$\begin{cases} \int_{S_\sigma} (\underset{\sim}{n} \cdot \Delta\dot{\underset{\sim}{t}} \cdot \delta\underset{\sim}{v}) dS = 0 \\ \int_{S_\sigma} [\underset{\sim}{n} \cdot \Delta\dot{\underset{\sim}{t}} - (\Delta\dot{J} - \underset{\sim}{n} \cdot \Delta\underset{\sim}{\varepsilon} \cdot \underset{\sim}{n})\underset{\sim}{T}] \cdot \delta\underset{\sim}{v} dS = 0 \ . \end{cases}$$

A sufficient condition for uniqueness is therefore that (6.4) has no solution among all pairs $\left\{(\dot{\underset{\sim}{t}}^1, \underset{\sim}{\omega}^1, \underset{\sim}{v}^1), (\dot{\underset{\sim}{t}}^2, \underset{\sim}{\omega}^2, \underset{\sim}{v}^2)\right\}$ in which the $\underset{\sim}{v}^i$ take the prescribed value $\bar{\underset{\sim}{v}}$ on S_v. We are unable to reduce (6.4) to a functional of $(\Delta\dot{\underset{\sim}{t}}, \Delta\underset{\sim}{\omega}, \Delta\underset{\sim}{v})$ alone except in the case that the constitutive function $\underset{\sim}{G}'$ has a distributive property

$$\underset{\sim}{G}'(\Delta\dot{\underset{\sim}{r}}, \underset{\sim}{\tau}) = \underset{\sim}{G}'(\dot{\underset{\sim}{r}}^2, \underset{\sim}{\tau}) - \underset{\sim}{G}'(\dot{\underset{\sim}{r}}^1, \underset{\sim}{\tau}) + \underset{\sim}{G}'(\underset{\sim}{0}, \underset{\sim}{\tau}) \ . \qquad (6.5)$$

In this case searching for solutions of (6.4) is precisely equivalent to searching for solutions of complementary virtual work (5.26) with homogeneous boundary conditions and no relaxation. Of course, the same materials satisfy the condition (6.5) which satisfied the condition (6.3). In the case of hypoelastic/plastic materials, (6.5) is not satisfied, but we note that the constitutive function of the associated linear comparison solid for a particular hypoelastic/plastic solid does satisfy (6.5). In view of the fact that uniqueness for the linear comparison solid is sufficient for uniqueness for the hypoelastic/plastic solid (and no restrictions are placed on the method by which we establish uniqueness for the linear comparison solid), we may use the constitutive equation of the linear comparison

solid in (6.4) to establish uniqueness for the hypoelastic/plastic solid. A proof of this sufficiency would be difficult if one started from (6.4), since plasticity theory is not formulated in terms of the stress rate $\dot{\underset{\sim}{\tau}}$. In the bifurcation study accompanying this work, the criterion (6.4) is used in conjunction with the constitutive equation of the linear comparison solid.

CHAPTER VII

A FINITE ELEMENT ALGORITHM

Introduction

The finite element method had its beginnings in structural analysis, but spread quickly and with great success to other areas of applied science. The underlying mathematical theory of finite elements resulted from the study of the method as applied by engineers, and is still being developed at this date. Extended introductions to the finite element method, both from the practitioner's point of view [39], [40], and from the mathematician's point of view [41], [42], are widely available, and therefore omitted from this work. For the discussion that follows, the finite element method may be regarded as a generalization of the approximate methods based on energy principles of linear elastostatics.*

The finite element algorithm described in this chapter is based upon the Second complementary virtual work principle (5.26). The advantage of starting from the 'work' principle, as opposed to starting from the 'energy' principle (5.46), is not only greater generality with regard to constitutive equations and boundary conditions, but greater clarity, since each of the equations of (5.26) corresponds to an equation of the general boundary value problem (5.1) through (5.9).

---

*see Washizu [36], especially sections 1.5 and 1.7 therein.

When the constitutive equation and boundary conditions are such that a complementary energy principle exists, the distinction between the 'work' and 'energy' formulations vanishes entirely. We do assume that the constitutive equation may be set in the form (5.5), and the traction boundary conditions are dealt with as if nominal traction rates were prescribed, but generalization to treat other materials and types of boundary conditions should present no difficulty for the reader familiar with finite element methods.

A Finite Element Algorithm

According to the Second complementary virtual work principle (5.26), the stress rate $\dot{\underset{\sim}{t}}$, spin $\underset{\sim}{\omega}$, and boundary velocity $\underset{\sim}{v}$ of a body are solutions of the following boundary value problem:

$$\left.\begin{aligned} &\int_V \left\{\left[(\underset{\approx}{W}^{-1} : (\dot{\underset{\sim}{r}} - \underset{\sim}{\Sigma}) + \underset{\sim}{\omega}) \cdot \underset{\sim}{\tau} + \dot{\underset{\sim}{t}}\right] : \delta\underset{\sim}{\omega}\right\} dV = 0 \\ &\int_V \left\{\left[-\underset{\approx}{W}^{-1} : (\dot{\underset{\sim}{r}} - \underset{\sim}{\Sigma}) + \underset{\sim}{\omega}\right] : \delta\dot{\underset{\sim}{t}}\right\} dV + \int_S \underline{n} \cdot \delta\underset{\sim}{t} \cdot \underline{v} dS = 0 \\ &\qquad \text{for all} \quad \delta\underset{\sim}{\omega}: \quad \delta\underset{\sim}{\omega} + \delta\underset{\sim}{\omega}^T = \underset{\sim}{0} \ ; \\ &\qquad\qquad\quad \delta\dot{\underset{\sim}{t}}: \quad \delta\dot{\underset{\sim}{t}} = \nabla \times \delta\underset{\sim}{\phi} \ ; \end{aligned}\right\} \qquad (7.1)$$

$$\left.\begin{aligned} &\int_{S_\sigma} (\underline{n} \cdot \dot{\underset{\sim}{t}} - \dot{\underline{T}}_t) \cdot \delta\underline{v} dS = 0 \\ &\qquad \text{for all} \quad \delta\underline{v}: \quad \int_{S_\sigma} \delta\underline{v} \cdot \delta\underline{v} dS \neq 0 \end{aligned}\right\} \qquad (7.2)$$

with the subsidiary conditions:

$$\dot{\underset{\sim}{t}} = \dot{\underset{\sim}{t}}^{o} + \dot{\underset{\sim}{t}}^{b} \; ; \qquad \dot{\underset{\sim}{t}}^{o} = \nabla \times \underset{\sim}{\phi} \; ; \qquad \nabla \cdot \dot{\underset{\sim}{t}}^{b} = -\rho \dot{\underset{\sim}{b}} \; ;$$

$$\dot{\underset{\sim}{r}} = \tfrac{1}{2}(\dot{\underset{\sim}{t}} + \underset{\sim}{\tau} \cdot \underset{\sim}{\omega} - \underset{\sim}{\omega} \cdot \underset{\sim}{\tau} + \dot{\underset{\sim}{t}}^{T}) \; ; \qquad \underset{\sim}{\omega} + \underset{\sim}{\omega}^{T} = \underset{\sim}{0} \; ;$$

$$\underset{\sim}{v} = \bar{\underset{\sim}{v}} \quad \text{on} \quad S_v \; .$$

In formulation of a finite element algorithm we regard the body as an assembly of sub-bodies called elements. We wish to represent the functions $\dot{\underset{\sim}{t}}$ and $\underset{\sim}{\omega}$ independently on each element. The stress rate $\dot{\underset{\sim}{t}}$ will be represented as indicated in the subsidiary conditions above on each element, but between elements $\dot{\underset{\sim}{t}}^{o}$ will generally be discontinuous. Such $\dot{\underset{\sim}{t}}$ is still admissible to the complementary virtual work principle providing it satisfies the generalized LMB (5.14).* Indicating by NELM the number of elements into which the body has been partitioned, we write LMB (5.14) as

$$\sum_{N=1}^{NELM} \left\{ \int_{V_N} [\dot{\underset{\sim}{t}} : \nabla \delta \underset{\sim}{v} - \rho \dot{\underset{\sim}{b}} \cdot \delta \underset{\sim}{v}] dV \right\} - \int_{S} \dot{\underset{\sim}{T}}_{t} \cdot \delta \underset{\sim}{v} dS = 0$$

for arbitrary $\delta \underset{\sim}{v}$ (continuous across interelement boundaries)

Integration by parts yields

*note that the original form of LMB (5.2) does not admit such $\dot{\underset{\sim}{t}}$.

$$\sum_{N=1}^{NELM}\left\{\int_{S_N}(\underline{n}\cdot\dot{\underline{t}}\cdot\delta\underline{v})dS\right\}-\int_{S}\dot{\underline{T}}_t\cdot\delta\underline{v}dS=0\ ,$$

where V_N and S_N are the element domain and boundary, respectively. Finally, setting $\dot{\underline{T}}_t$ to $\dot{\overline{\underline{T}}}_t$ on S_σ and $\delta\underline{v}$ to zero on S_v, we obtain

$$\sum_{N=1}^{NELM}\left\{\int_{S_N\sim(S_N\cap S_v)}(\underline{n}\cdot\dot{\underline{t}}\cdot\delta\underline{v})dS-\int_{(S_N\cap S_\sigma)}\dot{\overline{\underline{T}}}_t\cdot\delta\underline{v}dS\right\}=0\ . \tag{7.3}$$

We replace the traction boundary condition (7.2) by this last equation (7.3), which is easily seen to be no more than a statement of traction reciprocity. In the context of finite element terminology, it is called 'interelement traction reciprocity.' One should take special note that in (7.3) $\delta\underline{v}$ is required to be single valued on the interelement boundaries, since $\delta\underline{v}$ is required to possess a (generalized) gradient everywhere in V.

Since $\dot{\underline{t}}$, $\underline{\omega}$, $\delta\dot{\underline{t}}$, and $\delta\underline{\omega}$ are now independent on each element, (7.1) must be satisfied independently on each element. Thus, we replace the boundary value problem (7.1) and (7.2) by

$$\left.\begin{aligned}&\int_{V_N}\left\{[(\underline{\underline{W}}^{-1}:(\dot{\underline{r}}-\underline{\Sigma})+\underline{\omega})\cdot\underline{\tau}+\dot{\underline{t}}]:\delta\underline{\omega}\right\}dV=0\\&\int_{V_N}\left\{[-\underline{\underline{W}}^{-1}:(\dot{\underline{r}}-\underline{\Sigma})+\underline{\omega}]:\delta\dot{\underline{t}}\right\}dV+\int_{S_N}\underline{n}\cdot\delta\dot{\underline{t}}\cdot\underline{v}dS=0\\&\qquad\text{for all }\delta\underline{\omega}\text{: }\delta\underline{\omega}+\delta\underline{\omega}^T=\underline{0}\ ;\\&\qquad\text{for all }\delta\dot{\underline{t}}\text{: }\delta\dot{\underline{t}}=\nabla\times\delta\underline{\Phi}\end{aligned}\right\}\tag{7.4}$$

$$\sum_{N=1}^{NELM}\left\{\int_{S_N\sim(S_N\cap S_v)}(\underline{n}\cdot\dot{\underline{t}}\cdot\delta\underline{v})dS-\int_{(S_N\cap S_\sigma)}\dot{\overline{\underline{T}}}_t\cdot\delta\underline{v}dS\right\}=0 \tag{7.5}$$

with the subsidiary conditions

$$\dot{\underline{t}}=\dot{\underline{t}}^{o}+\dot{\underline{t}}^{b}\ ;\qquad \dot{\underline{t}}^{o}=\nabla\times\dot{\underline{\phi}}\ ;\qquad \nabla\cdot\dot{\underline{t}}^{b}=-\rho\dot{\underline{b}}\ ;$$

$$\underline{\omega}+\underline{\omega}^{T}=\underline{0}\qquad \dot{\underline{r}}=\tfrac{1}{2}(\dot{\underline{t}}+\underline{\tau}\cdot\underline{\omega}-\underline{\omega}\cdot\underline{\tau}+\dot{\underline{t}}^{T})\ ;$$

on each element, and globally

$$\underline{v}=\overline{\underline{v}}\ \text{ on }\ S_v;\qquad \delta\underline{v}=\underline{0}\ \text{ on }\ S_v\ ;$$

$\underline{v}$ and $\delta\underline{v}$ single valued along interelement boundaries.

To construct a finite element algorithm based on (7.4) and (7.5) we must be able to find representations for $\underline{v}$, $\delta\underline{v}$, $\underline{\omega}$, $\dot{\underline{t}}$, $\delta\underline{\omega}$, $\delta\dot{\underline{t}}$, and $\dot{\underline{r}}$ which satisfy all of the subsidiary conditions explicity. In the next few paragraphs such representations are discussed.

Let us represent the velocity *on the surface* of the N^{th} element by

$$\underline{v}(\underline{x})=\sum_{I=1}^{NQ}\underline{N}_I(\underline{x})\tilde{q}_N^I\qquad \tilde{q}=\begin{cases}\bar{q}\ \text{ on }\ S_N\cap S_v\\ q\ \text{ elsewhere}\end{cases} \tag{7.6}$$

where the $\underline{N}_i$ are (vector valued) isoparametric shape functions* and q^i are nodal velocity parameters. The shape functions are NQ in number. Those parameters determined by the velocity boundary condition are distinguished from the undetermined parameters by an overbar. The variation $\delta\underline{v}$ may be found from (7.6) as**

$$\delta\underline{v}(\underline{x}) = \sum_{i=1}^{NQ} \underline{N}_i(\underline{x})\,\delta q_N^i \,. \tag{7.7}$$

Note that $\underline{v} = \overline{\underline{v}}$ and $\delta\underline{v} = \underline{0}$ on S_v according to (7.6) and (7.7). Furthermore, when using the isoparametric shape functions, we can assure that $\underline{v}$ and $\delta\underline{v}$ are single valued along any interelement boundary simply by 'connecting' the nodes of the elements adjacent to that boundary. The easiest way to deal with this connectivity in practice is to index the velocity parameters node by node, for the whole body, instead of having indices which are independent on each element. The relation between the parameters with element-level indices (q_N^i) and those with global indices (Q^I) is formalized by the introduction of an 'assembly matrix' $[A_N]$ for each element such that

---

*see Ergatoudis et al. [43].

**It is unnecessary for $\underline{v}$ and $\delta\underline{v}$ to be so related when starting from a 'work' principle; similar statements may be made for $\underline{\omega}$ and $\delta\underline{\omega}$, $\dot{\underline{t}}$ and $\delta\dot{\underline{t}}$. We relate the total quantities to their variations so that 'work' and 'energy' formulations will coincide when an energy formulation exists.

$$\left.\begin{aligned} &\{\tilde{q}_N\} = [A_N]\{\tilde{Q}\} \ ; \qquad \tilde{Q} = \begin{cases} \bar{Q} \text{ on } S_v \\ Q \text{ elsewhere} \end{cases} \\ &\text{and} \\ &\{\delta q_N\} = [A_N]\{\delta Q\}. \end{aligned}\right\} \tag{7.8}$$

It turns out to be more natural to deal with the velocity boundary condition by constraining $\tilde{Q}$ than by constraining $\tilde{q}_N$, so the q_N and the $\tilde{q}_N$ (see 7.6) never need to be distinguished explicitly in practice. The total number of parameters $\tilde{Q}^I$ is called the 'number of degrees of freedom' of the finite element mesh, abbreviated NDOF.

We represent the spin $\underset{\sim}{\omega}$ and the stress function $\underset{\sim}{\Phi}$ in the N^{th} element's interior by

$$\underset{\sim}{\omega}(\underline{x}) = \sum_{i=1}^{NW} \underset{\sim}{QW}_i(\underline{x})\alpha_N^i \tag{7.9}$$

and

$$\underset{\sim}{\Phi}(\underline{x}) = \sum_{i=1}^{NT} \underset{\sim}{\Phi}_i(\underline{x})\beta_N^i \ ,$$

$\underset{\sim}{QW}_i$ and $\underset{\sim}{\Phi}_i$ being tensor valued shape functions. The actual functions used in the particular examples accompanying this work are detailed in Appendix C. The shape functions for the spin are chosen so that each satisfies

$$\underset{\sim}{QW}_i + \underset{\sim}{QW}_i^T = \underset{\sim}{0} \ . \tag{7.10}$$

The stress rate is represented in each element by

$$\dot{\underset{\sim}{t}}(\underset{\sim}{x}) = \sum_{i=1}^{NT} \underset{\sim}{QT}_i(\underset{\sim}{x})\beta_N^{\dot{i}} + \dot{\underset{\sim}{t}}^b(\underset{\sim}{x}) \tag{7.11}$$

where

$$\underset{\sim}{QT}_i(\underset{\sim}{x}) = \nabla \times \underset{\sim}{\phi}_i(\underset{\sim}{x}) \tag{7.12}$$

for each parameter $\beta_N^{\dot{i}}$. From (7.9) and (7.11) we obtain representations for $\delta\underset{\sim}{\omega}$ and $\delta\dot{\underset{\sim}{t}}$ as

$$\left.\begin{aligned} \delta\underset{\sim}{\omega}(\underset{\sim}{x}) &= \sum_{i=1}^{NW} \underset{\sim}{QW}_i(\underset{\sim}{x})\delta\alpha_N^{\dot{i}} \\ \delta\dot{\underset{\sim}{t}}(\underset{\sim}{x}) &= \sum_{i=1}^{NT} \underset{\sim}{QT}_i(\underset{\sim}{x})\delta\beta_N^{\dot{i}} \end{aligned}\right\} . \tag{7.13}$$

Finally we form $\dot{\underset{\sim}{r}} = \frac{1}{2}(\dot{\underset{\sim}{t}} + \underset{\sim}{\tau}\cdot\underset{\sim}{\omega} - \underset{\sim}{\omega}\cdot\underset{\sim}{\tau} + \dot{\underset{\sim}{t}}^T)$ as

$$\dot{\underset{\sim}{r}}(\underset{\sim}{x}) = \sum_{i=1}^{NT} \tfrac{1}{2}(\underset{\sim}{QT}_i + \underset{\sim}{QT}_i^T)\beta_N^{\dot{i}} + \sum_{i=1}^{NW} \tfrac{1}{2}(\underset{\sim}{\tau}\cdot\underset{\sim}{QW}_i - \underset{\sim}{QW}_i\cdot\underset{\sim}{\tau})\alpha_N^{\dot{i}} . \tag{7.14}$$

The functions $\underset{\sim}{v}$, $\delta\underset{\sim}{v}$, $\underset{\sim}{\omega}$, $\dot{\underset{\sim}{t}}$, $\delta\underset{\sim}{\omega}$, $\delta\dot{\underset{\sim}{t}}$, and $\dot{\underset{\sim}{r}}$, when represented in the forms (7.6), (7.7), (7.8), (7.9), (7.11), (7.13), and (7.14), satisfy all of the subsidiary conditions previously mentioned, and are therefore admissible to the boundary value problem as stated by (7.4) and (7.5).

Putting the representations for $\underset{\sim}{v}$, $\delta\underset{\sim}{v}$, $\underset{\sim}{\omega}$, $\dot{\underset{\sim}{t}}$, $\delta\underset{\sim}{\omega}$, $\delta\dot{\underset{\sim}{t}}$, and $\dot{\underset{\sim}{r}}$ into

the functionals (7.4) and (7.5) and carrying out the assigned integrations yields the following finite element equations (in which the index 'N' is suppressed on the stress and spin parameters):

$$\{\delta\alpha\}^T \left\{ -[H^{11} \quad H^{12}] \begin{Bmatrix} \alpha \\ \beta \end{Bmatrix} + \{P^{\alpha,b}\} + \{P^{\alpha,\Sigma}\} \right\} = 0 \tag{7.15}$$

$$\{\delta\beta\}^T \left\{ -[H^{21} \quad H^{22}] \begin{Bmatrix} \alpha \\ \beta \end{Bmatrix} + \{P^{\beta,b}\} + \{P^{\beta,\Sigma}\} + [G]\{\tilde{q}_N\} \right\} = 0 \tag{7.16}$$

$$\sum_{N=1}^{NELM} \left\{ \{\delta q_N\}^T [0 \quad G_H^T] \begin{Bmatrix} \alpha \\ \beta \end{Bmatrix} - \{\delta q_N\}^T \{F_N\} \right\} = 0 \ . \tag{7.17}$$

Henceforth we refer to (7.15) as AMB, to (7.16) as compatibility, and to (7.17) as TBC. The individual matrices are defined below:

$$H_{ij}^{11} = \int_{V_N} \{(\underset{\sim}{\tau} \cdot \underset{\sim}{QW}_i) : \underset{\approx}{D} : (\underset{\sim}{\tau} \cdot \underset{\sim}{QW}_j) + \underset{\sim}{\tau} : (\underset{\sim}{QW}_i \cdot \underset{\sim}{QW}_j)\} dV \tag{7.18}$$

$$H_{ij}^{12} = \int_{V_N} \{(\underset{\sim}{\tau} \cdot \underset{\sim}{QW}_i) : \underset{\approx}{D} : (\underset{\sim}{QT}_j) - \underset{\sim}{QW}_i : \underset{\sim}{QT}_j\} dV \tag{7.19}$$

$$H_{ij}^{21} = \int_{V_N} \{(\underset{\sim}{QT}_i) : \underset{\approx}{D} : (\underset{\sim}{\tau} \cdot \underset{\sim}{QW}_j) - \underset{\sim}{QT}_i : \underset{\sim}{QW}_j\} dV \tag{7.20}$$

$$H_{ij}^{22} = \int_{V_N} \{(\underset{\sim}{QT}_i) : \underset{\approx}{D} : (\underset{\sim}{QT}_j)\} dV \tag{7.21}$$

$$G_{ij} = \int_{S_N} \underset{\sim}{n} \cdot (\underset{\sim}{QT}_i) \cdot (\underset{\sim}{N}_j) dS \tag{7.22}$$

$$F_i = \int_{(S_N \cap S_\sigma)} \dot{\underline{T}}_t \cdot (\underline{N}_i) dS \tag{7.23}$$

$$P_i^{\alpha,b} = \int_{V_N} \left\{ (\underset{\sim}{QW}_i) : [\dot{\underline{t}}^b + (\underset{\approx}{D} : \dot{\underline{t}}^b) \cdot \underline{\tau} + \frac{1}{h} \underline{\tau}] \right\} dV \tag{7.24}*$$

$$P_i^{\beta,b} = \int_{V_N} \left\{ (\underset{\sim}{QT}_i) : (-\underset{\approx}{D} : \dot{\underline{t}}^b) \right\} dV \tag{7.25}$$

$$P_i^{\alpha,\Sigma} = \int_{V_N} \left\{ (\underline{\tau} \cdot \underset{\sim}{QW}_i) : \underset{\approx}{D} : \underline{\Sigma} \right\} dV \tag{7.26}$$

$$P_i^{\beta,\Sigma} = \int_{V_N} \left\{ (\underset{\sim}{QT}_i) : \underset{\approx}{D} : \underline{\Sigma} \right\} dV \tag{7.27}$$

and $\underset{\approx}{D}$ is obtained from $\underset{\approx}{W}^{-1}$ by symmetrization:

$$D_{ijkl} = \tfrac{1}{4}(W^{-1}_{ijkl} + W^{-1}_{jikl} + W^{-1}_{ijlk} + W^{-1}_{jilk}) \, . \tag{7.28}$$

This symmetrization is easily done after $\underset{\approx}{W}^{-1}$ is computed, and serves to reduce by a factor of four the number of multiplications required to compute the H matrices (7.18) through (7.21), and other matrices involving $\underset{\approx}{W}^{-1}$. The integrations must be performed numerically since the integrands and the domain of the element change during the deformation. In the examples accompanying this work only quadrilateral elements were used, so symmetric Gaussian quadrature rules were used for the integration.**

*the last term in the integrand is a residual whose significance is explained in the next chapter.

**see Tong and Rossettos [39], especially chapter six.

The procedure which leads one from equations (7.15) and (7.16) to the element stiffness matrix is virtually identical to that of Pian [3]. We define the element 'H-matrix' as

$$[H] = \begin{bmatrix} H^{11} & H^{12} \\ H^{21} & H^{22} \end{bmatrix} \tag{7.29}$$

and loads $\{P^b\}$ and $\{P^\Sigma\}$, due to body force and fluidity, respectively, as

$$\{P^b\} = \begin{Bmatrix} P^{\alpha,b} \\ P^{\beta,b} \end{Bmatrix} \quad ; \qquad \{P^\Sigma\} = \begin{Bmatrix} P^{\alpha,\Sigma} \\ P^{\beta,\Sigma} \end{Bmatrix} . \tag{7.30}$$

Then (7.15) and (7.16) may be collected into a single equation as

$$[H]\begin{Bmatrix} \alpha \\ \beta \end{Bmatrix} = \begin{bmatrix} 0 \\ G \end{bmatrix} \{\tilde{q}\} + \{P^b + P^\Sigma\}. \tag{7.31}$$

If $\underset{\approx}{D}$ is symmetric, that is, if $W^{-1}_{ijkl} = W^{-1}_{klij}$, then from (7.18) through (7.21) we easily determine that [H] is symmetric.

If the H-matrix is not singular, then we solve the matrix equation (NQ+1 right hand sides)

$$[H][H^{-1}G \quad H^{-1}P] = \left[\begin{array}{c|c} 0 & \\ G & P^b + P^\Sigma \end{array}\right] \tag{7.32}$$

on each element. Explicit calculation of the inverse of [H] is not only unnecessary, but substantially increases the time required to generate the element stiffness matrix. According to (7.31), the spin

and stress parameters on each element are given by

$$\begin{Bmatrix}\alpha\\ \beta\end{Bmatrix} = [H^{-1}G]\{\tilde{q}\} + \{H^{-1}P\}. \tag{7.33}$$

Using (7.33) to eliminate $\{\alpha/\beta\}$ from TBC (7.17) leads to

$$\sum_{N=1}^{NELM} \Big\{\{\delta q_N\}^T[K_N]\{\tilde{q}_N\} + \{\delta q_N\}^T [0 \quad G_N^T]\{H^{-1}P_n\} - \{\delta q_N\}^T\{F_N\}\Big\} = 0 \tag{7.34}$$

in which the element stiffness matrix has been identified as

$$[K_N] = [0 \quad G_N^T]\,[H^{-1}G_N]\,, \tag{7.35}$$

and the resultant nodal 'forces' are given by

$$-[0 \quad G_N^T]\,\{H^{-1}P_N\} + \{F_N\}\,. \tag{7.36}$$

It is easily verified that the element stiffness matrix [K] is symmetric if [H] is, and so the symmetry of [K] ultimately depends upon the symmetry of the constitutive matrix $\underset{\approx}{W}$.

To this point all of the finite element equations are independent on each element. The formal assembly of the global stiffness matrix and loads is accomplished by introduction of the assembly matrices (see 7.8) to (7.34) so that the element level velocity parameters may be expressed as functions of the global velocity

parameters. For $\{\tilde{q}\}$ and $\{\delta q\}$ we write

$$\{\tilde{q}_N\} = [A_N]\{Q + \overline{Q}\} \quad ; \qquad \{\delta q_N\} = [A_N]\{\delta Q\} \; ;$$

and from (7.34) thus obtain

$$\{\delta Q\}^T[K_G]\{Q\} = \{\delta Q\}^T\{P_G\} - \{\delta Q\}^T[K_G]\{\overline{Q}\} \; . \tag{7.37}$$

In equation (7.37) the global stiffness matrix $[K_G]$ and the loads $\{P_G\}$ are defined by

$$[K_G] = \sum_{N=1}^{NELM} [A_N]^T[K_N][A_N] \tag{7.38}$$

and

$$\{P_G\} = [A_N]^T \left\{ \{F_N\} - [0 \quad G_N^T]\{H^{-1}P_N\} \right\} . \tag{7.39}$$

The load matrix $\{P_G\}$ contains contributions from the prescribed body for rate $\dot{\underset{\sim}{b}}$, the relaxation $\underset{\sim}{\Sigma}$, and the traction boundary condition $\dot{\underline{T}}_t$. The global stiffness matrix, as defined by (7.38), will be singular for rigid translations, but not for rigid spin (except in the case that there is an 'axis of equilibrium' [44]). In order to solve the equation (7.37) we define a modified global stiffness matrix [K*] and a modified load {P*} as follows:

$$K^*_{IJ} = \begin{cases} \delta_{IJ} \text{ if } (\tilde{Q}_I = \bar{Q}_I) \text{ or } (\tilde{Q}_J = \bar{Q}_J) \\ K_{IJ} \text{ otherwise} \end{cases} \tag{7.40}$$

$$P^*_I = \begin{cases} Q_I \quad \text{if } (Q_I = \bar{Q}_I) \\ P_I - \sum_{J=1}^{NELM} K^G_{IJ}\bar{Q}_J \quad \text{otherwise} . \end{cases} \tag{7.41}$$

Then (7.37) may be replaced by

$$[K^*]\{\tilde{Q}\} = \{P^*\} . \tag{7.42}$$

If $[K^*]$ is not singular, then we solve (7.42) for $\{\tilde{Q}\}$,

$$\{\tilde{Q}\} = [K^*]^{-1}\{P^*\} . \tag{7.43}$$

By backsubstitution we obtain the velocity (on the boundary of each element), the spin and the stress rate on each element:

$$\{\tilde{q}_N\} = [A_N][K^*]^{-1}\{P^*\} \tag{7.44}$$

$$\begin{Bmatrix} \alpha_N \\ \beta_N \end{Bmatrix} = [H^{-1}G_N][A_N][K^*]^{-1}\{P^*\} + \{H^{-1}P_N\} \tag{7.45}$$

$$\underline{v}(\underline{x}) = [\underline{N}(\underline{x})][A_N][K^*]^{-1}\{P^*\} \tag{7.46}$$

C-2

$$\begin{Bmatrix} \underset{\sim}{\omega}(\underset{\sim}{x}) \\ \dot{\underset{\sim}{t}}(\underset{\sim}{x}) - \dot{\underset{\sim}{t}}^{b}(\underset{\sim}{x}) \end{Bmatrix}_N = \begin{bmatrix} \underset{\sim}{Q}\underset{\sim}{W}(\underset{\sim}{x}) & 0 \\ 0 & \underset{\sim}{Q}\underset{\sim}{T}(\underset{\sim}{x}) \end{bmatrix} \left\{ [H^{-1}G_N][A_N][K^*]^{-1}\{P^*\} + \{H^{-1}P_N\} \right\} \tag{7.47}$$

Equations (7.46) and (7.47) comprise the approximate solution of the boundary value problem.

The velocity $\underset{\sim}{v}(\underset{\sim}{x})$ is determined by (7.46) *on the element boundary only*. On an element's interior we may construct $\underset{\sim}{\varepsilon}(\underset{\sim}{x})$ from $\dot{\underset{\sim}{t}}(\underset{\sim}{x})$ and $\underset{\sim}{\omega}(\underset{\sim}{x})$ according to the constitutive equation (5.5). If our computations have produced an exact solution, then we can find the velocity field on the interior of an element by integration:

$$\underset{\sim}{v}(\underset{\sim}{x}) = \underset{\sim}{v}(\underset{\sim}{x}_o) + \int_{\underset{\sim}{x}_o}^{\underset{\sim}{x}} (\underset{\sim}{\varepsilon} + \underset{\sim}{\omega}) \cdot d\underset{\sim}{x} \quad ,$$

where $\underset{\sim}{x}_o$ is some point on the element's boundary. However the finite element algorithm generally will not produce exact solutions, so the integral expression above is of no use in defining the velocity on the interior of the element. Previous researchers using complementary work and energy based finite elements do not mention this problem, and it is left for the reader to assume that they found the velocity on the interior of the element by interpolation of the boundary velocities (by use of the isoparametric shape functions). If the reader will recall the discussion surrounding the derivation of the generalized compatibility (5.21), it is evident that there is reason to doubt the validity of this procedure. In the absence of supporting arguments, it amounts to assigning the velocity on the interior of the element in

an arbitrary manner.

A little light is shed on this problem by the following heuristic argument. In preparation, we consider rules by which fields $\underset{\sim}{v}$, $\underset{\sim}{\omega}$, and $\dot{\underset{\sim}{t}}$ may be judged 'admissible' or 'inadmissible' on a single element. Admissible velocity fields are those which satisfy

$$\int_V \{\underset{\sim}{v} \cdot \underset{\sim}{v} + (\nabla \underset{\sim}{v}) : (\nabla \underset{\sim}{v})\} dV < \infty \quad ; \tag{7.48}$$

and the admissible velocity fields comprise an inner product space R_v. Each velocity field in R_v takes on certain values on the boundary of the element, and the space made up of those boundary values we denote R_v^o. In a similar manner we define the space R_ω as the space of all tensors which satisfy

$$\int_V (\underset{\sim}{\omega} : \underset{\sim}{\omega}) dV < \infty ; \qquad \int_V (\underset{\sim}{\omega} + \underset{\sim}{\omega}^T) : (\underset{\sim}{\omega} + \underset{\sim}{\omega}^T) dV = 0 \quad ; \tag{7.49}$$

and the space R_t to be the space of all tensors which satisfy

$$\int_V (\dot{\underset{\sim}{t}} : \dot{\underset{\sim}{t}}) dV < \infty ; \qquad \int_V (\dot{\underset{\sim}{t}} : \nabla \delta \underset{\sim}{v}) dV = 0 \tag{7.50}$$

for arbitrary $\delta \underset{\sim}{v}$, $\delta \underset{\sim}{v} = \underset{\sim}{0}$ on S. An inner product on $R_\omega \times R_t$ is given by

$$(u,w)_{R_\omega \times R_t} = \int_V (\underset{\sim}{\omega} : \underset{\sim}{\omega}' + \dot{\underset{\sim}{t}} : \dot{\underset{\sim}{t}}') dV \tag{7.51}$$

where u and w are the ordered pairs of tensors

$$u = \langle \underset{\sim}{\omega}, \dot{\underset{\sim}{t}} \rangle \in R_\omega \times R_t; \qquad w = \langle \underset{\sim}{\omega}', \dot{\underset{\sim}{t}}' \rangle \in R_\omega \times R_t .$$

Now we define a linear map from $R_v^o \times R_\omega \times R_t$ to $R_\omega \times R_t$ by

$$w = B(u) \tag{7.52}$$

where $u = \langle \underset{\sim}{v}, \underset{\sim}{\omega}, \dot{\underset{\sim}{t}} \rangle$ is any element of $R_v^o \times R_\omega \times R_t$, and

$$w = \langle \tfrac{1}{2}[(\underset{\sim}{\varepsilon} + \underset{\sim}{\omega}) \cdot \underset{\sim}{\tau} + \dot{\underset{\sim}{t}} - \dot{\underset{\sim}{t}}^T - \underset{\sim}{\tau} \cdot (\underset{\sim}{\varepsilon} - \underset{\sim}{\omega})], \; -\underset{\sim}{\varepsilon} + \underset{\sim}{\omega} + \nabla \underset{\sim}{v} \rangle \tag{7.53}$$

is an element of $R_\omega \times R_t$ determined uniquely by u. In (7.53) we have written $\underset{\sim}{\varepsilon}$ for the constitutive function (5.5). The variational problem (7.4) may now be stated compactly as

$$\text{find} \quad u \in R_v^o \times R_\omega \times R_t \quad \text{such that for all} \quad \delta w \in R_\omega \times R_t$$

$$(\delta w, B(u))_{R_\omega \times R_t} = 0 \tag{7.54}$$

(that is, 7.54 is equivalent to 7.4). The problem in (7.52) of defining w uniquely for assigned u is solved if we can show there is a unique $\underset{\sim}{v}$ in R_v such that $(-\underset{\sim}{\varepsilon} + \underset{\sim}{\omega} + \nabla \underset{\sim}{v})$ belongs to R_t. We note in passing that this problem is identical to the problem in the finite element algorithm of defining $\underset{\sim}{v}$ on the interior of an element. The criterion that $(-\underset{\sim}{\varepsilon} + \underset{\sim}{\omega} + \nabla \underset{\sim}{v})$ must satisfy to be an element of R_t is given by (7.50):

$$\int_V \{(-\underset{\sim}{\varepsilon} + \underset{\sim}{\omega} + \nabla \underline{v}) : \nabla \delta \underline{v}\} dV = 0 \tag{7.55}$$

for arbitrary $\delta \underline{v}$, $\delta \underline{v} = \underline{0}$ on S. Equation (7.55), along with the boundary values of $\underline{v}$ (the first component of the argument of B), and the values of $\underset{\sim}{\varepsilon}$ and $\underset{\sim}{\omega}$ (from the second and third components of the argument of B) constitute a generalized Dirichlet problem, whose solution we presume to exist and be unique, and to depend linearly upon the argument of B. We conclude by remarking that the variational problem (7.54) would not make sense if $\underline{v}$ were assigned in an arbitrary manner.

The finite element counterpart of equation (7.55), including inhomogeneities from $\overset{\cdot b}{\underset{\sim}{t}}$ and $\underset{\sim}{\Sigma}$, is given by

$$[\hat{C}_N]\{\hat{q}\} = [L_N^1 \quad L_N^2] \begin{Bmatrix} \alpha_N \\ \beta_N \end{Bmatrix} - [C_N]\{\tilde{q}_N\}^{\cdot} + \{L^P\} , \tag{7.56}$$

where the individual matrices are defined below:

$$\hat{C}_{ij} = \int_{V_N} \nabla \underline{\hat{N}}_i : \nabla \underline{\hat{N}}_j \, dV \tag{7.57}$$

$$C_{ij} = \int_{V_N} \nabla \underline{\hat{N}}_i : \nabla \underline{N}_j \, dV \tag{7.58}$$

$$L^1_{ij} = \int_{V_N} \nabla \underline{\hat{N}}_i : [\underset{\approx}{D} : (\underset{\sim}{\tau} \cdot \underset{\sim}{QW}_j) + \underset{\sim}{QW}_j] dV \tag{7.59}$$

$$L^2_{ij} = \int_{V_N} \nabla \underline{\hat{N}}_i : [\underset{\approx}{D} : (\underset{\sim}{QT}_j)] dV \tag{7.60}$$

$$L^P_i = \int_{V_N} \nabla \underline{\hat{N}}_i : [\underset{\approx}{D} : (\overset{\cdot b}{\underset{\sim}{t}} - \underset{\sim}{\Sigma})] dV \, . \tag{7.61}$$

In equations (7.57) through (7.61) the $\underline{\hat{N}}_i$ are polynomial shape functions which vanish on S_N; that is, shape functions for 'internal' nodes, and the $\underline{N}_i$, $\underline{\underset{\sim}{QW}}_i$, and $\underline{\underset{\sim}{QT}}_i$ are the shape functions for boundary velocity, spin, and stress rate which have been previously discussed. Using (7.45) to eliminate $\{\alpha_N/\beta_N\}$ from (7.56) leads to

$$\{\hat{q}_N\} = [\hat{C}_N]^{-1}\left[[L_N^1 \quad L_N^2][H^{-1} \quad G_N] - [C_N]\right][A_N]\{\tilde{Q}\} \qquad (7.62)$$

$$+ [\hat{C}_N]^{-1}\left\{[L_N^1 \quad L_N^2]\{H^{-1} \quad P_N\} + \{L_N^P\}\right\}.$$

Equation (7.62) expresses the velocities of the internal nodes of an element as a function of the velocities of the boundary nodes. In the sense that the problem of determining the velocities of interior nodes is the inverse of the 'condensation' problem encountered in ordinary velocity-based finite element algorithms, we might call the procedure above 'inverse condensation.'

In view of the fact that use of the inverse condensation is potentially costly (because of the extra computation), an element for which interpolation of the boundary velocity to the interior is consistent with inverse condensation would be highly desirable. Consider the following examples in which result of inverse condensation is illustrated.

In the application of a stress-based finite element algorithm to beam problems,* usually one can only find a piecewise linear

*see Murakawa et al. [13], particularly Figure 2 therein.

approximation for the elastic curve, an approximation with 'corners' at the interelement boundaries. The only way to improve the approximation is to increase the number of elements per unit length of beam. Application of the inverse condensation procedure leads to (ignoring the length change of the beam)

$$v^2{}_{,11} = -\dot{M}/EI$$

a familiar formula from beam theory. If the moment $\dot{M}$ is piecewise linear and continuous at the interelement boundaries, then one may find a cubic spline for the elastic curve without any increase in the number of elements.

In the application of a stress-based finite element algorithm to two-dimensional problems, one typically uses four or eight noded quadrilateral elements. A simple example such as provided by beams is not available in this case, but we note that the lowest order polynomial function which vanishes on the boundary of a quadrilateral is *four*; being of the form

$$(x^2 - 1)(y^2 - 1) \ . \tag{7.63}$$

The immediate conclusion is that the highest order complete polynomial which may be represented exactly on a quadrilateral with boundary nodes only is *three*. The shape functions for four and eight noded quadrilaterals involve no fourth order terms, so one could expect to gain nothing in accuracy by adding an extra degree of freedom for the shape

(7.63). On the other hand, the shape functions for a 12 (or higher) noded quadrilateral do contain fourth order terms, so if terms of the form (7.63) are ignored, it amounts to assigning the velocity on the interior of the element in an arbitrary manner. Thus, the 'inverse condensation' is not necessary for the 'low order' four and eight noded elements, but should be used if 'higher order' elements are used. Similar arguments may be given for triangular elements and three dimensional elements. In the examples accompanying this work, only four and eight noded elements were used.

Numerical Stability Criteria

The finite element algorithm just described does not necessarily yield an approximation to the solution of the boundary value problem. In reviewing the development, we surmise that the algorithm may be carried through to obtain the approximate solution (7.46) and (7.47) if

$\underset{\approx}{W}$ is nonsingular in V (see 5.5) (7.64)

$[H_N]$ is nonsingular on each element (see 7.32) (7.65)

$[G_N]\{\tilde{q}_N\} = \{0\}$ only for rigid translations (7.66)

$[K^*]$ is nonsingular (see 7.42) . (7.67)

The first of these is satisfied by material models found in the engineering literature except for isolated states of stress. The last

of these is equivalent to the uniqueness criterion based on the Second complementary virtual work principle, presented in Chapter VI.

Satisfaction of the second and third conditions above depends strongly upon the particular functions $\underset{\sim}{N}_i$, $\underset{\sim}{QW}_i$, and $\underset{\sim}{QT}_i$ of the representations (7.6), (7.9), and (7.11). In this section we discuss criteria whose fulfillment is necessary for the satisfaction of (7.65) and (7.66). Such criteria are called 'numerical stability criteria.'

An analogue of the condition (7.66) arises in stress-based finite element algorithms in linear elastostatics. The analysis of Tong and Pian [45], with a minor modification, applies in the present case. The rank of the matrix [G] is usually

$$\min(NT, NQ - T) \tag{7.68}$$

where NT is the number of stress rate parameters, NQ the number of velocity parameters, and T the number of *translational* degrees of freedom of an element. It is well known that if $NT < NQ - T$, then 'kinematic modes' (deformations to which the element offers no resistance) will occur. The rank condition which is necessary (and usually sufficient) for the satisfaction of (7.66) is

$$NT \geq NQ - T \quad . \tag{7.69}$$

In the examples accompanying this work, the number of stress rate parameters always equalled or exceeded the number of velocity parameters,

and no kinematic mode was encountered.

A second type of kinematic mode can occur when the finite element algorithm is set up in a coordinate system which has singularities, such as cylinderical coordinates. This second type of mode occurs when

$$\underset{\sim}{N}_j dS = 0 \qquad \text{everywhere on } S_N \tag{7.70}$$

for some particular velocity shape function. An example is provided by an eight noded quadralateral element in cylinderical coordinates, with one edge along the z axis ($r = 0$). The shape function for the middle node on that edge vanishes everywhere on S except on the edge where dS is zero. Thus, the column in [G] corresponding to that node consists entirely of zeros. In such a case the kinematic mode may be avoided by eliminating the offending node entirely, or its value may be found by the inverse condensation procedure.

The condition (7.65) turns out to be the source of most of the difficulty of using the present stress-based finite element algorithm. Even when [H] is not singular, it may be so ill conditioned that an accurate solution of the matrix equation (7.32) can only be found by scaling.* In any case, the problem may be overcome by replacing $\underset{\sim}{QW}_i$ and $\underset{\sim}{QT}_i$ in a trial and error process until nonsingular [H] is found.

*that is, adjusting the magnitude of the stress and spin functions to improve the condition of [H].

Murakawa [10] gave the necessary (but not sufficient) rank condition that the number of stress functions exceed the number of spin functions.

After a number of trials, it became apparent that when [H] was singular, the spurious eigenmode consisted of a pure (but inhomogeneous) spin. Moreover, if a combination of functions $[\underset{\sim}{QW}]$ and $[\underset{\sim}{QT}]$ was found to be acceptable in the stress-free state, it remained so as the deformation progressed. Setting the initial stress to zero, the criterion sufficient for no spin mode to occur follows as

$$[H_o^{21}]\{\delta\alpha\} \neq 0 \; ; \qquad [H_o^{21}]_{ij} = \int_{V_N} (\underset{\sim}{QT}_i : \underset{\sim}{QW}_j)\, dV \quad . \tag{7.71}$$

A criterion similar to (7.71), but for a finite element algorithm of elastic membrane theory, was given by de Veubeke and Millard [6], but their conclusions differ slightly from our own. A necessary condition for the satisfaction of (7.71) is that

$$NT^* \geq NW \tag{7.72}$$

where NT* is the number of stress shape functions $\underset{\sim}{QT}_i$ whose skew parts do not vanish, and NW is the number of spin functions $\underset{\sim}{QW}_j$. In [6], the authors suggest that the polynomial degree of the spin field m be related to the polynomial degree of the stress field n as

$$m = n - 1 \quad , \tag{7.73}$$

calling the case m = n the "classical equilibrium model." In numerical experience with the present finite element algorithm we find that if m is less than n, then the angular momentum balance is not satisfied with reasonable (pointwise) accuracy. The degree of the spin field and the degree of the stress rate field were always the same in the examples accompanying this work. This amounts to the condition

$$[H_o^{21}]^T\{\delta\beta\} = 0 \tag{7.74}$$

only for $\{\delta\beta\}$ which produce symmetric stress rate fields.

CHAPTER VIII

INTEGRATION OF THE MOTION OF THE BODY

Introduction

Consider a body in a configuration C(t). We suppose that a particular finite element subdivision of the body has been defined, and that the stress $\underset{\sim}{\tau}$ is known at each quadrature point on each element of the body. Then for assigned body force rate $\dot{\underline{b}}$, nominal traction rate $\dot{\underline{T}}_t$ on S_σ, and velocity $\bar{\underline{v}}$ on S_v, the finite element algorithm presented in the previous chapter enables us to compute the (instantaneous) velocity $\underline{v}(\underline{x},t)$ and stress rate $\dot{\underset{\sim}{t}}(\underline{x},t)$. To be more explicit, the information above suffices to compute the matrices [H], [G], {F}, and {P} on each element,* and hence, the velocity and stress rate throughout the body (see 7.46 and 7.47, and development thereof). The matrices [H] and {P} each depend upon the constitutive matrix $\underset{\approx}{W}$ (through $\underset{\sim}{D}$), and hence upon the quadrature point values of the stress, but in an inexplicit way.**

We formally indicate the dependence of the nodal values of the velocity $\{\underline{v}\} = \{\underline{v}^1,\underline{v}^2,\ldots,\underline{v}^{ND}\}$ (ND being the number of nodes) and the quadrature point values of the stress rate $\{\dot{\underset{\sim}{t}}\} = \{\dot{\underset{\sim}{t}}^1,\dot{\underset{\sim}{t}}^2,\ldots,\dot{\underset{\sim}{t}}^G\}$ (G

---

*and if need be, the matrices $[\hat{C}]$, [C], [L], and $\{L^P\}$.

**when the constitutive matrix $\underset{\approx}{W}$ is a constant, the dependence of $\underset{\approx}{W}^{-1}$ on $\underset{\sim}{\tau}$ is approximately affine; see Appendix B.

being the number of quadrature points) upon the nodal positions $\{\underset{\sim}{x}\} = \{\underset{\sim}{x}^1, \underset{\sim}{x}^2, \ldots, \underset{\sim}{x}^{ND}\}$, the quadrature point values of the stress $\{\underset{\sim}{\tau}\} = \{\underset{\sim}{\tau}^1, \underset{\sim}{\tau}^2, \ldots, \underset{\sim}{\tau}^G\}$, and the time dependent prescribed loads by writing*

$$\{\underset{\sim}{v}\} = f[\{\underset{\sim}{x}\}, \{\underset{\sim}{\tau}\}, t] \tag{8.1}$$

$$\{\dot{\underset{\sim}{t}}\} = g[\{\underset{\sim}{x}\}, \{\underset{\sim}{\tau}\}, t] \quad . \tag{8.2}$$

Since each element node is associated with the same material point throughout a deformation, and likewise for each quadrature point, we may write each component of $\{x\}$, $\{v\}$, $\{\underset{\sim}{\tau}\}$, and $\{\dot{\underset{\sim}{t}}\}$ as

$$\underset{\sim}{x}^I = \underset{\sim}{\chi}_\tau(\underset{\sim}{X}^I, t) \ ;$$

$$\underset{\sim}{v}^I = \dot{\underset{\sim}{\chi}}_\tau(\underset{\sim}{X}^I, t) \ ;$$

$$\underset{\sim}{\tau}^I = (1/J_\tau^I)\underset{\sim}{F}_\tau^I \cdot \underset{\sim}{t}_\tau(\underset{\sim}{X}^I, t) \ ;$$

$$\dot{\underset{\sim}{t}}^I = (1/J_\tau^I)\underset{\sim}{F}_\tau^I \cdot \dot{\underset{\sim}{t}}_\tau(\underset{\sim}{X}^I, t) \ .$$

The quadrature point values of the deformation gradient

*The functions f and g are introduced specifically as a 'shorthand' for the solutions of the finite element equations, as given by (7.46) and (7.47). From (7.46) and (7.47) it is clear that integrations may be carried out on one element at a time.

$$\underset{\sim}{F}_{\tau}^{I} = (\nabla_{X}\underset{\sim}{\chi}_{\tau}(\underset{\sim}{X},t))^{T}\Big|_{\underset{\sim}{X}=\underset{\sim}{X}^{I}}$$

and its determinant

$$J_{\tau}^{I} = \det \underset{\sim}{F}_{\tau}^{I}$$

depend on the nodal positions through the isoparametric shape functions. The reference configuration indicated by the subscript τ is absolutely arbitrary and may be changed as frequently as desired. Typically it would be chosen on the basis of economy (e.g., to minimize storage requirements).

The equations (8.1) and (8.2) may now be written as

$$\{\dot{\underset{\sim}{\chi}}_{\tau}\} = f_{\tau}[\{\underset{\sim}{\chi}_{\tau}\},\{\underset{\sim}{t}_{\tau}\},t] \tag{8.3}$$

$$\{\dot{\underset{\sim}{t}}_{\tau}\} = g_{\tau}[\{\underset{\sim}{\chi}_{\tau}\},\{\underset{\sim}{t}_{\tau}\},t] \tag{8.4}$$

where f_{τ} and g_{τ} are defined by

$$f_{\tau}[\cdot,\{\dot{\underset{\sim}{t}}_{\tau}\},\cdot] = f[\cdot,\{\frac{1}{J_{\tau}}\underset{\sim}{F}_{\tau}\cdot\underset{\sim}{t}_{\tau}\},\cdot] \tag{8.5}$$

$$g_{\tau}[\cdot,\{\underset{\sim}{t}_{\tau}\},\cdot] = [J_{\tau}\underset{\sim}{F}_{\tau}^{-1}]g[\cdot,\{\frac{1}{J_{\tau}}\underset{\sim}{F}_{\tau}\cdot\underset{\sim}{t}_{\tau}\},\cdot]\ . \tag{8.6}$$

Equations (8.3) and (8.4) represent a system of nonlinear ordinary differential equations. On account of the complicated way in which

the finite element equations depend upon the stress, the functions f_τ and g_τ (or even f and g) cannot be written explicitly. This fact makes stability analyses such as those of Cormeau [46] and Hughes and Taylor [20] impossible for the equations (8.3) and (8.4).

An initial value problem may be set if initial values of $\underset{\sim}{\chi}_\tau$ and $\underset{\sim}{t}_\tau$, the constitutive equation, and a program of loads are given. It is assumed that solutions of the initial value problem exist for sufficiently smooth and physically tenable initial data, at least for some range of deformation from the initial configuration.

Numerical Integration of the Initial Value Problem

The initial value problem posed by (8.3), (8.4) and appropriate initial data is dependent upon the finite element equations as discussed in the first section. From that same discussion, and from the presentation of the finite element equations (Chapter VII), it is also clear that the finite element-initial value problem is predisposed to numerical integration. In this section we indicate the types of numerical integration schemes suitable for the present problem, and mention a few important differences between the various types.

The finite element-initial value problem may be integrated by single step explicit schemes, multistep explicit schemes, or (generally multistep) predictor-corrector schemes. A number of these schemes are discussed in the textbook of Conte and de Boor [47]. Three important facts to be kept in mind when choosing a particular scheme are

(1) the solution vector $<\{\underset{\sim}{\chi}_\tau(t_N)\},\{\underset{\sim}{t}_\tau(t_N)\}>$ at the time $t = t_N$

is of scalar dimension NDOF + 9 • G, where NDOF is the number of kinematic degrees of freedom of the mesh and G is the total number of quadrature points. Storage required for implementation of different integration schemes can vary appreciably.

(2) evaluation of $<f_\tau, g_\tau>$ is expensive on account of the complexity of the finite element equations.

(3) the functions f_τ and g_τ are generally discontinuous at points $<\{\underset{\sim}{\chi}_\tau\}, \{\underset{\sim}{t}_\tau\}>$ which correspond to material yield surfaces.

The multistep methods (explicit and predictor-corrector) require relatively few evaluations of $<f_\tau, g_\tau>$ per step; this is an attractive feature. However, multistep methods are not self starting, the time step is not easily changed, they have relatively large storage requirements (since several past values of $<f_\tau, g_\tau>$ must be carried along), and moreover, they cannot be expected to be accurate when the solution crosses a yield surface (since they are based on smooth polynomial interpolation of the solution over several time steps).

On the other hand, the single step methods (explicit and predictor-corrector) are easily started, the time step size is easily adjusted, and they have relatively small storage requirements. They can be expected to perform more favorably than the multistep methods when the solution crosses a yield surface since smoothing over several time steps is not built in. The disadvantage of the single step methods is that a relatively larger number of evaluations of $<f_\tau, g_\tau>$ are required per step to achieve a given accuracy when a yield surface is not crossed. However, the advantages of single step methods seem

to far outweigh the disadvantages.

In the examples accompanying this work the Euler and classical second and fourth order Runge-Kutta methods were used. Details of these methods may be found in the textbook of Conte and de Boor [47]. We note that the second order Runge Kutta method is equivalent to an Euler predictor and a single application of the trapezoid rule as a corrector. Errors of the Euler method were gauged (qualitatively) by step-halving and by comparison to results of second order integration for randomly selected time steps. Errors of the second order Runge-Kutta method were gauged in like manner; by step halving and comparison to results obtained by fourth order integration. The integration schemes used in the examples accompanying this work varied from problem to problem, and sometimes within a problem. Full details are given in the description of the individual problems, in the chapter following this one.

We assert that the stress $\underset{\sim}{t}_\tau$ (and hence $\underset{\sim}{\tau}$) integrated numerically satisfies LMB. As an example, consider the Euler-Trapezoid predictor-corrector pair for the stress at time (t_N+h):

predictor (Euler rule):

$$\{\underset{\sim}{\chi}_\tau^{(o)}(t_N + h)\} = \{\underset{\sim}{\chi}_\tau(t_N)\} + h\{\dot{\underset{\sim}{\chi}}_\tau(t_N)\}$$

$$\{\underset{\sim}{t}_\tau^{(o)}(t_N + h)\} = \{\underset{\sim}{t}_\tau(t_N)\} + h\{\dot{\underset{\sim}{t}}_\tau(t_N)\} \qquad (8.7)$$

corrector (trapezoid rule):

$$\{\underset{\sim}{\chi}_\tau^{(K+1)}(t_N+h)\} = \{\underset{\sim}{\chi}_\tau(t_N)\} + \tfrac{1}{2}h\{\dot{\underset{\sim}{\chi}}_\tau(t_N) + \dot{\underset{\sim}{\chi}}_\tau^{(K)}(t_N+h)\}$$

$$\{\underset{\sim}{t}_\tau^{(K+1)}(t_N+h)\} = \{\underset{\sim}{t}_\tau(t_N)\} + \tfrac{1}{2}h\{\dot{\underset{\sim}{t}}_\tau(t_N) + \dot{\underset{\sim}{t}}_\tau^{(K)}(t_N+h)\} \quad (8.8)$$

To verify the satisfaction of LMB, we check to see that

$$\int_V \underset{\sim}{t}^{(K+1)} : \nabla_X \underset{\sim}{x} dV = 0 \quad (8.9)$$

for all $\underset{\sim}{x}(\underset{\sim}{X})$ which vanishes on S (body force has been presumed to vanish, for simplicity). Elimination of $\underset{\sim}{t}_\tau^{(K+1)}(t_N+h)$ from (3.9) by use of the corrector (8.8), and assuming that $\underset{\sim}{t}_\tau^{(K)}(t_N)$ is balanced, yields

$$\int_V \left[\dot{\underset{\sim}{t}}_\tau(t_N) + \dot{\underset{\sim}{t}}_\tau^{(K)}(t_N+h)\right] : \nabla_X \underset{\sim}{x} dV = 0 \quad (?) \quad (8.10)$$

Since the stress rate is of the form

$$\dot{\underset{\sim}{t}} = \nabla \times \underset{\sim}{\Phi}(t) , \quad (8.11)$$

the stress rates $\dot{\underset{\sim}{t}}_\tau$ and $\dot{\underset{\sim}{t}}_\tau^{(K)}$ are of the forms

$$\dot{\underset{\sim}{t}}_\tau = \nabla_X \times \underset{\sim}{\Phi}_\tau(t_N) ; \qquad \dot{\underset{\sim}{t}}_\tau^{(K)} = \nabla_X \times \underset{\sim}{\Phi}_\tau^{(K)}(t_N+h) ; \quad (8.12)$$

where $\underset{\sim}{\Phi}_\tau$ and $\underset{\sim}{\Phi}_\tau^{(K)}$ are defined by

$$\underset{\sim}{\Phi}_\tau(t_N) = (\nabla_X \underset{\sim}{\chi}_\tau(t_N)) \cdot \underset{\sim}{\Phi}(t_N) \ ;$$

$$\underset{\sim}{\Phi}^{(K)}_\tau(t_N+h) = (\nabla_X \underset{\sim}{\chi}^{(K)}_\tau(t_N+h)) \cdot \underset{\sim}{\Phi}(t_N+h) \ .$$

Elimination of $\dot{\underset{\sim}{t}}_\tau$ and $\dot{\underset{\sim}{t}}^{(K)}_\tau$ from (8.10), and integration by parts affirms the satisfaction of (8.10). It is worthy of special note that the complementary work and energy principles provide no means whatever for checking the satisfaction of linear momentum balance by the stress, so it is of crucial importance that the numerical integration of the stress not introduce errors which lead to an unbalanced stress. This maintenance of balanced stress, necessary in stress-based finite element algorithms, is the counterpart of maintenance of compatible deformation, necessary in velocity-based finite element algorithms.

The true stress is found, after $\underset{\sim}{t}_\tau(t_N+h)$ and $\underset{\sim}{\chi}_\tau(t_N+h)$ are integrated, by the formula

$$\underset{\sim}{\tau}(t_N+h) = (1/J_\tau)(\nabla_X \underset{\sim}{\chi}_\tau(t_N+h))^T \cdot \underset{\sim}{t}_\tau(t_N+h) \ . \qquad (8.13)$$

The true stress given by (8.13) necessarily satisfies LMB since $\underset{\sim}{t}_\tau(t_N+h)$ does. It does not appear to be possible to integrate the true stress explicitly with out causing it to become unbalanced, so no further consideration is given to that alternative.

Angular momentum balance is satisfied only approximately by stresses computed in the present method. To keep the accumulated error small we embed the angular momentum balance as the stable

solution $\underset{\sim}{\Omega}_\tau(t) = 0$ of the following initial value problem:

$$\dot{\underset{\sim}{\Omega}}_\tau + \lambda \underset{\sim}{\Omega}_\tau = \underset{\sim}{0} \qquad \underset{\sim}{\Omega}_\tau(0) = \underset{\sim}{0} \; ; \tag{8.14}$$

where the tensor $\underset{\sim}{\Omega}_\tau$ is defined by

$$\underset{\sim}{\Omega}_\tau = \tfrac{1}{2}\left[\underset{\sim}{t}_\tau \cdot \underset{\sim}{F}_\tau^{-T} - \underset{\sim}{F}_\tau^{-1} \cdot \underset{\sim}{t}_\tau^{T}\right] \tag{8.15}$$

and $\lambda > 0$. In the course of numerical integration we adjust λ at the beginning of the time step from t_N to t_{N+1} as

$$\lambda = 1/h = 1/(t_{N+1} - t_N) \; . \tag{8.16}$$

The optimality of this choice is seen if (8.14) is replaced by the difference equation

$$\underset{\sim}{\Omega}_\tau(t_N + h) = (1 - \lambda h)\underset{\sim}{\Omega}_\tau(t_N) \; . \tag{8.17}$$

Equation (8.14) accounts for the 'AMB residual' term in the finite element equation (7.24).

Finally we note that frame indifference can be satisfied only in an approximate sense when one integrates the stress numerically. As an illustration consider the Euler method as applied by observers in frames which spin relative to each other. The first observer obtains

$$[\underset{\sim}{t}_\tau(t_N+h)] = \underset{\sim}{t}_\tau(t_N) + h\dot{\underset{\sim}{t}}_\tau(t_N) \tag{8.18}$$

and the second observer obtains (for the same material point and the same time step)

$$[\underset{\sim}{t}'_\tau(t_N+h)] = \underset{\sim}{t}'_\tau(t_N) + h\dot{\underset{\sim}{t}}'_\tau(t_N) \ . \tag{8.19}$$

We assume that $\underset{\sim}{t}_\tau(t_N)$, $\dot{\underset{\sim}{t}}_\tau(t_N)$, $\underset{\sim}{t}'_\tau(t_N)$, $\dot{\underset{\sim}{t}}'_\tau(t_N)$, and $\underset{\sim}{Q}(t)$ (the rotation between the two frames) are known exactly. According to the transformation rules, the exact $\underset{\sim}{t}_\tau$ and $\underset{\sim}{t}'_\tau$ satisfy, at each moment of time,

$$\underset{\sim}{t}'_\tau = \underset{\sim}{t}_\tau \cdot \underset{\sim}{Q}^T \ ; \qquad \dot{\underset{\sim}{t}}'_\tau = \dot{\underset{\sim}{t}}_\tau \cdot \underset{\sim}{Q}^T + \underset{\sim}{t}_\tau \cdot \dot{\underset{\sim}{Q}}^T \tag{8.20}$$

for arbitrary time dependent orthogonal $\underset{\sim}{Q}$. But at time (t_N+h) equations (8.18) and (8.19) yield

$$[\underset{\sim}{t}'_\tau(t_N+h)] - [\underset{\sim}{t}_\tau(t_N+h)] \cdot \underset{\sim}{Q}^T(t_N+h) = \tag{8.21}$$

$$[\underset{\sim}{t}_\tau(t_N)] \cdot [(\underset{\sim}{Q}^T(t_N) + h\dot{\underset{\sim}{Q}}^T(t_N)) - \underset{\sim}{Q}^T(t_N+h)]$$

$$+ h\dot{\underset{\sim}{t}}_\tau(t_N) \cdot [\underset{\sim}{Q}^T(t_N) - \underset{\sim}{Q}^T(t_N+h)] \ .$$

Since the right hand side of (8.21) does not vanish for all admissible $\underset{\sim}{Q}$ and $\dot{\underset{\sim}{Q}}$, the stress integrated by Euler's method will depend upon the frame of the observer.

Two courses of action are available. We might attempt to reformulate the initial value problem so that a frame indifferent stress is integrated, or we could attempt to integrate the stress in some special manner so as to remove the frame dependence. As previously discussed, integration of another stress besides $\underset{\sim}{t}_\tau$ leaves us with no way to ascertain the satisfaction of LMB, so we disregard the first option above.

For insight to the second option, let us consider integration of the stress when the deformation is homogeneous. Suppose that the spins $\underset{\sim}{\omega}$ and $\underset{\sim}{\omega}'$ vanish in the frames of the two observers of the previous example. According to the transformation rule for spin

$$\underset{\sim}{\omega}' = \underset{\sim}{Q} \cdot \underset{\sim}{\omega} \cdot \underset{\sim}{Q}^T + \dot{\underset{\sim}{Q}} \cdot \underset{\sim}{Q}^T$$

and since both $\underset{\sim}{\omega}$ and $\underset{\sim}{\omega}'$ vanish,

$$\dot{\underset{\sim}{Q}} = \underset{\sim}{0} \; ; \qquad \underset{\sim}{Q} = \underset{\sim}{Q}_o = \text{constant} \; .$$

In words, all the frames in which the spin vanishes rotate as one with the principal axes of the deformation. Keeping in mind that the deformation is homogeneous, suppose we permit Euler's method to be applied only in frames in which the spin vanishes. Then (8.21) is reduced to

$$[\underset{\sim}{t}'_\tau(t_N+h)] - [\underset{\sim}{t}_\tau(t_N+h)] \cdot \underset{\sim}{Q}_o^T = \underset{\sim}{0} \; . \tag{8.22}$$

From this equation we surmise that a frame indifferent stress may be found in any frame if the classical Euler's method is used *only in those frames in which the spin vanishes.*

Let $\underset{\sim}{t}_\tau(t_N+h)$ be the stress integrated in the frame of the principal axes of the stretching (of the homogeneous deformation), and let $\underset{\sim}{t}'_\tau(t_N+h)$ and $\underset{\sim}{t}''_\tau(t_N+h)$ be the stress in two arbitrary frames, determined from $\underset{\sim}{t}_\tau(t_N+h)$ as

$$\left.\begin{aligned} \underset{\sim}{t}'_\tau(t_N+h) &= \underset{\sim}{t}_\tau(t_N+h)\cdot\underset{\sim}{Q}'(t_N+h) \\ \underset{\sim}{t}''_\tau(t_N+h) &= \underset{\sim}{t}_\tau(t_N+h)\cdot\underset{\sim}{Q}''(t_N+h) \end{aligned}\right\}. \tag{8.23}$$

Then the stresses $\underset{\sim}{t}'_\tau(t_N+h)$ and $\underset{\sim}{t}''_\tau(t_N+h)$ are related as

$$\underset{\sim}{t}'_\tau(t_N+h) = \underset{\sim}{t}''_\tau(t_N+h)\cdot\underset{\sim}{Q}''^{T}(t_N+h)\cdot\underset{\sim}{Q}'(t_N+h)\ . \tag{8.24}$$

Thus, the stresses $\underset{\sim}{t}'_\tau(t_N+h)$ and $\underset{\sim}{t}''_\tau(t_N+h)$ are frame independent.

Equation (8.23) gives a clue as to how the stress may be integrated in a general frame (when the deformation is homogeneous). In (8.23) $\underset{\sim}{t}_\tau(t_N+h)$, the stress integrated in the frame of the principal axes of stretching, is given by

$$\underset{\sim}{t}_\tau(t_N+h) = \underset{\sim}{t}_\tau(t_N) + h\dot{\underset{\sim}{t}}_\tau(t_N)\ ,$$

which may be used along with the formulas (8.20) to write the first of

(8.23) in the form

$$\underset{\sim}{t}'_\tau(t_N+h) = [\underset{\sim}{t}'_\tau(t_N) + h(\dot{\underset{\sim}{t}}'_\tau(t_N) + \underset{\sim}{t}'_\tau(t_N)\cdot\underset{\sim}{\omega}'_N)]\cdot\underset{\sim}{Q}'^{T}(t_N)\underset{\sim}{Q}'(t_N+h) \tag{8.25}$$

In (8.25) $\underset{\sim}{\omega}'_N$ is the spin at the time t_N,

$$\underset{\sim}{\omega}'_N = \underset{\sim}{\omega}'(t_N)$$

and $\underset{\sim}{Q}'(t)$ is the solution of the initial value problem

$$\dot{\underset{\sim}{Q}}'^{T}(t) = \underset{\sim}{\omega}'(t)\cdot\underset{\sim}{Q}'^{T}(t)\ ; \qquad \underset{\sim}{Q}'(t_N) = \underset{\sim}{1}\ . \tag{8.26}*$$

The prime is dropped in the equations below, but the discussion is for general frames.

In a paper of related interest Rubinstein and Atluri [48] discuss approximate solutions of the initial value problem posed by (8.26) for orthogonal $\underset{\sim}{Q}(t)$. In practice usually only $\underset{\sim}{\omega}(t_N)$ is known. Then the best approximation for $\underset{\sim}{Q}^T(t_N)\cdot\underset{\sim}{Q}(t_N+h)$ is given by

$$\underset{\sim}{Q}^T(t_N)\cdot\underset{\sim}{Q}(t_N+h) = \underset{\sim}{1} - \frac{1}{\Omega}\sin(\Omega h)\underset{\sim}{\omega}_N + \frac{1}{\Omega^2}(1-\cos(\Omega h))\underset{\sim}{\omega}_N^2 \tag{8.27}$$

*since only $\underset{\sim}{Q}'^{T}(t_N)\cdot\underset{\sim}{Q}'(t_N+h)$ appears in (8.25), the initial value of $\underset{\sim}{Q}'$ only needs to be orthogonal, hence, $\underset{\sim}{Q}'(t_N) = \underset{\sim}{1}$.

where

$$\Omega^2 = \tfrac{1}{2}\, \underset{\sim}{\omega}_N : \underset{\sim}{\omega}_N \ . \tag{8.28}$$

Since only an approximation for $\underset{\sim}{Q}^T(t_N) \cdot \underset{\sim}{Q}(t_N + h)$ is available, application of (8.25) through (8.28) as an integration scheme has the effect of integrating the stress in a frame in which the spin *nearly* vanishes. However LMB is precisely satisfied since the approximation for $\underset{\sim}{Q}^T(t_N) \cdot \underset{\sim}{Q}(t_N + h)$ is precisely orthogonal.

For use in the finite element method one would replace $\underset{\sim}{\omega}_N$ by the mean spin (on each element)

$$\bar{\underset{\sim}{\omega}} = \frac{1}{V_N} \int_{V_N} \underset{\sim}{\omega}\, dV \ . \tag{8.29}$$

Then we call the equations (8.25), (8.27), and (8.29) the 'modified Euler method'; they are summarized below:

$$\underset{\sim}{t}_\tau(t_N + h) = [\underset{\sim}{t}_\tau(t_N) + h(\dot{\underset{\sim}{t}}_\tau(t_N) + \underset{\sim}{t}_\tau(t_N) \cdot \bar{\underset{\sim}{\omega}})] \cdot \underset{\sim}{Q}^T(t_N) \cdot \underset{\sim}{Q}(t_N + h)$$

$$\underset{\sim}{Q}^T(t_N) \cdot \underset{\sim}{Q}(t_N + h) = \underset{\sim}{1} - \frac{1}{\bar{\Omega}} \sin(\bar{\Omega} h)\bar{\underset{\sim}{\omega}} + \frac{1}{\bar{\Omega}^2}(1 - \cos(\bar{\Omega} h))\bar{\underset{\sim}{\omega}}^2$$

$$\bar{\Omega}^2 = \tfrac{1}{2}\, \bar{\underset{\sim}{\omega}} : \bar{\underset{\sim}{\omega}} \ . \tag{8.30}$$

As long as the spatial mesh is fine enough to render the spin nearly constant on each element, this scheme is equivalent to application of the classical Euler's method in a frame in which the spin nearly

vanishes.

By similar arguments we can establish frame indifferent Euler schemes for the true stress and Kirchhoff stress as

$$\underset{\sim}{\tau}(t_N+h) = \underset{\sim}{Q}^T(t_N+h)\cdot\underset{\sim}{Q}(t_N)\cdot[\underset{\sim}{\tau}(t_N)+h\dot{\underset{\sim}{\tau}}^*(t_N)]\cdot\underset{\sim}{Q}^T(t_N)\cdot\underset{\sim}{Q}(t_N+h)$$

$$\text{where}\quad \dot{\underset{\sim}{\tau}}^* = \dot{\underset{\sim}{\tau}} + \underset{\sim}{\tau}\cdot\underset{\sim}{\omega} - \underset{\sim}{\omega}\cdot\underset{\sim}{\tau}$$

and

$$\underset{\sim}{\sigma}_\tau(t_N+h) = \underset{\sim}{Q}^T(t_N+h)\cdot\underset{\sim}{Q}(t_N)\cdot[\underset{\sim}{\sigma}_\tau(t_N)+h\,\dot{\underset{\sim}{\sigma}}^*_\tau(t_N)]\cdot\underset{\sim}{Q}^T(t_N)\cdot\underset{\sim}{Q}(t_N+h)$$

$$\text{where}\quad \dot{\underset{\sim}{\sigma}}^*_\tau = \dot{\underset{\sim}{\sigma}}_\tau + \underset{\sim}{\sigma}_\tau\cdot\underset{\sim}{\omega} - \underset{\sim}{\omega}\cdot\underset{\sim}{\sigma}_\tau$$

Of course $\underset{\sim}{Q}^T(t_N)\cdot\underset{\sim}{Q}(t_N+h)$ is computed approximately according to equation (8.30).

To illustrate the advantage of using the modified Euler method, consider the integration of the stress in a body which spins rigidly; that is

$$\underset{\sim}{t}_\tau(t) = \underset{\sim}{t}_o\cdot\underset{\sim}{Q}(t); \qquad \underset{\sim}{Q}(0) = \underset{\sim}{I};$$

$$\dot{\underset{\sim}{t}}_\tau(t) = \underset{\sim}{t}_o\cdot\dot{\underset{\sim}{Q}}(t);$$

where $\underset{\sim}{t}_o$ is a constant. An initial value problem for the stress $\underset{\sim}{t}_\tau(t)$ (in the frame in which body appears to spin) may be set as

$$\dot{\underset{\sim}{t}}_\tau(t) = -\underset{\sim}{t}_\tau(t)\cdot\underset{\sim}{\omega}_o; \qquad \underset{\sim}{t}_\tau(0) = \underset{\sim}{t}_o;$$

where $\underset{\sim}{\omega}_o = -\underset{\sim}{Q}^T(t)\cdot\dot{\underset{\sim}{Q}}(t)$ = constant. Euler's method applied to this initial value problem gives the result:

$$\underset{\sim}{t}_{\tau}(Nh) = \underset{\sim}{t}_{o} \cdot (\underset{\sim}{I} - h\underset{\sim}{\omega}_{o})^{N} .$$

The accumulated error grows without bound. On the other hand, the modified Euler method gives the exact answer:

$$\underset{\sim}{t}_{\tau}(Nh) = \underset{\sim}{t}_{o} \cdot \underset{\sim}{Q}(Nh)$$

since $\underset{\sim}{Q}(t) = \underset{\sim}{I} - \frac{1}{\Omega}\sin(\Omega t)\underset{\sim}{\omega}_{o} + \frac{1}{\Omega^2}(1 - \cos(\Omega t))\underset{\sim}{\omega}_{o}^{2}$, and, for constant $\underset{\sim}{\omega}_{o}$, $\underset{\sim}{Q}(Nh) = [\underset{\sim}{Q}(h)]^{N}$.

In the integration of the examples accompanying this work the term $(h\underset{\sim}{\omega})$ was always so small as to make the classical and modified Euler methods indistinguishable. However, in the general case one must take special precautions in the integration of tensors to insure that a frame dependence is not induced by the integration scheme.

Stability of Numerical Integration of the Initial Value Problem

It is possible that the difference between two supposed numerical solutions of a given initial value problem is much larger than would be expected to arise from discretization error alone. As an example, consider integration of the stress in a material of the type (4.20) by the Euler method. We suppose, for the sake of simplicity, that $\underset{\sim}{\varepsilon}(t)$ is given and $\underset{\sim}{\Sigma}(\underset{\sim}{\tau}) = -2\mu(\frac{3}{2}\gamma\underset{\sim}{\tau}')$, so that the difference between two solutions satisfies

$$\Delta\overset{\circ}{\underset{\sim}{\sigma}}^{*} = [\underset{\sim}{V}(\underset{\sim}{\tau} + \Delta\underset{\sim}{\tau}) - \underset{\sim}{V}(\underset{\sim}{\tau})] : \underset{\sim}{\varepsilon}(t) - (3\mu\gamma)\Delta\underset{\sim}{\tau}' . \qquad (8.31)$$

If the elastic matrix and stretching are such that, in the Euclidean norm,

$$\| [\underset{\approx}{V}(\underset{\sim}{\tau} + \Delta\underset{\sim}{\tau}) - \underset{\approx}{V}(\underset{\sim}{\tau})] : \underset{\sim}{\varepsilon}(t) \| \; / \; \| \Delta\underset{\sim}{\tau} \| \to 0 \tag{8.32}$$

as $\| \Delta\underset{\sim}{\tau} \| \to 0$, then for sufficiently small $\| \Delta\underset{\sim}{\tau} \|$, equation (8.31) may be replaced by

$$\Delta\dot{\underset{\sim}{\sigma}}^{*} = -(3\mu\gamma)\Delta\underset{\sim}{\tau}' \; . \tag{8.33}$$

Defining $\Delta\sigma$ as $\Delta\sigma = J_o \sqrt{\frac{3}{2} \Delta\underset{\sim}{\tau}' : \Delta\underset{\sim}{\tau}'}$, we may reduce (8.33) to a scalar equation in the invariant $\Delta\sigma$:

$$\frac{d}{dt} (\Delta\sigma) = -(3\mu\gamma)\Delta\sigma \; . \tag{8.34}$$

For an initial value $\Delta\sigma(0)$ (small), the closed form solution of (8.34) is

$$\Delta\sigma(t) = \Delta\sigma(0) e^{-(3\mu\gamma)t} \; . \tag{8.35}$$

Euler's method yields

$$\Delta\sigma_N = \Delta\sigma(0)(1 - 3\mu\gamma h)^N \; . \tag{8.36}$$

It is clear from (8.35) that $\Delta\sigma$ decays to zero as time passes. This

means that the closed form solution of the equation

$$\overset{\nabla}{\underset{\sim}{\sigma}}^{*} = \underset{\approx}{V} : \underset{\sim}{\varepsilon}(t) + \underset{\sim}{\Sigma} \; ; \qquad \underset{\sim}{\tau}(0) = \underset{\sim}{\tau}_{o} \tag{8.37}$$

is stable with respect to sufficiently small perturbations of the deviatoric part of $\underset{\sim}{\tau}$. On the other hand, the numerical solution (8.36) attenuates as time passes only if

$$|(1 - 3\mu\gamma h)| < 1 \; . \tag{8.38}$$

This means that the numerical solution of (8.37) is stable with respect to small perturbations of the deviatoric part of $\underset{\sim}{\tau}'$ only so long as the time step h is bounded above as

$$|h| < 2/(3\mu\gamma) \quad . \tag{8.39}$$

This bound is identical to the bound given by Cormeau [46] (see equations 16 and 54 in this reference). It is not surprising that time steps such as (8.39) are found to be necessary for stability of numerical solutions of the finite element-initial value problem presented in this work. According to Hughes and Taylor [20]:

> The time step restriction of the Zienkiewicz-Cormeau algorithm . . . is a stringent one in practice. For slowly varying loads, or when equilibrium response is of prime interest, stability requires that time steps be selected which are much smaller than those necessary for accuracy.

Argyris et al. [19] remark that this time step restriction amounts to

limiting the inelastic strain increment to be smaller than the elastic strain. Since the elastic strain is usually very small in metals such as those used in structures, this implies that a finite deformation analysis would entail an impractically large number of steps.

The work of Kanchi et al. [49] and Atluri and Murakawa [14] suggests the modification we now describe. To improve the estimate of the inelastic strain increment in a time step, we replace $\underset{\sim}{\varepsilon}^P(\underset{\sim}{\tau}_N)$ by an estimate of the mean value of the inelastic stretching in that time step:

$$\underset{\sim}{\varepsilon}^P(\underset{\sim}{\tau}(t_N+\theta h)) \doteq \underset{\sim}{\varepsilon}^P(\underset{\sim}{\tau}(t_N)) + \theta h \left.\frac{d\underset{\sim}{\varepsilon}^P}{d\underset{\sim}{\tau}}\right|_{\underset{\sim}{\tau}=\underset{\sim}{\tau}_N} : \dot{\underset{\sim}{\sigma}}^* \tag{8.40}$$

where the parameter θ, $0 \leqslant \theta \leqslant 1$, serves to locate the time at which the mean value is achieved. As θ goes from zero to one, the estimate of the creep-stretch becomes increasingly more conservative.

Equation (8.40) may be introduced to the finite element algorithm through the constitutive equation; (4.20) becomes

$$\dot{\underset{\sim}{\sigma}}^* = \underset{\approx}{V}_\theta : \underset{\sim}{\varepsilon} + \underset{\sim}{\Sigma}_\theta \tag{8.41}$$

where

$$\underset{\approx}{V}_\theta = \left[\underset{\approx}{V}^{-1} + \theta h \frac{d\underset{\sim}{\varepsilon}^P}{d\underset{\sim}{\tau}}\right]^{-1} ; \quad \underset{\sim}{\Sigma}_\theta = -\underset{\approx}{V}_\theta : \underset{\sim}{\varepsilon}^P .$$

From $\underset{\approx}{V}_\theta$ (8.41) we derive $\underset{\approx}{W}_\theta$ just as we derived $\underset{\approx}{W}$ from $\underset{\approx}{V}$:

$$\underset{\approx}{W}_\theta = \underset{\approx}{V}_\theta - \underset{\approx}{T} \; ; \qquad T_{ijkl} = \tfrac{1}{2}(\tau_{ik}\delta_{lj} + \delta_{ik}\tau_{lj}) \; ;$$

$$\underset{\sim}{\Sigma}_\theta = -\underset{\approx}{V}_\theta : \underset{\sim}{\varepsilon}^P = -(\underset{\approx}{W}_\theta + \underset{\approx}{T}) : \underset{\sim}{\varepsilon}^P \quad . \tag{8.42}$$

When a material which exhibits relaxation is to be analyzed, $\underset{\approx}{W}_\theta$ and $\underset{\sim}{\Sigma}_\theta$ are introduced to the finite element algorithm for $\underset{\approx}{W}$ and $\underset{\sim}{\Sigma}$.

If Euler's method is used to integrate the initial value problem which results from the modification described above, then, in the terminology of Argyris et al. [19], an explicit 'forward gradient scheme' is recovered. If the 'gradient' $(d\underset{\sim}{\varepsilon}^P/d\underset{\sim}{\tau})$ is evaluated at $\underset{\sim}{\tau} = \underset{\sim}{\tau}_\theta = (1-\theta)\underset{\sim}{\tau}_N + \theta\underset{\sim}{\tau}_{N+1}$, then an implicit forward gradient scheme, counterpart to that proposed by Hughes and Taylor [20] is recovered. Finally, if the 'gradient' $(d\underset{\sim}{\varepsilon}^P/d\underset{\sim}{\tau})$ is replaced altogether by a function $\underset{\approx}{g}_\theta$, defined through

$$\underset{\sim}{\varepsilon}^P(\underset{\sim}{\tau}) = \underset{\approx}{g}(\underset{\sim}{\tau}) : \underset{\sim}{\tau} \quad ; \qquad \underset{\approx}{g}_\theta = \underset{\approx}{g}(\underset{\sim}{\tau}_\theta) \; ; \tag{8.43}$$

then an implicit 'finite approximation technique,' counterpart to that proposed by Argyris et al. [19] is recovered. The implicit schemes must be solved by iterating on each time step, keeping θ fixed. The iterative schemes amount to special predictor-corrector techniques. An important fact that is exploited in our numerical studies is that for the material (8.31), with $\mu\gamma$ constant, all of these schemes are equivalent.

CHAPTER IX

EXAMPLES: FINITE DEFORMATION PROBLEMS

Introduction

In this chapter we present several examples as demonstrations of the feasibility and performance of the finite element algorithm. All of the examples may be described either as plane or axisymmetric, so we begin by discussing specializations of the algorithm for such problems.

The examples fall into two categories--homogeneous deformations and inhomogeneous deformations. By treatment of homogeneous deformations (for which closed form solutions are known), several important aspects of the performance of the finite element algorithm can be clearly identified and studied. The studies of inhomogeneous deformations, the results of which are compared to both analytical and other numerical results, indicate the potential of the algorithm for treatment of problems of technological interest.

In the discussions of the examples the time integration scheme used is indicated as Euler, Runge-Kutta second order (RK2), or Runge-Kutta fourth order (RK4). In all cases the classical schemes (i.e., those described in [47]) have been used.

Plane Strain

All but one of the deformations studied in this chapter are plane strain in character. Just as for formulations using ordinary

stresses, a number of the components of the velocity, spin, and stress rate vanish if a Cartesian coordinate system is chosen with one axis normal to the plane of deformation. We have chosen the x^2 coordinate line to be normal to the plane of deformation, so that the velocity, spin, stress rate, and stress are of the forms

$$\underset{\sim}{v} = v^1 \underset{\sim}{e}_1 + v^3 \underset{\sim}{e}_3$$

$$\underset{\sim}{\omega} = \omega^{13} \underset{\sim}{e}_1 \underset{\sim}{e}_3 + \omega^{31} \underset{\sim}{e}_3 \underset{\sim}{e}_1$$

$$\overset{\nabla}{\underset{\sim}{t}} = \overset{\nabla}{t}{}^{11} \underset{\sim}{e}_1 \underset{\sim}{e}_1 + \overset{\nabla}{t}{}^{13} \underset{\sim}{e}_1 \underset{\sim}{e}_3 + \overset{\nabla}{t}{}^{22} \underset{\sim}{e}_2 \underset{\sim}{e}_2 + \overset{\nabla}{t}{}^{31} \underset{\sim}{e}_3 \underset{\sim}{e}_1 + \overset{\nabla}{t}{}^{13} \underset{\sim}{e}_3 \underset{\sim}{e}_3 \ .$$

$$\underset{\sim}{\tau} = \tau^{11} \underset{\sim}{e}_1 \underset{\sim}{e}_1 + \tau^{13} \underset{\sim}{e}_1 \underset{\sim}{e}_3 + \tau^{22} \underset{\sim}{e}_2 \underset{\sim}{e}_2 + \tau^{31} \underset{\sim}{e}_3 \underset{\sim}{e}_1 + \tau^{33} \underset{\sim}{e}_3 \underset{\sim}{e}_3 \ .$$

None of the components depends upon x^2. The velocity is represented on each element as

$$\underset{\sim}{v} = \sum_{i=1}^{NQ} \underset{\sim}{N}_i q^i \ .$$

The shape functions $\underset{\sim}{N}_i$ are described in Appendix C. Similarly the spin and stress rate are represented as

$$\underset{\sim}{\omega} = \sum_{i=1}^{NW} \underset{\sim}{QW}_i \alpha^i \quad ; \qquad \overset{\cdot}{\underset{\sim}{t}} = \sum_{i=1}^{NT} \underset{\sim}{QT}_i \beta^i$$

and those shape functions are given in Appendix C also.

We note that this approach requires minimal specialization in programming for the particular case of plane strain. The plane strain condition is not satisfied a priori; that is,

$$\delta\varepsilon_{22} = (\underset{\sim}{e}_2\underset{\sim}{e}_2) : \underset{\approx}{W}^{-1} : \delta\overset{\cdot}{\underset{\sim}{r}} \neq 0$$

for arbitrary $\delta\overset{\cdot}{\underset{\sim}{r}}$. Rather, $\varepsilon_{22} = 0$ follows from the stationary condition (a component of 7.1):

$$\int_V \left[-\varepsilon_{22}(\overset{\cdot}{\underset{\sim}{t}}, \underset{\sim}{\omega})\right] \delta\overset{\cdot}{t}^{22} \, dV = 0 \quad .$$

In using the finite element algorithm the plane strain condition is only satisfied approximately. In practice a qualitative check for satisfaction of the plane strain condition can be made by seeing that the stress component τ^{22} and the mean stress are nearly equal. This method for checking $\varepsilon_{22} = 0$ works so long as the inelastic stretching is proportional to the stress deviator (in the constitutive equation).

As an alternative to approximate satisfaction of the plane strain condition, it is possible to 'split' the constitutive equation

into two equations. The first involves only the in-plane components of the stretching and stress rate, all that is actually required for the finite element algorithm for plane strain problems. After in-plane components of the stress rate and spin have been found, the stress rate component $\dot{t}^{22}$ can be assigned so as to give precise satisfaction of the plane strain condition. This alternative is attractive from the point of view of efficiency, for storage could be reduced and the analytic inverse for the constitutive equation could be used, but it requires considerable specialization in programming. Because of the inflexibility of this approach, it was not pursued in programming.

Axisymmetric Deformations

One of the deformations studied in this chapter is axisymmetric in character, that of creep of a pipe from internal pressure. We have used a right circular cylindrical coordinate system to describe the problem, indexing the coordinates as $x^1 = r$, $x^2 = \theta$, and $x^3 = z$. Of course the z axis is along the centerline of the pipe, and r is a constant on the interior and exterior surfaces of the pipe at any particular time. The velocity, spin, stress rate, and stress are of the same forms as for plane strain; that is

$$\underset{\sim}{v} = v^1 \underset{\sim}{e}_1 + v^3 \underset{\sim}{e}_3$$

$$\underset{\sim}{\omega} = \omega^{13} \underset{\sim}{e}_1 \underset{\sim}{e}_3 + \omega^{31} \underset{\sim}{e}_3 \underset{\sim}{e}_1$$

$$\dot{\underset{\sim}{t}} = \dot{t}^{11} \underset{\sim}{e}_1 \underset{\sim}{e}_1 + \dot{t}^{13} \underset{\sim}{e}_1 \underset{\sim}{e}_3 + \dot{t}^{22} \underset{\sim}{e}_2 \underset{\sim}{e}_2 + \dot{t}^{31} \underset{\sim}{e}_3 \underset{\sim}{e}_1 + \dot{t}^{33} \underset{\sim}{e}_3 \underset{\sim}{e}_3$$

$$\underset{\sim}{\tau} = \tau^{11}\underline{e}_1\underline{e}_1 + \tau^{13}\underline{e}_1\underline{e}_3 + \tau^{22}\underline{e}_2\underline{e}_2 + \tau^{31}\underline{e}_3\underline{e}_1 + \tau^{33}\underline{e}_3\underline{e}_3 \ .$$

None of the components above depends upon $x^2 = \theta$. The representations for the velocity, spin, and stress rate are of the same forms as for plane strain; the shape functions are described in Appendix C.

Homogeneous Deformations

Through the study of homogeneous deformations various important aspects of the performance of the finite element algorithm can be identified and studied. Since closed form solutions to problems of homogeneous deformation are widely available, questions of the accuracy of the finite element solutions can be resolved quickly and absolutely. If we immediately engaged problems complicated by inhomogeneous deformation, the accuracy of any solution we obtained would be no more than a subject for speculation. It was demonstrated by the example in Chapter VIII that homogeneous deformations are as difficult to integrate from the point of view of time step stability as inhomogeneous deformations (since the same time step bound was found). Thus, homogeneous deformations are convenient subjects for studies of time step stability, and in the present case, for studies of the effect of the forward gradient scheme on accuracy. Finally, the results of this study serve to underscore the fact that the material models themselves are too idealized to be used in problems of technological interest when strains are very large.

Finite Plane Extension

We begin our study of homogeneous deformations by considering

finite plane extension of (i) the hypoelastic material (4.31), (ii) a hypoelastic/plastic material, and (iii) a creeping viscoplastic material. The geometry of the specimen for these examples is given in Figure 1. These examples serve to demonstrate the relative efficiencies (accuracy/cost) of the Euler, RK2, and RK4 time integration schemes, the performance of those schemes when the loading path crosses a material yield surface, and the effect on accuracy of the forward gradient scheme.

Hypoelastic Material. For the first problem we consider the hypoelastic material defined by the constitutive equation (4.31):

$$\overset{\nabla}{\underset{\sim}{\sigma}}{}^{*} = \lambda(\underset{\sim}{I} : \underset{\sim}{\varepsilon})\underset{\sim}{I} + 2\mu\underset{\sim}{\varepsilon} \quad . \tag{9.1}$$

It is convenient to introduce the normalized stress $\underset{\sim}{s}$, defined as $\underset{\sim}{s} = \underset{\sim}{\tau}/2\mu$. Then (9.1) may be written

$$\overset{\nabla}{\underset{\sim}{s}}{}^{*} = \left(\frac{\nu}{1-2\nu}\right)(\underset{\sim}{I} : \underset{\sim}{\varepsilon})\underset{\sim}{I} + \underset{\sim}{\varepsilon} \quad . \tag{9.2}$$

For homogeneous plane extension of this material from a stress free state, the stresses are given by

$$\begin{aligned} s^{11}(1) &= 0 \\ s^{22}(1) &= \nu s^{33}(1) \\ s^{33}(1) &= \left(\frac{1}{1-2\nu}\right)(1 - 1^{-\bar{\nu}}) \end{aligned} \tag{9.3}$$

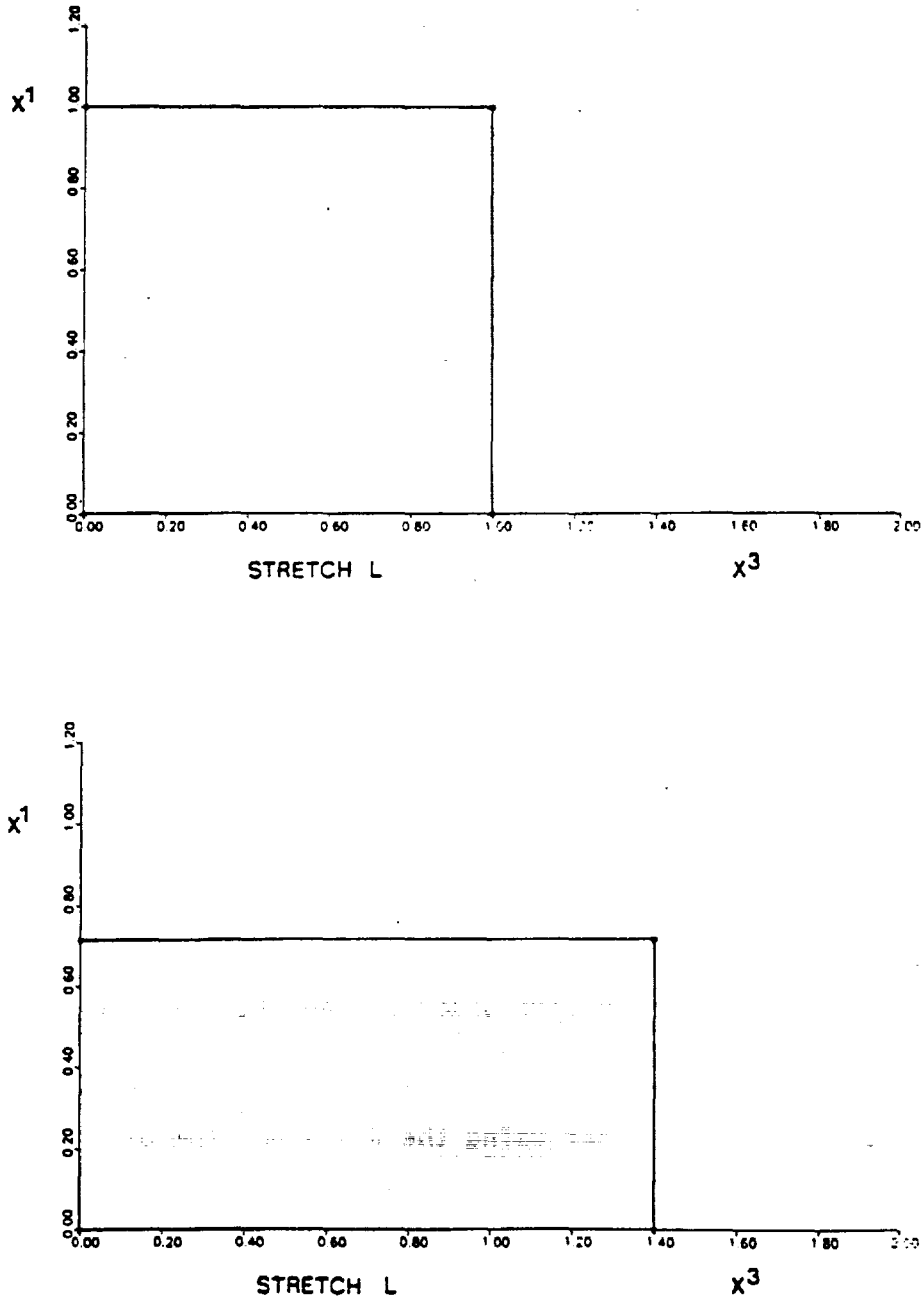

Figure 1. Plane Extension Specimen

where $\bar{\nu} = (1 - 2\nu)/(1 - \nu)$. In Figures 2, 3, and 4 the stresses found by application of the finite element algorithm are compared to the closed form solution (9.3) for $\nu = 1/3$. Euler, RK2, and RK4 time stepping algorithms are used. The Euler algorithm underestimates the strain-softening of the material slightly, but the RK2 and RK4 algorithms provide data indistinguishable from the closed form solution. The reader should note that the stretch increment for each time step is (0.01), (0.02), and (0.04), for the Euler, RK2, and RK4 algorithms, respectively. Thus, the computational effort is the same in each of these three cases (1 element stiffness matrix evaluation per stretch increment of 0.01). In view of the differences in accuracy, we rank the RK4 algorithm as most efficient, followed by RK2 and Euler.

One of the methods used to get qualitative estimates of the local error of the Euler and RK2 algorithms is based on the assumption that greater accuracy will always be achieved by the next higher order time stepping algorithm when the solution is smooth. To check the error of the Euler algorithm on a given time step, we integrate the time step a second time using the RK2 algorithm. The local error is then assumed to be of the same order of magnitude as the difference between those two solutions. The error of the RK2 algorithm may be checked in a similar manner using the RK4 algorithm as a 'reference.'

Plastic Material. As a second example we consider plane extension of a hypoelastic/plastic material from a stress free state. The specimen geometry is identical to that of the previous example (see Figure 1). The material is characterized by uniaxial test data as

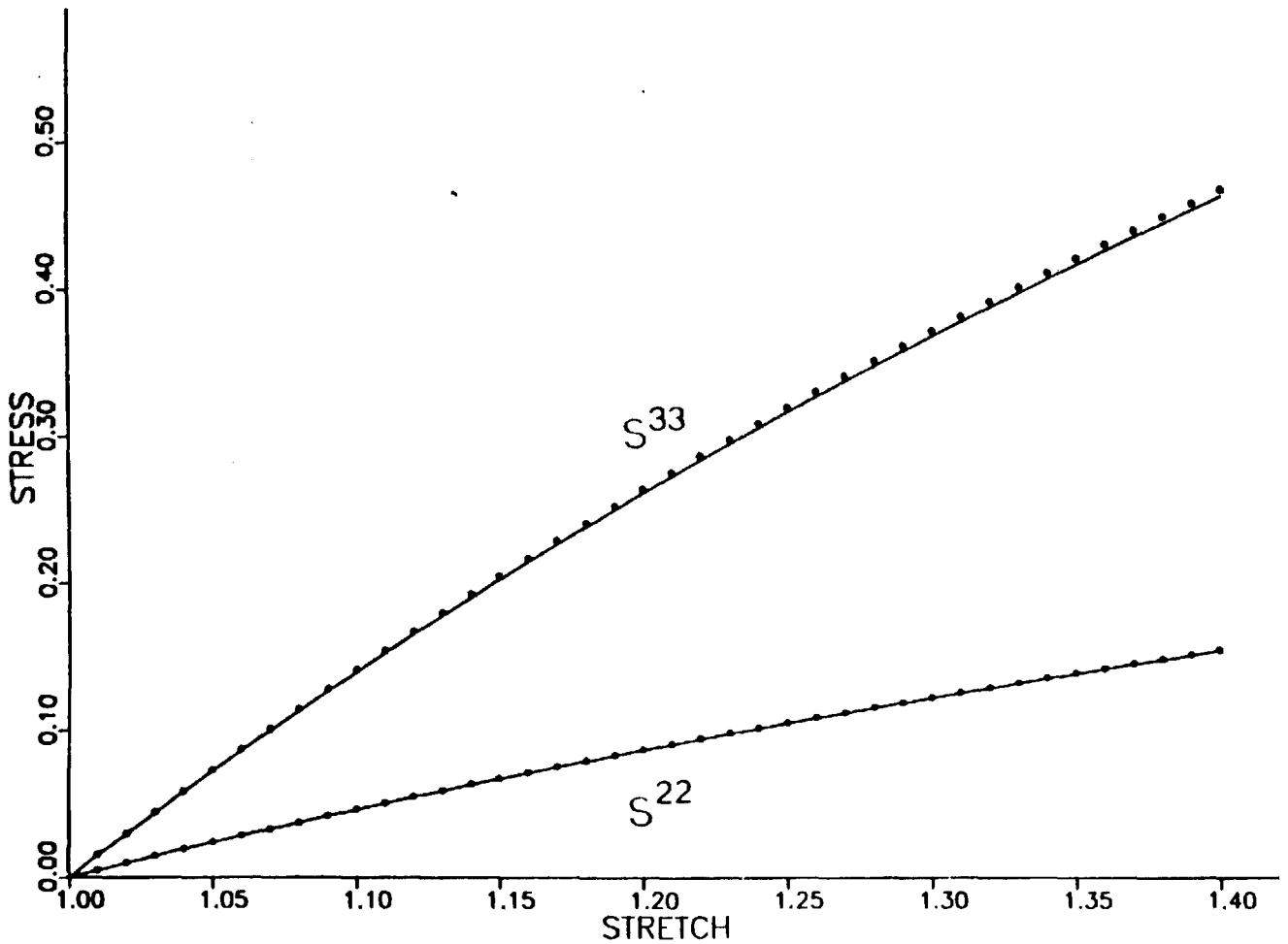

Figure 2. Stress Accompanying Plane Extension of a Hypoelastic Material--Euler Integration

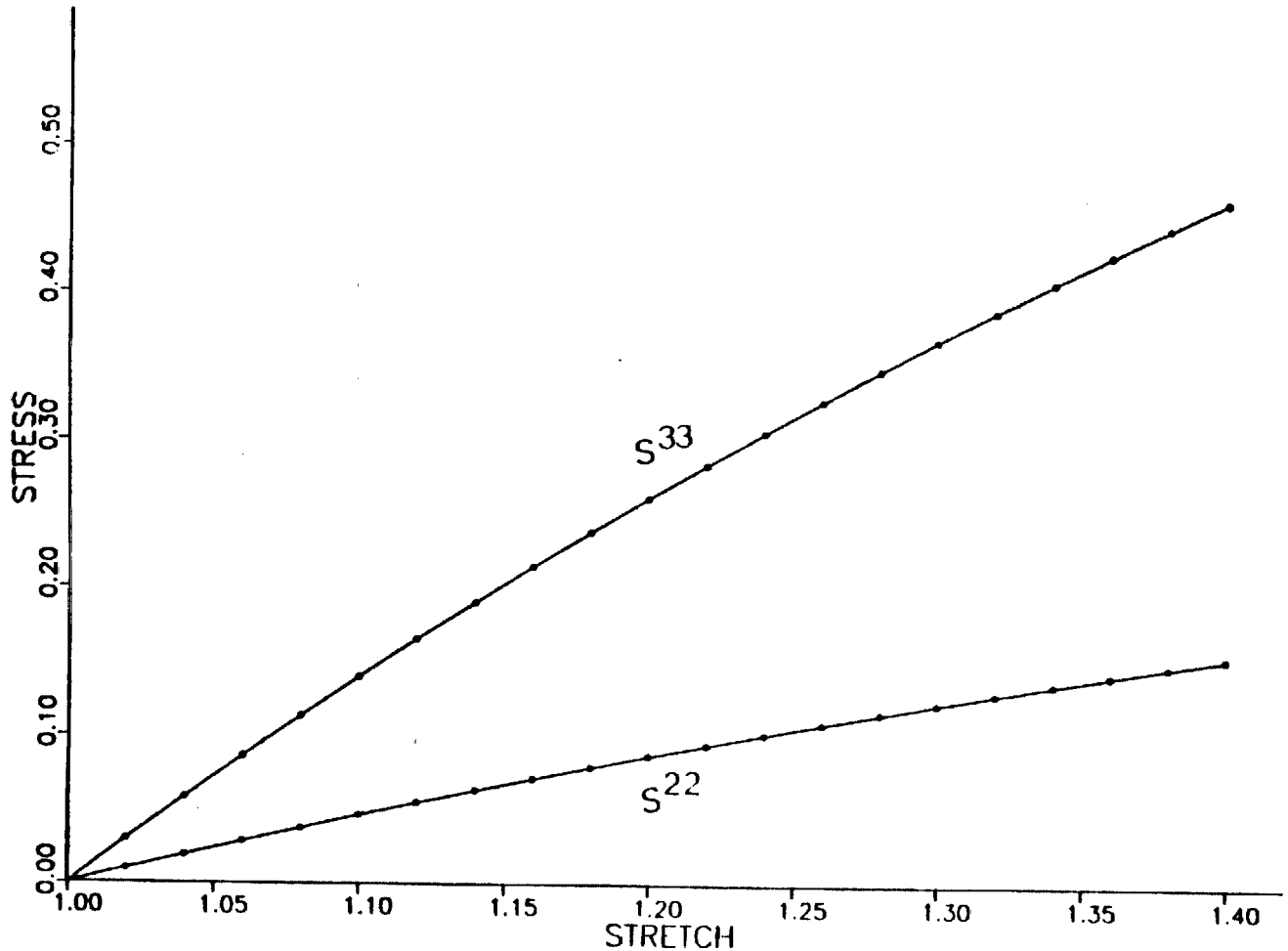

Figure 3. Stress Accompanying Plane Extension of a Hypoelastic Material--RK2 Integration

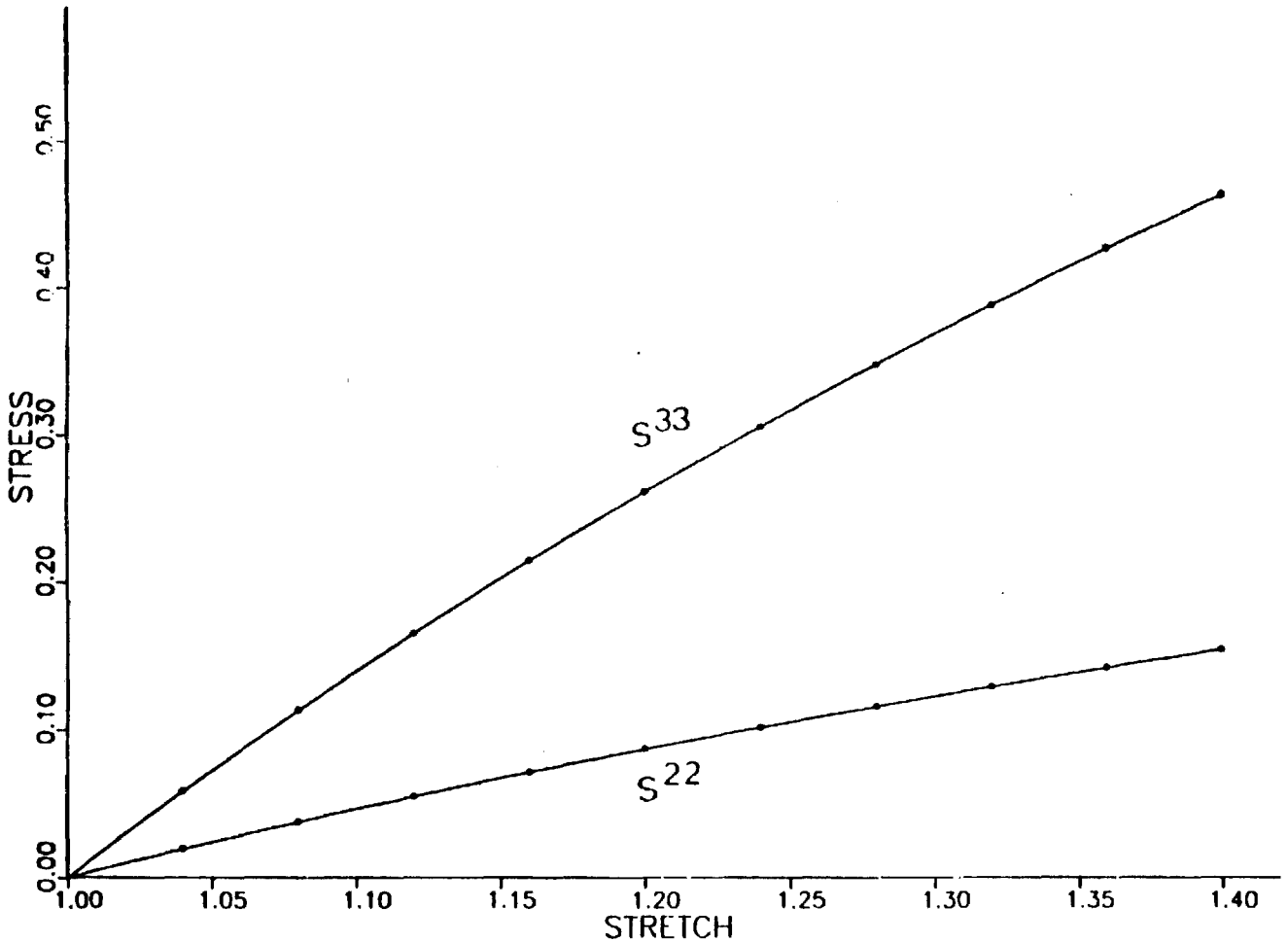

Figure 4. Stress Accompanying Plane Extension of a Hypoelastic Material--RK4 Integration

$$\left.\begin{aligned} \dot{\sigma}_o^{11}/\varepsilon_{11} &= J_o E \qquad (\tau^{11} < \tau_y) \\ \dot{\sigma}_o^{11}/\varepsilon_{11} &= J_o E_t = J_o E\left\{N\left(\frac{\tau^{11}}{\tau_y}\right)^{N-1}\right\}^{-1} \qquad (\tau^{11} \geq \tau_y) \end{aligned}\right\} \tag{9.4}$$

The associated constitutive equation is

$$\underset{\sim}{\varepsilon} = \underset{\sim}{\varepsilon}^e + \underset{\sim}{\varepsilon}^P = \underset{\approx}{V} : \dot{\underset{\sim}{\sigma}}^* \tag{9.5}$$

$$\left.\begin{aligned} \underset{\sim}{\varepsilon}^e &= \left(\frac{1+\nu}{E}\right)\dot{\underset{\sim}{\sigma}}^* - \left(\frac{\nu}{E}\right)(\underset{\sim}{I} : \dot{\underset{\sim}{\sigma}}^*)\underset{\sim}{I} \\ \underset{\sim}{\varepsilon}^P &= \alpha\,\frac{9}{4h}\left(\frac{3}{2} I'\right)^{-1}(\underset{\sim}{\tau}' : \dot{\underset{\sim}{\sigma}}^*)\underset{\sim}{\tau}' \end{aligned}\right\} \tag{9.6}$$

In accordance with (4.44) h is defined as

$$1/h = 1/E_t - 1/E = (1/E)\left\{N\left(\frac{\sqrt{1.5\, I'}}{\tau_y}\right)^{N-1} - 1\right\} \tag{9.7}$$

where $I' = \underset{\sim}{\tau}' : \underset{\sim}{\tau}'$, and $\alpha = 0$ or $\alpha = 1$ as the material is elastic or plastic. It is convenient in this case to normalize the stress by its yield value in plane extension:

$$\underset{\sim}{s} = \sqrt{3}\,\underset{\sim}{\tau}/2\tau_y \,. \tag{9.8}$$

The stress accompanying plane extension from a stress free state of the material (9.5) are easily found when $\nu = \frac{1}{2}$ as

$$s^{11}(1) = 0 \; ; \qquad s^{22}(1) = \tfrac{1}{2} s^{33}(1)$$

$$s^{33}(1) = [\ln(1)/\ln(1_y)] \qquad s < 1 \tag{9.9}$$

$$s^{33}(1) = [\ln(1)/\ln(1_y)]^{\frac{1}{N}} \qquad s \geq 1$$

where 1_y is the nominal strain at the initial yield of the incompressible material in plane extension:

$$\ln(1_y) = \sqrt{3}\ \tau_y/2E \; . \tag{9.10}$$

In the examples we take $(E/\tau_y) = 200$, $N = 4$, and $\nu = (1/3)$. In Figures 5, 6, and 7 the stresses found by application of the finite element algorithm are compared to the stresses in the incompressible material with the same Young's modulus (E/τ_y) and hardening exponent N. The discrepancy in the elastic range is due entirely to the difference in the Poisson ratio; for both $\nu = (\frac{1}{2})$ and $\nu = (\frac{1}{3})$ the stress $\tau^{22} = \nu\tau^{33}$, as we have determined it should in the previous example (see 9.3). We note that the numerical solution 'overshoots' the yield surface for Euler, RK2, and RK4 algorithms, but the error appears to be least for the higher order methods. As plastic deformation progresses, the stress in the compressible body falls slightly below the stress in the incompressible body. This is to be expected, for the compressible body is more compliant. One other point made by this example is that the deformation in the plastic range (beyond about 2% stretch) is

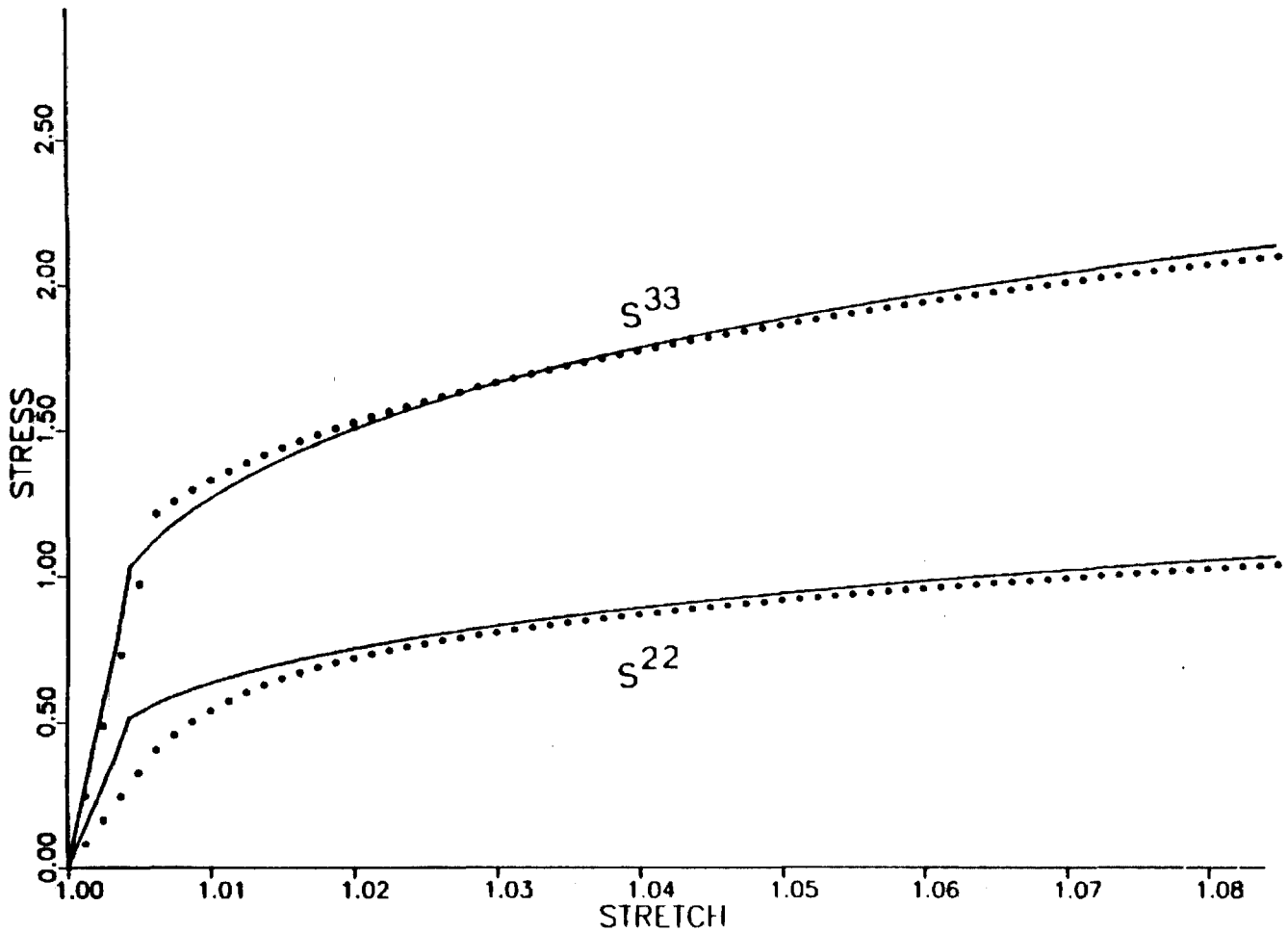

Figure 5. Stress Accompanying Plane Extension of a Plastic Material--Euler Integration

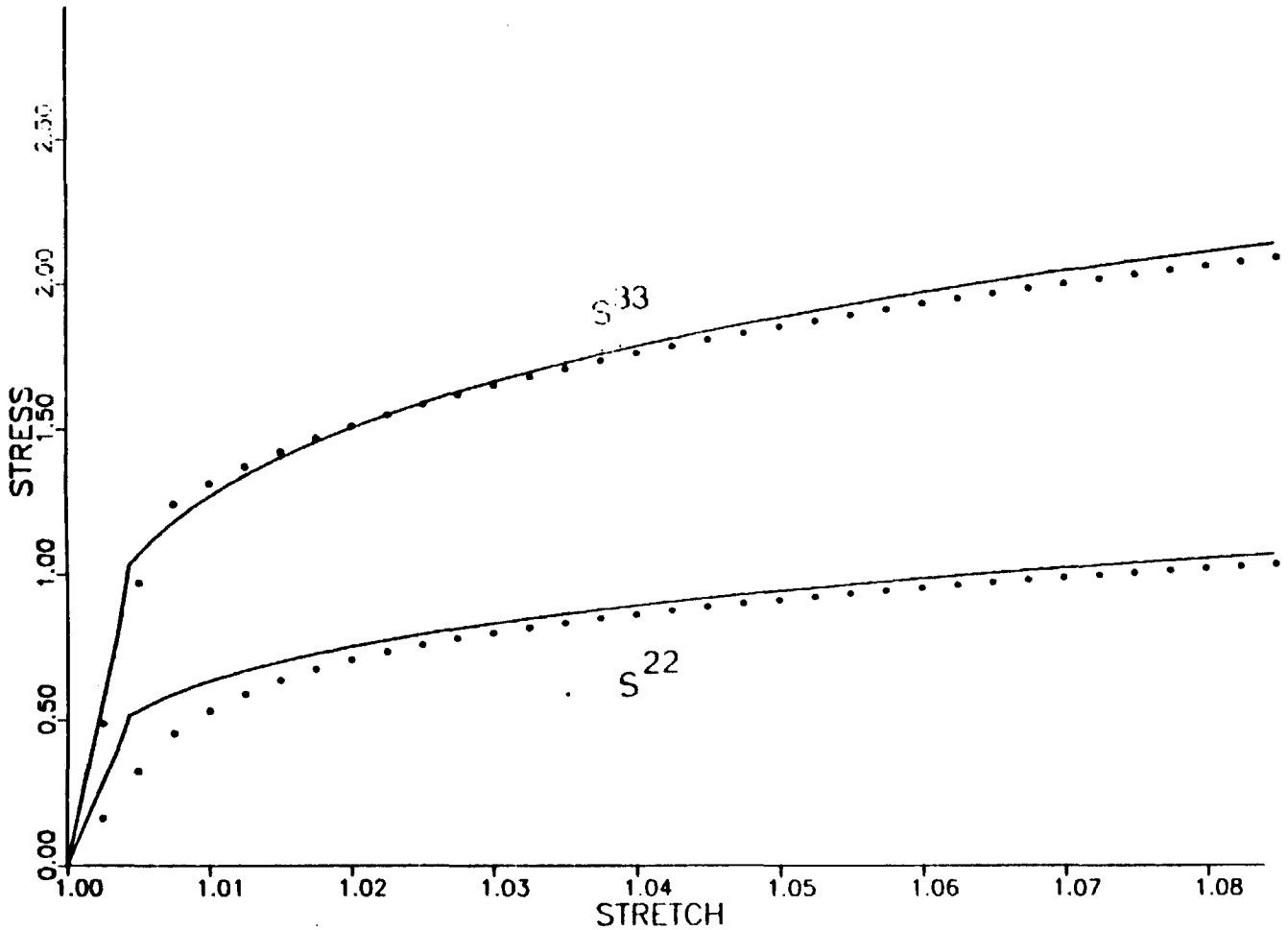

Figure 6. Stress Accompanying Plane Extension of a Plastic Material--RK2 Integration

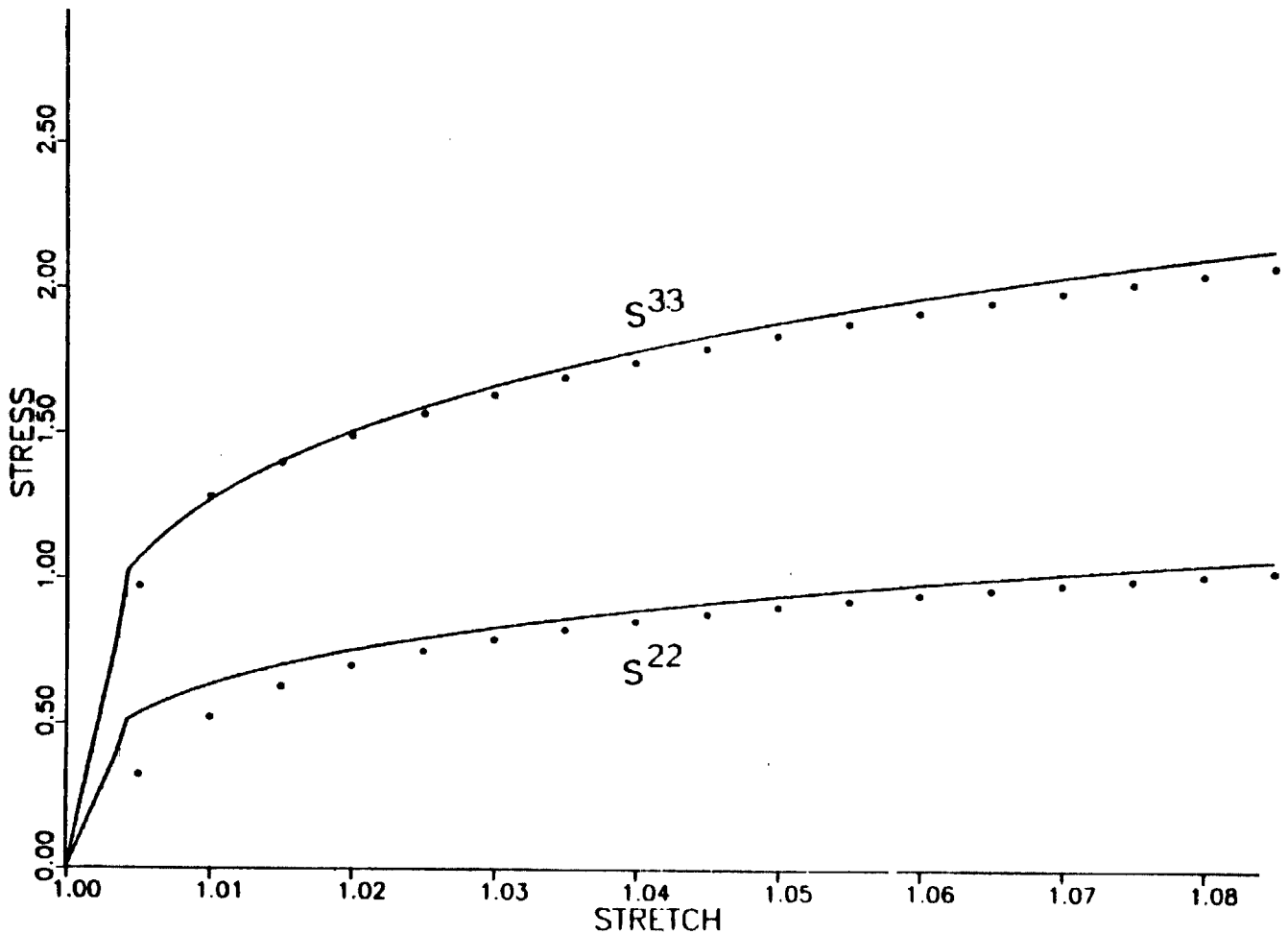

Figure 7. Stress Accompanying Plane Extension of a Plastic Material--RK4 Integration

essentially isochoric. This is not because the material is any less compressible in the plastic range; rather, it occurs because of the drastic lowering of the shear rigidity of the material by the plasticity mechanism. The condition number of the constitutive matrix $\underset{\approx}{V}$ can be used as an indicator of the relative shear rigidity; as that number decreases, an unconstrained deformation becomes more and more like the deformation of an incompressible body.

In Figure 8 of the stress accompanying the deformation out to a stretch of 1.92 is plotted for the same materials as above. The RK4 algorithm was used for this integration, with a stretch increment of (0.04).

Creeping Viscoplastic Material. As final examples of plane extension we consider a viscoplastic material which creeps (i) from an initially stressed state, and (ii) from a stress free state. The specimen geometry is the same as that of the previous two examples. The material behavior is governed by

$$\underset{\sim}{\varepsilon} = \dot{\underset{\sim}{s}}^{*} - \left(\frac{\nu}{1+\nu}\right)(\underset{\sim}{1} : \dot{\underset{\sim}{s}}^{*})\underset{\sim}{1} + \frac{1}{T}\left(\underset{\sim}{s} - \frac{1}{3}(\underset{\sim}{s} : \underset{\sim}{1})\underset{\sim}{1}\right) \tag{9.11}$$

where $\underset{\sim}{s} = \underset{\sim}{\tau}/2\mu$, $\dot{\underset{\sim}{s}}^{*} = \dot{\underset{\sim}{\sigma}}^{*}/2\mu$, and $T = 1/3\mu\gamma$. When the material is incompressible, the stress accompanying plane extension are easily found as

$$s^{11}(t) = 0$$

$$s^{22}(t) = \tfrac{1}{2} s^{33}(t)$$

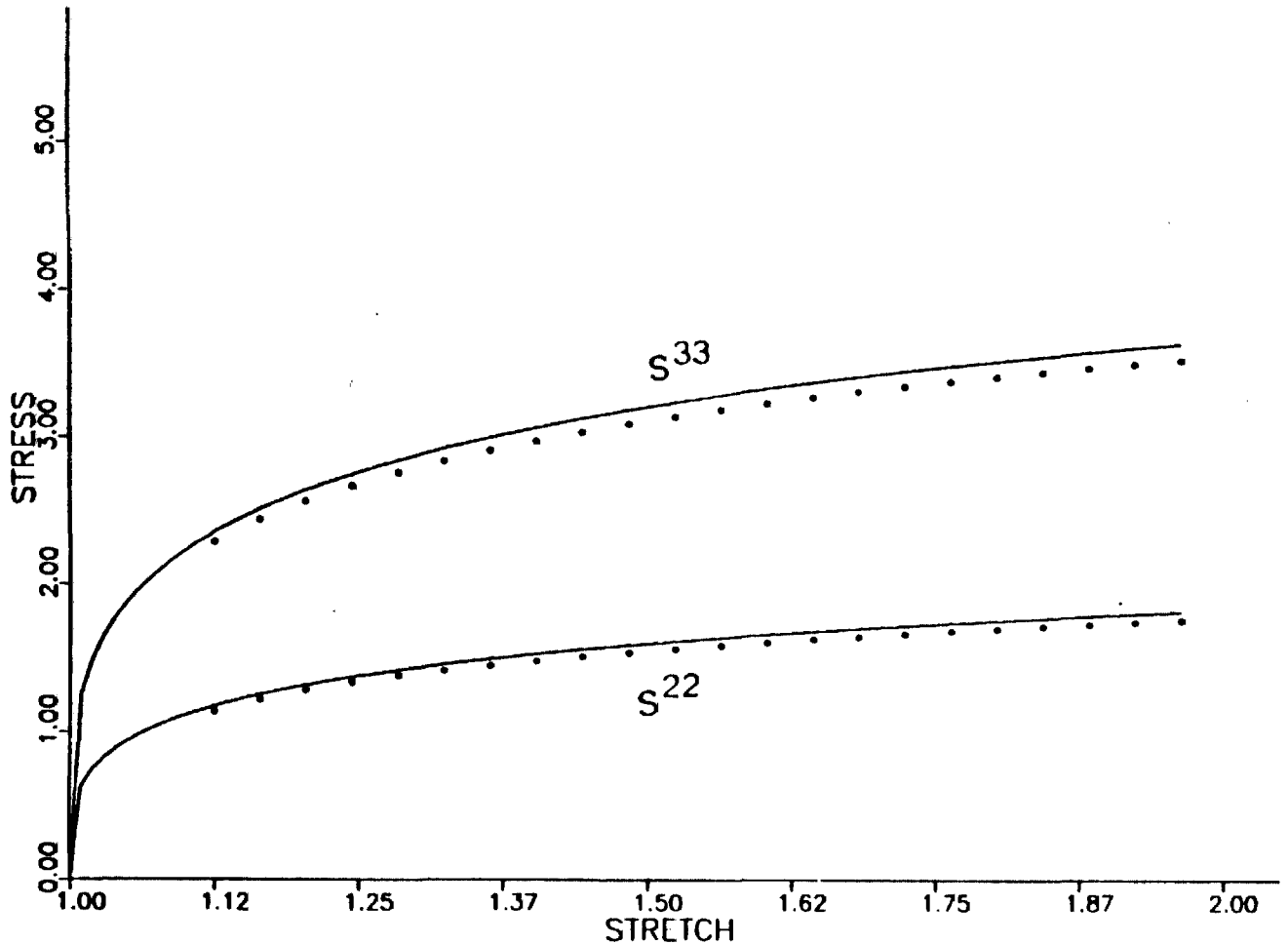

Figure 8. Stress Accompanying Plane Extension of a Plastic Material--to I = 1.92

$$s^{33}(t) = s^{33}(0)e^{-t/T} + 2\int_0^t \varepsilon^{33}(\zeta)e^{-(t-\zeta)/T}\,d\zeta \ . \qquad (9.12)$$

For the stretch history $l(t) = 1 + Vt$, the stretching $\varepsilon^{33}(t)$ is

$$\varepsilon^{33}(t) = V/(1 + Vt) \ . \qquad (9.13)$$

The stresses for this stretch history take the form

$$s^{11}(1) = 0$$

$$s^{22}(1) = \tfrac{1}{2}s^{33}(1)$$

$$s^{33}(1) = s^{33}(0)e^{-(1-1)/L} + 2e^{-1/L}\left\{Ei(1/L) - Ei(1/L)\right\} \qquad (9.14)$$

where $L = VT$, and $Ei(\cdot)$ is the exponential integral, defined

$$Ei(x) = \int_{-\infty}^{x} (e^z/z)dz \ .$$

Values of Ei may be found in tables [53]. In the present case Ei was evaluated by a subroutine in the IMSL Mathematical and Statistical Library (FORTRAN). The subroutine (MMDEI) returns a value to the calling program which is based on interpolation of tables.

In both of the cases which follow we take $V = 10^{-14}$ sec^{-1} (nominal stretch rate) and $T = \frac{1}{2}\left(\frac{56}{90}\right) \times 10^{12}$ sec. Cormeau's [46] time step bound is $h < h_c = 2T$.

In the first case we assign the initial stress as if it arose from viscosity alone:

$$s^{11}(0) = 0 \; ; \qquad s^{22}(0) = \tfrac{1}{2} s^{33}(0) = VT \; .$$

We take time steps $h = (90/56)h_c$, $2(90/56)h_c$, and $4(90/56)h_c$ (for stretch increments of 0.01, 0.02, and 0.04, respectively), applying Euler, RK2, and RK4 algorithms, respectively. The stability parameter θ is set as $\theta = \frac{1}{2}$. The stresses found by application of the finite element algorithm are compared to the closed form solution (9.14) for the incompressible body with the same characteristic time T in Figures 9, 10, and 11. It is apparent from these figures that the numerically integrated stress is slightly greater than the stress in the incompressible material, which is surprising. One would expect the more compliant material to have the lower stress.

We note that the introduction of the stability parameter θ has the net effect of replacing (9.11) by

$$\underset{\sim}{\varepsilon} = \left(1 + \frac{\theta h}{T}\right) \underset{\sim}{\dot{s}}^{*} - \left(\frac{\nu}{1+\nu} + \frac{1}{3}\frac{\theta h}{T}\right) (\underset{\sim}{1} : \underset{\sim}{\dot{s}}^{*}) \underset{\sim}{1}$$

$$+ \frac{1}{T}\left(\underset{\sim}{s} - \frac{1}{3}(\underset{\sim}{1} : \underset{\sim}{s})\underset{\sim}{1}\right).$$

Dividing through this equation by $\left(1 + \frac{\theta h}{T}\right)$, setting $\nu = \frac{1}{2}$, and defining $T_\theta = T + \theta h$ gives

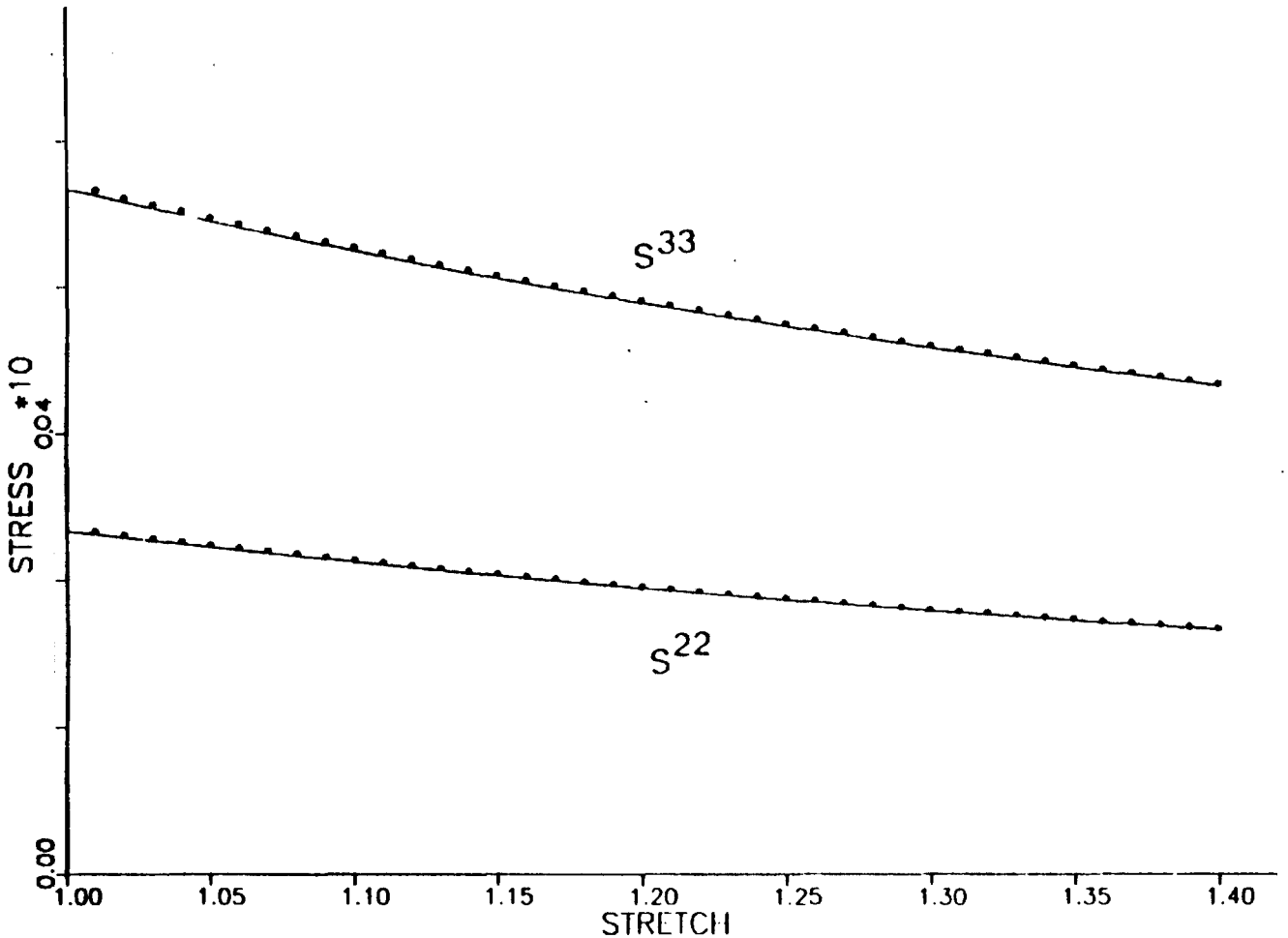

Figure 9. Stress Accompanying Plane Extension of a Viscoplastic Material--Euler Integration

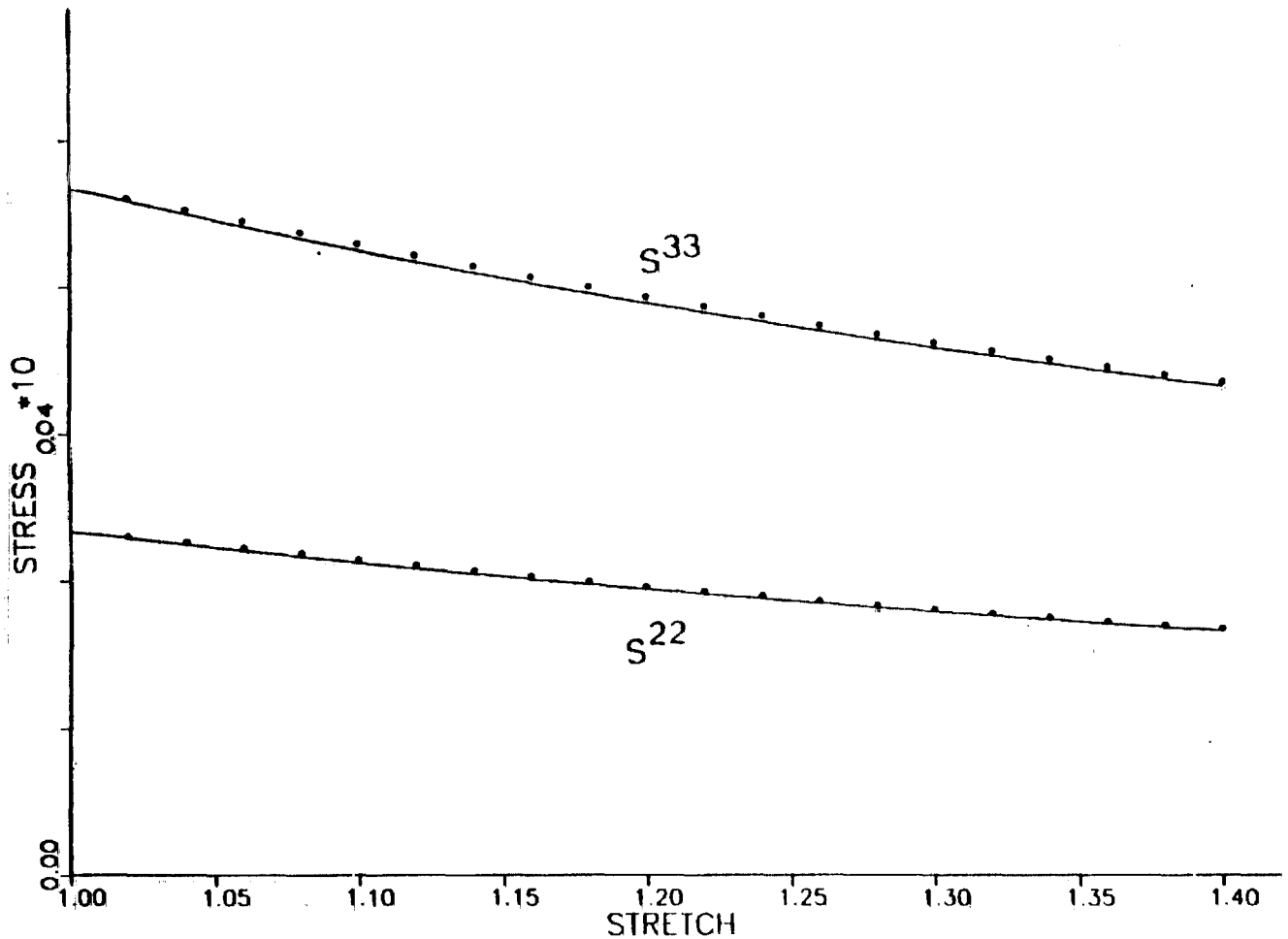

Figure 10. Stress Accompanying Plane Extension of a Viscoplastic Material--RK2 Integration

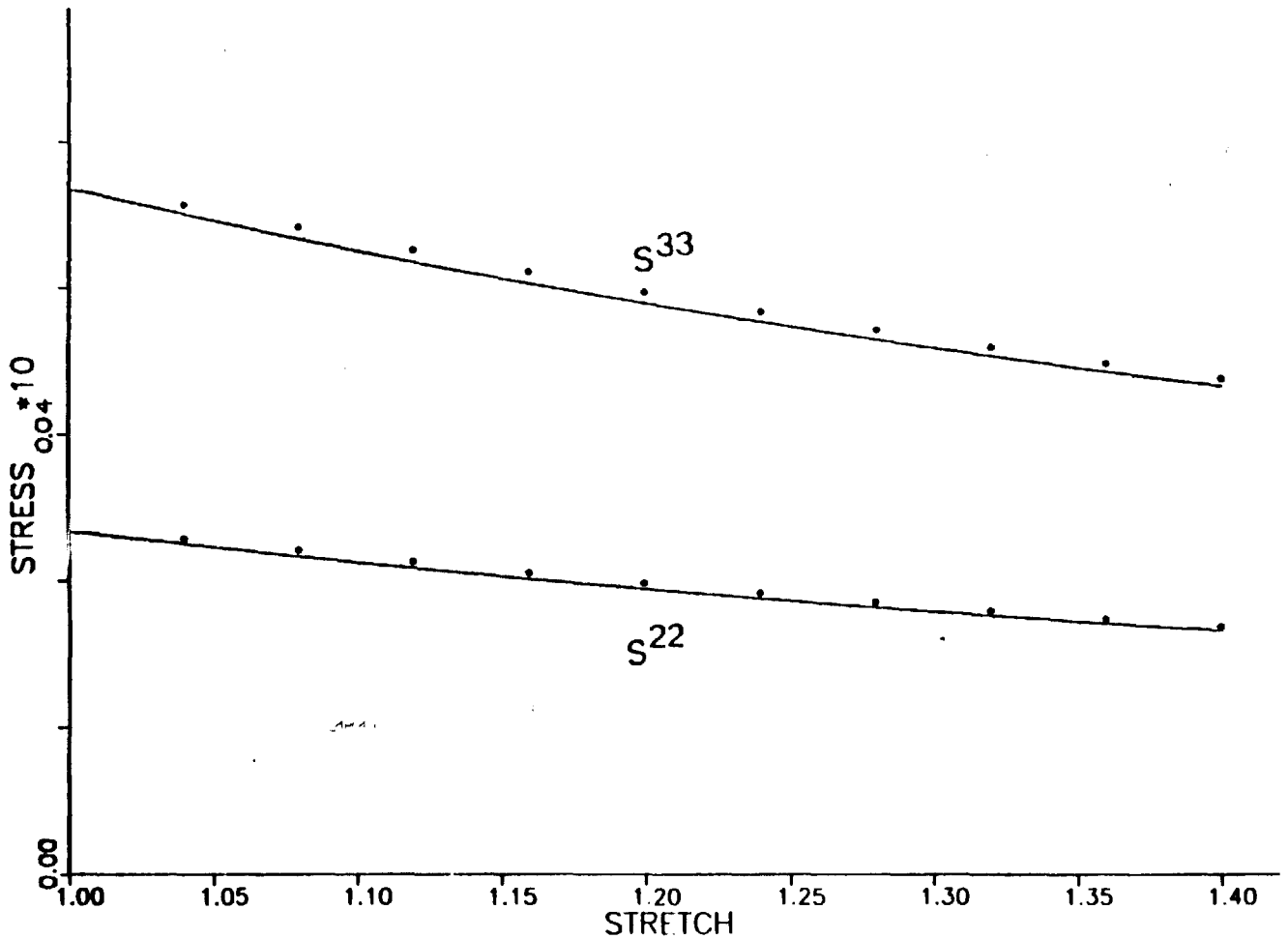

Figure 11. Stress Accompanying Plane Extension of a Viscoplastic Material--RK4 Integration

$$\left(\frac{T}{T_\theta}\right)\underset{\sim}{\varepsilon} = \overset{\cdot}{\underset{\sim}{s}}^{*} - \left(\frac{0.5}{1+0.5}\right)(\underset{\sim}{1} : \overset{\cdot}{\underset{\sim}{s}}^{*})\underset{\sim}{1} + \frac{1}{T_\theta}\left(\underset{\sim}{s} - \frac{1}{3}(\underset{\sim}{s} : \underset{\sim}{1})\underset{\sim}{1}\right). \quad (9.15)$$

But this equation has already been integrated for plane extension. From (9.12) we can immediately write

$$s^{11}(t) = 0 \; ; \qquad s^{22}(t) = \tfrac{1}{2} s^{33}(t)$$

$$s^{33}(t) = s^{33}(0)e^{-t/T_\theta} + \frac{2T}{T_\theta}\int_0^t \varepsilon^{33}(\zeta)e^{-(t-\zeta)/T_\theta}\, d\zeta \; . \quad (9.16)$$

Now we consider the special case that $\varepsilon^{33}(t)$ is a constant. Integration of (9.12) gives

$$s^{33}(t) = s^{33}(0)e^{-t/T} + 2T\varepsilon^{33}(0)(1 - e^{-t/T}) \; . \quad (9.17)$$

At times t much later than t = T the stress attains a steady state value of $2\varepsilon^{33}(0)T$. Integration of (9.16) yields

$$s_\theta^{33}(t) = s^{33}(0)e^{-t/T_\theta} + 2T\varepsilon^{33}(0)\left(1 - e^{-t/T_\theta}\right), \quad (9.18)$$

and at late times $s_\theta^{33}(t) \to 2\,\varepsilon^{33}(0)T$. Thus, the steady state value of the stress in plane extension is unaffected by the introduction of the stability parameter θ. The important difference between (9.17) and (9.18) is the rate at which the stress approaches the steady state value. It is clear that $s^{33}(t)$ and $s_\theta^{33}(t)$ are related as

$$s^{33}(t) = s_\theta^{33}\left(t\left(1 + \frac{\theta h}{T}\right)\right) .$$

Simply put, the stress s_θ^{33} 'lags' the correct stress. This is exactly what is observed in Figures 9, 10, and 11. That lag becomes increasingly apparent as the order of the integration scheme is increased, since the numerical solution tends towards $s_\theta^{33}(t)$, not $s^{33}(t)$. We conclude the discussion of this example by remarking that this lagging of the stress must be expected any time the stability parameter $\theta \neq 0$, and the lag increases with $(\theta h/T)$.

In the second case of plane stretching of a creeping viscoplastic material we set the initial stresses to zero. As before, $V = 10^{-4}\text{sec}^{-1}$ (nominal stretch rate), $T = \frac{1}{2}(56/90)10^{12}$ sec (characteristic time), and Cormeau's [46] time step bound is $h < h_c = 2T$. The stress in this example differs from the stress in the previous example solely because of the different initial stress, and that difference attenuates like $e^{-t/T}$. For times t much later than $t = T$, the stress in this example is indistinguishable from that of the previous example. We use Euler's method for integration, taking time steps of $h = \frac{1}{2}(90/56)h_c$, $(90/56)h_c$, and $2(90/56)h_c$ (for stretch increments of 0.005, 0.01, and 0.02, respectively). We set the stability parameter θ to unity, $\theta = 1$ (giving $\theta h/T = (90/56)$, $2(90/56)$, and $4(90/56)$, respectively). In Figures 12, 13, and 14 the stresses found by application of the finite element algorithm are compared to the closed form solution (9.12) for the incompressible body with the same characteristic time T, and also to the closed form solution for the

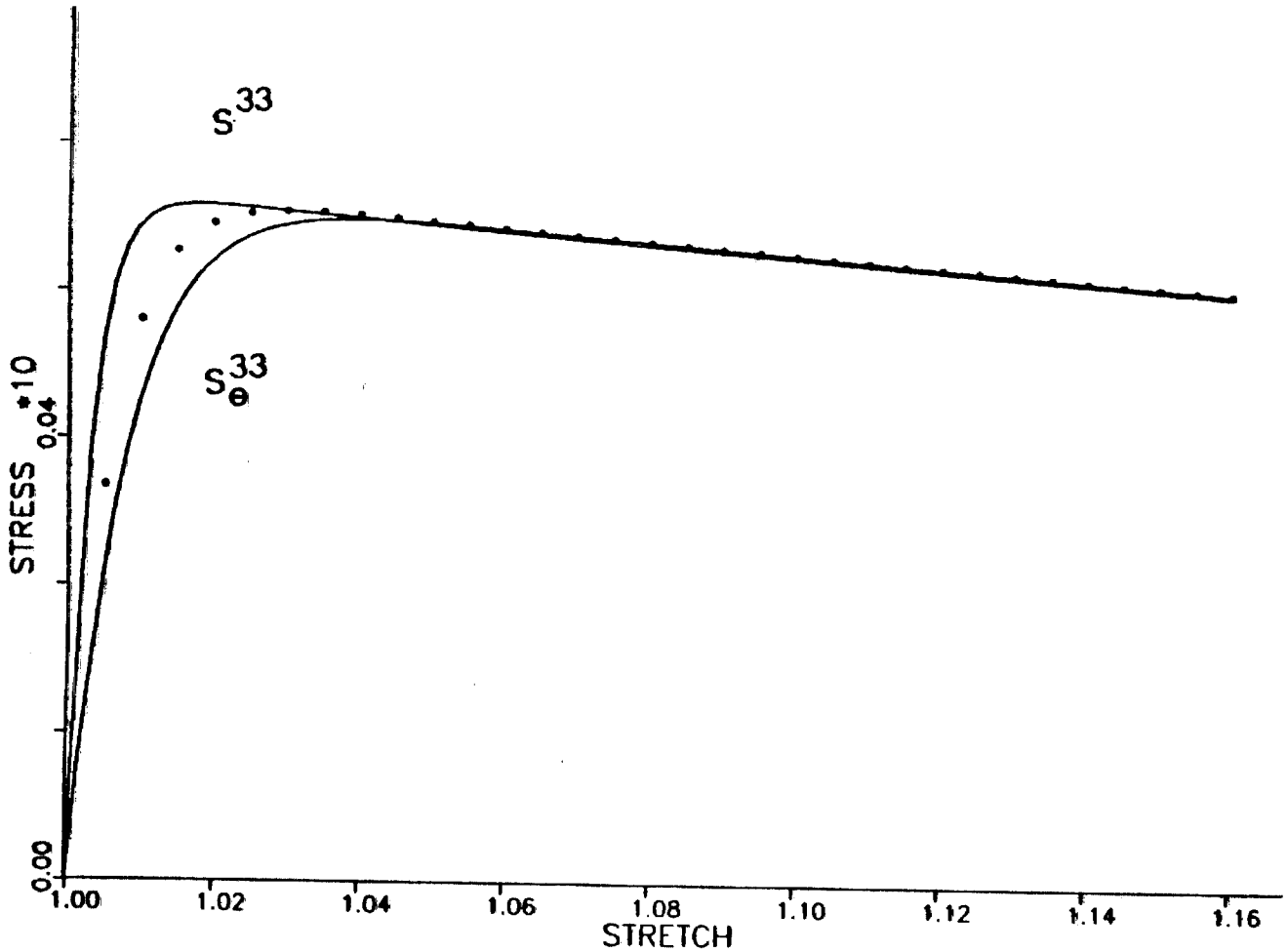

Figure 12. Stress Accompanying Plane Extension of a Viscoplastic Material--($\theta h/T$) = (90/56)

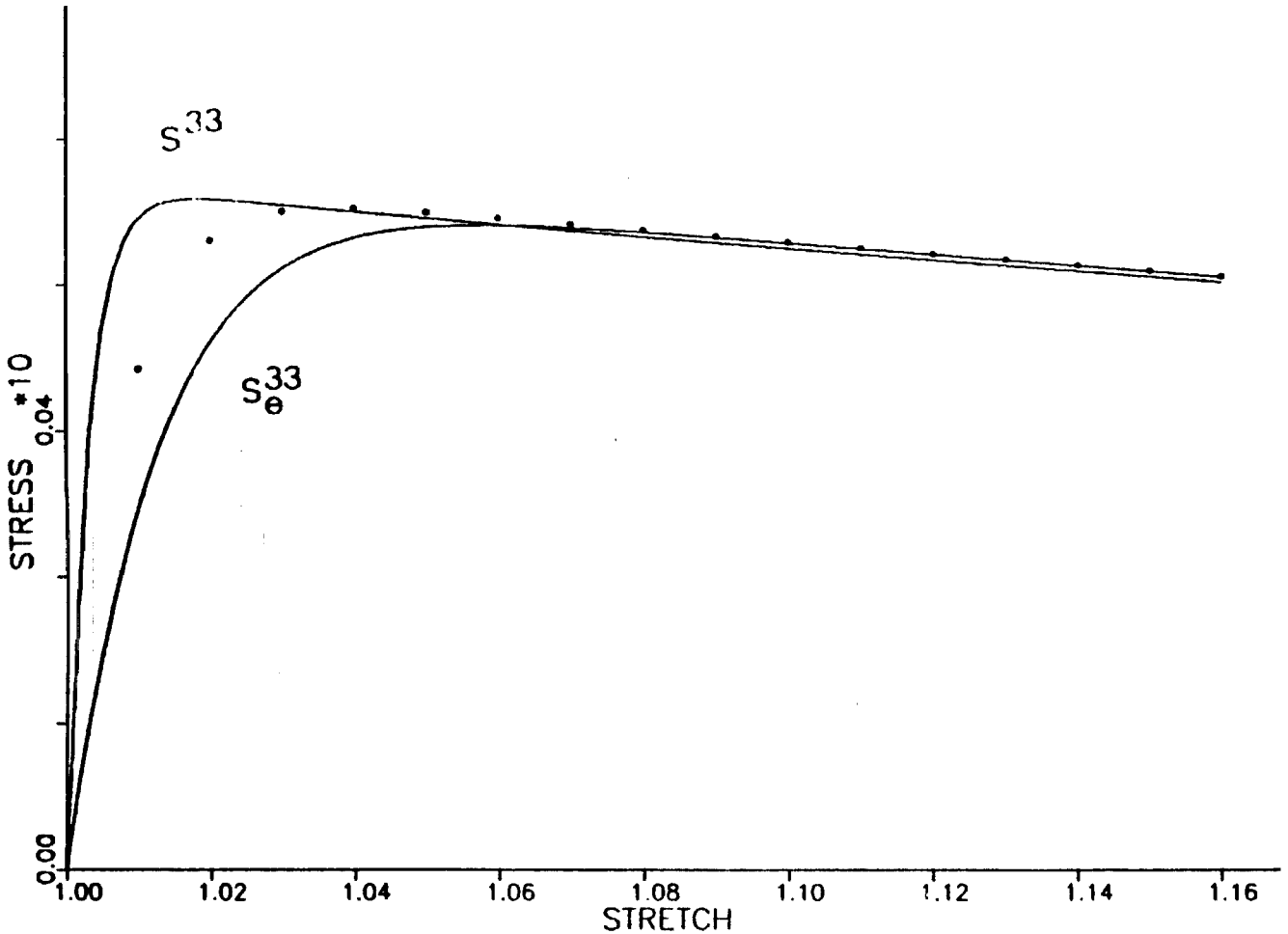

Figure 13. Stress Accompanying Plane Extension of a Viscoplastic Material--(θh/T) = 2(90/56)

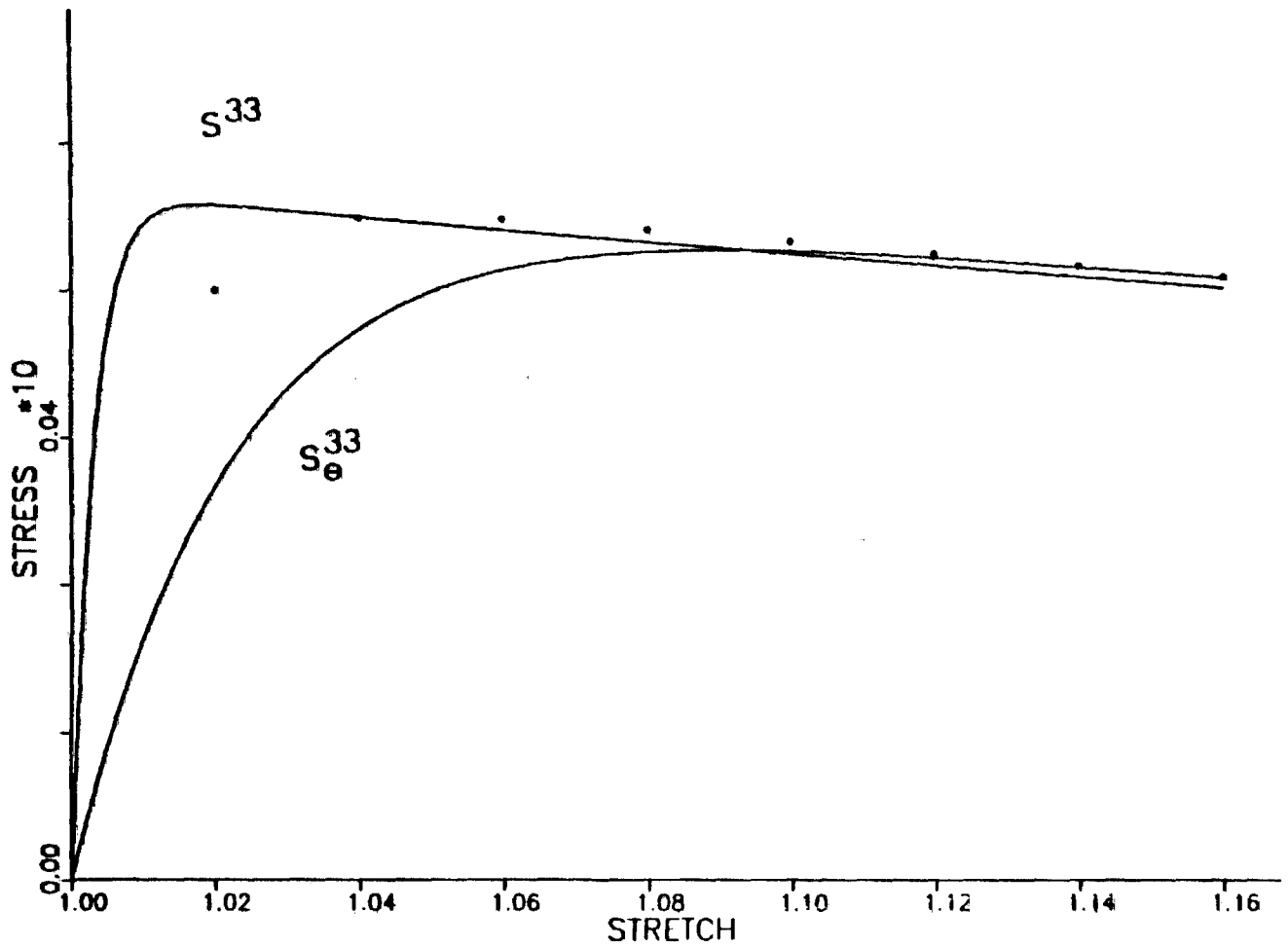

Figure 14. Stress Accompanying Plane Extension of a Viscoplastic Material--(θh/T) = 4(90/56)

incompressible body with the θ-modified characteristic time T_θ. It is clear from these figures that only a qualitative estimate of the transient stress response is given by the finite element algorithm; and that estimate is degraded as (θh/T) increases. More important though is the fact that use of a higher order time stepping algorithm (for the same (θh/T)) *cannot* improve the accuracy of the numerical solution, since that solution would be drawn closer to $\underset{\sim}{s}_\theta$, not $\underset{\sim}{s}$. It is therefore senseless to use methods other than Euler's when θh is of the same order of magnitude as the characteristic time T.

Finite Rectilinear Shear

We continue our study of homogeneous deformations by considering finite rectilinear shear of (i) the hypoelastic material (9.2), (ii) a second hypoelastic material which resembles an elastic-perfectly plastic material, and (iii) a creeping viscoplastic material. The geometry of the specimen is given in Figure 15. These examples serve not only to further demonstrate the performance of the finite element algorithm, but also to portray aspects of the finite deformation behavior of the materials themselves. Consistent with the conclusions of the previous section, we use only higher order integration schemes for the two hypoelastic materials (on the basis of efficiency). It happens that for this completely constrained deformation stable integration of the stress in the viscoplastic material may be achieved without relying on the forward gradient technique. We take advantage of this situation by comparing the accuracy of the finite element algorithm with and without the forward gradient scheme for the same deformation. From the results one can only conclude that further research is needed.

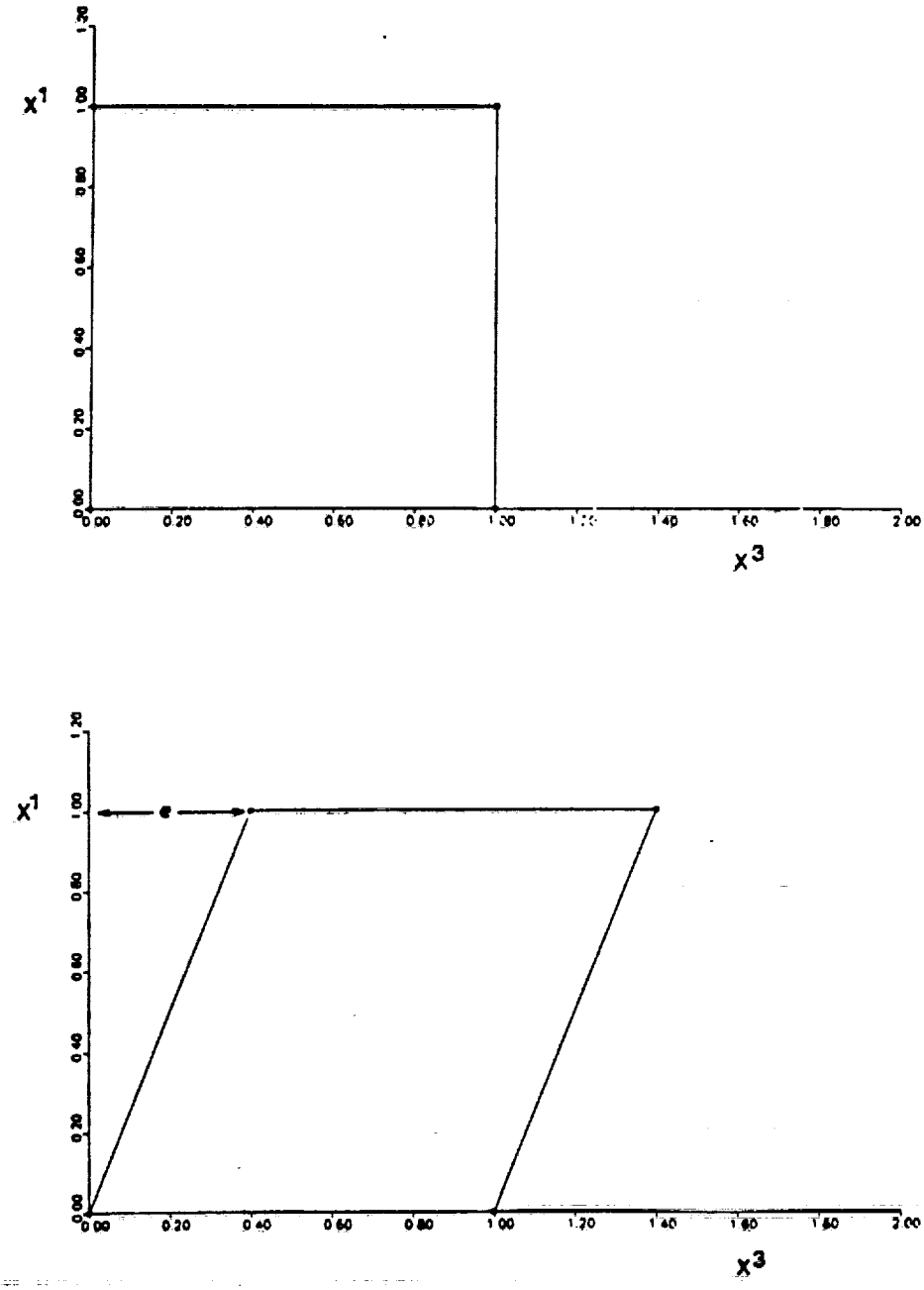

Figure 15. Rectilinear Shear Specimen

Hypoelastic Material. We consider for a second time the hypoelastic material defined by (9.2). For homogeneous rectilinear shearing of this material from a stress free state, $v^1 = v^2 = 0$, $v^3 = \dot{e}x^1$, the normalized stress $\underset{\sim}{s}$ is given by

$$s^{33}(e) = -s^{11}(e) = \tfrac{1}{2}(1 - \cos(e))$$
$$s^{13}(e) = \tfrac{1}{2}\sin(e) \quad . \tag{9.19}$$

We compare the stresses found by application of the finite element algorithm to the closed form solution in Figure 16. The RK2 algorithm was used, with time steps corresponding to (nominal) shear increments of (0.16). As discussed in Chapter IV, constitutive equation (9.2) is invalid beyond the nominal shear strain $e = \frac{1}{2}\pi$. This is of little consequence if one is interested only in metals such as used in structures, because some mechanism of inelasticity always sets in long before such a large shear strain as $e = \frac{1}{2}\pi$ is reached. However, since (9.2) is typically used to model the elastic part of the stretching in constitutive equations for inelasticity, one must ask whether or not similar periodic behavior will be observed when a hypoelastic/plastic or hypoelastic/viscoplastic material is subjected to such large shear strains.

A Second Hypoelastic Material. We consider a second hypoelastic material whose constitutive equation resembles that of an elastic-perfectly plastic material. This material is studied in

Figure 16. Stress Accompanying Rectilinear Shear of a Hypoelastic Material

place of a truly plastic material because of the availability of a closed form solution [27]. It would have been possible to 'splice' solutions for an elastic material and the present material at the yield surface to obtain a closed form solution for a truly elastic-plastic material, but there would have been little to gain in the way of illustration. The new hypoelastic material is defined by

$$\overset{\nabla}{\underset{\sim}{\sigma}}^{*} = 2\mu\underset{\sim}{\varepsilon} + \lambda(\underset{\sim}{I} : \underset{\sim}{\varepsilon})\underset{\sim}{I} - \frac{2\mu}{\frac{2}{3}\tau_y^2}(\underset{\sim}{\tau}' : \underset{\sim}{\varepsilon})\underset{\sim}{\tau}' \quad . \tag{9.20}$$

By defining $K^2 = \frac{2}{3}(\tau_y/2\mu)^2$, introducing the normalized stress $\underset{\sim}{s} = \underset{\sim}{\tau}/2\mu$, and prescribing rectilinear shearing, we deduce

$$\overset{\nabla}{\underset{\sim}{s}}^{*} = \underset{\sim}{\varepsilon} - \frac{1}{K^2}\underset{\sim}{s}(\underset{\sim}{s} : \underset{\sim}{\varepsilon}) \quad . \tag{9.21}$$

For materials such as those used in structures the parameter K is typically of the order of (0.01). The stresses accompanying rectilinear shearing from a stress free state were found in [27] as

$$\begin{aligned} s^{13}(\phi) &= \tfrac{1}{2} K \sin(\phi)/(\tfrac{1}{2} + K^2)^{\frac{1}{2}} \\ s^{33}(\phi) &= -s^{11}(\phi) = \tfrac{1}{2} K^2(1 - \cos(\phi))/(\tfrac{1}{2} + K^2) \end{aligned} \tag{9.22}$$

where

$$\tan(\tfrac{1}{2}\phi) = \left(\frac{\frac{1}{2} + K^2}{\frac{1}{2} - K^2}\right)^{\frac{1}{2}} \tanh\left(\frac{(\frac{1}{2} - K^2)^{\frac{1}{2}}}{2K} e\right); \qquad K^2 < \tfrac{1}{2} \quad .$$

In Figure 17 we compare the stresses found by application of the finite element algorithm to the closed form solution (9.22) or the special value K = (0.10). The RK2 time stepping algorithm was used for the computation. The closed form solution has a peak at [27]

$$e_c = \frac{K}{\left(\frac{1}{2} - K^2\right)^{\frac{1}{2}}} \ln \frac{\frac{1}{2} + \left(\frac{1}{4} - K^2\right)^{\frac{1}{2}}}{K^2} = 0.656431$$

but this is completely lost in the numerical solution. At shear strains larger than e_c above, the shear stress s^{13} is a decreasing function of e; one must conclude that the model (9.20) is unacceptable beyond that level of strain.

Creeping Viscoplastic Material. As final examples of rectilinear shear we consider a viscoplastic material wh creeps from a stress free state at several different rates. For a second time we use the material defined by (9.11). The specimen geometry is the same as in the previous two examples. The stress accompanying the deformation is

$$s^{33}(e) = -s^{11}(e) = s_\infty^{13}\left\{ E - \exp\left(\frac{-e}{E}\right)[\sin(e) + E\cos(e)]\right\}$$

$$s^{13}(e) = s_\infty^{13}\left\{1 - \exp\left(\frac{-e}{E}\right)[\cos(e) - E\sin(e)]\right\} \qquad (9.23)$$

where $E = \dot{e}T$, and $s_\infty^{13} = \frac{1}{2}E/(1 + E^2)$. The characteristic time T is the same in this case as in the plane extension examples. We took values of E as (0.5), (1.0), and (2.0), corresponding to nominal shear strain

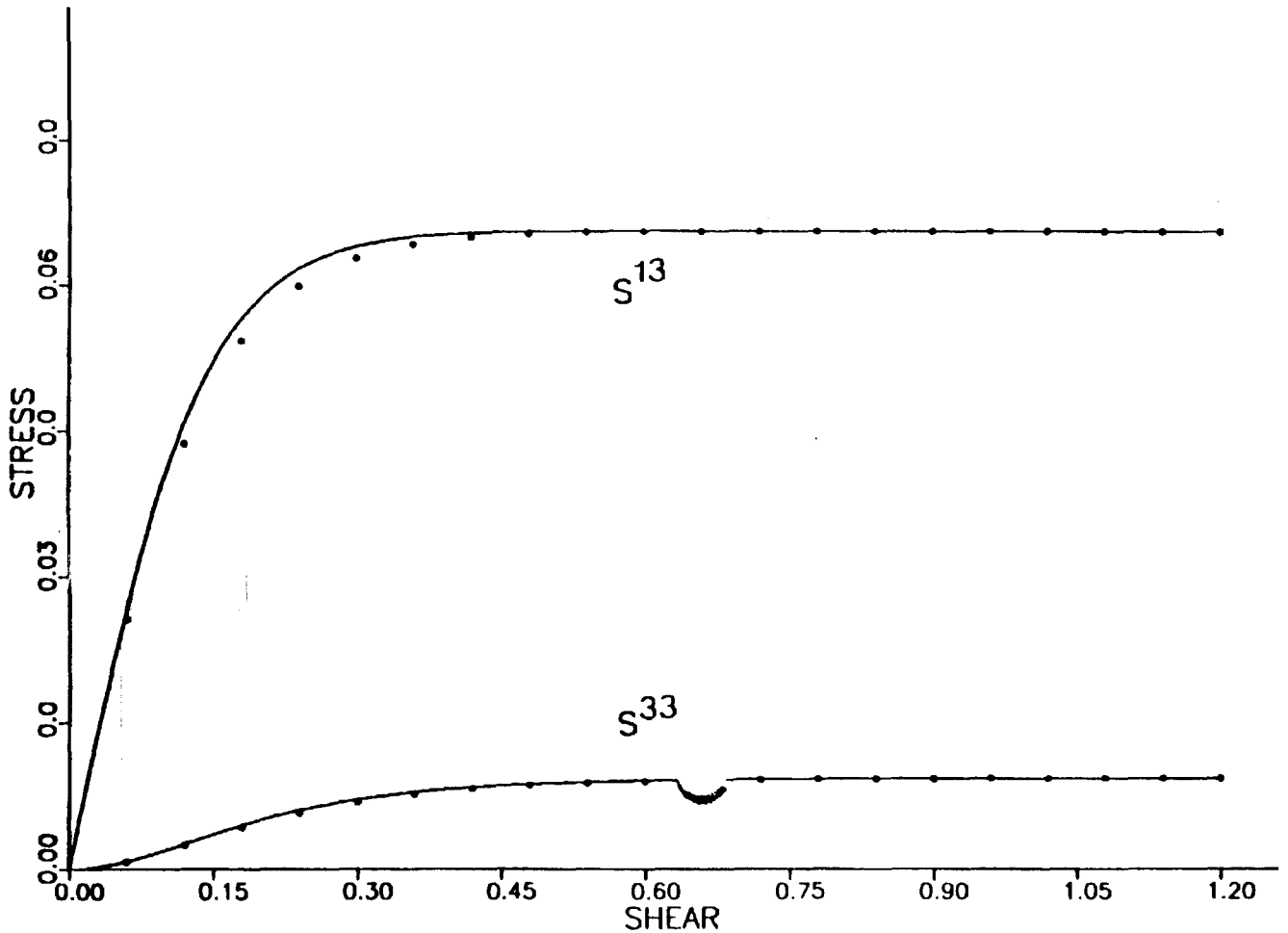

Figure 17. Stress Accompanying Rectilinear Shear of a Second Hypoelastic Material

rates of $(45/28) \times 10^{-12}$, $(45/14) \times 10^{-12}$, and $(45/7) \times 10^{-12}$, respectively. The reader should note that these strain rates are indeed very slow. The stresses found by application of the finite element algorithm are compared to the closed form solution in Figures 18, 19, and 20. The RK2 algorithm was used for time integration, with time steps corresponding to nominal shear strain increments of (0.2). The first stress peak is at $e = \frac{1}{2}\pi$, and the final shear strain is (8.0). The reader should note that the behavior is (qualitatively) similar to the purely hypoelastic behavior (period) and to rigid-viscoplastic (or viscous fluid) behavior at late times.

In the three cases above it was not necessary to use the forward gradient scheme since the deformation was completely constrained. However we can still introduce the stability parameter for the purpose of finding out what error it leads to. Just as for the examples of plane extension, it is possible to integrate the modified equations in closed form. The solution of the θ-modified problem is found by replacing E by $E(1 + \theta h/T)$ in (9.23) everywhere except in the numerator of s_∞^{13}. The stresses found by application of the finite element algorithm, with $\theta = 1$, are plotted in Figure 21, along with the solutions of the true and modified problems, for the case $E = 2$. All the other data is unchanged. The reader should note that at late times the two solutions do not coincide; rather, we get the ratios

$$s_\theta^{13}/s^{13} \to (1 + E^2)/(1 + E_\theta^2)$$

$$s_\theta^{11}/s^{11} \to (E_\theta/E)(s_\theta^{13}/s^{13}) \quad . \tag{9.24}$$

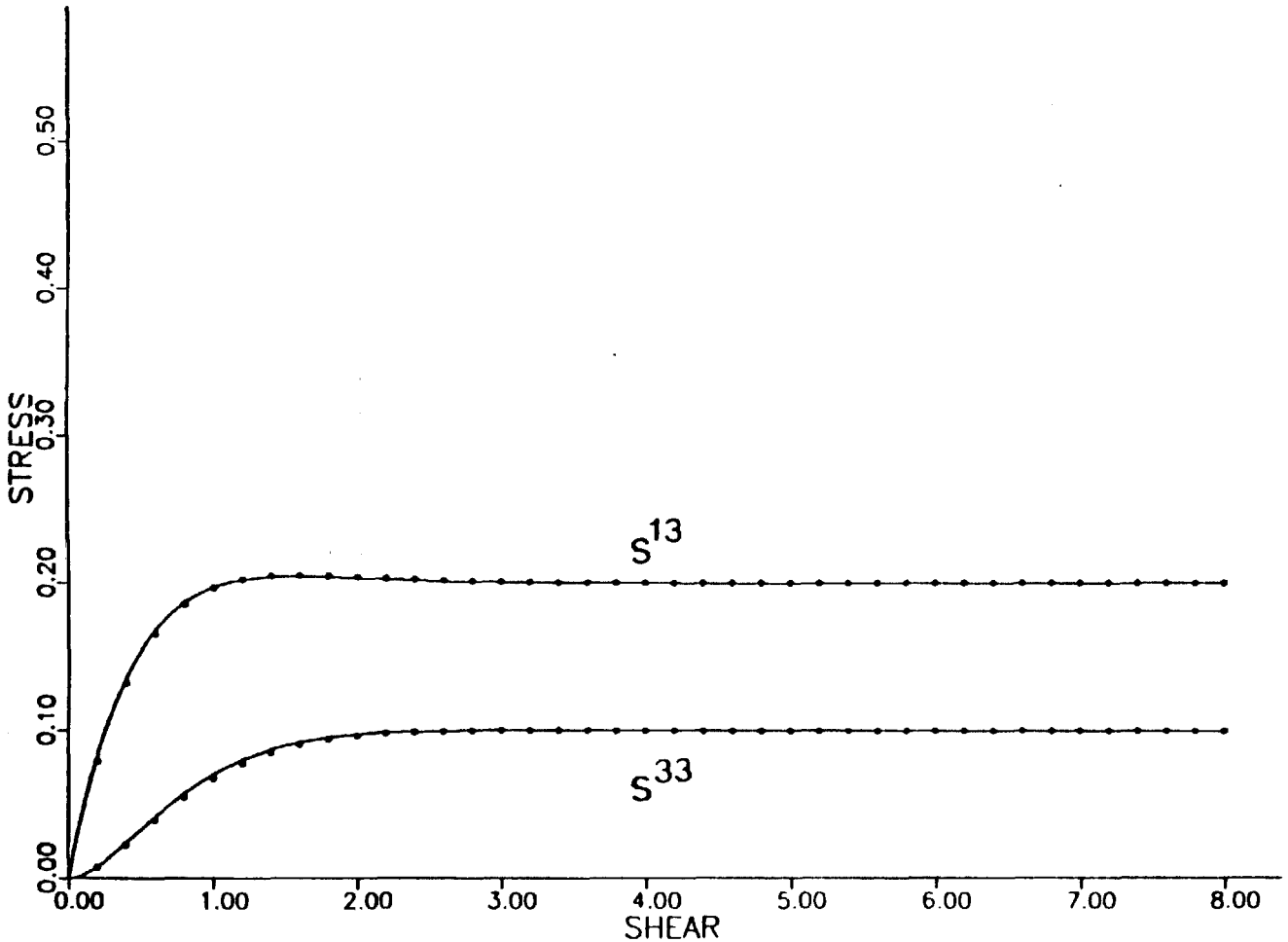

Figure 18. Stress Accompanying Rectilinear Shear of a Viscoplastic Material--E = 0.5

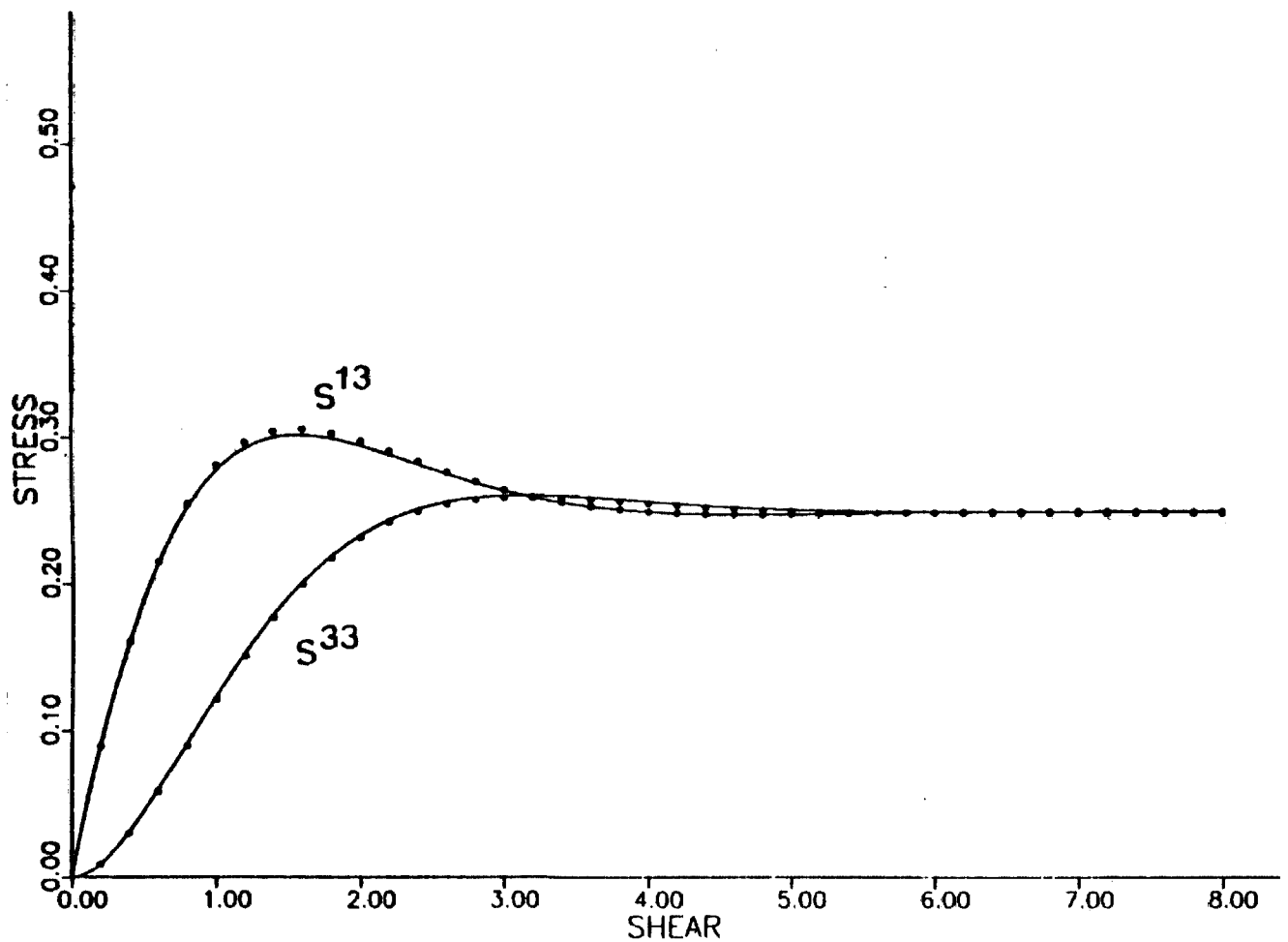

Figure 19. Stress Accompanying Rectilinear Shear of a Viscoplastic Material--E = 1.0

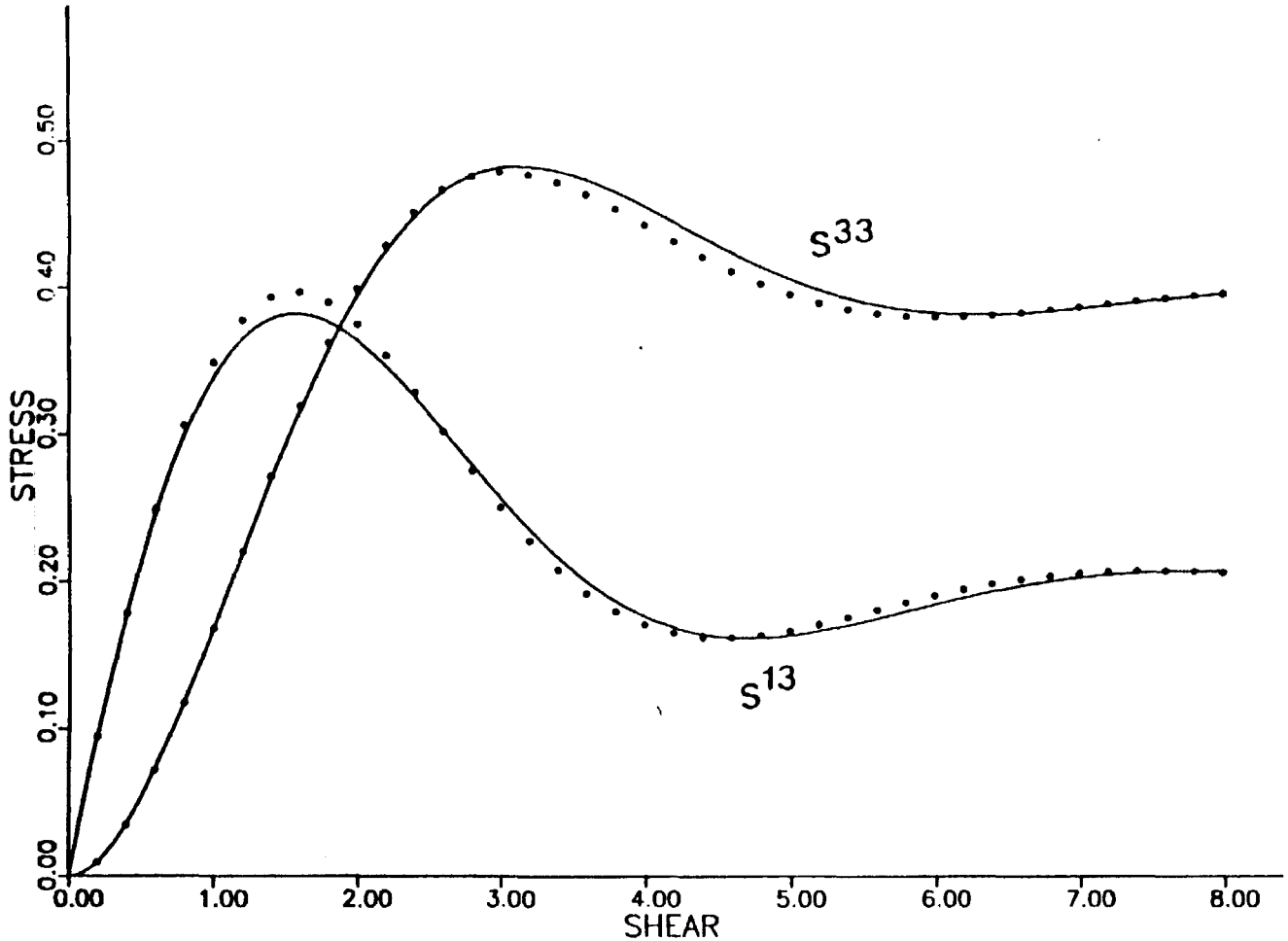

Figure 20. Stress Accompanying Rectilinear Shear of a Viscoplastic Material--E = 2.0

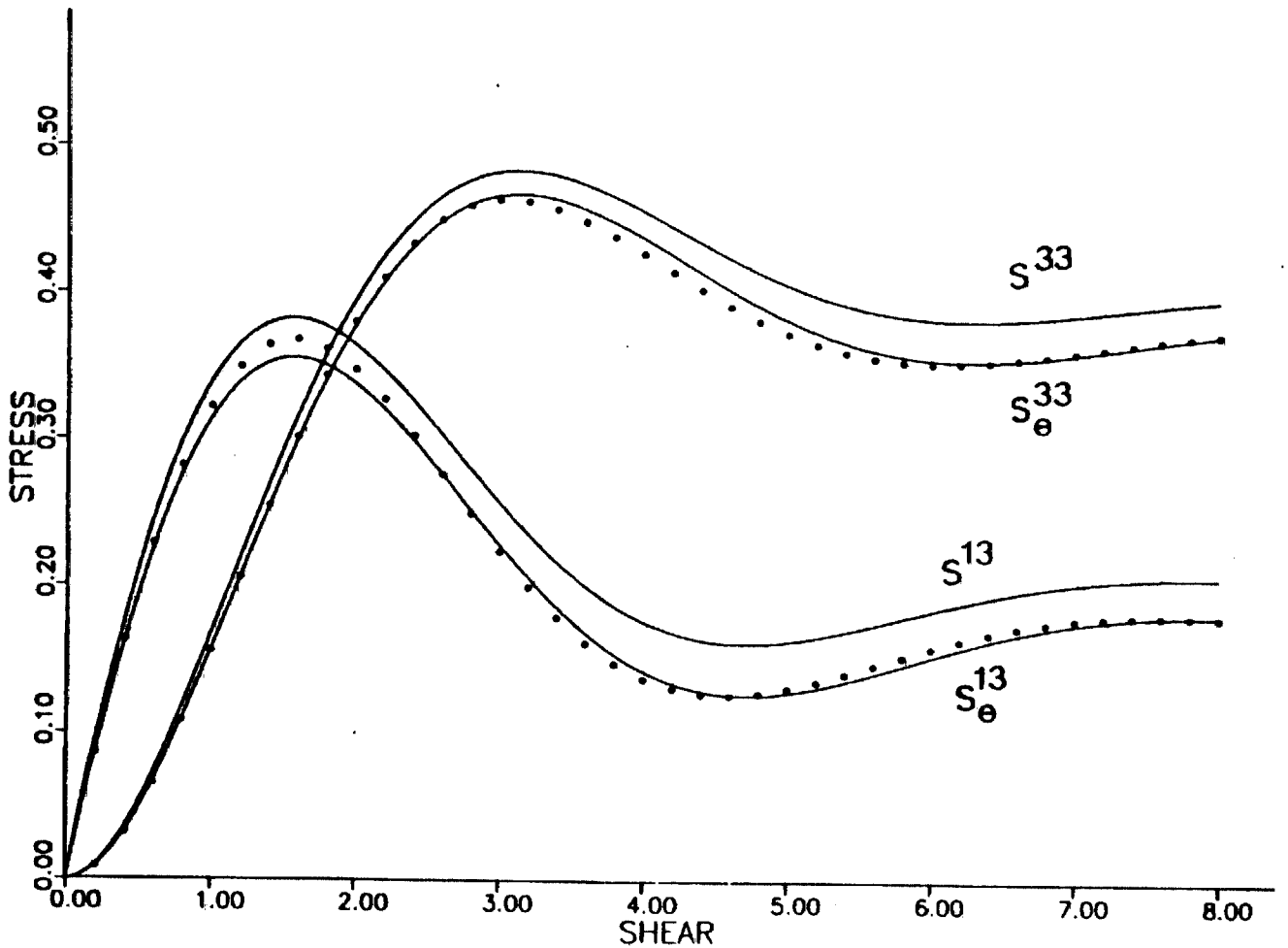

Figure 21. Stress Accompanying Rectilinear Shear of a Viscoplastic Material--$\theta = 1$

From (9.15) it is easily seen that the influence of the parameter θ will vanish at late times (for any deformation) only so long as $\overset{\bullet}{\underset{\sim}{s}}^*$ vanishes at late times. In other words, the forward gradient scheme presented here will only give correct steady state values of the stress for deformations in which the spin or the total stress vanishes at late times. Rectilinear shearing does not meet either of these conditions. Further research is needed to determine whether or not this defect in the forward gradient scheme, which is probably only important for large deformations, can be overcome.

Inhomogeneous Deformations

We conclude this chapter with three studies of inhomogeneous deformations. In the first, a study of creep in a pipe due to internal pressure, the numerical solution is compared to closed form solutions for elastic and rigid-plastic bodies (at different stages of the deformation), as well as to other numerical results. In the second problem, a study of the onset of necking in the plane tensile test, results are compared to closed form results for an incompressible body as well as to other numerical results. In the third problem, a study of plane void growth in a creeping viscoplastic medium, comparison is made to other numerical results. As shall be seen, the stress-rate based finite element algorithm compares very well in every case.

Creep of a Pipe from Internal Pressure

The problem geometry and boundary conditions are given in Figure 22. The problem may be analyzed in three stages: (1) rapid elastic inflation, (2) transient stress stage, and (3) large strain

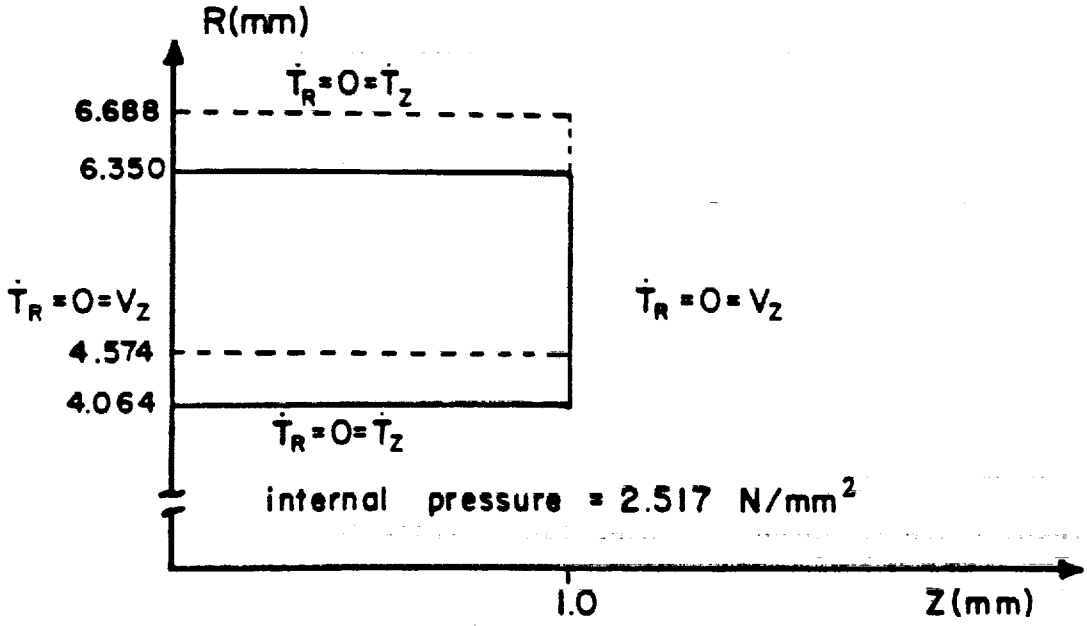

Figure 22. Pipe Creep Specimen

creep stage. The first two parts of this problem have been studied by Greenbaum and Rubenstein [54], and Pian and Lee [55]. The creep behavior is characterized by the uniaxial relation

$$\varepsilon_{11}^{P} = \gamma(\tau^{11})^{N} M t^{M-1} \qquad (9.25)^{*}$$

where $\gamma = 2.073 \times 10^{-8} (hr)^{-1} (N/mm^2)^{-N}$, $N = 4.4$, and $M = 0.7$. The elastic and inelastic components of the stretching are

$$\underset{\sim}{\varepsilon}^{e} = \left(\frac{1+\nu}{E}\right) \overset{\nabla}{\underset{\sim}{\sigma}}^{*} - \left(\frac{\nu}{E}\right) (\underset{\sim}{I} : \overset{\nabla}{\underset{\sim}{\sigma}}^{*}) \underset{\sim}{I} \qquad (9.26)$$

$$\underset{\sim}{\varepsilon}^{P} = \frac{3}{2} \gamma \left(\sqrt{\frac{3}{2} \underset{\sim}{\tau}' : \underset{\sim}{\tau}'} \right)^{N-1} (M t^{M-1}) \underset{\sim}{\tau}'$$

As in [55], time integration is carried out with respect to the parameter $\lambda = t^{M}$. Real time is recovered after integration as $t = \lambda^{1/M}$. In the example we take $E = 1.379 \times 10^{11}$ Pa, $\nu = 0.45$, $\theta = \frac{1}{2}$, and use Euler integration exclusively.

Rapid Elastic Inflation. The pipe is taken from a stress free state to an elastically strained state in a single Euler step by imposing a nominal pressure rate on the inside wall of the pipe of $\dot{T}_1 = 2517$ $(N/mm^2 \cdot sec^{M})$ for a λ-time step of 0.001 $(sec)^{M}$. The pressure in the pipe at the end of elastic inflation is 2.517 (N/mm^2). In Figure 23 the stresses found by application of the finite element

*when the parameter $M < 1$, the material age-hardens.

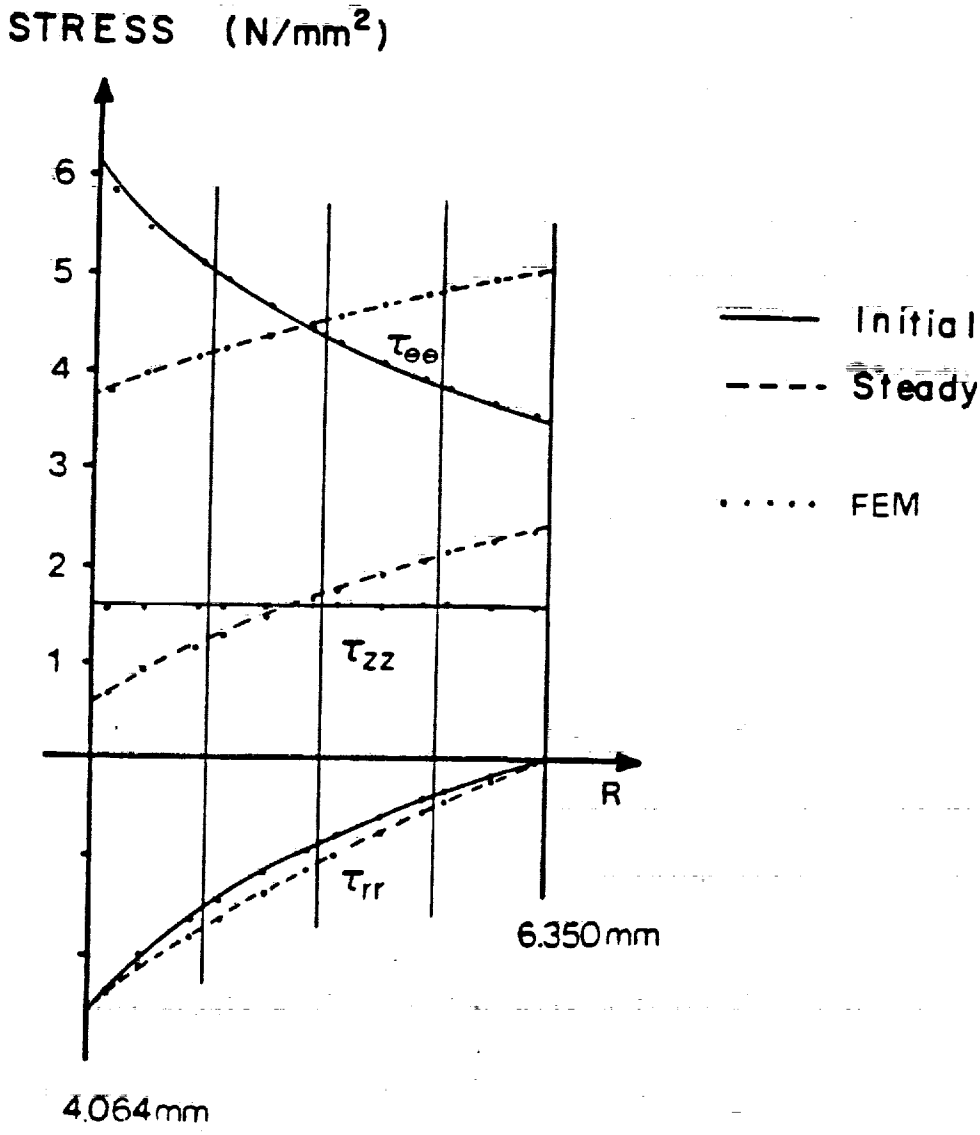

Figure 23. Stress Profiles in Pipe Creep Specimen

algorithm are compared to those predicted by the infinitesimal displacement theory of elasticity. As is evident, the two solutions are virtually indistinguishable.

Transient Stress Stage. In this stage the creep mechanism causes the stresses to redistribute themselves through the thickness of the pipe, and the pipe itself to expand slightly. In this stage the nominal traction rate on the inner wall was set to zero, and the λ-time step was set as $\Delta\lambda = 0.5\ (\text{sec})^M$. In Figure 23 the new distribution of stresses is compared to the stresses that would be obtained if the material were rigid plastic. These latter stress distributions are given by Hult [56]. Again, the two solutions are virtually indistinguishable. In Figure 24 the small deformation displacement history of the inner wall of the pipe is plotted against the result of Pian and Lee [55].

Large Strain Creep Stage. This stage is a continuation of the relatively steady creep that characterized the latter part of the previous stage. The only difference in the computation was the λ-time step was set to 400. In Figure 25 the maximum hoop stress history (at the outside wall) is plotted against the history for the rigid-plastic material. In this stage it is important to note that the traction boundary condition on the inside wall, $\dot{T}_1 = 0$ does not correspond to constant pressure; rather from the equation (3.36) we find that the pressure rate is

$$\dot{p} = -(\dot{a}/a)p \tag{9.27}$$

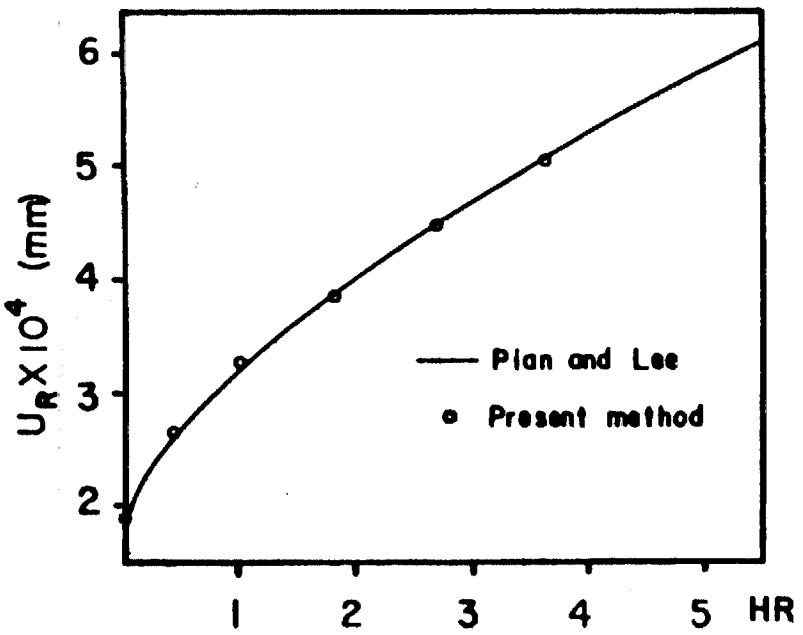

Present mtd

time	$U_R X 10^4$
0.0	1.90
0.37	2.60
1.00	3.24
1.79	3.85
2.69	4.46
3.70	5.07

Figure 24. Small Displacement History of Inner Wall of Pipe

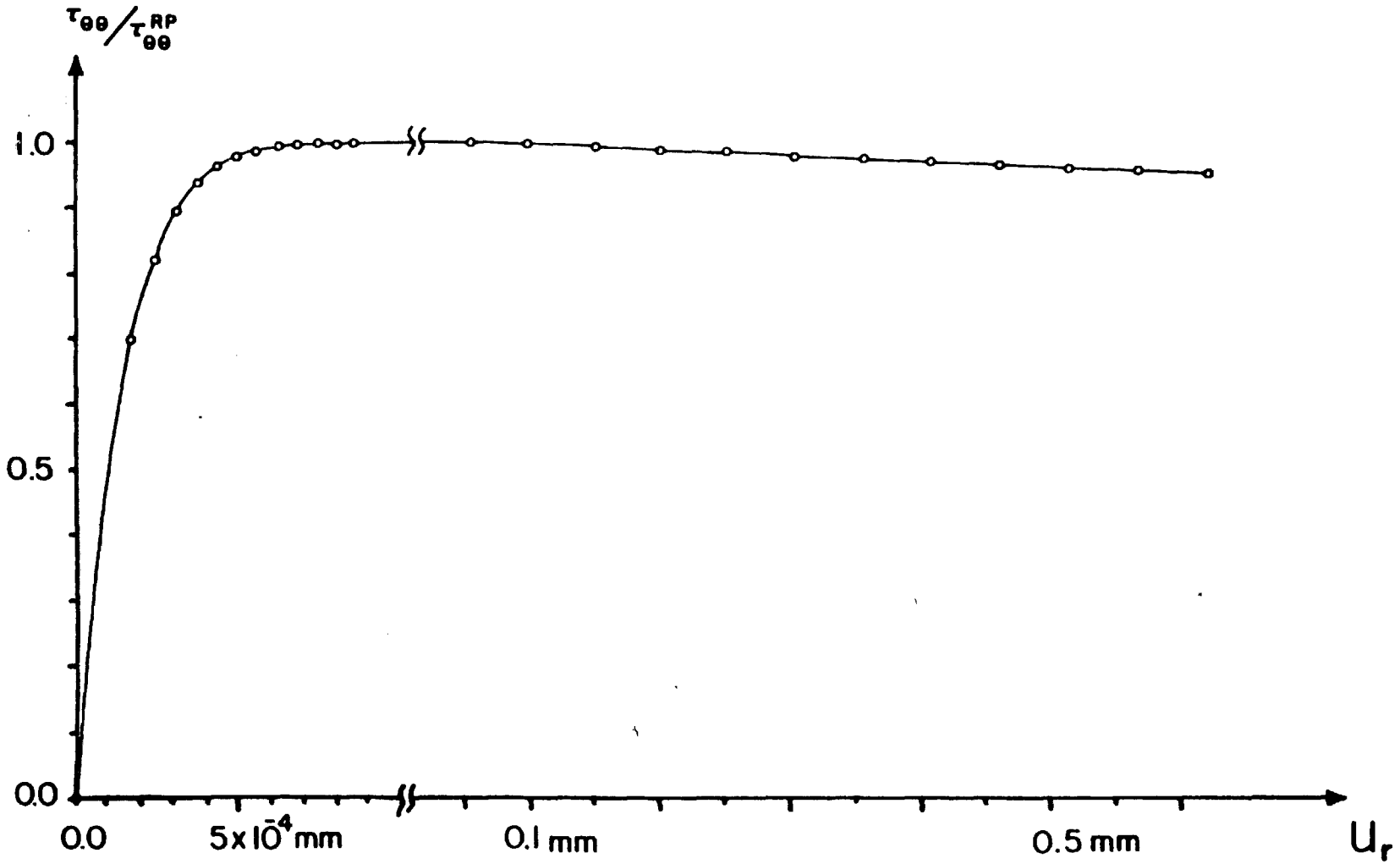

Figure 25. Maximum Hoop Stress History for Pipe

where a is the instantaneous inner radius of the pipe. Integration gives

$$p = (a_o p_o)/a \quad . \tag{9.28}$$

This traction boundary condition was chosen simply for convenience. For constant pressure, the nominal traction rate and velocity on the inner wall would have to satisfy

$$\dot{T}_1 - (\dot{a}/a)p_o = 0 \quad . \tag{9.29}$$

This boundary condition could be dealt with by iteration, using (9.29) to form 'residual loads,' or by recasting the traction boundary condition (7.2) as

$$\int_{S_\sigma} \left[\dot{T}_1 - (\dot{a}/a)p\right] \delta\dot{a} \, dS = 0 \quad . \tag{9.30}$$

The Onset of Necking in Plane Extension

It is well known that in tensile tests of metals (plane or uniaxial) the deformation prior to the attainment of the maximum load is essentially homogeneous. At some point after the maximum load point a 'neck' forms and the specimen fails almost immediately. In experiment, the point at which necking begins is sensitive to the slenderness of the specimen, the rate of strain hardening of the material, and the presence of geometric imperfections or inclusions.

Mathematically it is possible to consider specimens absolutely

free from geometric imperfections, and throughout which material properties are perfectly homogeneous. For such a 'perfect' specimen homogeneous stretching (such as discussed earlier in this chapter) to any extension is a solution of the general boundary value problem. However, to reach configurations of pure extension far beyond the maximum load point, the perfect specimen must pass through a (possibly infinite) number of configurations from which bifurcation is possible. For the classical elastic/plastic solid with a smooth yield surface the first possible mode of bifurcation is that of necking.

Within the past few years mathematical analyses of bifurcation from configurations of pure extension have been presented by Hutchinson and Miles [57], Miles [58], and Hill and Hutchinson [59]. The first two of these are concerned with the onset of necking in cylinderical and rectangular specimens of an incompressible elastic-plastic material. In the third an extensive study of general bifurcation phenomena of incompressible materials in the plane tension test is presented. For the classical elastic/plastic solid this study indicates that the first possible mode of bifurcation is that of necking.

Here we present a numerical study of the onset of necking of (hypo-) elastic/plastic solids in the plane tension test. To aid in the comparison of our results to those of Hill and Hutchinson [59], certain of their notations are adopted; these are explained as they are presented. The material we consider is slightly compressible*;

---

*the loading surface does not depend upon the pressure.

in order to compare our results to those of Hill and Hutchinson we must assume that the effect of this compressibility is slight, though not necessarily ignorable. So that the performance of the present finite element method may be contrasted to the performance of a velocity-based finite element algorithm, we have chosen particular materials identical to those used in the bifurcation study of Burke and Nix [60]. This appears to be the only other numerical study of bifurcation of classical elastic/plastic materials in plane extension in the literature.

Finally, we investigate the sensitivity of our results to variations in the number, shape, and type* of elements in the finite element mesh. This latter study serves not only to graphically demonstrate the stability of the finite element algorithm, but also to help characterize the approximation thus obtained.

Bifurcation Analysis. As discussed in Chapter VI, a condition sufficient for uniqueness of a deformation of an (hypo-) elastic/plastic body is that the second complementary virtual work principle have only the trivial solution for the 'linear comparison solid' when homogeneous boundary conditions are imposed. In as much as the finite element algorithm is based on that work principle, we equate the uniqueness criterion with the condition that the finite element equations have only the trivial solution for the linear comparison solid when homogeneous boundary data is imposed. Searching for possible

*the type is determined by the number of boundary nodes, the number of spin parameters, and the number of stress parameters.

bifurcation points amounts to looking for configurations of the body in which the global stiffness matrix $[K_L^*]$ is singular. The subscript L is to indicate that the stiffness matrix is formed as if loading occurs throughout the plastically stressed portions of the body; in extension problems this condition can be satisfied a posteriori by judicious superposition of the homogeneous and necking modes.

We consider a specimen of initial length $2a_o^3$ and thickness $2a_o^1$. We assume that the bifurcation mode will be symmetric in the sense that the velocity field may be reflected across the x^3 axis (see Figure 26). This is consistent with usage of the adjective 'symmetric' by Hill and Hutchinson. The finite element mesh is over the area $a^1 \times 2a^3$. The specimen is composed of the hypoelastic/plastic material of equations (9.5) through (9.7), and the subsequent discussions pertain only to that material.

To ease the comparison of our results to those of Hill and Hutchinson [59] we introduce the plane strain tangent modulus $4\mu^*$, defined by

$$\frac{\mathring{\sigma}_o^{33}}{J_o \varepsilon_{33}} = 4\mu^* \quad . \tag{9.31}$$

Assuming that as the bifurcation point is approached the stresses satisfy (approximately--see Figure 8)

$$\mathring{\sigma}^{22} = \tfrac{1}{21}\mathring{\sigma}^{33} \; ; \qquad \mathring{\sigma}^{22} = \tfrac{1}{2}\mathring{\sigma}^{33} \; ; \tag{9.32}$$

the constitutive equations (9.5) through (9.7) yield (without further

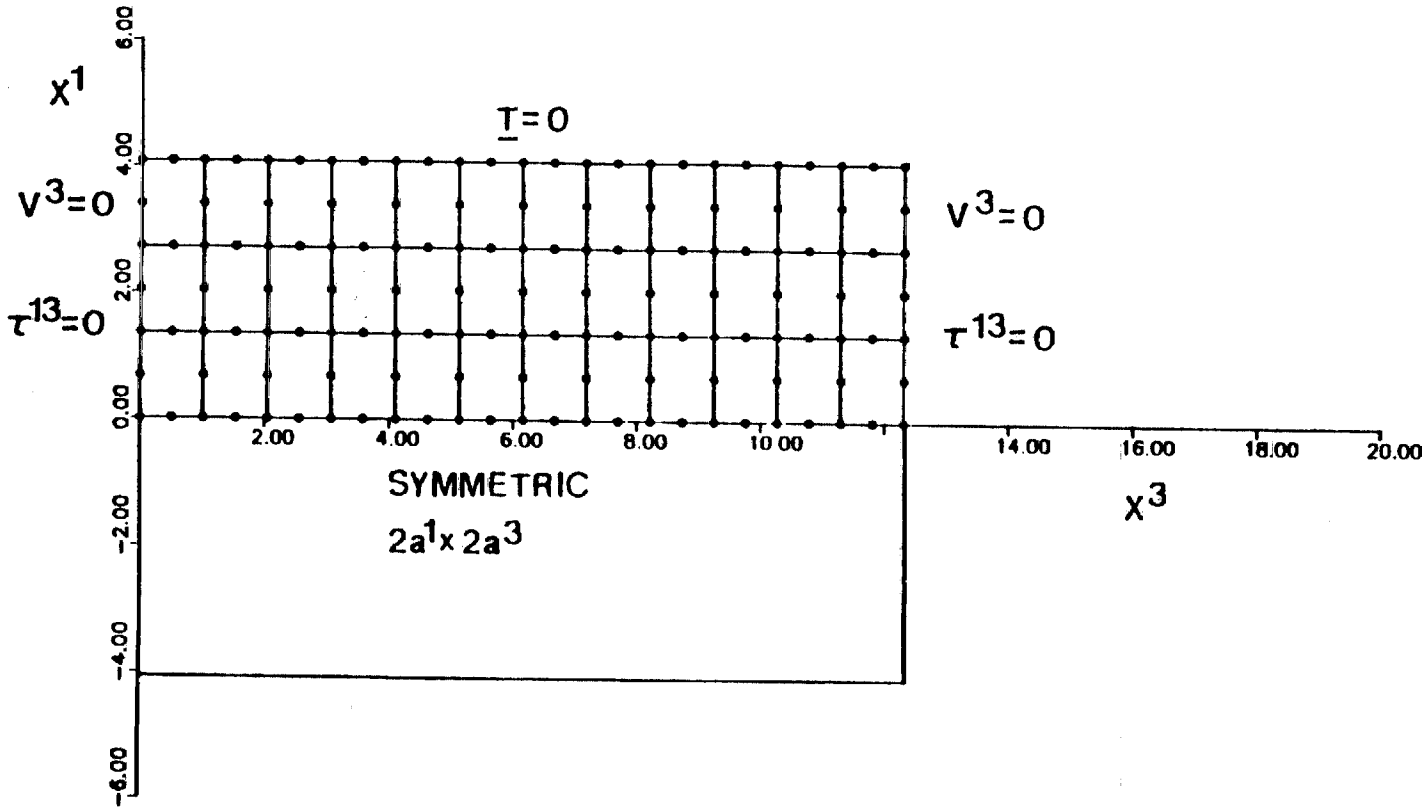

Figure 26. Specimen for Necking Analysis

approximation)

$$\frac{1}{4\mu^*} = \frac{1}{4E}\left[(1 - 2\nu) + 3N\left(\frac{\sqrt{3}\,\tau^{33}}{2\tau_y}\right)^{N-1}\right]. \qquad (9.33)$$

In our calculations the stress τ^{33} at the onset of necking was always at a level of stretch at which (i) (9.32) was a very good approximation, and (ii) the influence of ν on $4\mu^*$ was negligible.

The dimensionless stress $(\tau^{33}/4\mu^*)$ arises naturally in the analysis of Hill and Hutchinson. When the material (9.5)-(9.7) is incompressible, considering (9.9), we find

$$\frac{\tau^{33}}{4\mu^*} = \frac{\sqrt{3}\,N\tau_y}{2E}\left(\frac{\sqrt{3}\,\tau^{33}}{2\tau_y}\right)^{N} = -\tfrac{1}{2}N \ln (X/X_o) \qquad (9.34)^*$$

where $X = (a^1/2a^3)$ is the *stubbiness*, and $X_o = (a_o^1/2a_o^3)$. It is well known that the maximum load occurs when the tangent modulus (as defined by 4.39 or 9.31) falls to equal the stress; (i.e. when $(\tau^{33}/4\mu^*) = 1$).** No bifurcation can occur before this point [23].

The tangent modulus continues to decline after the maximum load, so $4\mu^* < \tau^{33}_{\text{max load}} \ll \mu$; that is, the tangent modulus is much smaller than the shear modulus in the neighborhood of the bifurcations points. As such, the critical stress $(\tau^{33}/4\mu^*)$ may be found by the asymptotic formula***

---

*note the latter equation is independent of any elasticity.

**this can be shown by computing $\dot{P} = 0$ in equation (4.34).

***see Hill and Hutchinson [59], equation 6.8 therein.

$$(\tau^{33}/4\mu^*) = \tfrac{1}{2} + \frac{\gamma}{\sin 2\gamma} \tag{9.35}$$

$$+ \frac{2\mu^*}{\mu}\left\{\left(\frac{\gamma}{\sin 2\gamma}\right)^3(1+\cos 2\gamma) - \frac{1}{8} - \frac{\gamma}{\sin 2\gamma}\left(\frac{1}{4}+\frac{1}{3}\gamma^2\right)\right\}$$

$$+ \mathcal{O}\left(\frac{\mu^*}{\mu}\right)^2$$

where $\gamma = m\pi X$, m an integer. As $(2\mu^*/\mu) \to 0$, this formula reduces to that of Cowper and Onat [61] for a rigid-plastic solid. We could use (9.34) to eliminate either $(\tau^{33}/4\mu^*)$ or X from (9.35) to get eigenvalue equations for X or $(\tau^{33}/4\mu^*)$, respectively, but for clarity it is better to plot (9.34) and (9.35) independently in the $X - (\tau^{33}/4\mu^*)$ plane. The critical configurations in plane extension are then identified as the points at which the curves intersect. This is the approach we take, marking the critical configurations found by application of the finite element algorithm on the same plot.

For numerical study we take Young's modulus $E = 6.895 \times 10^4$ MPa, $\nu = (1/3)$, and $\tau_y = 344.75$ MPa. Six individual cases are considered, corresponding to values of the hardening exponent $N = 4$ and $N = 8$, for initial slendernesses of $1/X_o = 2$, 3, and 4. These same six cases were studied by Burke and Nix [60]. The problem may be treated in two parts: (i) generation of the solution for homogeneous extension, and (ii) location of the critical configurations through which the specimen passes in the course of homogeneous extension.

To generate the solution for homogeneous extension for all six cases it is only necessary to find the solutions for extensions of a

unit cube of the two materials involved. These solutions consist of a sequence of configurations through which the specimen passes in the course of plane extension. It is anticipated that the bifurcation analysis will be sensitive to small variations of the stress and stubbiness, so an accurate integration of the homogeneous extension is essential. We use one element. For the material whose hardening exponent N equals four, a single RK2 step brings the material from the stress free state to the yield surface. This is followed by 30 RK4 steps to bring the specimen out to nominal stretch $l = 1.04$. Subsequent steps are (all RK4) stretch increments $\Delta l = 0.002$ out to $l = 1.10$, followed by $\Delta l = 0.01$ out to $l = 1.45$. For the material whose hardening exponent N is eight, 40 steps were taken from the yield surface to get out to $l = 1.05$, followed by stretch increments $\Delta l = 0.01$ out to $l = 1.25$ (all RK4). For both $N = 4$ and $N = 8$ post maximum load calculations were repeated using $\Delta l = 0.002$. This gave not only an accuracy check, but also a refined sequence of configurations in the neighborhood of the bifurcations points. One result of this increase in accuracy (over the example among the homogeneous deformations) is that the stress, as a function of the nominal stretch, is found to be virtually indistinguishable from the stress in the incompressible material: only the thickness of the specimen varied appreciably, and this difference is not distinguishable on the figures which follow.

In the second part of the problem, location of the critical configurations, estimates for those locations were provided by the results of Burke and Nix [60]. The global stiffness matrix $[K_L^*]$

was formed using a uniform mesh of eight-noded elements, three elements through the (half-) thickness a^1 and twelve elements along the length $2a^3$. Then the first eigenvalue (smallest in absolute value) was found.* The first eigenvalue has the physical significance of force required to produce 'unit' necking. The search for the critical configuration was extended towards or away from the maximum load point as this eigenvalue was negative or positive. The critical configurations are given in Table 1. Linear interpolation was used to get configurations intermediate to those found in part one of this problem. In Figures 27 and 28 the present results are compared to the closed form results of Hill and Hutchinson [59] and to the numerical results of Burke and Nix [60], for N = 4 and N = 8, respectively.**

In each of Figures 27 and 28 the three nearly vertical lines represent the closed form solutions (9.34) for $X_o = (1/2)$, $(1/3)$, and $(1/4)$. The stubbiness X decreases and the stress $(\tau^{33}/4\mu^*)$ rises as extension progresses. Along the loading paths bifurcation is first possible when the curve (9.35) (for m = 1) is encountered.*** Special

---

*IMSL (FORTRAN) Library subroutines were used to accomplish this.

**Burke and Nix [60] do not report the critical configurations, so it was necessary to reconstruct from information they do give. The stubbiness X can be recovered from equations 46a, 46b, and Table 2 (in that paper). The stress $(\tau 33/4\mu^*)$ is then assigned according to (9.34)--in this paper. We remark that their results are considerably more accurate than entries in (their) Table 2 would have the reader believe; the error in that table results from mis-application of the asymptotic formula (7.6) from the paper of Hill and Hutchinson [59].

***to show the proximity of the next bifurcation point, (9.35) for m = 2 has been plotted also.

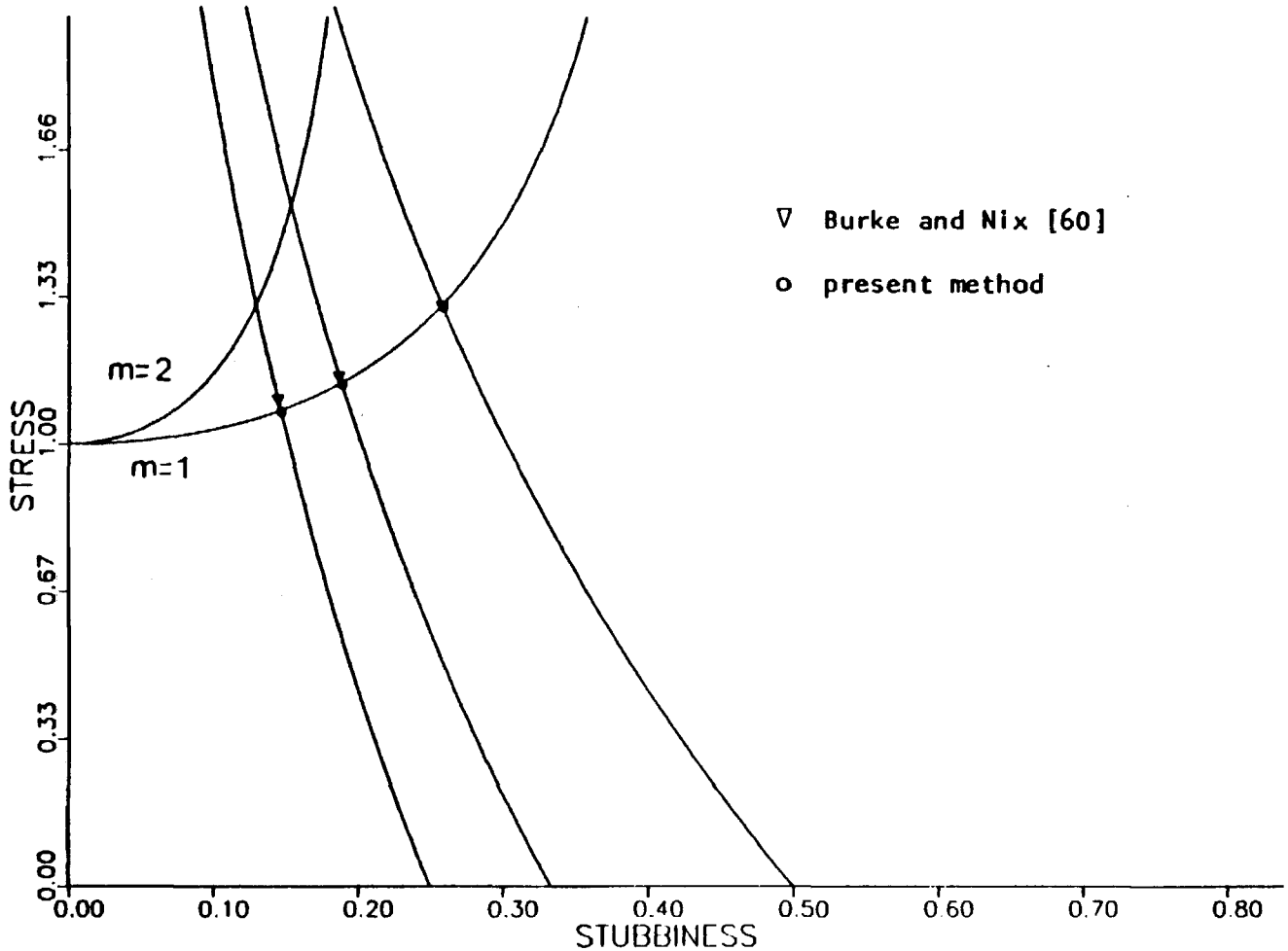

Figure 27. Results of Necking Analysis--N = 4

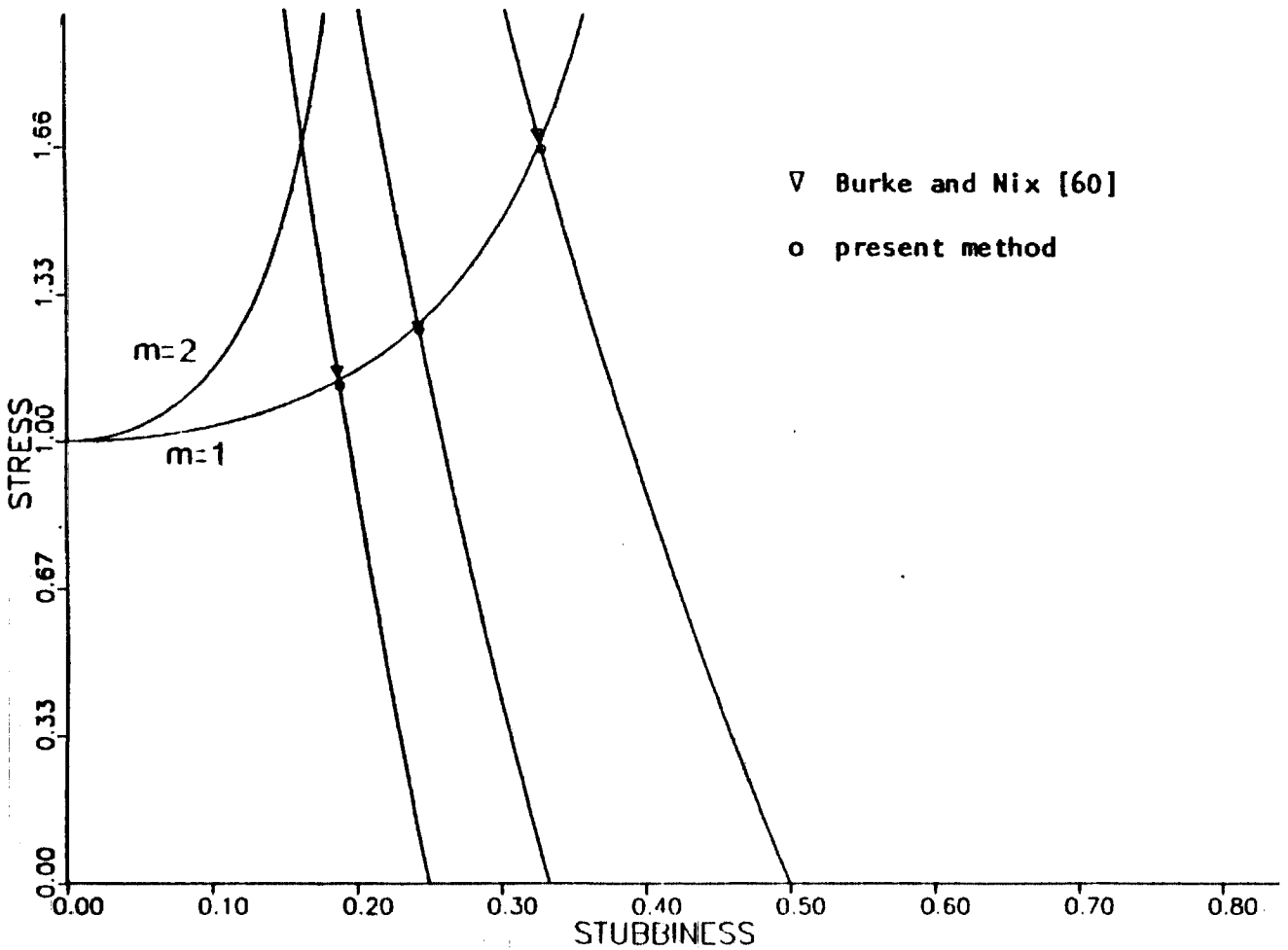

Figure 28. Results of Necking Analysis--N = 8

symbols have been placed on the plots to indicate the critical configurations found by the present finite element method and by the velocity-based finite element method used by Burke and Nix [60].

Perhaps the most striking feature of these figures is that in every case the present method indicates bifurcation at a stress below the critical stress for an incompressible body, while the results of Burke and Nix indicate the opposite. While the velocity-based method is certainly providing an upper bound for the critical stress, it would be imprudent to assume from this single result that the stress-based method is leading to a lower bound. In fact, counterexamples to such a supposition are abundant. As an experiment, the Poisson ratio was varied between $\nu = 0.1$ and $\nu = 0.49$. It was found that as ν increased, bifurcation was *delayed*. This is certainly not proof, but it supports the idea that the bifurcation stress of the incompressible body is an upper bound for the bifurcation stress of compressible bodies. In that light, the numerical results found by the present method must be more accurate than Figures 27 and 28 indicate, and the question of whether they lie above or below the correct critical stress (for $\nu = \frac{1}{3}$) is still open. Moreover, the present result was obtained using only 36 elements (239 unconstrained velocity parameters), whereas 75 elements (479 unconstrained velocity parameters) were required in the velocity-based analysis to obtain a result less accurate.*

*Since a precise account of the critical configurations is not given by Burke and Nix [60], it is impossible to say whether or not the difference in the results can be attributed to the accuracy with which the extension was integrated.

One could ask whether or not the symmetry we imposed on the velocity field (see Figure 26) resulted in the suppression of an anti-symmetric bifurcation mode, such as one that formation of a shear band might give rise to. This is unlikely, since the bifurcations all occur at stress levels too low to support the formation of a shear band in the incompressible material. That stress, for incompressible materials, is (see [60])

$$(\tau^{33}/4\mu^*) > \sqrt{2(\mu/2\mu^*) - 1} \tag{9.36}$$

Finally we note that the present bifurcation problems are well conditioned in the senses that (i) no other bifurcation points are close by, and (ii) the loading path and locus of critical stresses cross at a large angle. The results of Hill and Hutchinson [59] provide a basis for evaluation of the performance of a finite element algorithm under much more demanding circumstances.

A Parameter Study. In this section we investigate the sensitivity of the results of the previous bifurcation analysis to variations of number, shape, and type of elements in the finite element mesh. The 'type' of element is determined by the number of boundary nodes, the number of spin parameters, and the number of stress rate parameters. It is desired that a 'small' change in the character of the mesh result in a 'small' (or at least predictable) change in the approximate solution. Moreover, it is hoped that the accuracy of that result will increase monotonically with the computational effort, measured roughly by the number of unconstrained velocity parameters.

Finally, it is very important in practice to know whether an approximate load is an upper or lower bound for the actual load.

Four different types of elements are considered. The first two are eight and four-noded elements satisfying all of the rank conditions given in Chapter VII. Third, a four-noded element whose spin field is of polynomial degree one less than the stress-rate field is considered. Finally, a constant stress--constant spin element is considered. In all of the cases that follow, the configuration and stress of the body are fixed at values given in Table 2. The material is identical to that considered in the previous section with hardening parameter $N = 8$. Though the precise eigenvalue of the configuration (Table 2) is not known, it is believed to be small and positive.

In Figure 29 the smallest eigenvalue of the global stiffness matrix $[K^*]$ is plotted as a function of the total number of unconstrained velocity parameters. The finite element meshes were made up of uniform eight-noded quadrilaterals with 21 stress parameters and 6 spin parameters. Complete data is given in Table 3. As can be seen in the Figure, the eigenvalue is quite insensitive to the particular arrangement of elements, depending almost exclusively upon the total number of degrees of freedom in the mesh. Every estimate for the eigenvalue was positive.

In Figure 30 the smallest eigenvalue of the global stiffness matrix $[K^*]$ is plotted as a function of the total number of unconstrained velocity parameters. The finite element meshes were made up of uniform four-noded quadrilaterals with 13 stress parameters and 3 spin parameters. Complete data is given in Table 4. In contrast to

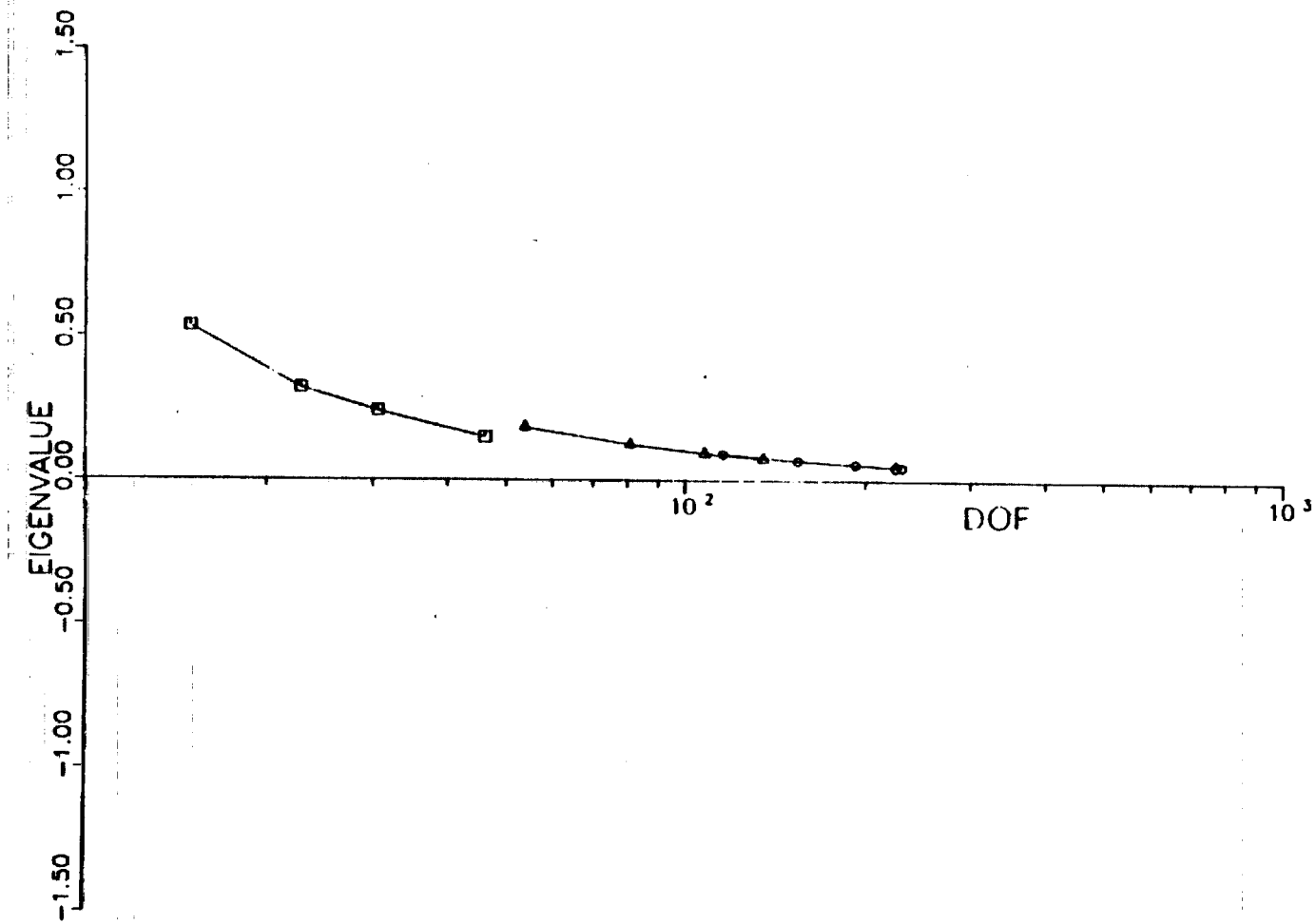

Figure 29. Necking Eigenvalue for Various Finite Element Meshes--Eight Node Elements

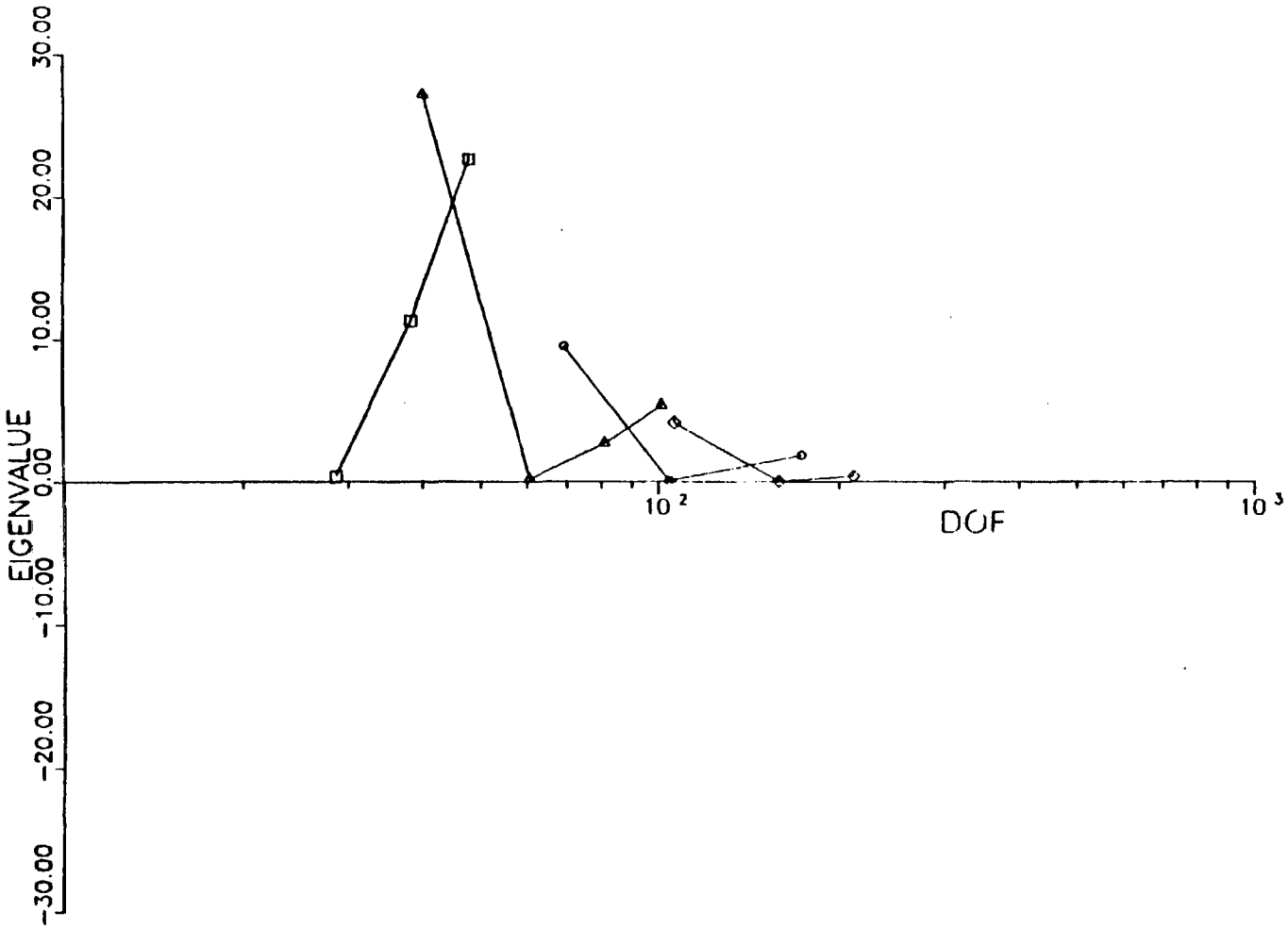

Figure 30. Necking Eigenvalue for Various Finite Element Meshes--Four Node Elements (NT = 13, NW = 3)

the eight-noded elements, the four-noded elements show a marked sensitivity to mesh arrangement. They are also substantially stiffer. In spite of the existence of preferred meshes, the eigenvalue estimate appears to improve as the degrees of freedom in the mesh increases.* Every estimate for the eigenvalue was positive.

In Figure 31 the smallest eigenvalue of the global stiffness matrix $[K^*]$ is plotted as a function of the total number of unconstrained velocity parameters. The finite element meshes were made up of uniform four-noded quadrilaterals with 13 stress parameters and 1 spin parameter. Complete data is given in Table 5. The stress-rate field on this element contained linear terms, while the spin field was a constant. Thus, angular momentum balance is generally satisifed only in the mean by this element. The reader should note the dramatic increase in stiffness of this element, as well as the relative insensitivity to mesh arrangement. Every estimate for the eigenvalue was positive.

From these three examples it is readily seen that the compliance increases with the number of kinematic degrees of freedom (velocity and spin parameters), just as it would in a velocity-based finite element algorithm. However the type of element makes a bigger difference than does the number of elements in the mesh. This is important from the point of view of efficiency, since it means that

*the reader should note that the angularity of the lines connecting meshes in a sequence would be reduced if a refined sequence were used in the plot.

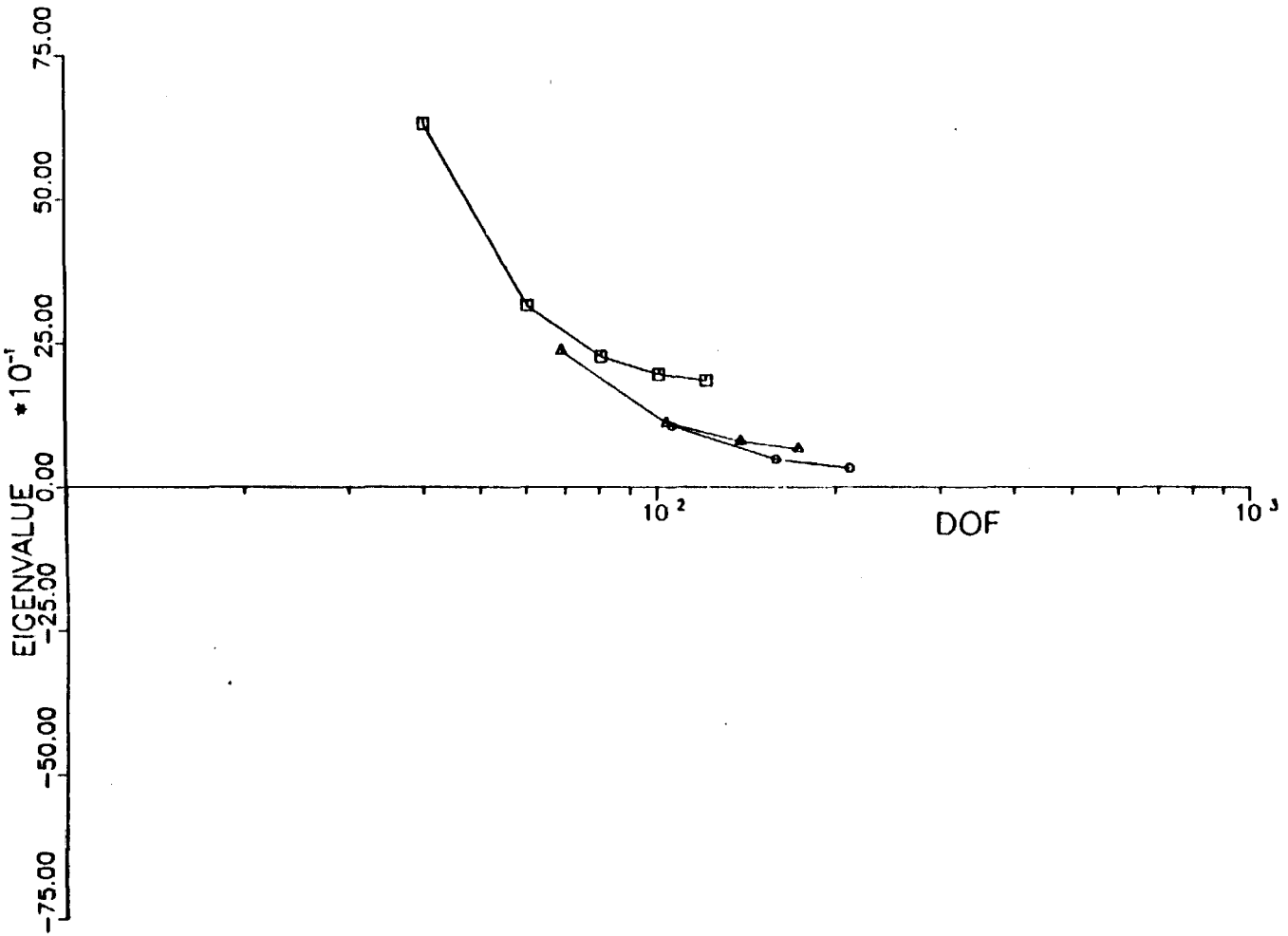

Figure 31. Necking Eigenvalue for Various Finite Element Meshes--Four Node Elements (NT = 13, NW = 1)

it is better to go to a 'higher order' element than to refine the finite element mesh to achieve greater accuracy. It is also clear from these examples that the finite element algorithm is not providing a lower bound for the eigenvalue.*

We would expect that decreasing the number of stress parameters would have just the opposite effect that decreasing the number of kinematic parameters had--decrease the stiffnesses (see Pian [3]). However, we found no difference in the necking eigenvalue for four-noded elements when 13 or 21 stress parameters were used, for either 1, 3, 4, or 6 spin parameters. This result is summarized in Table 6.

As a final example we consider meshes of four-noded elements, each with 5 stress-rate parameters and 1 spin parameter. Each element has two kinematic modes, but when the global stiffness matrix $[K^*]$ is assembled and the kinematic boundary conditions enforced, these modes disappear. The element is interesting because the equations of compatibility and angular momentum balance are satisifed precisely on the interior of each element. As such, a velocity field of the form

$$\underline{v} = (a^i x + b^i y)\underline{e}_i \tag{9.37}$$

may be integrated on the interior of each element. However such a velocity field is incapable of matching the boundary velocities of a

*as might have been inferred from the results of the bifurcation analysis.

C-3

four-noded quadrilateral except in the mean sense (since they contain an 'xy' term). Therefore, across element boundaries this velocity field must generally be discontinuous.

According to Washizu,* one of Rayleigh's principles states that "if the prescribed boundary conditions are partly relaxed, all the eigenvalues decrease." In using the elements above, the actual problem has been replaced by a problem in which interelement velocity continuity has been partly relaxed. Thus, it is not surprising that for some meshes the finite element algorithm overestimates the compliance of the body. However, as the element mesh is refined, it can be imagined that the disparity between the boundary velocity and interior velocity diminishes (how rapidly would depend upon the particular sequence of meshes). In Table 7 two sequences of meshes are detailed. Any smooth velocity field could be approximated to any degree of accuracy by continuation of either of these sequences. In Figure 32 the sequences of eigenvalues corresponding to these two sequences are plotted. These simple elements apparently are converging to the same value as all the other elements at a rate matched only by the eight-noded 'high-order' elements. But the most striking feature is that one of the sequences of approximate eigenvalues is converging from above while the other from below.

The natural tendency would be to attribute this behavior to the presence of kinematic modes on the element level. However, for sufficiently distorted meshes of other-wise well-behaved elements,

*Washizu [36], p. 48.

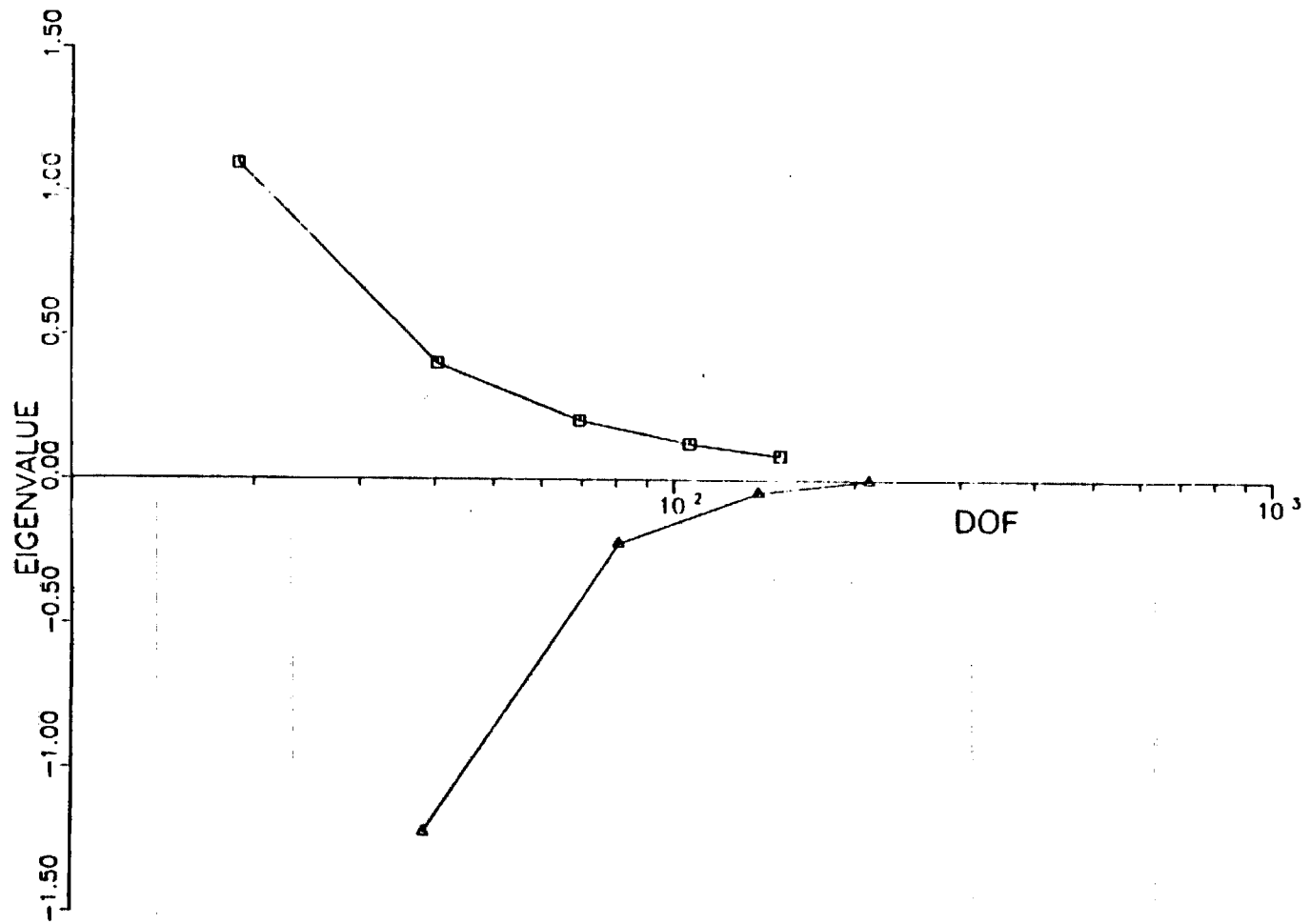

Figure 32. Necking Eigenvalue for Various Finite Element Meshes--Four Node Elements (NT = 5, NW = 1)

similar behavior can be observed.* This example supports the idea that the present method does not necessarily lead to an upper or lower bound.

Growth of a Void in a Viscoplastic Medium

In this final example we examine the growth of a void in a hypoelastic/viscoplastic medium. This problem has been studied (numerically) by Burke and Nix [62], who treated the material as rigid/viscoplastic. We present the problem as a further demonstration of the performance of the finite element algorithm. The material exhibits stress relaxation, so the forward gradient scheme must be used to stabilize the time integration. Thus, only a qualitative picture of the stress and deformation can be expected of our analysis. Nevertheless, the present results agree quite closely with those of Burke and Nix [62].

The motion is assumed to be plane strain, and throughout the body is a doubly periodic array of cylinderical voids. Due to the symmetry we need analyze only one quadrant of one rectangular cell of the body. The finite element mesh and boundary conditions are described in Figure 33.

Burke and Nix motivate their study by explaining that certain theories for the initiation of creep fracture suppose that the growth

*For a (1 x 10) mesh of eight-noded elements an eigenvalue of -30.3368 was found; it was not determined whether this value was simply erratic (due to the irregular element shape), or whether similar negative values could be found for 'nearby' meshes (such as 1x9 or 1x11).

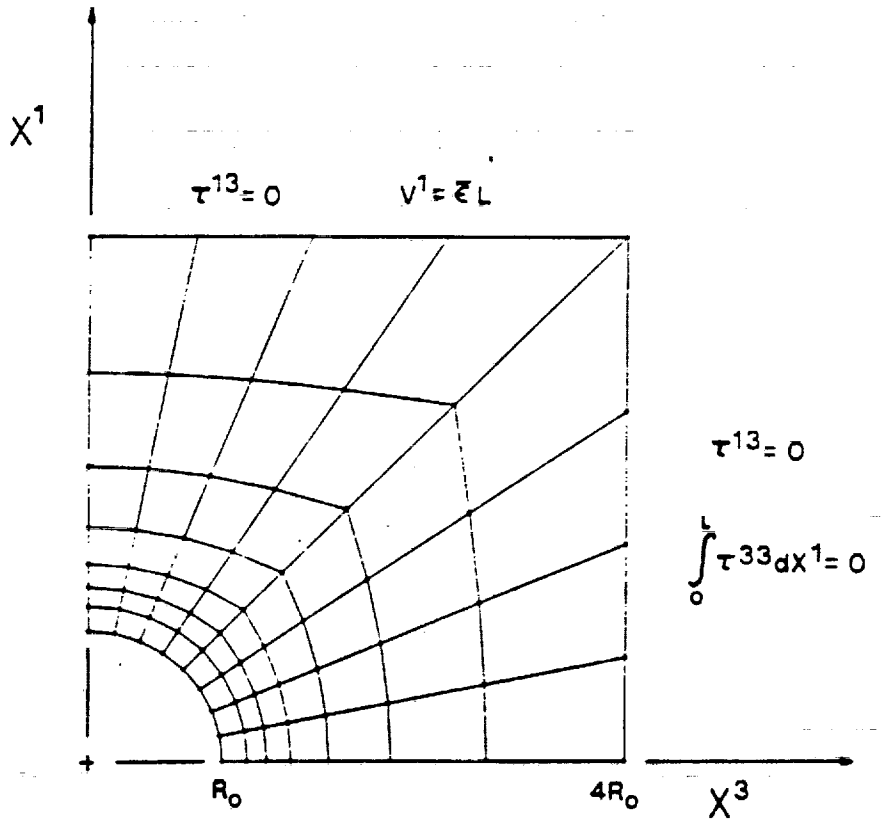

Figure 33. Finite Element Mesh and Boundary Conditions for Void Growth Problem

of voids can be "attributed to the inhomogeneous plastic deformation of the surrounding grains." Furthermore, "finite fracture strains can be predicted only when a void lies in the neighborhood of another void." Such a study necessarily involves a number of special cases. For our purposes, that of demonstration, only one case is taken.

The problem has been analyzed in three parts, much as the pipe-creep problem was. In the first part the cell is brought rapidly from the virgin state (stress-free) to a state of purely elastic strain. This is accomplished by a single RK2 step. In the second part, relatively small time steps are taken while the stress relaxes from the elastic distribution to a nearly steady creep distribution. In the third part, time steps are taken which produce 1% nominal elongation of the cell in each step. To stabilize time integration in the second and third parts the forward gradient scheme is used, the stability parameter θ set as $\theta = 1/2$ and $3/4$, respectively. Consistent with our earlier discussions regarding use of the forward gradient scheme, only the Euler time stepping scheme has been used in the second and third parts of the problem.

The material model is identical to (9.11):

$$\underset{\sim}{\varepsilon} = \underset{\sim}{\varepsilon}^{e} + \underset{\sim}{\varepsilon}^{P}$$

$$\underset{\sim}{\dot{\varepsilon}}^{e} = \left(\frac{1+\nu}{E}\right) \underset{\sim}{\dot{\sigma}}^{*} - \left(\frac{\nu}{E}\right) (\underset{\sim}{I} : \underset{\sim}{\dot{\sigma}}^{*}) \underset{\sim}{I}$$

$$\underset{\sim}{\dot{\varepsilon}}^{P} = \frac{3}{2} \dot{\gamma} \underset{\sim}{\tau}' \quad .$$

This model corresponds to that of Burke and Nix [62] with (their) creep exponent $n = 1$. The fluidity γ is set as $\gamma = 1 \times 10^{-19}$ $(\text{psi-sec})^{-1}$. The velocity at the top of the cell (see Figure 33) was adjusted so that a specimen with no void would experience a homogeneous constant stretching $\bar{\varepsilon}^{11}$ of $\bar{\varepsilon}^{11} = 0.25 \times 10^{-14}$ sec^{-1}. Since the material was treated as rigid/viscoplastic in [62], our choice of elastic constants is somewhat arbitrary. We have taken Young's modulus $E = 3 \times 10^{7}$ psi and Poisson ratio $\nu = 0.4$, so the material is like mild steel in its elastic response.

In Figures 34, 35, and 36 the contours of stress τ^{11}, mean stress, and stress τ^{33} have been plotted for L (the elongation of the cell) $L = 1.01$. The stress concentration where the hole edge crosses the x^3 axis is approximately 2.7.* This is quite reasonable since the theoretical value for an isolated void in a purely elastic medium is 3.0 [63]. In Reference 62 an approximate value of 2.66 was found for the rigid plastic material. In Figure 37 the contours of effective strain rate $\sqrt{\frac{2}{3}\,\underset{\sim}{\varepsilon}^{P} : \underset{\sim}{\varepsilon}^{P}}$ are plotted for $L = 1.01$. Qualitatively this compares very well to Figure 7 in [62].

In Figure 38 the deformation is traced from $L = 1.0$ to $L = 1.5$. These deformations are physically tenable. We remark that no indication of any numerical instability was observed in the course of integrating this deformation.

In Figures 39, 40, and 41 the contours of stress τ^{11}, mean stress, and τ^{33} have been plotted for $L = 1.50$. They compare very well

*A stress concentration of approximately 2.59 was observed for the elastically stressed medium.

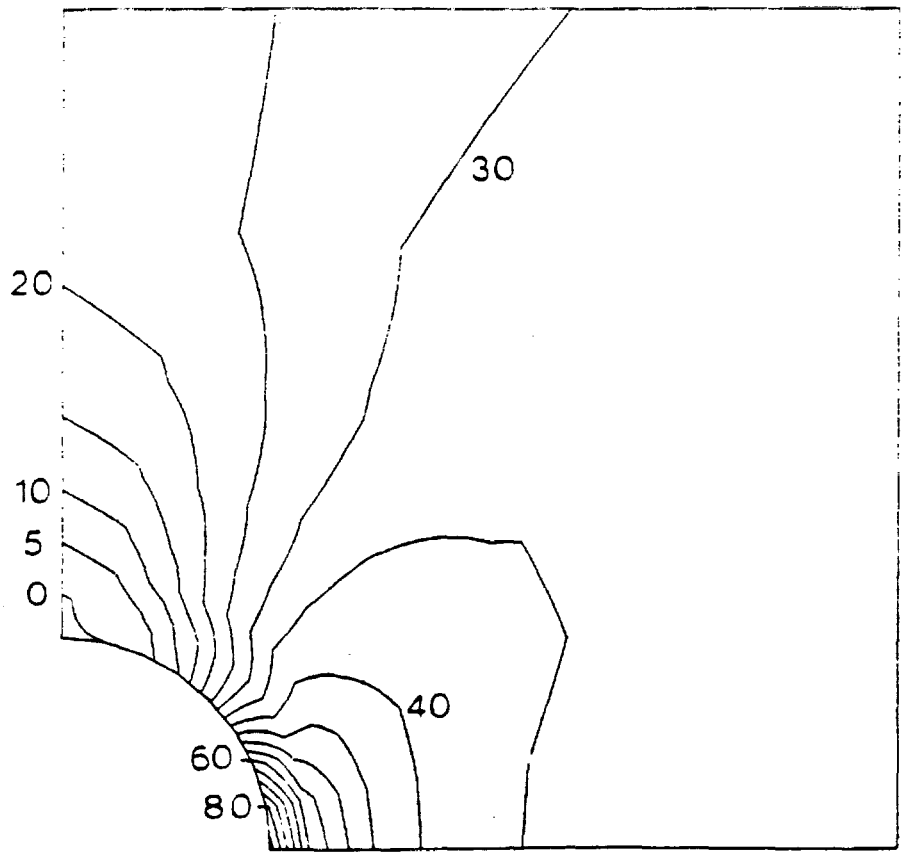

Figure 34. Contours of Stress τ^{11} at L = 1.01

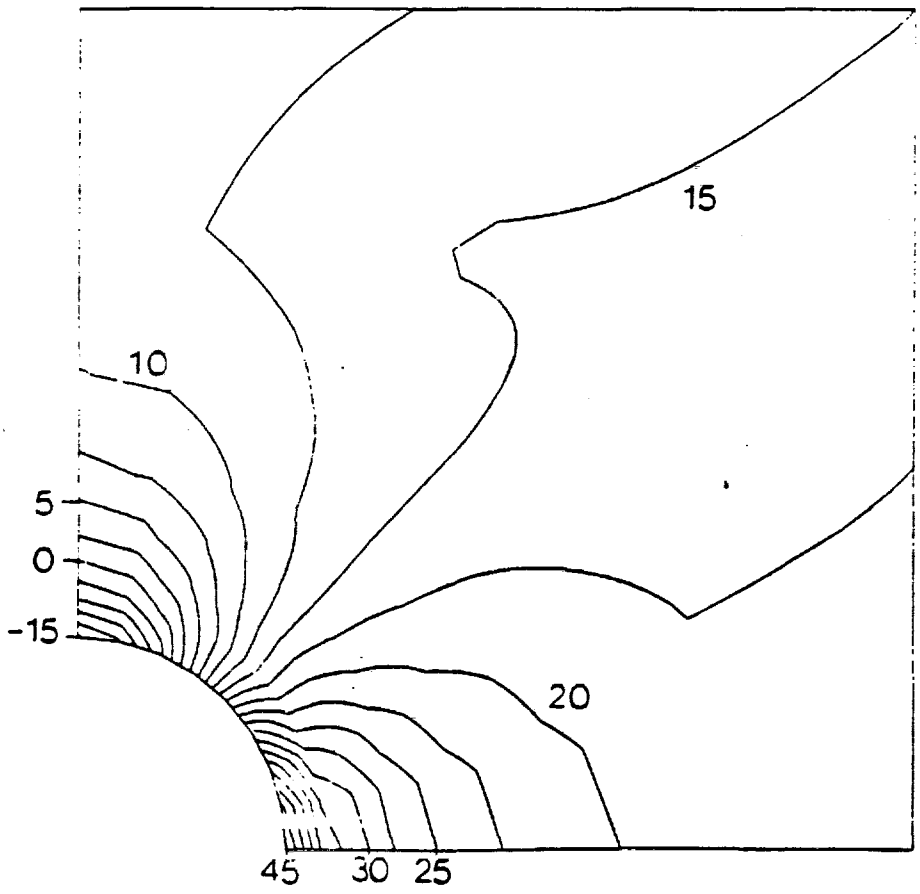

Figure 35. Contours of Mean Stress at L = 1.01

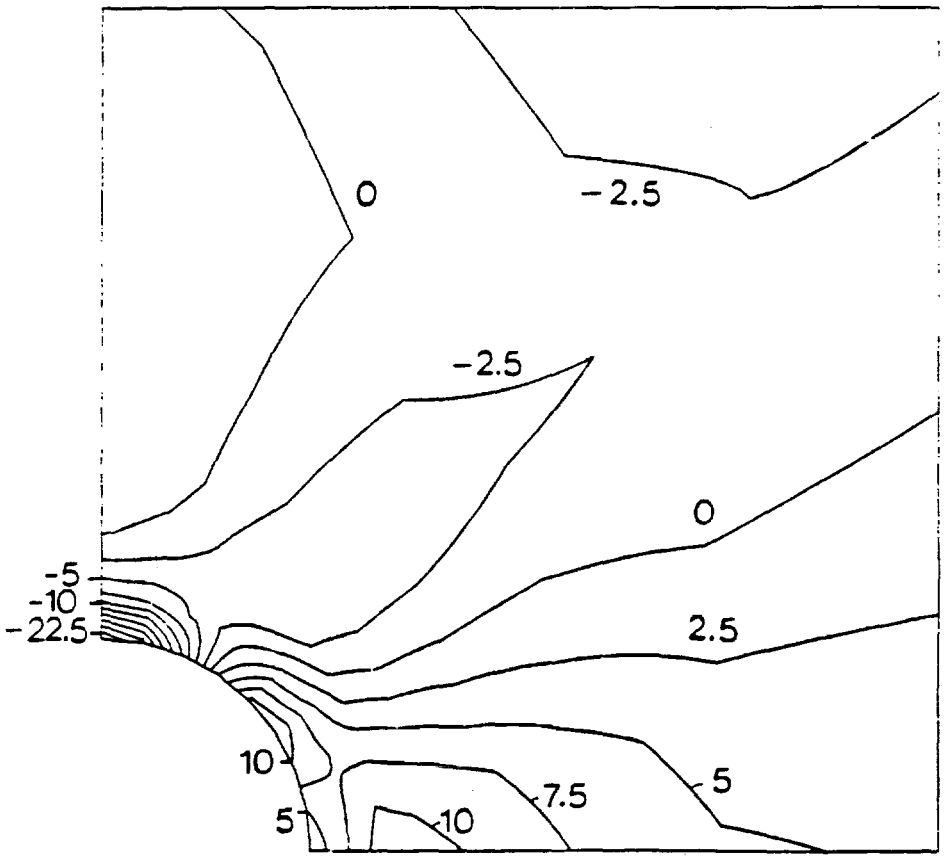

Figure 36. Contours of Stress τ^{33} at L = 1.01

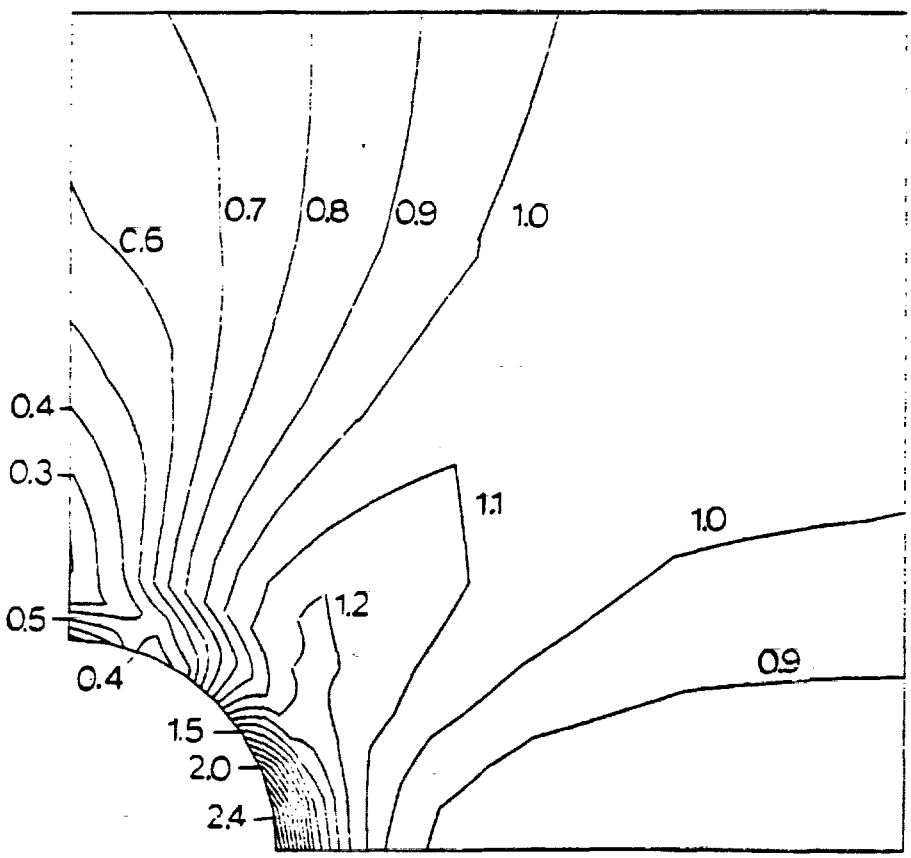

Figure 37. Contours of Effective Strain Rate $\dot{\varepsilon}^p/\bar{\varepsilon}$ at L = 1.01

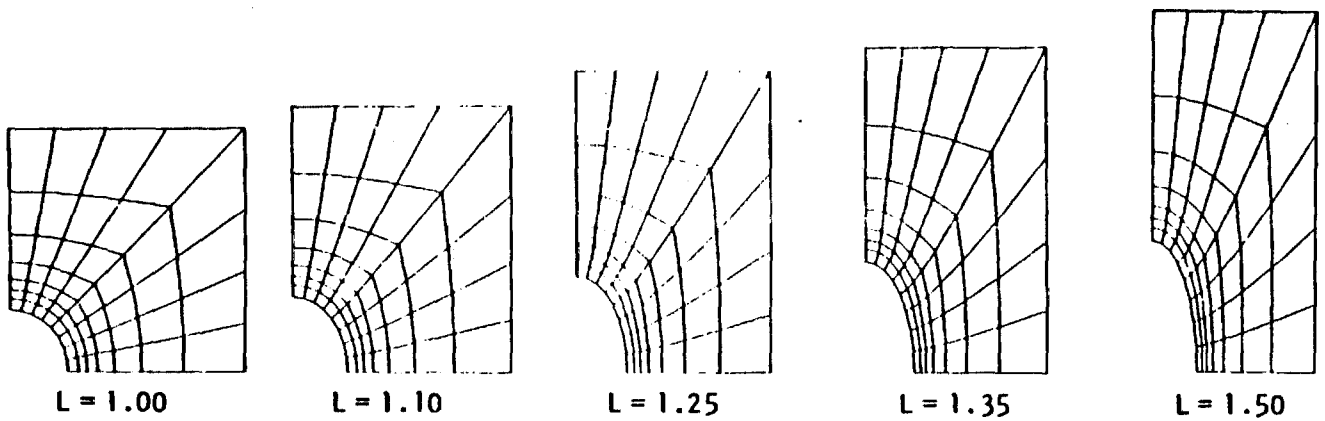

Figure 38. Deformation History of Cell

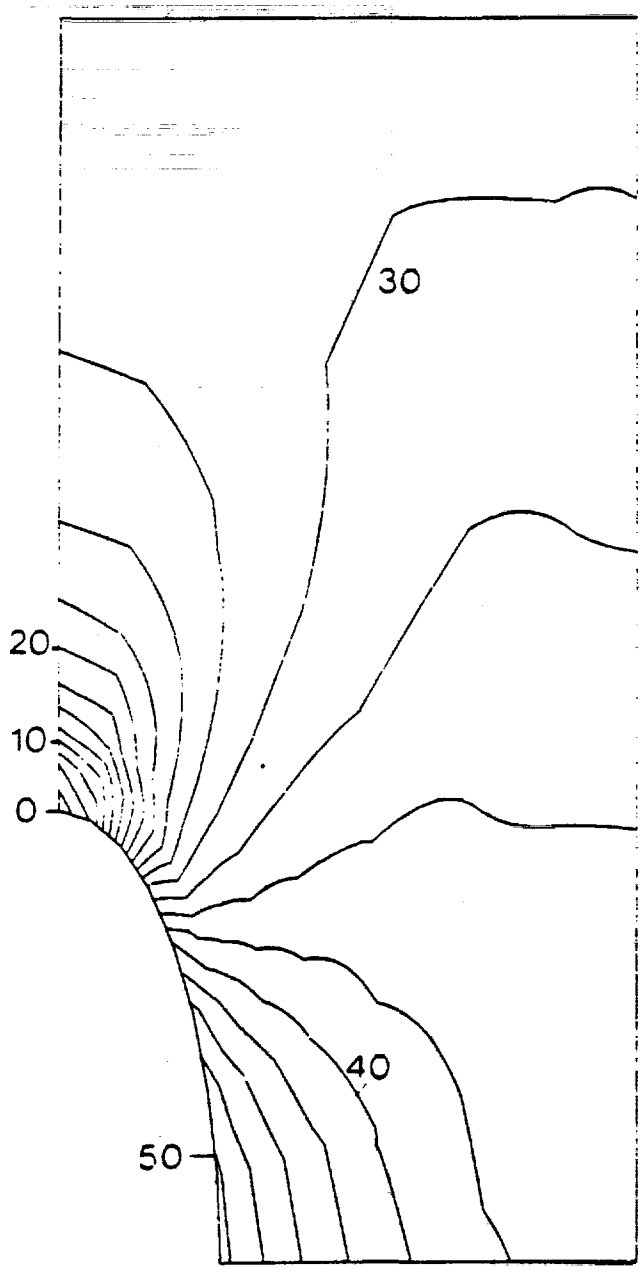

Figure 39. Contours of Stress τ^{11} at L = 1.5

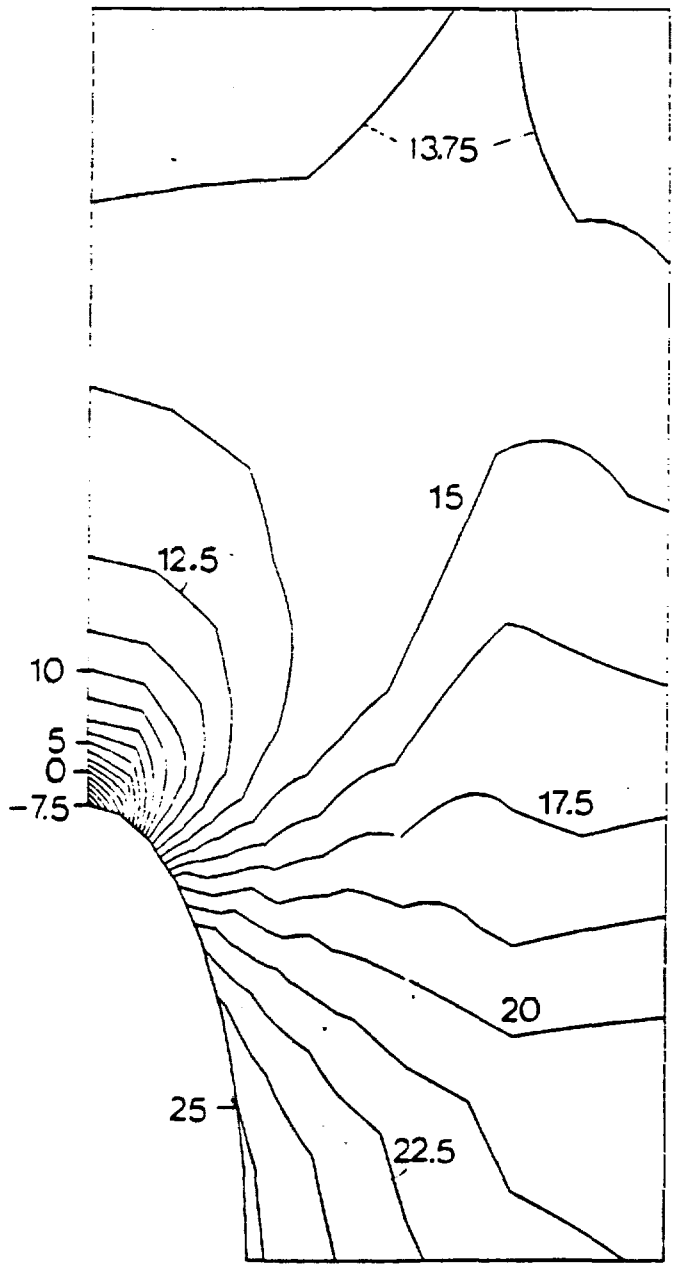

Figure 40. Contours of Mean Stress at L = 1.5

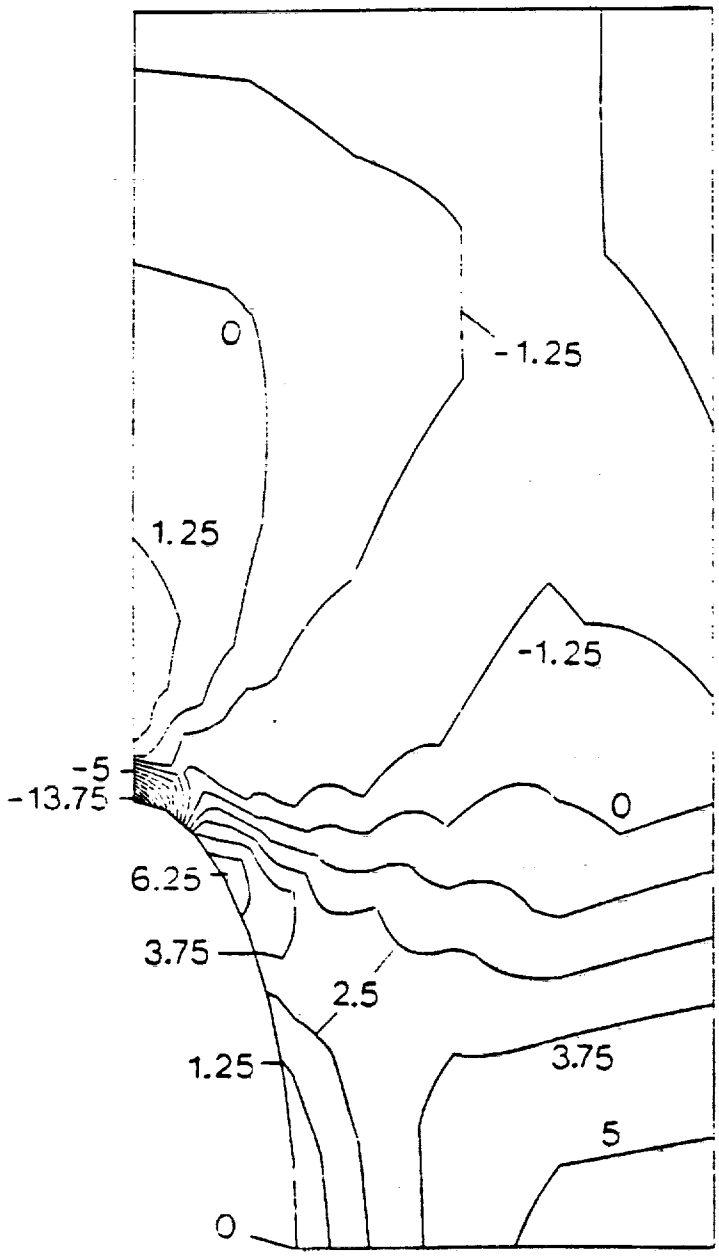

Figure 41. Contours of Stress τ^{33} of L = 1.5

to the stresses found in [62] (see Figure 8 there). We note that the stress concentration has dropped to 1.71. The stress concentration depends strongly on the geometry of the specimen; as such, it was observed to decline steadily throughout the deformation. In Figure 42 the contours of effective strain rate are plotted for L = 1.5. Again, the qualitative agreement with the results of Burke and Nix [62] is noted (see Figure 9 there).

The present calculation was terminated at L = 1.5 because of the unstable traction boundary condition* at $x^3 = 0.0$ and the edge of the hole, and the general breakdown of (total) traction reciprocity conditions on the interior of the cell. This problem is easily avoided by incorporation of traction residuals.

We conclude by noting that in the present analysis only 56 four noded elements were used, as compared to 56 eight noded elements used in the analysis of Burke and Nix. Considering the agreement between their results and our own, the present method appears to have performed very well, in spite of the large disparity in the degrees of freedom of the finite element mesh.

---

*see discussion and footnote accompanying equation (3.37).

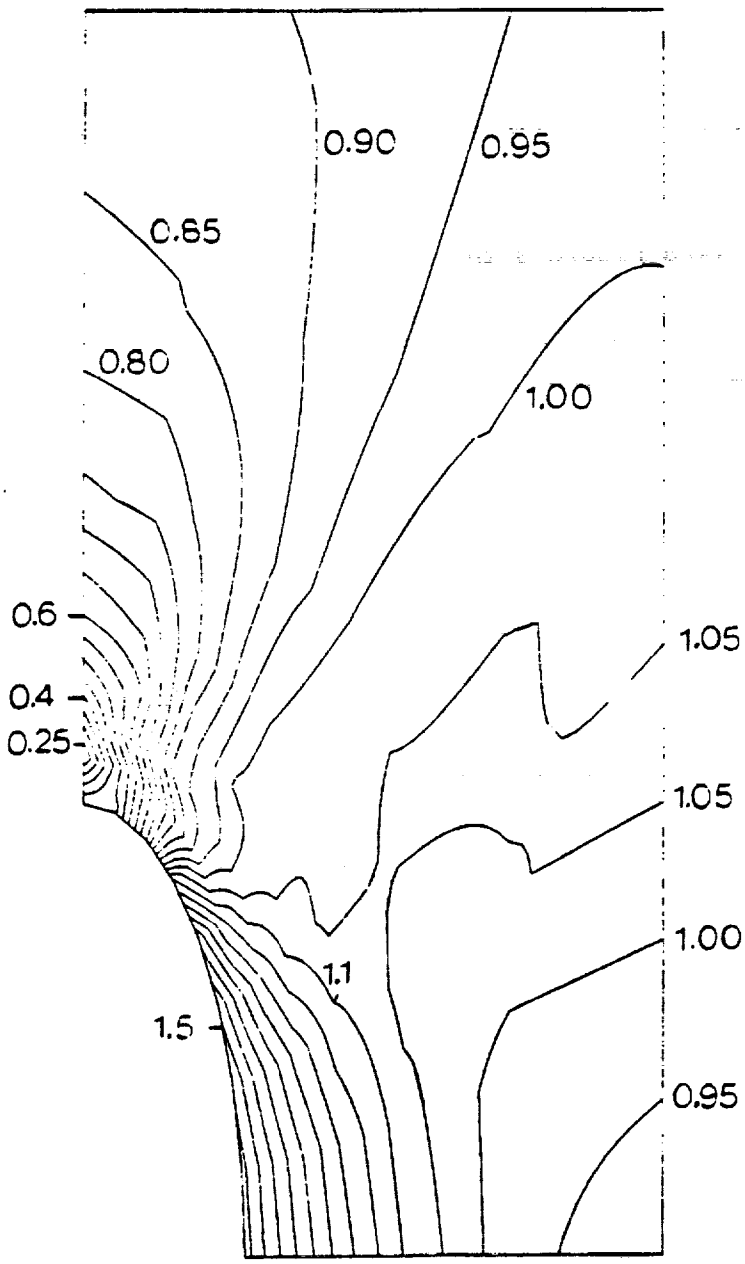

Figure 42. Contours of Effective Strain Rate $\dot{\varepsilon}^P/\bar{\dot{\varepsilon}}$ at L = 1.5

CHAPTER X

CONCLUSIONS AND RECOMMENDATIONS

Conclusions

In this work a new hybrid stress finite element algorithm, suitable for analyses of large quasistatic deformations of inelastic solids, has been presented. The feasibility and performance of the algorithm has been demonstrated in a number of example problems.

Principal variables in the formulation are the nominal stress rate and spin. As such, consistent reformulation of the constitutive equation is necessary. This is discussed at length, as are alternatives to direct numerical inversion of constitutive matrices involved in that reformulation.

The principal variables in most finite element algorithms for solids are either displacement increments or stress increments (as opposed to actual time derivatives). In problems involving elastic bodies the accumulated error of such an algorithm may be kept small by 'residual load' iterations; however, in problems involving inelastic bodies, the accumulated error of the incremental approach is like that of the Euler scheme for integration of ordinary differential equations. In the present work the notion of 'increments' has been discarded entirely. As a consequence, the finite element equations give rise to an initial value problem (which may be treated independently). Integration has been accomplished by Euler and Runge-Kutta schemes,

and the superior accuracy of the higher order schemes is noted.

It has been shown that there is an ambiguity inherent in finite element methods based on complementary work and energy principles surrounding the appropriate definition of the velocity (or displacement) on the interior of the element. Heuristic arguments have been given as justification for the method by which those velocities were found in the present work. Those arguments indicate that mathematical consistency requires that special techniques be used to find the velocity on the interior of 'high order' elements, but that the velocity on the interior of a 'low order' element may be found by interpolation of the boundary velocities.

In the course of integration of the stress (in time) it has been demonstrated that classical schemes such as Euler's and Runge-Kutta may lead to strong frame dependence. The problem can be traced to the integration schemes themselves. As a remedy, modified integration schemes have been proposed. The potential of the new schemes for suppressing frame dependence of numerically integrated stress is demonstrated by an example.

Time integration of the stress in materials which exhibit stress relaxation is complicated by the necessity that one take very small time steps in order to avoid numerical instability. The applicability of explicit and implicit forward gradient schemes to improve stability of integration in large deformation problems has been investigated. These schemes are known to be both stable and accurate in problems involving small deformations. It has been found that in large deformation problems the schemes are indeed stable, but potentially inaccurate.

The capability of the stress-based finite element algorithm for extremely accurate bifurcation analysis was demonstrated. Moreover, it was shown that one could expect the result of such an analysis to be stable with respect to variations of the finite element mesh, so long as the same type of element was used in every mesh. If the type of element was varied, the result changed in a (qualitatively) predictable manner. It was demonstrated that the method did not necessarily lead to an upper or lower bound for the critical load.

Finally, it was made evident through examples that stresses obtained by the present method were of exceptional accuracy; much more than could be expected of a velocity-based algorithm. Traction boundary conditions and the traction reciprocity conditions were met with a correspondingly high accuracy, though their accuracy could have been improved by incorporation of residuals (to keep the accumulated error small).

Recommendations

The principal defect of the algorithm presented in this work is its inability to accurately integrate the stress in bodies which exhibit stress relaxation, unless of course, the time steps are kept inordinately small. Evidently, this defect is present in the algorithm of Kanchi et al [49], though no mention is made of it. This appears to be the only other application of a 'forward gradient' technique to finite deformation problems. In the context of small deformation problems, the error of (generalized) gradient techniques was studied numerically by Argyris et al. [19]. On that basis they concluded that 'midstep

weighting techniques' (that is, $\theta = \frac{1}{2}$) were accurate. However, the present results indicate that the accuracy of generalized gradient techniques is highly problem dependent, and that no one choice of θ assures optimal accuracy. A minimal requirement to be made of any scheme for stabilization of numerical integration is that it give correct results under steady, or nearly steady conditions; this requirement is not met by the generalized gradient techniques currently available. It is recommended that an effort be made to develop schemes for stabilization of numerical integration of stress for finite element-initial value problems whose accuracy can be proved.

Secondly, it was demonstrated that the present method could not be relied upon to give either an upper or lower bound for the critical load in a bifurcation analysis. It is suspected that the character of the approximate load obtained by the present method may be linked to the rank conditions (7.69) and (7.73). Further research, both from the mathematical point of view and numerical point of view is needed before a practically applicable criteria for critical load characterization can be given. A mathematically accurate discussion of the problem of assigning the velocity on the interior of an element (for hybrid stress methods) might aid in this characterization.

Finally, the materials considered in this work all have the common property that their constitutive equations are isotropic functions. Though the generalization of the present method to anisotropic material behavior is conceptually straightforward, there may be special problems in an implementation. The performance and special problems of the present method, when applied to anisotropic materials, should be investigated.

APPENDICES

APPENDIX A

DIRECT, DYADIC, AND INDEX NOTATIONS FOR TENSORS

Let $\underline{r}$ denote the position vector in E. We write X^I for an arbitrary (smooth) system of coordinates in E. Then a triad of vectors $\underline{e}_I$, called the 'natural base vectors' of the coordinate system, are defined by the equation

$$\underline{e}_I = \frac{\partial}{\partial X^I}(\underline{r}) \quad . \tag{A.1}$$

We assume that these vectors are linearly independent; that is,

$$(\underline{e}_1 \times \underline{e}_2) \cdot \underline{e}_3 \neq 0 \quad . \tag{A.2}$$

Then a conjugate triad of base vectors is defined by the equation

$$\underline{e}^I \cdot \underline{e}_J = \begin{cases} 1 \text{ if } I = J \\ 0 \text{ otherwise} \end{cases} \quad . \tag{A.3}$$

Any vector in E may be represented as a linear combination of the base vectors $\underline{e}_I$ or $\underline{e}^I$:

$$\underline{v} = v^I \underline{e}_I = v_I \underline{e}^I \quad . \tag{A.4}$$

The components v^I are called 'contravariant' and the components v_I are

called 'covariant.' They are defined by

$$v^I = \underline{e}^I \cdot \underline{v} \; ; \qquad v_I = \underline{e}_I \cdot \underline{v} \; . \tag{A.5}$$

To every triplet $\langle v^1, v^2, v^3 \rangle$ there corresponds a unique vector in E, and vice versa, for any linearly independent set of base vectors $\underline{e}_I$. This important fact is the basis of the index notation for vectors and tensors. If a linearly independent set of base vectors is given (for example by specifying a coordinate system), then no ambiguity arises in writing $\langle v^1, v^2, v^3 \rangle$, or simply v^I, for $\underline{v}$. In continuum mechanics one frequently is forced to work with more than one coordinate system at a time; then the dyadic notation, indicated by (A.4), is more convenient.

The relation between the contravariant and covariant components is found by 'dotting' the representation (A.4):

$$v^I = (\underline{e}^I \cdot \underline{e}^J) v_J \; ; \qquad v_I = (\underline{e}_I \cdot \underline{e}_J) v^J \; . \tag{A.6}$$

Just as the triad $\underline{e}_I$ constitutes a vector basis in E, the dyads $(\underline{e}_I \underline{e}_J)$ are a basis for second order tensors in E. Any second order tensor may be represented as a linear combination of these dyads, for example

$$\underset{\sim}{T} = T^{IJ} \underline{e}_I \underline{e}_J \; ; \qquad T^{IJ} = (\underline{e}^I \underline{e}^J) : \underset{\sim}{T} = \underline{e}^J \cdot (\underline{e}^I \cdot \underset{\sim}{T}) \; . \tag{A.7}$$

Other components for $\underset{\sim}{T}$ may be defined for the dyads $(\underline{e}^I \underline{e}^J)$, $(\underline{e}^I \underline{e}_J)$,

and $(\underline{e}_I \underline{e}^J)$, and they are called 'covariant,' 'mixed,' and 'mixed,' respectively. To every 3 x 3 matrix there corresponds a unique second order tensor in E, and vice versa, for any linearly independent set of dyads. Therefore the index notation may be used for second order tensors also.

A fundamental tensor in E is the identity tensor, defined as that tensor with the property

$$\underline{v} = \underset{\sim}{I} \cdot \underline{v} \tag{A.8}$$

for every vector in E. We may represent $\underset{\sim}{I}$ as

$$\underset{\sim}{I} = \delta^I{}_J \underline{e}_I \underline{e}^J ,$$

where $\delta^I{}_J$ is the matrix of components of $\underset{\sim}{I}$ for the dyad $(\underline{e}_I \underline{e}^J)$. According to (A.5) we may represent $\underline{v}$ by $v^I \underline{e}_I$, so (A.8) may be set in the form

$$(v^I - \delta^I_J v^J)\underline{e}_I = \underline{0} \quad . \tag{A.9}$$

For (A.9) to be satisfied for arbitrary v^I it is necessary that $\delta^I{}_J$ be defined as

$$\delta^I{}_J = \left\{ \begin{matrix} 1 \text{ if } I = J \\ 0 \text{ otherwise} \end{matrix} \right\} = (\underline{e}^I \cdot \underline{e}_J) \quad . \tag{A.10}$$

Components of $\underset{\sim}{I}$ may be obtained for the other dyads in a similar manner as

$$\delta^{IJ} = (\underline{e}^I \cdot \underline{e}^J) \; ; \quad \delta_{IJ} = (\underline{e}_I \cdot \underline{e}_J) \; ; \quad \delta_I{}^J = (\underline{e}_I \cdot \underline{e}^J) \; . \tag{A.11}$$

In some applications $\underset{\sim}{I}$ is called the 'metric tensor.'

The relation (A.6) between contravariant and covariant vector components may be written as

$$v^I = \delta^{IJ} v_J \; ; \qquad v_I = \delta_{IJ} v^J \; . \tag{A.12}$$

Similarly, the relations between the various components of a second order tensor may be written as

$$T^{IJ} = \delta^{KJ} T^I{}_K = \delta^{KI} T_K{}^J = \delta^{KI} \delta^{LJ} T_{KL} \; . \tag{A.13}$$

The apparent rule for raising and lowering indices may be shown to be valid for tensors of all orders.

When differentiating vectors along a coordinate line, one must take into account not only the rate of change of the components, but also the rate of change of the base vectors themselves:

$$\frac{\partial}{\partial X^I} (\underline{v}) = \frac{\partial}{\partial X^I} (v^K) \underline{e}_K + v^K \frac{\partial}{\partial X^I} (\underline{e}_K) \; . \tag{A.14}$$

The derivative of a base vector is a vector itself, and may be

represented as a linear combination of the base vectors:

$$\frac{\partial}{\partial X^I}(\underline{e}_K) = \gamma^J_{IK}\,\underline{e}_J \quad . \tag{A.15}$$

The components in the representation (A.15) are called Christoffel symbols (of the second kind); they are defined in the same manner as components of any other vector, by use of (A.5). Using the representation (A.15), the derivative of the vector in (A.14) may be written

$$\frac{\partial}{\partial X^I}(\underline{v}) = \left(\frac{\partial}{\partial X^I}(v^J) + v^K \gamma^J_{KI}\right)\underline{e}_J \quad . \tag{A.16}$$

The coefficient in (A.16) is called the 'covariant derivative' of the component v^J. Covariant derivatives of the components of second order tensors may be defined in a similar manner. It should be noted that the Christoffel symbols are not components of third order tensors.

The operators GRAD, DIV, and CURL may be represented as the vector operators

$$\begin{aligned} \text{GRAD}\ \underline{v} &= \nabla \underline{v} \\ \text{DIV}\ \underline{v} &= \nabla \cdot \underline{v} \\ \text{CURL}\ \underline{v} &= \nabla \times \underline{v} \end{aligned} \tag{A.17}$$

where ∇ is the symbolic gradient operator:

$$\nabla = \underline{e}^K \frac{\partial}{\partial X^K} . \tag{A.18}$$

In dyad notation (A.17) may be written out as

$$\begin{aligned} \text{GRAD } \underline{v} &= \nabla \underline{v} = (v^J)_{,I} \underline{e}^I \underline{e}_J \\ \text{DIV } \underline{v} &= \nabla \cdot \underline{v} = (v^J)_{,J} \\ \text{CURL } \underline{v} &= \nabla \times \underline{v} = (v^I)_{,J} e^J{}_{IK} \underline{e}^K \end{aligned} \tag{A.19}$$

where $(\ )_{,I}$ denotes the covariant derivative with respect to X^I, and $e^I{}_{JK}$ is the alternating tensor, defined by

$$e^I{}_{JK} = (\underline{e}^I \times \underline{e}_J) \cdot \underline{e}_K = \delta^{IN} (\underline{e}_N \times \underline{e}_J) \cdot \underline{e}_K = \delta^{IN} e_{NJK} . \tag{A.20}$$

A convenient summary of formulas of vector analysis is given by Spiegel [50]; an extensive treatment of the subject is given by Phillips [51]. The remainder of this appendix is devoted to special notations used in this work.

The special notations used in this work are summarized in the formulas below. In accordance with (A.7) we write a second order tensor $\underline{\underline{T}}$ as

$$\underline{\underline{T}} = T^{IJ} \underline{e}_I \underline{e}_J = T^I{}_J \underline{e}_I \underline{e}^J = T_I{}^J \underline{e}^I \underline{e}_J = T_{IJ} \underline{e}^I \underline{e}^J .$$

The transpose is given by

$$\underset{\sim}{T}^T = T^{IJ}\underline{e}_J\underline{e}_I = T^I{}_J\underline{e}^J\underline{e}_I = T_I{}^J\underline{e}_J\underline{e}^I = T_{IJ}\underline{e}^J\underline{e}_I \ . \tag{A.21}$$

A fourth order tensor $\underset{\approx}{E}$ may be written out as

$$\underset{\approx}{E} = E^{IJKL}\underline{e}_I\underline{e}_J\underline{e}_K\underline{e}_L \ . \tag{A.22}$$

The scalar product of two second order tensors $\underset{\sim}{S}$ and $\underset{\sim}{T}$ is

$$\underset{\sim}{S} : \underset{\sim}{T} = S^{IJ}T_{IJ} \ . \tag{A.23}$$

The product of a fourth order tensor $\underset{\approx}{E}$ and a second order tensor $\underset{\sim}{T}$ is

$$\underset{\approx}{E} : \underset{\sim}{T} = E^{IJKL}T_{KL}\underline{e}_I\underline{e}_J \ ; \tag{A.24}$$

$$\underset{\sim}{T} : \underset{\approx}{E} = T_{KL}E^{KLIJ}\underline{e}_I\underline{e}_J \ .$$

The product of two fourth order tensors $\underset{\approx}{D}$ and $\underset{\approx}{E}$ is

$$\underset{\approx}{D} : \underset{\approx}{E} = D_{IJKL}E^{KLMN}\underline{e}^I\underline{e}^J\underline{e}_M\underline{e}_N \ . \tag{A.25}$$

Finally, differentiation by a tensor is defined

$$\frac{\partial R}{\partial \underset{\sim}{T}} = \frac{\partial R}{\partial T_{IJ}}\underline{e}_I\underline{e}_J \ ; \qquad \frac{\partial \underset{\sim}{S}}{\partial \underset{\sim}{T}} = \frac{\partial S^{IJ}}{\partial T_{KL}}\underline{e}_I\underline{e}_J\underline{e}_K\underline{e}_L \ . \tag{A.26}$$

APPENDIX B

ALTERNATIVES TO DIRECT NUMERICAL INVERSION OF THE CONSTITUTIVE EQUATION

Formulation of the stiffness matrix involves inversion of the (9×9) constitutive matrix $\underset{\approx}{W}$ at each quadrature point in the body, each time the stiffness matrix is evaluated. In practice it is found that these inversions figure significantly in the total computational effort. In this appendix we investigate the possibility of (1) analytic inversion of matrices of the form (4.21), and (2) approximation of the inverse of a matrix $\underset{\approx}{W} = \underset{\approx}{V} - \underset{\approx}{T}$ when $\underset{\approx}{V}^{-1}$ and $\underset{\approx}{T}$ are known. The reader is referred to the articles of Rivlin and Ericksen [25], and Rivlin [52] for discussions of representations of symmetric isotropic matrix functions.

Analytic Inversion of the Constitutive Equation

We begin by inverting the counterpart of (4.21) which arises in plane stress and plane strain problems. We consider a symmetric isotropic matrix function of the form

$$\dot{\underset{\sim}{\sigma}}^{*} = \underset{\approx}{V} : \underset{\sim}{\varepsilon} + \underset{\sim}{\Sigma} \tag{B.1}$$

where $\dot{\underset{\sim}{\sigma}}^{*}$, $\underset{\sim}{\varepsilon}$, and $\underset{\sim}{\Sigma}$ are (2×2) matrices, and

$$\underset{\approx}{V} = \sum_{I,J=1}^{2} \lambda^{IJ} \underset{\sim}{z}_I \underset{\sim}{z}_J + 2\mu \underset{\approx}{I} \tag{B.2}$$

$$\underset{\sim}{\Sigma} = \sum_{I=1}^{2} \eta^{I} \underset{\sim}{z}_{I} \tag{B.3}$$

$$\underset{\sim}{z}_{1} = \underset{\sim}{I} \; ; \qquad \underset{\sim}{z}_{2} = \underset{\sim}{\tau}. \tag{B.4}$$

If $\underset{\approx}{V}$ is invertible, then we may write (B.1) as

$$\underset{\sim}{\varepsilon} = \underset{\approx}{V}^{-1} : \overset{\circ}{\underset{\sim}{\sigma}}^{*} + \underset{\sim}{\Sigma}^{I} \tag{B.5}$$

where

$$\underset{\approx}{V}^{-1} = \sum_{I,J=1}^{2} \Lambda^{IJ} \underset{\sim}{z}_{I} \underset{\sim}{z}_{J} + 2M \underset{\approx}{I} \tag{B.6}$$

and

$$\underset{\sim}{\Sigma}^{I} = -\underset{\approx}{V}^{-1} : \underset{\sim}{\Sigma} \quad . \tag{B.7}$$

Of course $\underset{\approx}{V}$ and $\underset{\approx}{V}^{-1}$ satisfy

$$\underset{\approx}{V} : \underset{\approx}{V}^{-1} = \underset{\approx}{V}^{-1} : \underset{\approx}{V} = \underset{\approx}{I} \tag{B.8}$$

so multiplication of (B.2) and (B.6) must yield

$$\left[\lambda^{IJ}\Lambda^{KL}(\underset{\sim}{z}_{J} : \underset{\sim}{z}_{K}) + 2M\lambda^{IL} + 2\mu\Lambda^{IL}\right]\underset{\sim}{z}_{I}\underset{\sim}{z}_{L} + [4\mu M]\underset{\approx}{I} = \underset{\approx}{I} \; . \tag{B.9}$$

(in which the summation convention is used). From the linear

independence of the basis $\underset{\sim}{z}_I \underset{\sim}{z}_L$, $\underset{\approx}{I}$, we conclude that

$$4\mu M = 1 \; ; \tag{B.10}$$

$$\lambda^{IJ}\Lambda^{KL}(\underset{\sim}{z}_J : \underset{\sim}{z}_K) + 2M\lambda^{IL} + 2\mu\Lambda^{IL} = 0 \; . \tag{B.11}$$

From (B.10) we get

$$2M = 1/(2\mu) \; . \tag{B.12}$$

Elimination of 2M for (B.11) leads to a (2×2) matrix equation for Λ^{IJ}:

$$\left[[\lambda][Z] + 2\mu[I]\right][\Lambda] = -\frac{1}{2\mu}[\lambda] \tag{B.13}$$

where

$$[\lambda] = \begin{bmatrix} \lambda^{11} & \lambda^{12} \\ \lambda^{21} & \lambda^{22} \end{bmatrix} \quad ; \quad [\Lambda] = \begin{bmatrix} \Lambda^{11} & \Lambda^{12} \\ \Lambda^{21} & \Lambda^{22} \end{bmatrix} \; ;$$

and

$$Z_{IJ} = (\underset{\sim}{z}_I : \underset{\sim}{z}_J) \; .$$

The solution of (B.13) is easily found by Kramer's rule:

$$\Lambda^{11} = -\frac{1}{2\mu\Delta}\left[(\lambda^{11}\lambda^{22} - \lambda^{12}\lambda^{21})(tr\underset{\sim}{\tau}^2)\right] - \frac{\lambda^{11}}{\Delta}$$

$$\Lambda^{21} = \frac{1}{2\mu\Delta}\left[(\lambda^{11}\lambda^{22} - \lambda^{12}\lambda^{21})(tr\underset{\sim}{\tau})\right] - \frac{\lambda^{21}}{\Delta}$$

$$\Lambda^{12} = \frac{1}{2\mu\Delta}\left[(\lambda^{11}\lambda^{22} - \lambda^{12}\lambda^{21})(tr\underset{\sim}{\tau})\right] - \frac{\lambda^{12}}{\Delta} \qquad (B.14)$$

$$\Lambda^{22} = -\frac{1}{2\mu\Delta}\left[(\lambda^{11}\lambda^{22} - \lambda^{12}\lambda^{21})(2)\right] - \frac{\lambda^{22}}{\Delta}$$

$$\Delta = (\lambda^{11}\lambda^{22} - \lambda^{12}\lambda^{21})(2(tr\underset{\sim}{\tau}^2) - (tr\underset{\sim}{\tau})^2)$$

$$+ 2\mu(2\lambda^{11} + (\lambda^{12} + \lambda^{21})(tr\underset{\sim}{\tau}) + \lambda^{22}(tr\underset{\sim}{\tau}^2)) + 4\mu^2 .$$

Thus $2M$ and Λ^{IJ} in the representation of $\underset{\approx}{V}^{-1}$ (B.6) are all explicitly determined by μ, λ^{IJ}, and the stress.

The problem of inverting $\underset{\approx}{V}$ (4.21) for general problems may be attacked in precisely the same way as for two dimensional problems. For $\underset{\approx}{V}$ and $\underset{\approx}{V}^{-1}$ we write

$$\left.\begin{aligned} \underset{\approx}{V} &= \lambda^{IJ}\underset{\sim}{z}_I\underset{\sim}{z}_J + 2\mu^I\underset{\approx}{\phi}_I \ ; \\ \underset{\approx}{V}^{-1} &= \Lambda^{IJ}\underset{\sim}{z}_I\underset{\sim}{z}_J + 2M^I\underset{\approx}{\phi}_I \ ; \end{aligned}\right\} \qquad (B.15)$$

where

$$\underset{\sim}{z}_1 = \underset{\sim}{I} \ ; \qquad \underset{\sim}{z}_2 = \underset{\sim}{\tau}' \ ; \qquad \underset{\sim}{z}_3 = \underset{\sim}{s} = \underset{\sim}{\tau}' \cdot \underset{\sim}{\tau}' \ ;$$

and

$$[\phi_1]_{ijkl} = \delta_{ik}\delta_{lj}$$

$$[\phi_2]_{ijkl} = \tfrac{1}{2}(\tau'_{ik}\delta_{lj} + \delta_{ik}\tau'_{lj})$$

$$[\phi_3]_{ijkl} = \tfrac{1}{2}(s_{ik}\delta_{lj} + \delta_{ik}s_{lj}) \ .$$

The equation $\underset{\approx}{V}^{-1} : \underset{\approx}{V} = \underset{\approx}{I}$ gives the following relation among the λ^{IJ}, μ^I, Λ^{IJ}, and M^I:

$$\left[\lambda^{IJ}\Lambda^{KL}(\underset{\sim}{z}_L : \underset{\sim}{z}_I)\underset{\sim}{z}_K\underset{\sim}{z}_J + 2\mu^M\Lambda^{KL}\underset{\sim}{z}_K(\underset{\sim}{z}_L : \underset{\sim}{\phi}_M)\right. \tag{B.16}$$

$$\left. + 2M^N\lambda^{IJ}(\underset{\approx}{\phi}_N : \underset{\sim}{z}_I)\underset{\sim}{z}_J + 4M^N\mu^M(\underset{\approx}{\phi}_N : \underset{\approx}{\phi}_M)\right] = \underset{\approx}{I} \ .$$

It is tedious but straightforward to resolve the expressions $(\underset{\sim}{z}_I : \underset{\approx}{\phi}_J)$, $(\underset{\approx}{\phi}_I : \underset{\sim}{z}_J)$, and $(\underset{\approx}{\phi}_I : \underset{\approx}{\phi}_J)$ in the basis $\underset{\sim}{z}_I\underset{\sim}{z}_J$, $\underset{\approx}{\phi}_I$. The formulas given by Rivlin [52] (generalizations of the Hamilton-Cayley theorem) are particularly useful.

<u>Resolutions</u>: (B.17)

$$\underset{\approx}{\phi}_1 : \underset{\sim}{z}_I = \underset{\sim}{z}_I : \underset{\approx}{\phi}_1 = \underset{\sim}{z}_I \qquad I = 1,2,3 \ .$$

$$\underset{\approx}{\phi}_2 : \underset{\sim}{z}_1 = \underset{\sim}{z}_1 : \underset{\approx}{\phi}_2 = \underset{\sim}{z}_2$$

$$\underset{\approx}{\phi}_2 \ \underset{\sim}{z}_2 = \underset{\sim}{z}_2 : \underset{\approx}{\phi}_2 = \underset{\sim}{z}_3$$

$$\underset{\approx}{\phi}_2 : \underset{\sim}{z}_3 = \underset{\sim}{z}_3 : \underset{\approx}{\phi}_2 = (\det \underset{\sim}{\tau}')\underset{\sim}{z}_1 + \tfrac{1}{2}(\mathrm{tr}\ \underset{\sim}{s})\underset{\sim}{z}_2$$

$$\underset{\approx}{\phi}_3 : \underset{\sim}{z}_1 = \underset{\sim}{z}_1 : \underset{\approx}{\phi}_3 = \underset{\sim}{z}_3$$

$$\underset{\approx}{\phi}_3 : \underset{\sim}{z}_2 = \underset{\sim}{z}_2 : \underset{\approx}{\phi}_3 = \underset{\approx}{\phi}_2 : \underset{\sim}{z}_3$$

$$\underset{\approx}{\phi}_3 : \underset{\sim}{z}_3 = \underset{\sim}{z}_3 : \underset{\approx}{\phi}_3 = (\det \underset{\sim}{\tau}')\underset{\sim}{z}_2 + \tfrac{1}{2}(\mathrm{tr}\ \underset{\sim}{s})\underset{\sim}{z}_3$$

$$\underset{\approx}{\phi}_1 : \underset{\approx}{\phi}_1 = \underset{\approx}{\phi}_1 : \underset{\approx}{\phi}_1 = \underset{\approx}{\phi}_1 \qquad I = 1,2,3$$

$$\underset{\approx}{\phi}_2 : \underset{\approx}{\phi}_2 = -\tfrac{1}{2}\underset{\approx}{\phi}_3 - \tfrac{1}{4}(\mathrm{tr}\ \underset{\sim}{s})\underset{\sim}{z}_1\underset{\sim}{z}_1 + \tfrac{1}{2}\underset{\sim}{z}_2\underset{\sim}{z}_2$$

$$+ \tfrac{1}{2}(\underset{\sim}{z}_1\underset{\sim}{z}_3 + \underset{\sim}{z}_3\underset{\sim}{z}_1) + \tfrac{1}{4}(\mathrm{tr}\ \underset{\sim}{s})\underset{\approx}{I}$$

$$\underset{\approx}{\phi}_2 : \underset{\approx}{\phi}_3 = \underset{\approx}{\phi}_3 : \underset{\approx}{\phi}_2 = \tfrac{1}{4}(\mathrm{tr}\ \underset{\sim}{s})\underset{\approx}{\phi}_2 + \tfrac{1}{4}(\det \underset{\sim}{\tau}')\underset{\approx}{I}$$

$$+ \tfrac{1}{4}(\underset{\sim}{z}_3\underset{\sim}{z}_2 + \underset{\sim}{z}_2\underset{\sim}{z}_3) + \tfrac{1}{4}(\det \underset{\sim}{\tau}')\underset{\sim}{z}_1\underset{\sim}{z}_1$$

$$\underset{\approx}{\phi}_3 : \underset{\approx}{\phi}_3 = \frac{3}{4}(\mathrm{tr}\ \underset{\sim}{s})\underset{\approx}{\phi}_3 - \tfrac{1}{2}(\det \underset{\sim}{\tau}')\underset{\approx}{\phi}_2 - \tfrac{1}{2}(\mathrm{tr}\ \underset{\sim}{s})^2\underset{\approx}{I}$$

$$+ \tfrac{1}{2}\underset{\sim}{z}_3\underset{\sim}{z}_3 - \tfrac{1}{4}(\mathrm{tr}\ \underset{\sim}{s})(\underset{\sim}{z}_3\underset{\sim}{z}_1 + \underset{\sim}{z}_1\underset{\sim}{z}_3)$$

$$+ \tfrac{1}{2}(\det \underset{\sim}{\tau}')(\underset{\sim}{z}_1\underset{\sim}{z}_2 + \underset{\sim}{z}_2\underset{\sim}{z}_1) + \frac{1}{8}(\mathrm{tr}\ \underset{\sim}{s})^2\underset{\sim}{z}_1\underset{\sim}{z}_1 .$$

After resolution of the terms in (B.16) into the basis of the

representation of $\underset{\approx}{V}$ (i.e. $\underset{\sim}{z}_I\underset{\sim}{z}_J$ and $\underset{\approx}{\phi}_I$), the coefficient of $\underset{\approx}{I}$ is set to one and the coefficients of the other terms are set to zero. The coefficients of the $\underset{\approx}{\phi}_I$ involve the generalized shear moduli μ^I and M^I and stress only:

$$\begin{matrix} \underset{\approx}{I}: \\ \underset{\approx}{\phi}_2: \\ \underset{\approx}{\phi}_3: \end{matrix} \begin{bmatrix} 4\mu^1 & \mu^2(\mathrm{tr}\underset{\sim}{s}) + \mu^3(\det\underset{\sim}{\tau}') & -2\mu^3(\mathrm{tr}\underset{\sim}{s})^2 + \mu^2(\det\underset{\sim}{\tau}') \\ 4\mu^2 & 4\mu^1 + \mu^3(\mathrm{tr}\underset{\sim}{s}) & \mu^2(\mathrm{tr}\underset{\sim}{s}) - 2\mu^3(\det\underset{\sim}{\tau}') \\ 4\mu^3 & -2\mu^2 & 4\mu^1 + 3\mu^3(\mathrm{tr}\underset{\sim}{s}) \end{bmatrix} \begin{Bmatrix} M^1 \\ M^2 \\ M^3 \end{Bmatrix} = \begin{Bmatrix} 1 \\ 0 \\ 0 \end{Bmatrix} \tag{B.18}$$

In general (B.18) could just as well be solved numerically as analytically. In a special case of great practical importance though, when μ^2 and μ^3 both vanish, it follows immediately that $2M^1 = (1/2\mu^1)$, $2M^2 = 2M^3 = 0$. In any case, the remaining equations form a (3×3) matrix equation for the Λ^{IJ}. When $2M^1 = (1/2\mu^1)$ and the other M^I vanish, the equation for the Λ^{IJ} is of the same form as (B.13):

$$\Big[[\lambda][Z] + 2\mu[I]\Big][\Lambda] = -\frac{1}{2\mu}[\lambda] \tag{B.19}$$

where the matrices $[\lambda]$, $[\Lambda]$, and $[Z]$ are the identical counterparts of those in (B.13).

Though an analytic expression for $\underset{\approx}{V}^{-1}$ was not found in the general case, the numerical problem of inverting a (9×9) matrix was replaced by the problem of solving (at most) two (3×3) matrix equations. Finally we remark that no assumption as to the symmetry of the

[λ] matrix was made.

Approximation of W

Suppose that we are given the constitutive equation for a body in the form

$$\underset{\sim}{\varepsilon} = \underset{\approx}{V}^{-1} : \overset{\circ}{\underset{\sim}{\sigma}}^{*} + \underset{\sim}{\varepsilon}^{P} \tag{B.20}$$

and we wish to obtain the form

$$\underset{\sim}{\varepsilon} = \underset{\approx}{W}^{-1} : \overset{\circ}{\underset{\sim}{r}} + \overset{\nabla}{\underset{\sim}{\varepsilon}}^{P} . \tag{B.21}$$

Since $\overset{\circ}{\underset{\sim}{\sigma}}^{*} = \overset{\circ}{\underset{\sim}{r}} + \underset{\approx}{T} : \underset{\sim}{\varepsilon}$, we can get the implicit equation

$$\underset{\sim}{\varepsilon} = \underset{\approx}{V}^{-1} : (\overset{\circ}{\underset{\sim}{r}} + \underset{\approx}{T} : \underset{\sim}{\varepsilon}) + \underset{\sim}{\varepsilon}^{P} \tag{B.22}$$

directly. If we try to solve (B.22) for $\underset{\sim}{\varepsilon}$ (when $\overset{\circ}{\underset{\sim}{r}}$ is assigned) by iteration,

$$\underset{\sim}{\varepsilon}^{N+1} = \underset{\approx}{V}^{-1} : (\overset{\circ}{\underset{\sim}{r}} + \underset{\approx}{T} : \underset{\sim}{\varepsilon}^{N}) + \underset{\approx}{\varepsilon}^{P} \tag{B.23}$$

then we are led to define $\underset{\approx N}{W}^{-1}$ as

$$\underset{\approx N}{W}^{-1} = \underset{\approx}{V}^{-1} + \underset{\approx}{V}^{-1} : \underset{\approx}{T} : \underset{\approx}{V}^{-1} + \ldots + (\underset{\approx}{V}^{-1} : \underset{\approx}{T})^{N} : \underset{\approx}{V}^{-1} \tag{B.24}$$

and the first neglected term is $(\underset{\approx}{V}^{-1} : \underset{\approx}{T})^{N+1} : \underset{\sim}{\varepsilon}$, where $(N+1)$ is the

number of terms in the series (B.24). If the eigenvalue of $(\underset{\approx}{V}^{-1} : \underset{\approx}{T})$ whose absolute value is greatest is of absolute value less than one, then the remainder vanishes as $N \to \infty$, so the series converges; that is $\underset{\approx}{W}_N^{-1} \to \underset{\approx}{W}^{-1}$. The eigenvalues of $\underset{\approx}{T}$ coincide with those of the true stress, and the eigenvalue of $\underset{\approx}{V}^{-1}$ whose absolute value is greatest is a shear compliance. Thus, for metals in the elastic range $\underset{\approx}{W}_1^{-1}$ can be expected to be in error by less than 0.01%. We find that in practice if more than two terms in (B.24) are needed, it is more efficient to compute $\underset{\approx}{W}^{-1}$ by some other means. The main appeal of (B.24) with two terms taken is in large deformation--small strain analyses, such as in structures.

Construction and Inversion of Constitutive Equations for Plane Problems

We first indicate the class of problems which may be considered 'planar.' The class consists of those problems in which the true stress $\underset{\sim}{\tau}$, the (general) stress rate $\overset{\circ}{\underset{\sim}{s}}$, and the stretching $\underset{\sim}{\varepsilon}$ are of the forms

$$\begin{aligned} \underset{\sim}{\tau} &= \tau^{\alpha\beta}\underset{\sim}{e}_\alpha\underset{\sim}{e}_\beta + \tau^{33}\underset{\sim}{e}_3\underset{\sim}{e}_3 \\ \overset{\circ}{\underset{\sim}{s}} &= \overset{\circ}{s}{}^{\alpha\beta}\underset{\sim}{e}_\alpha\underset{\sim}{e}_\beta + \overset{\circ}{s}{}^{33}\underset{\sim}{e}_3\underset{\sim}{e}_3 \\ \underset{\sim}{\varepsilon} &= \varepsilon^{\alpha\beta}\underset{\sim}{e}_\alpha\underset{\sim}{e}_\beta + \varepsilon^{33}\underset{\sim}{e}_3\underset{\sim}{e}_3 \end{aligned} \qquad \text{(B.25)}$$

where the Greek indices range from 1 to 2. Substitution of (B.25)

into the constitutive equation

$$\dot{\underset{\sim}{s}} = \underset{\approx}{V} : \underset{\sim}{\varepsilon} + \underset{\sim}{\Sigma} \tag{B.26}$$

yields the component equations

$$\begin{Bmatrix} \dot{s}^{\alpha\beta} \\ \dot{s}^{33} \end{Bmatrix} = \begin{bmatrix} V^{\alpha\beta}{}_{\gamma\delta} & V^{\alpha\beta}{}_{33} \\ V^{33}{}_{\gamma\delta} & V^{33}{}_{33} \end{bmatrix} \begin{Bmatrix} \varepsilon^{\gamma\delta} \\ \varepsilon^{33} \end{Bmatrix} + \begin{Bmatrix} \Sigma^{\alpha\beta} \\ \Sigma^{33} \end{Bmatrix} \tag{B.27}$$

(B.28)

The tensors $\underset{\approx}{V}''$ and $\underset{\sim}{\Sigma}''$, defined as

$$\begin{aligned} \underset{\approx}{V}'' &= V^{\alpha\beta}{}_{\gamma\delta}\underset{\sim}{e}_\alpha\underset{\sim}{e}_\beta\underset{\sim}{e}^\gamma\underset{\sim}{e}^\delta \\ \underset{\sim}{\Sigma}'' &= \Sigma^{\alpha\beta}\underset{\sim}{e}_\alpha\underset{\sim}{e}_\beta \end{aligned} \tag{B.29}$$

are necessarily of the forms (B.2) and (B.3) when $\underset{\approx}{V}$ and $\underset{\sim}{\Sigma}$ are of the forms (4.21) and (4.22), respectively. We define $\dot{\underset{\sim}{s}}''$, $\underset{\sim}{\varepsilon}''$, and $\underset{\sim}{\tau}''$ as

$$\dot{\underset{\sim}{s}}'' = \dot{s}^{\alpha\beta}\underset{\sim}{e}_\alpha\underset{\sim}{e}_\beta \; ; \quad \underset{\sim}{\varepsilon}'' = \varepsilon^{\alpha\beta}\underset{\sim}{e}_\alpha\underset{\sim}{e}_\beta ; \quad \underset{\sim}{\tau}'' = [\underset{\sim}{\tau}' : (\underset{\sim}{e}^\alpha\underset{\sim}{e}^\beta)](\underset{\sim}{e}_\alpha\underset{\sim}{e}_\beta) \; .$$

For plane strain (B.27) may be written

$$\begin{aligned} \dot{\underset{\sim}{s}}'' &= \underset{\approx}{V}'' : \underset{\sim}{\varepsilon}'' + \underset{\sim}{\Sigma}'' \\ \dot{s}^{33} &= \underset{\sim}{V}^{33} : \underset{\sim}{\varepsilon}'' + \Sigma^{33} \end{aligned} \tag{B.30}$$

For plane stress (B.27) becomes

$$\begin{aligned} \overset{\cdot}{\underset{\sim}{s}}'' - \underset{\sim}{V}_{33}\varepsilon^{33} &= \underset{\approx}{V}'' : \underset{\sim}{\varepsilon}'' + \underset{\sim}{\Sigma}'' \\ - V_{33}^{33}\varepsilon^{33} &= \underset{\sim}{V}^{33} : \underset{\sim}{\varepsilon}'' + \Sigma^{33} \ . \end{aligned} \tag{B.31}$$

It is apparent that if we can write $\underset{\approx}{V}''$ in the form (B.2) then analytic inversion is possible. To find the necessary coefficients we set the components so that

$$(\underset{\sim}{e}_\alpha\underset{\sim}{e}_\beta) : \underset{\approx}{V} : (\underset{\sim}{e}_\gamma\underset{\sim}{e}_\delta) - (\underset{\sim}{e}_\alpha\underset{\sim}{e}_\beta) : \underset{\approx}{V}'' : (\underset{\sim}{e}_\gamma\underset{\sim}{e}_\delta) = 0 \tag{B.32}$$

where $\underset{\approx}{V}$ is written for (4.21) and $\underset{\approx}{V}''$ for (B.2). We let λ^{IJ} and μ^I be the coefficients in (4.21) and l^{IJ} and m be the coefficients in (B.2). Then (B.32) leads directly to

$$l^{11} = \lambda^{11} - q(\lambda^{13} + \lambda^{31}) + q^2\lambda^{33} - (p\mu^2 + p^2\mu^3)$$

$$l^{12} = \lambda^{12} + p(\lambda^{13} + \mu^3) - q\lambda^{32} - qp\lambda^{33} + \mu^2$$

$$l^{21} = \lambda^{21} + p(\mu^{31} + \mu^3) - q\lambda^{23} - qp\lambda^{33} + \mu^2$$

$$l^{22} = \lambda^{22} + p(\lambda^{23} + \lambda^{32}) + p^2\lambda^{33}$$

$$2m = 2\mu^1 + p\mu^2 + (p^2 - 2q)\mu^3$$

where $p = \tau'_{\eta\eta}$ and $q = \frac{1}{2}(p^2 - \tau'_{\eta\theta}\tau'_{\eta\theta})$. The planar inverse is found by putting 1^{IJ} for λ^{IJ}, m for μ, p for $\mathrm{tr}\,\underset{\sim}{\tau}$, and $(p^2 - 2q)$ for $\mathrm{tr}(\underset{\sim}{\tau}^2)$ in (B.14). Though (B.33) and (B.14) are algebraically complicated, their effect is to reduce the problem of construction and inversion of $\underset{\approx}{W}''$ for planar problems to about ten lines of ordinary FORTRAN.

APPENDIX C

SHAPE FUNCTIONS FOR VELOCITY, STRESS RATE, AND SPIN

Shape Functions for Plane Strain

$$x^1 = x \; ; \qquad x^3 = z$$

Velocity Shape Functions

$$\underline{N}_i = N_{1,i}\underline{e}_1 + N_{3,i}\underline{e}_3$$

Four Noded Element:

$$N_{1,i} = \begin{cases} \frac{1}{4}(1+\xi\xi_i)(1+\eta\eta_i) & i = 1,2,3,4. \\ 0 & i = 5,6,7,8 \end{cases}$$

$$N_{3,i} = \begin{cases} 0 & i = 1,2,3,4 \\ \frac{1}{4}(1+\xi\xi_{i-4})(1+\eta\eta_{i-4}) & i = 5,6,7,8 \end{cases}$$

$$|\xi| \leq 1, \qquad |\eta| \leq 1,$$

$$\xi_1 = -1, \quad \xi_2 = 1, \quad \xi_3 = 1, \quad \xi_4 = -1$$

$$\eta_1 = -1, \quad \eta_2 = -1, \quad \eta_3 = 1, \quad \eta_4 = 1$$

Eight Noded Element

$$N_{1,i} = \begin{cases} H_i & i = 1,2,\ldots,8 \\ 0 & i = 9,10,\ldots,16 \end{cases}$$

$$N_{3,i} = \begin{cases} 0 & i = 1,2,\ldots,8 \\ H_{i-8} & i = 9,10,\ldots,16 \end{cases}$$

$$H_i = \begin{cases} \frac{1}{2}(1-\xi^2)(1+\eta\eta_i) & i = 2,6 \\ \frac{1}{2}(1+\xi\xi_i)(1-\eta^2) & i = 4,8 \\ \frac{1}{4}(1+\xi\xi_i)(1+\eta\eta_i)(\xi\xi_i+\eta\eta_i-1) & i = 1,3,5,7 \end{cases}$$

$$\xi_1 = \xi_7 = \xi_8 = -1; \quad \xi_2 = \xi_6 = 0; \quad \xi_3 = \xi_4 = \xi_5 = +1;$$

$$\eta_1 = \eta_2 = \eta_3 = -1; \quad \eta_4 = \eta_8 = 0; \quad \eta_5 = \eta_6 = \eta_7 = +1 .$$

Shape Functions for Spin

$$\underset{\sim}{QW}_i = QW_{13,i}\ \underline{e}_1\underline{e}_3 + QW_{31,i}\ \underline{e}_3\underline{e}_1$$

where

$$QW_{13,1} = c_1$$

$$QW_{31,1} = -c_1$$

If NW = 3 add the following shape functions

$$QW_{13,2} = xc_2$$

$$QW_{13,3} = zc_3$$

$$QW_{31,2} = -xc_2$$

$$QW_{31,3} = -zc_3$$

If NW = 4 add the following shape functions

$$QW_{13,4} = xyc_4$$

$$QW_{31,4} = -xyc_4$$

If NW = 6 add the following shape functions

$$QW_{13,5} = xxc_5$$

$$QW_{13,6} = zzc_6$$

$$QW_{31,5} = -xxc_5$$

$$QW_{31,6} = -zzc_6$$

The constants were used to improve the condition of [H].

Stress Shape Functions

$$\underset{\sim}{QT}_i = QT_{11,i}\ \underline{e}_1\underline{e}_1 + 0 + QT_{13,i}\ \underline{e}_1\underline{e}_3$$

$$+ 0 + QT_{22,i}\ \underline{e}_2\underline{e}_2 + QT_{31,i}\ \underline{e}_3\underline{e}_1 + 0 + QT_{33,i}\ \underline{e}_3\underline{e}_3$$

$$QT_{11,1} = 1$$

$$QT_{31,2} = -1$$

$$QT_{22,3} = 1$$

$QT_{13,4} = -1$

$QT_{33,5} = 1$

For NT = 13 add the following stress shape functions

$QT_{11,6} = x$

$QT_{31,6} = -z$

$QT_{31,7} = -x$

$QT_{22,8} = x$

$QT_{13,9} = -x$

$QT_{33,9} = z$

$QT_{33,10} = x$

$QT_{11,11} = z$

$QT_{13,12} = -z$

$QT_{22,13} = z$

For NT = 21 add the following stress shape functions

$QT_{11,14} = .5xx$

$QT_{31,14} = -xz$

$QT_{31,15} = -xx$

$QT_{13,16} = -.5xx$

$QT_{33,16} = xz$

$QT_{33,17} = xx$

$QT_{11,18} = xz$

$QT_{31,18} = -.5zz$

$QT_{11,19} = zz$

$QT_{13,20} = -xz$

$QT_{33,20} = .5zz$

$QT_{13,21} = -zz$

1 x 1 Gauss quadrature for 'constant' shapes;

3 x 3 Gauss quadrature for 'linear' shapes;

4 x 4 Gauss quadrature for 'quadratic' shapes.

Shape Functions for Axisymmetric Deformation

$r = x^1$; $z = x^3$

$\underline{e}_1 = \underline{e}_r$; $\underline{e}_2 = \underline{e}_\theta$; $\underline{e}_3 = \underline{e}_z$;

Components $N_{1,i}$, $N_{2,i}$, and $N_{3,i}$ are identical to plane strain shape functions. Spin functions are identical except r replaces x, $\underline{e}_r$ replaces $\underline{e}_x$.

Stress Rate Shape Functions

$$\underset{\sim}{QT}_i = QT_{11,i}\ \underline{e}_1\underline{e}_1 + 0 + QT_{13,i}\ \underline{e}_1\underline{e}_3$$

$$+ 0 + QT_{22,i}\ \underline{e}_2\underline{e}_2 + 0 + QT_{31,i}\ \underline{e}_3\underline{e}_1 + 0 + QT_{33,i}\ \underline{e}_3\underline{e}_3$$

where

$$QT_{11,1} = c/r \ .$$

$$QT_{31,2} = c/r \ .$$

$$QT_{13,3} = c/r \ .$$

$$QT_{33,4} = c/r \ .$$

$$QT_{11,5} = 1 \ .$$

$$QT_{22,5} = 1 \ .$$

$$QT_{31,6} = 1 \ .$$

$$QT_{13,7} = c \ .$$

$$QT_{33,7} = -cz/r \ .$$

$$QT_{33,8} = cz/r \ .$$

$$QT_{11,10} = z \ .$$

$$QT_{22,10} = z \ .$$

$$QT_{13,11} = cz/r \ .$$

$$QT_{11,12} = (r-c)/c \ .$$

$$QT_{22,12} = (2r-c)/c \ .$$

$$QT_{31,13} = (r-c)/c \ .$$

$$QT_{13,14} = (r-c)/c \ .$$

$$QT_{33,14} = -z(2r-c)/rc \ .$$

$$QT_{33,15} = (r-c)/c$$

where c is chosen to improve the condition of matrix [H]. (3 x 3) Gaussian quadrature was used on this element. The constant c was assigned as the value of r at the center quadrature point on each element.

APPENDIX D

TABLES

Table 1. Critical Configurations in Plane Extension

$2a_o^3/a_o^1$	a_c^1	$2a_c^3$	τ_c^{22}	τ_c^{33}
N = 4				
2	3.6191	13.9342	584.79	1173.34
3	3.7800	20.0053	564.15	1132.54
4	3.8388	26.2625	556.25	1116.87
N = 8				
2	4.0714	12.3385	322.63	646.19
3	4.2852	17.5819	311.39	623.93
4	4.3533	23.0741	307.26	615.77

Table 2. Configuration for Parameter Study

$2a_o^3/a_o^1$	a^1	$2a^3$	τ^{22}	τ^{33}
2	4.0752	12.3271	322.44	645.83

Table 3. Data for Figure 29 (8 Noded Element, NT = 21, NW = 6)

Mesh	Symbol	Degrees of Freedom	Eigenvalue
1 x 2	□	15	0.5341
1 x 3	□	23	0.3221
1 x 4	□	31	0.2416
1 x 6	□	47	0.1505
2 x 4	△	55	0.1850
2 x 6	△	83	0.1259
2 x 8	△	111	0.0957
2 x 10	△	139	0.0772
3 x 6	○	119	0.0925
3 x 8	○	159	0.0703
3 x 10	○	199	0.0568
3 x 12	○	239	0.0476
4 x 9	◇	233	0.0495

Table 4. Data for Figure 30 (4 Noded Element, NT = 13, NW = 3)

Mesh	Symbol	Degrees of Freedom	Eigenvalue
2 x 6	□	29	0.3732
2 x 8	□	39	11.2843
2 x 10	□	49	22.6500
3 x 6	△	41	27.1690
3 x 9	△	62	0.1777
3 x 12	△	83	2.7302
3 x 15	△	104	5.4067
4 x 8	○	71	9.5265
4 x 12	○	107	0.1059
4 x 20	○	179	1.8974
5 x 10	◇	109	4.1738
5 x 15	◇	164	0.0706
5 x 20	◇	219	0.4415

Table 5. Data for Figure 31 (4 Noded Element, NT = 13, NW = 1)

Mesh	Symbol	Degrees of Freedom	Eigenvalue
3 x 6	□	41	633.077
3 x 9	□	62	316.414
3 x 12	□	83	228.714
3 x 15	□	104	197.089
3 x 18	□	125	185.583
4 x 8	△	71	237.617
4 x 12	△	107	117.908
4 x 16	△	143	80.444
4 x 20	△	179	68.967
5 x 10	○	109	107.518
5 x 15	○	164	49.623
5 x 20	○	219	35.078

Table 6. Necking Eigenvalue--(2 x 6 Mesh, 4 Noded Elements)

	NT = 13	NT = 21
NW = 1	1253.19	1253.19
NW = 3	0.3732	0.3732
NW = 4	0.3732	0.3732
NW = 6	0.3732	0.3732

Table 7. Data for Figure 32 (4 Noded Element, NT = 5, NW = 1)

Mesh	Symbol	Degrees of Freedom	Eigenvalue
2 x 4	□	19	1.0948
3 x 6	□	41	0.4043
4 x 8	□	71	0.2074
5 x 10	□	109	0.1269
6 x 12	□	155	0.0862
2 x 8	△	39	-1.2258
3 x 12	△	83	-0.2204
4 x 16	△	143	-0.0426
5 x 20	△	219	0.0003

BIBLIOGRAPHY

1. Love, A. E. H., *A Treatise on the Mathematical Theory of Elasticity*, 4th ed., Dover, Publications, 1944.

2. Reissner, E., "The Effect of Transverse Shear Deformation on the Bending of Elastic Plates," Journal of Applied Mechanics, Vol. 12, No. 2, June 1945, pp. 69-77.

3. Pian, T. H. H., "Derivation of Element Stiffness Matrices by Assumed Stress Distributions," AIAA Journal, Vol. 2, No. 7, 1964, pp. 1333-1336.

4. Herrmann, L. R., "Elasticity Equations for Incompressible Materials by a Variational Theorem," AIAA Journal, Vol. 3, No. 10, October 1965, pp. 1896-1900.

5. de Veubeke, B. F., "A New Variational Principle for Finite Elastic Deformations," International Journal of Engineering Science, Vol. 10, 1972, pp. 745-763.

6. de Veubeke, B. F., and Millard, A., "Discretization of Stress Field in the Finite Element Method," Journal of the Franklin Institute, Vol. 302, Nos. 5 & 6, 1976, pp. 389-412.

7. Sander, G., and Carnoy, E., "Equilibrium and Mixed Formulations in Stability Analysis," in Proceedings of the International Conference on Finite Elements in Nonlinear Solid and Structural Mechanics, Geilo, Norway, 1977, pp. 87-105.

8. Koiter, W. T., "Complementary Energy, Neutral Equilibrium, and Buckling," Proc. Kon. Ned. Akad., Wetensch., Series B, 1977, pp. 183-200.

9. Wunderlich, W., and Obrecht, H., "Large Spatial Deformations of Rods Using Generalized Variational Principles," in *Nonlinear Finite Element Analysis in Structural Mechanics*, Wunderlich, W., Stein, E., and Bathe, K.-J., Editors, Springer-Verlag, 1981.

10. Murakawa, H., "Incremental Hybrid Finite Element Methods for Finite Deformation Problems (with Special Emphasis on the Complementary Energy Principle)," Ph.D. Dissertation, Georgia Inst. of Technology, August, 1978.

11. Murakawa, H., and Atluri, S. N., "Finite Elasticity Solutions Using Hybrid Finite Elements Based on a Complementary Energy

Principle," Journal of Applied Mechanics, Vol. 45, 1978, pp. 539-548.

12. Murakawa, H., and Atluri, S. N., "Finite Elasticity Solutions Using Hybrid Finite Elements Based on a Complementary Energy Principle - II, Incompressible Materials," Journal of Applied Mechanics, Vol. 46, 1979, pp. 71-78.

13. Murakawa, H., Reed, K. W., Atluri, S. N., and Rubinstein, R., "Stability Analysis of Structures via a New Complementary Energy Principle," in *Computational Methods in Nonlinear Structural and Solid Mechanics*, Noor, A. K., and McCome, H. G., Editors, Pergamon, 1981.

14. Atluri, S. N., and Murakawa, H., "New General and Complementary Energy Theorems, Finite Strain, Rate Sensitive Inelasticity and Finite Elements: Some Computational Studies," in *Nonlinear Finite Element Analysis in Structural Mechanics*, Wunderlich, W., Stein, E., and Bathe, K.-J., Editors, Springer-Verlag, 1981.

15. Atluri, S. N., "On Some New General and Complementary Energy Theorems for the Rate Problems of Finite Strain, Classical Elasto-Plasticity," Journal of Structural Mechanics, Vol. 8, No. 1, 1980, pp. 61-92.

16. Levinson, M., "The Complementary Energy Theorem in Finite Elasticity," Journal of Applied Mechanics, Vol. 87, 1965, pp. 826-828.

17. Zubov, L. M., "The Stationary Principle of Complementary Work in Nonlinear Theory of Elasticity," Journal of Applied Mathematics and Mechanics (trans; Prikl. Mat. Meh.), Vol. 34, 1970, pp. 228-232.

18. Dill, E. H., "The Complementary Energy Principle in Nonlinear Elasticity," Letters in Applied and Engineering Sciences, Vol. 5, 1977, pp. 95-106.

19. Argyris, J. H., Vaz, L. E., and William, K. J., "Improved Solution Methods for Inelastic Rate Problems," Computer Methods in Applied Mechanics and Engineering, Vol. 16, 1978, pp. 231-277.

20. Hughes, T. R. J., and Taylor, R. L., "Unconditionally Stable Algorithms for Quasi-Static Elasto-Visco-Plastic Finite Element Analysis," Computers and Structures, Vol. 8, 1978, pp. 169-173.

21. Prager, W., *Introduction to the Mechanics of Continua*, Ginn and Co., 1961.

22. Truesdell, C., and Noll, W., *The Nonlinear Field Theories of Mechanics*, Handbuch der Physik, III/3, Springer-Verlag, 1965.

23. Hill, R., "Some Basic Principles in the Mechanics of Solids without a Natural Time," J. Mech. Phys. Solids, Vol. 7, 1959, pp. 209-225.

24. Ogden, R. W., "Inequalities associated with the inversion of elastic stress-deformation relations and their implications," Math. Proc. Camb. Phil. Soc., Vol. 81, 1977, pp. 313-324.

25. Rivlin, R. S., and Ericksen, J. L., "Stress-Deformation Relations for Isotropic Materials," J. Rat. Mech. Anal., Vol. 4, 1955, pp. 323-425.

26. Truesdell, C., "Hypo-elasticity," J. Rat. Mech. Anal., Vol. 4, 1955, pp. 83-133. Note corrections, pp. 1019-1020.

27. Truesdell, C., "Hypo-elastic Shear," Journal of Applied Physics, Vol. 27, No. 5, 1956, pp. 441-447.

28. Green, A. E., and McInnis, B. C., "Generalized Hypo-Elasticity," Proc. Roy. Soc. Edinburg A67, 1967, pp. 220-230.

29. Kachanov, L. M., *Fundamentals of the Theory of Plasticity*, Mir Publishers, 1974 (English trans. by M. Konyaeva).

30. Hill, R., *The Mathematical Theory of Plasticity*, Oxford, 1971.

31. Christoffersen, J., and Hutchinson, J. W., "A Class of Phenomenological Corner Theories of Plasticity," J. Mech. Phys. Solids, Vol. 27, 1979, pp. 465-487.

32. Tvergaard, V., Needleman, A., and Lo, K. K., "Flow Localization in the Plane Strain Tensile Test," J. Mech. Phys. Solids, Vol. 29, 1981, pp. 115-142.

33. Prager, W., *An Introduction to Plasticity*, Addison-Wesley Publishing Co., 1959.

34. McMeeking, R. M., and Rice, J. R., "Finite Element Formulations for Problems of Large Elastic-Plastic Deformation," Int. J. Solids Structures, Vol. 11, 1975, pp. 601-616.

35. Perzyna, P., "Fundamental Problems in Viscoplasticity," in Advances in Applied Mechanics, Vol. 9, 1966, pp. 243-377.

36. Washizu, K., *Variational Methods in Elasticity and Plasticity*, Second edition, Pergamon Press, 1975.

37. Hill, R., "Aspects of Invariance in Solid Mechanics," in Advances in Applied Mechanics, Vol. 18, 1978, pp. 1-75.

38. Hill, R., "A General Theory of Uniqueness and Stability in Elastic-Plastic Solids," J. Mech. Phys. Solids, Vol. 6, 1958, pp. 236-249.

39. Tong, P., and Rossettos, J. N., *Finite Element Method; Basic Technique and Implementation,* The MIT Press, 1977.

40. Zienkiewicz, O. C., *The Finite Element Method in Engineering Science,* McGraw-Hill, 1971.

41. Strang, G. and Fix, G. J., *An Analysis of the Finite Element Method,* Prentice-Hall, 1973.

42. Oden, J. T., *Finite Elements for Nonlinear Continua,* McGraw-Hill, 1972.

43. Ergatoudis, I., Irons, B. M., and Zienkiewicz, O. C., "Curved, Isoparametric, Quadralateral Elements for Finite Element Analysis," Int. J. Solids Structures, Vol. 4, 1968, pp. 31-42.

44. Hill, R., "Eigenmodal Deformations in Elastic/Plastic Continua," J. Mech. Phys. Solids, Vol. 15, 1967, pp. 371-386.

45. Tong, P., and Pian, T. H. H., "A Variational Principle and the Convergence of a Finite Element Method Based on Assumed Stress Distribution," Int. J. Solids Structures, Vol. 5, 1969, pp. 463-472.

46. Cormeau, I., "Numerical Stability in Quasistatic Elasto-Visco-plasticity," Int. J. Numer. Meths. in Eng., Vol. 9, 1975, pp. 109-127.

47. Conte, S. D., and de Boor, C., *Elementary Numerical Analysis,* McGraw-Hill, Second Edition, 1972.

48. Rubinstein, R., and Atluri, S. N., "Objectivity of Incremental Constitutive Relations Over Finite Time Steps in Computational Finite Deformation Analyses," Computer Methods in Applied Mechanics and Engineering, to appear.

49. Kanchi, M. B., Zienkiewicz, O. C., and Owen, R. J., "The Visco-Plastic Approach to Problems of Plasticity and Creep Involving Geometric Nonlinear Effects," Int. J. Numer. Meths. Eng., Vol. 12, 1978, pp. 169-181.

50. Spiegel, M. R., *Vector Analysis,* McGraw-Hill, 1959.

51. Phillips, H. B., *Vector Analysis,* J. Wiley, 1933.

52. Rivlin, R., "Further Remarks on the Stress-Deformation Relations

for Isotropic Materials," J. Rat. Mech. Anal., Vol. 4, 1955, pp. 681-702.

53. Abramowitz, M., and Stegun, I. A., Editors, *Handbook of Mathematical Functions*, Ninth Printing, Dover, 1970.

54. Greenbaum, G. A., and Rubenstein, M. F., "Creep Analysis of Axisymmetric Bodies Using Finite Elements," Nuclear Engineering and Design, Vol. 7, 1968, pp. 379-397.

55. Pian, T. H. H., and Lee, S. W., "Creep and Viscoplastic Analysis by Assumed Stress Finite Elements," in *Finite Elements in Nonlinear Mechanics*, Vol. II, Bergan, P. G., et al., Editors, Tapir Press, Norway, 1977.

56. Hult, J. A. H., *Creep in Engineering Structures*, Blaisdell, 1966.

57. Hutchinson, J. W., and Miles, J. P., "Bifurcation Analysis of the Onset of Necking in an Elastic/Plastic Cylinder Under Uniaxial Tension," J. Mech. Phys. Solids, Vol. 22, 1974, pp. 61-71.

58. Miles, J. P., "The Initiation of Necking in Rectangular Elastic/Plastic Specimens Under Uniaxial and Biaxial Tension," J. Mech. Phys. Solids, Vol. 23, 1975, pp. 197-213.

59. Hill, R., and Hutchinson, J. W., "Bifurcation Phenomena in the Plane Tension Test," J. Mech. Phys. Solids, Vol. 23, 1975, pp. 239-264.

60. Burke, M. A., and Nix, W. D., "A Numerical Study of Necking in the Plane Tension Test," Int. J. Solids Structures, Vol. 15, 1979, pp. 379-393.

61. Cowper, G. R., and Onat, E. T., "The Initiation of Necking and Buckling in Plane Plastic Flow," in *Proceedings of the Fourth U.S. National Congress of Applied Mechanics*, Rosenberg, R. M., editor, ASME, 1962.

62. Burke, M. A., and Nix, W. D., "A Numerical Analysis of Void Growth in Tension Creep," Int. J. Solids Structures, Vol. 15, 1979, pp. 55-71.

63. Timoshenko, S. P., and Goodier, J. N., *Theory of Elasticity*, Third Edition, McGraw-Hill, 1970.

VITA

Kenneth Wayne Reed was born in [redacted] on [redacted] He received his Bachelor of Engineering degree in Engineering Mechanics from Georgia Institute of Technology in March, 1978. He entered the graduate school at Georgia Institute of Technology and obtained the degree of Master of Science in Engineering Mechanics in August, 1979. He was enrolled as a doctoral student in the School of Civil Engineering of Georgia Institute of Technology in September, 1979.

Corrections to

"Analysis of Large Quasistatic Deformations of Inelastic Solids by a New Stress Based Finite Element Method"

p. 17, last line:
replace "$\underline{n}\ (\underline{x},\tau)$" by "$\underline{n}(\underline{X},\tau)$".

p. 20, equation (3.26):
replace "0" by "$\underset{\sim}{0}$".

p. 27, equation (3.52):

replace "$\frac{\partial}{\partial\tau}$" by $\frac{\partial}{\partial t}$".

p. 43, 8th line from page bottom:
replace "In any case" by "In the case of solids without a natural time"
5th line from page bottom
replace "so the choice" by "so then the choice".

p. 91, last line:
replace "v" by "w".

p. 225, 3rd line from bottom of page:

replace "μ^{21}" and "μ^{31}" by "λ^{21}" and "λ^{31}", respectively.

REPORT DOCUMENTATION PAGE

Form Approved
OMB No. 0704-0188

1. AGENCY USE ONLY (*Leave blank*)	2. REPORT DATE	3. REPORT TYPE AND DATES COVERED
	1992	Final Contractor Report

4. TITLE AND SUBTITLE

Analysis of Large Quasistatic Deformations of Inelastic Solids by a New Stress Based Finite Element Method

5. FUNDING NUMBERS

WU–590–21–11
G–NAG3–38

6. AUTHOR(S)

Kenneth W. Reed

7. PERFORMING ORGANIZATION NAME(S) AND ADDRESS(ES)

Georgia Institute of Technology
Atlanta, Georgia 30332

8. PERFORMING ORGANIZATION REPORT NUMBER

9. SPONSORING/MONITORING AGENCY NAMES(S) AND ADDRESS(ES)

National Aeronautics and Space Administration
Lewis Research Center
Cleveland, Ohio 44135–3191

10. SPONSORING/MONITORING AGENCY REPORT NUMBER

NASA CR–189235

11. SUPPLEMENTARY NOTES

Project Manager, C.C. Chamis, Structures Division, NASA Lewis Research Center, (216) 433–3252. This report was submitted by Kenneth Wayne Reed as a thesis in partial fulfillment of the requirements for the degree Doctor of Philosophy in Civil Engineering to Georgia Institute of Technology, Atlanta, Georgia.

12a. DISTRIBUTION/AVAILABILITY STATEMENT

Unclassified - Unlimited
Subject Category 39

12b. DISTRIBUTION CODE

13. ABSTRACT ***(Maximum 200 words)***

A new hybrid stress finite element algorithm suitable for analyses of large quasistatic deformation of inelastic solids is presented. Principal variables in the formulation are the nominal stress rate and spin. The finite element equations which result are discrete versions of the equations of compatibility and angular momentum balance. Consistent reformulation of the constitutive equation, and accurate and stable time integration of the stress are discussed at length. Examples which bring out the feasibility and performance of the algorithm conclude the work.

14. SUBJECT TERMS

Hybrid element; Kinematic dynamics; Hypoelastic; Yield surfaces; Plastic bodies; Viscoplastic bodies; Uniqueness; Stablility criteria; Initial value

15. NUMBER OF PAGES
254

16. PRICE CODE
A12

17. SECURITY CLASSIFICATION OF REPORT	18. SECURITY CLASSIFICATION OF THIS PAGE	19. SECURITY CLASSIFICATION OF ABSTRACT	20. LIMITATION OF ABSTRACT
Unclassified	Unclassified	Unclassified	